N°d'ordre NNT : 2020LYSEI025

THESE de DOCTORAT DE L'UNIVERSITE DE LYON
opérée au sein de
INSA de Lyon

Ecole Doctorale N° 162
Mécanique, Energétique, Génie Civil, Acoustique (MEGA)

Spécialité/ discipline de doctorat :
Mécanique

Soutenue publiquement le 07/04/2020, par :

Amira Hannoun

Tribological role of pyrocarbon in articular cartilage regeneration.
Application in the shoulder arthroplasty

Devant le jury composé de :

Pinzano, Astrid	CR-CNRS, HDR	Université de Lorraine	Rapportrice
Wimmer, Markus	PR	Rush University Medical Center	Rapporteur
Mallein-Gérin, Frédéric	DR-CNRS	IBCP	Examinateur
Drouet, Cristophe	DR-CNRS	CIRIMAT Toulouse	Examinateur
Hassler, Michel	Directeur Principal	Wright Medical/Tornier	Invité
Bougault, Carole	Maître de conférences	Université Lyon 1	Invitée
Pasal Boileau	PR-Chirurgien	Hôpital Pasteur 2 Nice	Invité
Berthier, Yves	DR-CNRS, Emérite	INSA Lyon	Directeur de thèse
Trunfio-Sfarghiu, Ana-Maria	CR-CNRS, HDR	INSA Lyon	Co-directrice de thèse

Département FEDORA – INSA Lyon - Ecoles Doctorales – Quinquennal 2016-2020

SIGLE	ECOLE DOCTORALE	NOM ET COORDONNEES DU RESPONSABLE
CHIMIE	**CHIMIE DE LYON** http://www.edchimie-lyon.fr Sec. : Renée EL MELHEM Bât. Blaise PASCAL, 3e étage secretariat@edchimie-lyon.fr INSA : R. GOURDON	**M. Stéphane DANIELE** Institut de recherches sur la catalyse et l'environnement de Lyon IRCELYON-UMR 5256 Équipe CDFA 2 Avenue Albert EINSTEIN 69 626 Villeurbanne CEDEX directeur@edchimie-lyon.fr
E.E.A.	**ÉLECTRONIQUE, ÉLECTROTECHNIQUE, AUTOMATIQUE** http://edeea.ec-lyon.fr Sec. : M.C. HAVGOUDOUKIAN ecole-doctorale.eea@ec-lyon.fr	**M. Gérard SCORLETTI** École Centrale de Lyon 36 Avenue Guy DE COLLONGUE 69 134 Écully Tél : 04.72.18.60.97 Fax 04.78.43.37.17 gerard.scorletti@ec-lyon.fr
E2M2	**ÉVOLUTION, ÉCOSYSTÈME, MICROBIOLOGIE, MODÉLISATION** http://e2m2.universite-lyon.fr Sec. : Sylvie ROBERJOT Bât. Atrium, UCB Lyon 1 Tél : 04.72.44.83.62 INSA : H. CHARLES secretariat.e2m2@univ-lyon1.fr	**M. Philippe NORMAND** UMR 5557 Lab. d'Ecologie Microbienne Université Claude Bernard Lyon 1 Bâtiment Mendel 43, boulevard du 11 Novembre 1918 69 622 Villeurbanne CEDEX philippe.normand@univ-lyon1.fr
EDISS	**INTERDISCIPLINAIRE SCIENCES-SANTÉ** http://www.ediss-lyon.fr Sec. : Sylvie ROBERJOT Bât. Atrium, UCB Lyon 1 Tél : 04.72.44.83.62 INSA : M. LAGARDE secretariat.ediss@univ-lyon1.fr	**Mme Sylvie RICARD-BLUM** Institut de Chimie et Biochimie Moléculaires et Supramoléculaires (ICBMS) - UMR 5246 CNRS - Université Lyon 1 Bâtiment Curien - 3ème étage Nord 43 Boulevard du 11 novembre 1918 69622 Villeurbanne Cedex Tel : +33(0)4 72 44 82 32 sylvie.ricard-blum@univ-lyon1.fr
INFOMATHS	**INFORMATIQUE ET MATHÉMATIQUES** http://edinfomaths.universite-lyon.fr Sec. : Renée EL MELHEM Bât. Blaise PASCAL, 3e étage Tél : 04.72.43.80.46 infomaths@univ-lyon1.fr	**M. Hamamache KHEDDOUCI** Bât. Nautibus 43, Boulevard du 11 novembre 1918 69 622 Villeurbanne Cedex France Tel : 04.72.44.83.69 hamamache.kheddouci@univ-lyon1.fr
Matériaux	**MATÉRIAUX DE LYON** http://ed34.universite-lyon.fr Sec. : Stéphanie CAUVIN Tél : 04.72.43.71.70 Bât. Direction ed.materiaux@insa-lyon.fr	**M. Jean-Yves BUFFIÈRE** INSA de Lyon MATEIS - Bât. Saint-Exupéry 7 Avenue Jean CAPELLE 69 621 Villeurbanne CEDEX Tél : 04.72.43.71.70 Fax : 04.72.43.85.28 jean-yves.buffiere@insa-lyon.fr
MEGA	**MÉCANIQUE, ÉNERGÉTIQUE, GÉNIE CIVIL, ACOUSTIQUE** http://edmega.universite-lyon.fr Sec. : Stéphanie CAUVIN Tél : 04.72.43.71.70 Bât. Direction mega@insa-lyon.fr	**M. Jocelyn BONJOUR** INSA de Lyon Laboratoire CETHIL Bâtiment Sadi-Carnot 9, rue de la Physique 69 621 Villeurbanne CEDEX jocelyn.bonjour@insa-lyon.fr
ScSo	**ScSo*** http://ed483.univ-lyon2.fr Sec. : Véronique GUICHARD INSA : J.Y. TOUSSAINT Tél : 04.78.69.72.76 veronique.cervantes@univ-lyon2.fr	**M. Christian MONTES** Université Lyon 2 86 Rue Pasteur 69 365 Lyon CEDEX 07 christian.montes@univ-lyon2.fr

*ScSo : Histoire, Géographie, Aménagement, Urbanisme, Archéologie, Science politique, Sociologie, Anthropologie

Tribological role of pyrocarbon in articular cartilage regeneration.

Application in the shoulder arthroplasty

Abstract

Degenerative shoulder pathologies are currently treated by total shoulder arthroplasty (joint replacement) or hemiarthroplasty. Despite the success of this treatment, the complication rate reaches 22 % due to the complex nature of joint mechanics and limited bone stock. In this context, for young patients with degenerative glenohumeral joints, a new generation of interposition implant has been developed. The implant, designed with an original spherical shape, is inserted without fixation between the glenoid cartilage and a surgically created humeral bone cavity.

Cobalt-chromium (CoCr) is the most used biomaterial in shoulder arthroplasty; however, Pyrocarbon (PyC) is selected for the new implant for its elastic modulus similar to that of cortical bone.

Short-term clinical results showed minimal bone and cartilage wear and good bone remodelling in contact with the implant. However, the origin of these results is not yet well understood.

In this framework, the previous study on human explants in the laboratory showed that humeral bone remodelling involves the synthesis of a neocartilaginous tissue, which partly explains the favourable clinical results. However, these results are more controversial on the scapula side because of cartilage erosion. Therefore, the effect of PyC and the geometry of the implant on the remodelling of the surrounding tissues need investigation. Thus, this thesis aims to understand the origin of tissue remodelling on the bone and cartilage side. The first step of our strategy is to carry out three parallel studies to dissociate the role of the biology (cellular response), the impact of the material (PyC vs CoCr), and the involvement of mechanical stresses transmission (living tribological triplet). The second step is to validate the results thus obtained by associating the different aspects in an *in vitro* model based on tissue bioengineering principles. Consequently, our methodology was based on 1) the expertise of retrieved explants; 2) the analysis of murine primary chondrocytes cultures in contact with PyC and CoCr; 3) the testing of *in vitro* biotribological simulations; and 4) the design and validation of a simulator allowing to combine the biological, physicochemical and tribological results obtained previously.

The final results showed better chondrogenic and osteogenic cell activity in the case of PyC compared to CoCr. They were correlated on the one hand with better adsorption of the lubricating molecules, phospholipids, on the surface of PyC and the other hand with an optimal transmission of the mechanical stress due to its properties and geometry. Furthermore, the *in vivo* control of transmission of mechanical stresses is essential to guarantee good results in the long term. Besides, this thesis opens up fresh perspectives on the control of this transmission through biomaterials and their geometries for cartilage regeneration.

Rôle tribologique du pyrocarbone dans la régénération du cartilage articulaire. Application aux arthroplasties d'épaule

Résumé

Les pathologies dégénératives de l'épaule sont actuellement traitées par arthroplastie totale ou hémiarthroplastie. Malgré le succès de ce traitement, le taux d'échec augmente à 22 % à cause de la complexité de la mécanique articulaire de l'épaule. Dans ce cadre, pour des patients ayant un stock osseux très limité, une nouvelle génération d'implants d'interposition a été développée. L'implant, dont l'originalité est la forme sphérique, est introduit sans fixation dans l'articulation. Il est en contact direct avec le cartilage de l'omoplate et une cavité humérale osseuse créée chirurgicalement. Bien que le chrome-cobalt (CrCo) soit le matériau le plus utilisé pour l'arthroplastie de l'épaule, le pyrocarbone (PyC) a été choisi pour le nouvel implant car il a un module d'élasticité proche de celui de l'os.

Les résultats cliniques à court terme ont montré une usure minimale du cartilage et un bon remodelage osseux au contact avec l'implant. Cependant, l'origine de ces résultats n'est pas encore bien comprise. Dans ce contexte, les précédents travaux au laboratoire ont montré que le remodelage osseux côté humérus implique la synthèse d'un tissu néocartilagineux expliquant en partie les bons résultats cliniques. En revanche, ces résultats du côté de l'omoplate sont beaucoup plus controversés car ils présentent une érosion du cartilage. Par conséquent, des interrogations se posent sur l'effet du PyC et de la géométrie de l'implant sur le remodelage des tissus adjacents. Cette thèse vise donc à comprendre l'origine de ce remodelage coté humérus et omoplate. Pour cela, notre stratégie est d'effectuer en première étape trois études parallèles pour découpler le rôle de la biologie (réponse cellulaire), du matériau (PyC vs CrCo) et de la transmission des contraintes mécaniques (triplet tribologique vivant). En deuxième étape, notre stratégie consiste à coupler les différents aspects dans un modèle *in vitro* s'appuyant sur les principes de la bio-ingénierie tissulaire. Pour ce faire notre méthodologie a été basée sur : 1) l'expertise d'explants *in vivo* (analyses histologiques et lipidomiques), 2) le développement *in vitro* des cultures cellulaires primaires de chondrocytes murins en contact avec les deux matériaux, 3) les simulations bio-tribologiques *in vitro et* 4) la conception et la validation d'un simulateur qui a permis de combiner les résultats biologiques, physicochimiques et tribologiques obtenus précédemment.

Les résultats ont montré une meilleure activité cellulaire chondrogénique et ostéogénique dans le cas du PyC par rapport au CrCo. Cela a été corrélé d'une part à une meilleure adsorption des molécules lubrifiantes, les phospholipides, sur la surface du PyC et d'autre part à une transmission optimale des contraintes mécaniques due à ses propriétés et à sa géométrie. Par ailleurs, le contrôle de la transmission des contraintes mécaniques *in vivo* est essentiel pour garantir de bons résultats à long terme. De plus, cette thèse ouvre des perspectives vers le contrôle de cette transmission via les biomatériaux et leurs géométries afin de régénérer le cartilage.

Content

Amira HANNOUN/ Thesis in Biomechanics 2020/ INSA Lyon

List of abbreviations

APA	Amplified Piezo Actuators
BLC	Bone-like Conditions
CoCr	Cobalt-chromium
COF	Coefficient of friction/friction factor
CLC	Cartilage-like Conditions
CS	Chondroitin Sulphate
CTE	Thermal Expansion Coefficient
CVD	Chemical Vapour Deposition
DMMB	Dimethylmethylene Blue Assay
DMEM	Dulbecco's Modified Eagle Medium
DMSO	Dimethyl sulfoxide
DMA	Dynamic Mechanical Analysis
DOPC	Dioleoyl phosphatidylcholine
DPPC	Dipalmitoyl phosphatidylcholine
DS	Dermatan Sulphate
EDS	Energy-dispersive X-ray spectroscopy
ES	Sterol Esters
FBS	Foetal Bovine Serum
FRAP	Fluorescence Recovery After Photo-bleaching
GAG	Glycosaminoglycan
GC	Gas Chromatography
HA	Hyaluronic Acid
HACs	Human Articular Chondrocytes
HAS	Hemiarthroplasty
HES	Haematoxylin-Eosin-Saffron
HS	Heparan Sulphate
ITS	Insulin-Transferrin-Sodium selenite
KS	Keratan Sulphate

LDH	Lactate dehydrogenase
LTI	Low-Temperature Isotropic
MCP	Metacarpophalangeal
OA	Osteoarthritis
PBS	Phosphate Buffered Saline
PC	Phosphatidylcholine
PE	Phosphatidylethanolamine
PEEK	Polyether ether ketone
PG	Proteoglycans
PMMA	Polymethyl methacrylate
PS	Phosphatidylserine
PVC	Polyvinyl chloride
PyC	Pyrocarbon
RSA	Reverse Shoulder Arthroplasty
SAP	Surface-active protein
SAPLs	Surface-active phospholipids
SO	Safranin O
Sph	Sphingomyelin
TG	Triglycerides
TL	Total amount of lipids
TNAP	Tissue Non-specific Alkaline Phosphatase
TPL	Total amount of phospholipids
TSA	Total Shoulder Arthroplasty
WOF	Wheel On Flat

List of figures

Amira HANNOUN/ Thesis in Biomechanics 2020/ INSA Lyon

10

11

List of tables

Context and strategy

Osteoarthritis affects about 10 % of the world's population aged more than 60 years [1]. The joints are altered, sometimes consecutively to trauma, and the disease leads to cartilaginous tissue wear. This induces severe disability, and no treatment allows the total repair of this tissue [2]. The inefficiency of the treatments is mainly caused by the difficulty in detecting earlier the first symptoms of cartilage degradation [3].

The impact in terms of public health is significant. Osteoarthritis is ranked within the 15 most reported chronic diseases in Europe, according to the European Health and Social Protection Survey 2014: 20 % of people aged more than 15 years old suffer from osteoarthritis [4]. Notably, in France, around 50 % of the population aged more than 65 years old is affected by osteoarthritis [5]. The same study showed that 10 % of the hospital stays of people aged more than 45 years old are caused by articular system disorders [5].

Among several solutions for osteoarthritis, two leading solutions are still very promising: either the joint replacement by a prosthesis (arthroplasty) or restoring the cartilage structure using grafts [6]. Currently, arthroplasty is recognized as a valid treatment for osteoarthritis. Despite the general success of this treatment, failures have also been recorded. The clinical results of approximately 25 % of patients with total knee arthroplasty showed no significant improvement. In addition, with the ageing of the population, 13 % of patients undergoing arthroplasty worldwide are re-operated within the next ten years [7].

Despite many efforts to improve the different existent prostheses, their *in vivo* lifespan is still very disappointing compared to that extrapolated from *ex vivo* simulations. This discrepancy is mainly attributed to the *ex vivo* tribological test conditions, insufficiently realistic regarding the mechanical and physicochemical particularities of the biological environment. Thus, implants optimization requires a realistic tribological analysis which, because of the limits in the resolution of *in vivo* investigation techniques, can only be conducted from *ex vivo* model. Such a study must consider all the parameters of the *in vivo* environment (the contact, the loads, the lubricant).

Our study focuses mainly on the case of shoulder arthroplasty. The available surgical procedures are divided into three main types: hemiarthroplasty (HAS), total shoulder arthroplasty (TSA) and reverse total shoulder arthroplasty (RSA) [8][9]. Several factors must be considered when choosing an implant: the age and activity level of the patient, his/her bone stock and rotator cuff status. HAS is primarily used in rather young patients with healthy glenoid cartilage. However, TSA is widely used for centred glenohumeral arthritis, and RSA is used for pathologies involving the rotator cuff and rather older

patients [10]. The complication rate with these solutions reaches 22 % with an average follow-up of six years due to the complex nature of joint mechanics and limited bone stock [11].

Consequently, a new generation of interposition implant has been developed [12]. The implant is designed with an original spherical shape. It is inserted without fixation between the glenoid cartilage and a surgically-created humeral bone cavity. Thus, the new implant replaces the anatomical humeral head [13]. Cobalt-chromium (CoCr) is the most used biomaterial in shoulder arthroplasty; however, pyrocarbon (PyC) is selected for the new implant for its elastic modulus similar to that of bones [12]. Also, PyC has excellent tissue biocompatibility and good wear properties [14][15].

Clinical evaluations, radiographic outcomes and implant survival of the new PyC implant have been assessed at a 2-years follow-up [12][16]. Short-term clinical results showed minimal bone and cartilage wear and good bone remodelling in contact with the implant. These studies revealed satisfactory clinical results. The implant achievements were comparable to those of HAS but still inferior to those of TSA. However, the origin of these results is not yet well understood.

In this framework, in a recent study on human explants in the laboratory, a neosynthesized tissue at the extremity of the humeral metaphyseal cavity in contact with the PyC implant was observed. The histological analysis suggested that this new tissue had cartilage-like characteristics (unpublished data from a previous PhD study of Ghassen Ouenzerfi: Tribological behaviour of pyrocarbon against bone promotes cartilage regeneration? Proceedings of the 42nd Leeds-Lyon Symposium on Tribology 2015) [17]. These data suggested that the humeral bone remodelling involves the synthesis of a neocartilaginous tissue, which partly explains the favourable clinical results and confirms that the proper functioning of this implant is related to the "biological adaptability" of the surrounding tissues [18]. However, these results are more controversial on the scapula side, where glenoid cavity erosion was observed.

Therefore, the effect of PyC and the geometry of the implant on the remodelling of the surrounding tissues need investigations. Thus, this thesis aims to understand the origin of tissue remodelling on the bone and cartilage side. Our strategy is: first, to carry out a retrieval analysis to identify the *in vivo* effect of the PyC on the living tribological triplet compared to the CoCr; second, to carry out three parallel studies to dissociate the role of the biology (cellular response of the first bodies) of the material (PyC vs CoCr) and the transmission of mechanical stresses (third body and mechanism); and finally, to validate the results thus obtained by associating the different aspects in an *in vitro* model based on tissue bioengineering principles. Consequently, our methodology is based on:

① The expertise of retrieved explants (shoulder hemi-prostheses) made of PyC or CoCr. Histological analysis is performed to identify the effect of the biomaterials on the surrounding tissues (the 1st bodies in the live biotribological triplet). Also, lipidomic analyses are performed

to evaluate the adsorbed biological molecules on the surfaces of the implants, to identify the effect and the interaction of the biomaterials on/ with the natural lubricant;

② The analysis of murine primary chondrocytes cultures in contact with PyC and CoCr: this section aims to identify the effect of the biomaterials on the 1st bodies *in vitro,*

③ The development of a new lubricant for *in vitro* biotribological simulations based on the information obtained from the retrieval analysis,

④ The *in vitro* biotribological simulations: this section aims to validate the new developed 3rd body (the lubricant) and to evaluate the biomaterials effect on live bovine cartilage with different mechanisms,

⑤ The design and validation of a biotribological simulator "Tribo-bioreactor" which allowed to combine *ex vivo* the biological, physicochemical and tribological results obtained previously.

The methodology of this project is summarized in the diagram below:
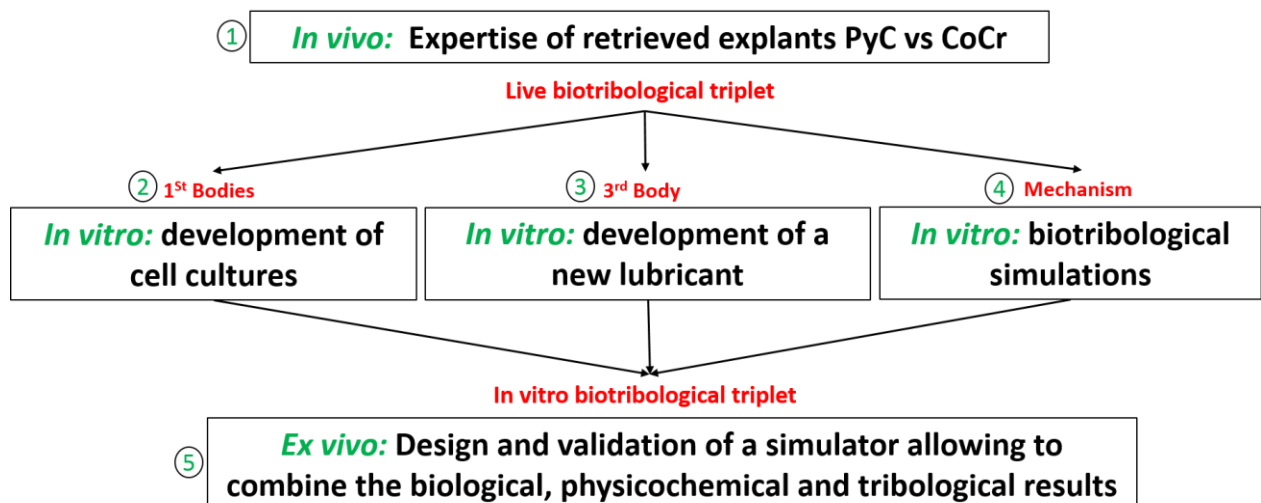
Figure 0-1 Diagram illustrating the followed method during the work of this thesis

Reproducing the appropriate biological environment *ex vivo* is still a complex task, and the *in vivo* experiments are insufficient to allow studying the natural contact between cells and the biomaterials used in the arthroplasty. This thesis investigated the *in vivo* results of different shoulder Hemi-prostheses in various disciplines as biochemistry, biology, and biomechanics to conceive an *ex vivo* model allowing to reproduce the *in vivo* results.

Thus, the work in this thesis is divided into seven chapters:

Chapter A: offers a bio-tribological approach to the joint. It presents the articular contact as a mechanical system with its different components, from the two bodies in contact to the perfect natural lubricant. Particularly, it gives the different aspects of the tribology and its applications in the human body with a bibliography summary.

Chapter B: presents the history of the PyC material from its use from nuclear studies to the arthroplasty. It shows different applications of the PyC, particularly in the shoulder arthroplasty. In this chapter, the context and the main aim of the thesis are presented. The preliminarily results obtained previously in the laboratory are also presented.

The remaining chapters present the different approaches performed to understand the promising results of the interposition implant made with PyC observed *in vivo*.

Chapter C: presents an investigation of the PyC effect on the human body. Retrieval analysis of different shoulder hemi-prostheses made either of PyC or CoCr is performed to the *in vivo* effect of the biomaterial on the components of the living tribological triplet, particularly on the natural lubricant and on the surrounding tissues.

Chapter D: presents the "biological approach" to understand the proper functioning of the PyC from a biological point of view. Cell culture of murine chondrocytes in the presence of discs of PyC is performed in comparison with the CoCr. Multi-physical characterisations are performed to evaluate the biomaterials effects on cells. This part of the work is a collaboration between the Contact and Structure Mechanics Laboratory (LaMCoS) in INSA Lyon and the Metabolism, Enzymes and Molecular Mechanisms Laboratory (MEM^2) in Institute of Molecular and Supramolecular Chemistry and Biochemistry (ICBMS).

Chapter E: presents the "tribological approach" to develop a new realistic 3rd body. A newly developed lubricant mimics the healthy synovial fluid with lubricating properties. The new lubricant is favourable for biotribological simulations. It ensures cell viability in simulations using live cartilage explants. The work presented in this chapter is performed as a part of an internship in the tribology laboratory of Rush university medical centre (Chicago, USA).

Chapter F: presents the "tribological approach" to investigate the tribological behaviour of the PyC against living articular cartilage in comparison with the CoCr. Wear testing against living bovine cartilage with the PyC and CoCr is performed using a specific bioreactor "shoulder simulator". This bioreactor allows to apply the same movements of the shoulder, and it is available in the tribology laboratory of Rush university medical centre (Chicago, USA). The work presented in this chapter is a part of an internship in the tribology laboratory.

And finally,

Chapter G: presents the compilation of all the information obtained from the different approaches in a global test. An *ex vivo* model to reproduce an appropriate *in vivo* configuration is developed. The

simulator used was conceived in the laboratory. In this chapter, its validation for the different experiments is presented. And finally, the results of the first primary test are presented.

Discussions and preliminary conclusions are presented at the end of each chapter to facilitate the lecture of the manuscript. General findings are offered at the end with some perspectives of the study.

Chapter A

The synovial joint is a perfect tribological system

A. Chapter A: The synovial joint is a perfect tribological system

This chapter aims to introduce the global context of this project: the synovial joint and its tribological properties. It is necessary to introduce this theme here to understand and justify the choices that animated these three years of research. In the first part, notions related to tribology is mentioned to appreciate the rest of the chapter. Then, a bio-tribological approach of the synovial joint is described.

1. Tribology

Tribology is the science studying the friction between two bodies in contact. It includes the themes of lubrication, friction and wear. The tribology is usually applied in the context of industrial applications. However, it is a part of our daily life. We blink our eyes. We chew and taste our food. We put on shoes to run or for a walk. In all these actions, tribology is present.

Most of the daily problems related to the friction could be clarified using the laws of friction. These laws are described for the first time by Leonard de Vinci (1699). Vinci proposed that in the case of two solids in contact, the tangential force is proportional to the load and does not depend on the contact surface. Later, Amontons (1699) and Coulomb (1781) checked the main laws governing the friction between two solids.

Back to the primary concern, let's consider two solids in contact, subject to a normal load F, and sliding between each other with speed V. In this case, a tangential force T appears to oppose the displacement of these two solids. In 1785, Coulomb laws suggested a new parameter $\mu = T/F$ called the "coefficient of friction". This parameter is particularly important. It allows us to walk without sliding, but it leads in other cases to significant damages in surfaces, like the wear.

Lubricants are used to avoid damages caused by a high coefficient of friction. They are defined by their viscosities. The choice of the lubricant type depends on the surfaces in contact and the contact environment.

To better study the contact, Godet defined a model called the "tribological triplet" [19]. This model helps to understand better the friction and wear mechanisms [20]. Thus, the tribological triplet became a regular tool used in the tribology. Briefly, it is composed of the first bodies (the two solids in contact), the third body (the lubricant) and the mechanism (mechanical system containing the first bodies).

The first bodies undergo surface transformations due to the tribological constraints. The third body is the intercalary zone between them and allows accommodation of the velocity difference. It can be produced *in situ* (natural 3rd body) or introduced into the contact (artificial 3rd body). It allows to separate the first bodies and limit their wear, to transmit and distribute the load, to accommodate the shear rates between the first bodies, and to evacuate the heat from the contact [21].

The mechanism is the origin of the stresses applied to the contact. It combines the tribological and the mechanical, thermal and physicochemical behaviours [22]. Therefore, friction depends as much on the mechanism as on the materials in contact. The "coefficient of friction" is usually used as the "friction factor".

Many studies looked to enhance the contact between two surfaces on different scales, from the contact wheel/rail to the contact between cells in the human body. These studies tried to obtain a perfect tribological system. Such a system is present in the human body: the synovial joint which represents a specific branch of the tribology: the biotribology.

2. Biotribology

The biotribology is introduced by Dowson and Wright in 1973 [23], to study the live tribological triplets. The synovial joint is considered as a very efficient tribo-system which runs for a lifetime, ensuring a minimum of friction and wear at the contact level [24]. These exceptional tribological performances [25][26] are due mainly to the "living" materials in contact, which:

- facilitate the motion between their surfaces by the synthesis of natural molecules that act as natural lubricants
- reduce their wear

Despite the exceptional performance of the living environment, researchers are still not able to explain:

- How do biological contacts resist wear?
- Why do some live contacts end up wearing with age?

Consequently, it is essential to understand the different components of the structure of the synovial joint "the natural tribological triplet".

3. The synovial joint: elements and structure of the articular triplet

The synovial joint is the most common type of joint in the human body. It is found in the knee, the hip, the shoulder or the fingers. It is composed of two bones in contact covered by hyaline cartilage, embedded in an articular capsule that contains the synovial membrane, as shown in figure 1.

This membrane produced the synovial fluid, which ensures the cartilage nutrition and contact lubrication [27]. This system acquires its tribological properties from embryogenesis to the first months of life. During this period, initial cartilage cracks to decrease the load in the articular contact, which gives the geometry of the first bodies [28][29]. The damping of mechanical solicitations depends on the cartilage thickness and is controlled by the embryonic stage during endochondral ossification. During this process, the cartilaginous tissue is transformed into bone tissue [30]. The thickness of the

cartilage is then regulated according to the external solicitations [31][32]: the areas with the highest loads are the thickest [33].
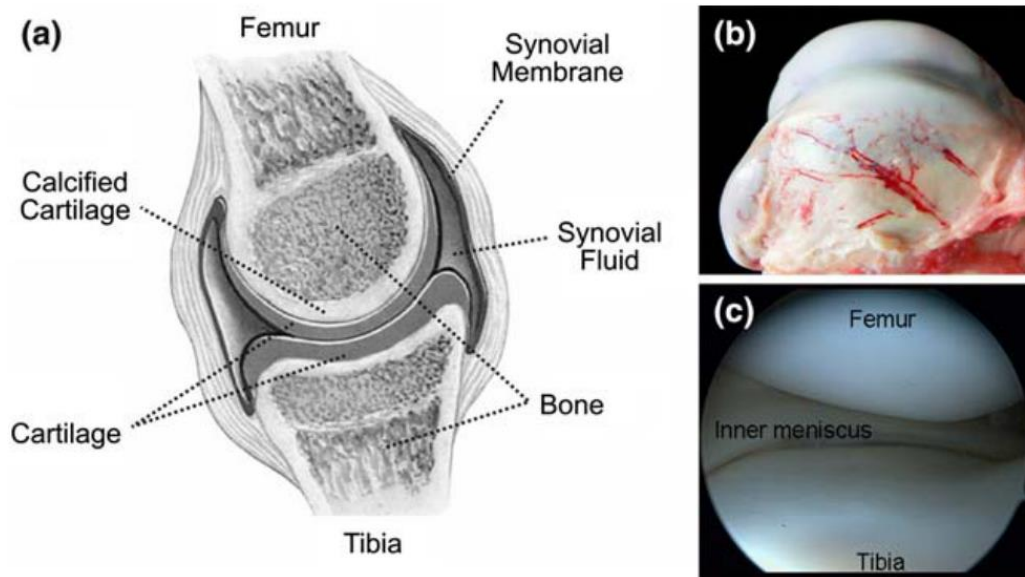
Figure A-1 Sketch of a knee joint (a), side view on the femoral condyle of an open joint (b), and arthroscopic view of a healthy human knee joint (c) [27]

The coefficient of friction (µ) of this system is around 0.001-0.05 [34]. For years, many studies have been conducted to understand how this coefficient could be so low, but there is still no consensus. In fact, beyond the purely mechanical characteristics of the system, it is necessary to consider the biological and physicochemical phenomena at the contact level.

From a tribological point of view, to better understand the articular functioning, we must consider the tribological triplet that forms the synovial joint and the different interactions between its components (figure 2) [35]. Considering the anatomical structure of a synovial joint, the tribological triplet joint, as shown in figure 2, consists of:

- The 1st bodies: represented by the articular cartilages which form the surfaces in contact,
- The 3rd body: represented by the synovial fluid which separates the 1st bodies and ensures the lubrication,
- The mechanism: represented by the muscular-ligamentous system, which imposes the global solicitations.

3.1. The mechanism

The mechanism sets in motion the first bodies of the articular contact via the neuromuscular and the ligament system [36]:

• The neuromuscular system generates an order using an electrical tool, the nerve fibre. This fibre transmits the information in the form of an electric shock to the mechanical tool, the muscular tissue. The muscle is then set in motion.

• The ligament system (consisting of the joint capsule, ligaments, and surrounding musculotendinous system) modulates the electric shock, and therefore the movement, to avoid any sudden changes and to respond ideally to the initial order. It also maintains the two bony ends of the joint, to stabilize and limit the movement.
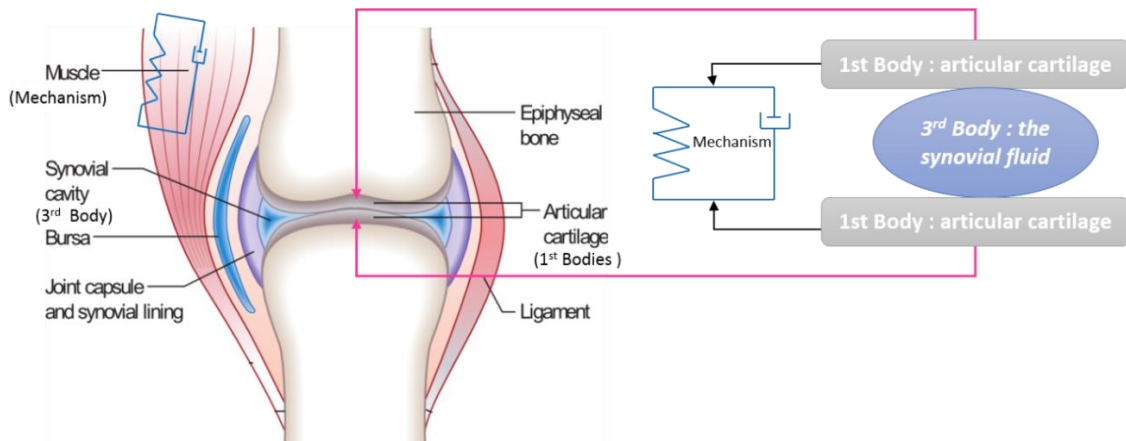
Figure A-2 Tribological triplet of the synovial joint showing the 1st bodies (the articular cartilage), the 3rd body (the synovial cavity/synovial fluid) and the mechanism (the muscle)

3.2. The first bodies: Cartilage

Articular cartilage is a soft tissue that covers the surfaces of the bones in contact. It is smooth, flexible and elastic, compressible and extensible [3]. This cartilage provides low friction, wear-resistance, and useful load support. In adults, the thickness of this tissue varies from 0.5 to 5 mm depending on where the joint is located. In weight-bearing joints (hip, knee), the maximum thickness is detected in the zones supporting the maximum load. Thus, on the patella, the thickness of the cartilage can reach up to 7 mm. In general, articular cartilage is a bit thicker in men than in women. This thickness could be estimated as a function of the pressure at the surface of contact [37].

Adult cartilage is an avascular (its nutrition is possible by diffusion from the synovial fluid) and non-innervated connective tissue: its remodelling is slow. Besides, cartilage is a non-lymphatic tissue which results in a little immune resistance to disease. In the case of cartilage degeneration, such as in osteoarthritic joints, the pain appears when the cartilage lesions reach the bone.
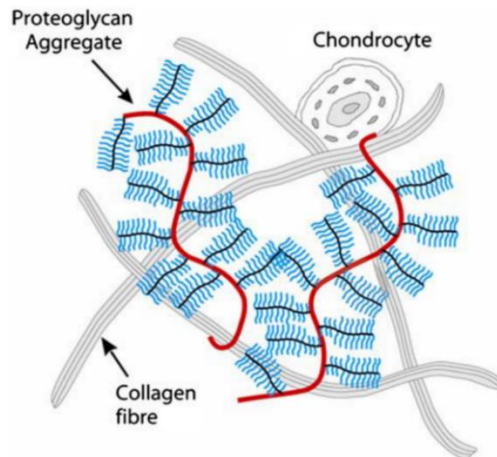
Figure A-3 Illustration of the extracellular matrix organization of articular cartilage [27]

Its structure is complex and composed of 80 % of water, 20 % of the extracellular matrix, and less than 1 % of cells (% by mass), as shown in figure 3 [27]. The important biomechanical properties of articular cartilage depend on the structure of the extracellular matrix secreted by the chondrocytes (cartilage cells). This matrix is composed of a network of collagen fibres and a well-hydrated substance, consisting of proteoglycans (PG), glycoproteins, and large macromolecules, binding proteins as well as phospholipids and elastin. This structure is anisotropic and heterogeneous. Cartilage is considered a viscoelastic, permeable and highly organized.

3.2.1. The macromolecular components specific to articular cartilage

3.2.1.1. Collagens

Collagens present about 55 % of the dry weight of cartilage. They are proteins: molecules formed by long chains of amino acids. Nine different types of collagen are detected in the hyaline cartilage [38]. However, the most redundant one is type II collagen, which presents from 90 to 95 % of the existent collagen. It is fibrillar collagen made up of three alpha chains, which are wrapped around each other to form a "fibril". At each end of the fibril, the collagen binds to another collagen fibril periodically. Consequently, the arrangement of the collagen fibrils with each other produces a robust mesh network.

In cartilage, type II collagen forms a heterotrimeric bonding with type IX and XI collagens. Type IX collagen attaches to the fibre and binds the proteoglycans to the type II collagen network. Type XI collagen is localized within type II collagen fibres to organize fibrils structure (Figure 4).

Other types of collagen (types III, VI, XII, XIII and XIV) are present in the articular cartilage in small amounts. Collagen type I is not detected in cartilage structure despite it represents around 90 % of the total collagen in the human body.

Generally, collagen fibrils allow a tensile strength and a tissue organisation in the same directions of the mechanical constraints.
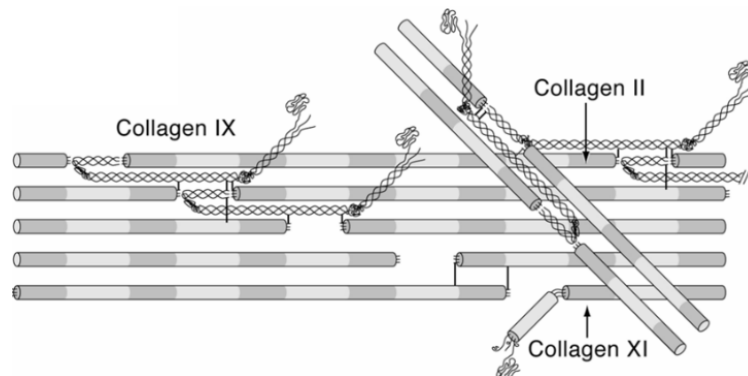
Figure A-4 the collagen II/IX/XI heterofibril. (a) An interaction model between surface collagen IX molecules and the collagen II polymer that can accommodate all known IX-to-IX and IX-to-II cross-links and potential interfibrillar cross-links (the figure is taken from [38]

3.2.1.2. Proteoglycans (PG)

Proteoglycans present about 20 % of the dry weight of cartilage. They are macromolecules formed by a central fibrillar protein on which chains of glycosaminoglycan (GAG) and sugars (oligosaccharides) are attached via small connecting proteins (figure 5). Four types of glycosaminoglycan chains are present mainly in cartilage: chondroitin sulphate (CS), dermatan sulphate (DS), heparan sulphate (HS), and keratan sulphate (KS).

The chemical structure of these chains shows the presence of negative charges of sulphate and carboxyl type. Their charge density is the origin of their strong hydration: proteoglycans can attract up to 50 times their weight in water. It generates a significant osmotic pressure in the extracellular matrix. Besides, the liquid phase of the cartilage contains multiple ions. Their concentration in the cartilage matrix depends on the local concentration of proteoglycans and their charge density.

For example, cations of Na^+ (240-350 mM), K^+ (7-12 mM), Ca_2^+ (6-20 mM), and Cl^- anions (600-100 mM) are found in femoral head cartilage [39] [40]. These ions affect the proteoglycans conformation and therefore, the mechanical properties of the tissue.

Thanks to their high-water retention, proteoglycans ensure excellent resistance to the compression and shock of the cartilaginous tissue. They allow the diffusion and the fixation of many molecules (growth factors, cytokines, nutrients, hormones ...) necessary for the viability and the proper functioning of the cells. Their size and composition are highly variable and promote non-covalent bonds with the collagen fibres. These multiple interactions inhibit the transport of large molecules and stabilize the extracellular matrix, hence its viscoelastic behaviour [41].

26
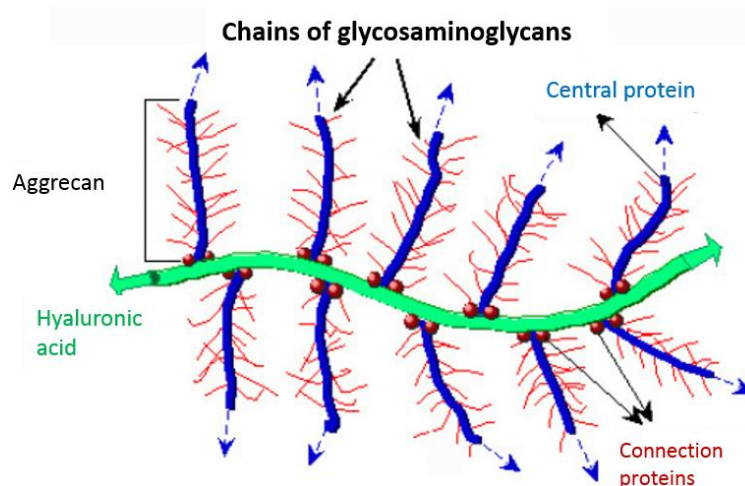
Figure A-5 Aggrecan aggregates (cartilage extract) composed of a chain of hyaluronic acid on which are grafted carrier core proteins through binding proteins

The metabolism of proteoglycans is affected by the biomechanical factors of the joint. When the joint is immobilized, the proteoglycans decreased inducing cartilage thinning. In the case of osteoarthritis, the loss of proteoglycans leads to a significant decrease in shock resistance [42][43].

3.2.1.3. Cartilage cells: Chondrocytes

Articular cartilage contains only one type of cells (chondrocytes) with a total volume of 1 % from the cartilage volume. Chondrocytes have a very low capacity of multiplication (regeneration) but a robust metabolic activity (synthesis of the solid phase by biochemical reactions).

During embryonic development, stem cells (present initially in the mesenchyme of the embryo) differentiate into pre-chondroblasts. Pre-chondroblasts are active cells able to proliferative into chondroblasts [44]. For up to 8 years, chondroblasts can differentiate into chondrocytes and vice-versa. After eight years, their differentiation into chondrocytes is definitive. The extracellular matrix of cartilage is mainly developed by chondroblasts, but maintained by chondrocytes [45].

Chondrocytes have a round shape and regular morphology with a diameter from 10 to 40 µm, incorporated in the cartilaginous matrix. In cartilaginous tissue, chondrocytes are isolated from each other. That's why there is no contact between cells, but they are firmly in connection with the matrix. Consequently, the chondrocyte is sensitive to the transmitted charges through the extracellular matrix via various receptors and proteins [29][46].

The size, shape, and arrangement of the chondrocytes depend on their location in the depth of the cartilage:

- In the superficial zone: they are organized according to the orientation of the collagen fibres. They are not very active metabolically.
- In the transition zone: they are spherical and distributed randomly.

Amira HANNOUN/ Thesis in Biomechanics 2020/ INSA Lyon

- In the deep zone: they form columns perpendicular to the surface of the subchondral bone. The number of chondrocytes increases in the direction of the bone.

Chondrocytes ensure extracellular matrix maintenance. They regulate the balance between anabolism hyaluronic acid to the information of the external environment. Thus, their differentiation is controlled by the biophysical forces, the mechanical stresses and the deformations received at the cellular level.

3.2.1.4. Mechanisms of mechanotransduction of chondrocytes

Mechanical signals induce changes in the chondrocyte environment. Thus, chondrocytes are affected. When the cartilage is under mechanical constraints, the extracellular matrix and cells undergo a deformation. This deformation generates locally interstitial fluid flows, hydrostatic pressure forces, osmotic pressure variations, electrical potential, cell volume changes, and variations in ionic composition and pH in the interstitial fluid. These changes depend on the type of pressure.

- The cyclic charges increase the pressure rapidly, momentarily deform the cells and cause short peaks of liquid flow without loss of liquid which. In general, such strains stimulate cell biosynthesis of matrix molecules.
- Static charges with long duration, cause an increase in the concentration of proteoglycans and osmolarity as well as a drop in pH, and a slow deformation of the tissue. As a result, the static charge usually causes a decrease in the production of the molecules that form the cartilage matrix.

Chondrocytes thus react to the mechanical stresses applied by their mechanical environment and their extracellular matrix. Mechano-sensitive components are responsible for cell mechanotransduction, which is the process of translating external physical forces into intracellular biochemical and biological responses. They include ion channels and integrins, for instance [47][48][49][50] (Figure 6). They react directly to mechanical stress or transmit it to another mechano-sensitive component. When these components are located on the cell surface, they are called mechano-sensitive receptors.

For each receptor stimulation, a specific cascade of intracellular reactions, known as the "mechanotransduction pathway", leads to a specific cellular response (figure 6). The transmission of the forces from the outside to the inside of the cells also involves a reorganization of the internal architecture of the cellular cytoskeleton.

Briefly, the transmission of mechanical forces between cells and their environment is one of the essential processes in the coordination of cellular functions such as adhesion, migration or differentiation.
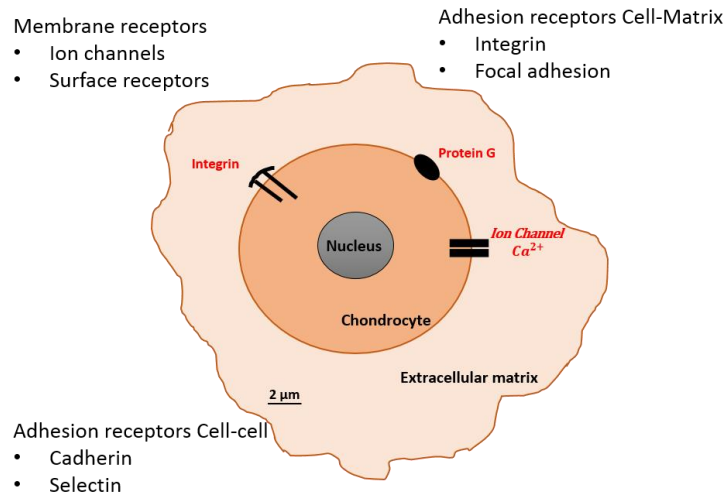
Figure A-6 The pathways of cell mechanotransduction: membrane receptors - the ion channels are the most important, their activation inducing the change of the ionic concentration in the cell; cell-matrix adhesion receptors - the integrins are in charge of the adhesion of the cell to its environment, and they have been associated calveolae and protein G; cell-cell adhesion receptors are receptors that play a role in the mechanotransduction only when we have cells in contact, these receptors establish adhesions between two neighbouring cells

3.2.2. Mechanical constraints and structure of articular cartilage

In vivo, cartilage undergoes a wide range of mechanical stresses such as compression, shear and liquid flow which are imposed by the dynamics and the kinematics of the joint:

- Compression: for example, in the hip, 1 MPa for a static standing position, from 0.1 to 4 MPa while walking with peaks up to 10-20 MPa to climb steps. *In vivo*, the articular surfaces are exposed to cyclic contact pressures, with frequencies between 0.1 and 1 Hz over periods generally less than 1 hour. These cyclic loading periods are interrupted by partial or total recovery periods which, cumulatively, represent at least 16 hours per day [51][31].

- Shear: It is considered that in the healthy joint, the relative movement of the two cartilages in contact is accommodated by a strongly localized shear in the lubricant film (volume of the synovial fluid trapped between the two cartilages). The cartilaginous tissue is sheared in its deep zone, in contact with the subchondral bone. Due to the difference in modulus of elasticity cartilage/bone, the deformed material cannot transmit all the movements which cause micro-fractures. These micro-fractures are usually filled by the biological activity of the bone tissue (bone remodelling).

- Liquid flow: The compression and shear of lubricant film as well as the bi-phasic structure of the articular cartilages cause a flow of liquid between the intra-articular space and the cartilage.

The transmission of mechanical stresses is not uniform through the thickness of articular cartilage [51] [52]. The extracellular matrix and the chondrocytes are spread out over four zones with different biomechanical properties [45][53][54]. From the superficial to the deep zone, the number of chondrocytes is decreased. At the same time, the dimension and metabolic activity are increased [27] (as shown in 7 taken from *Anatomy and Physiology of Equine Joints – Colorado State University*).

- Zone 1: superficial zone resistant in shear due to the tangential organizations of the collagen fibres and the synthesis of proteins with the lubricant behaviour.
- Zone 2: intermediate zone, resistant in compression by the fibrillar arch structure of collagen.
- Zone 3: radial/deep zone, resistant in compression by the collagen fibres which are perpendicular to the surface, and the highest concentration of proteoglycan against the lowest concentration of water.
- Zone 4: a thin and calcified zone, the collagen fibres are anchored to the subchondral bone underneath; only a few chondrocytes appear here.

Thus, thanks to this structure, articular cartilage has remarkable biomechanical properties against its principal stresses: shear, compression, friction, and traction. Besides, the synovial fluid reduces friction by lubricating the joint.
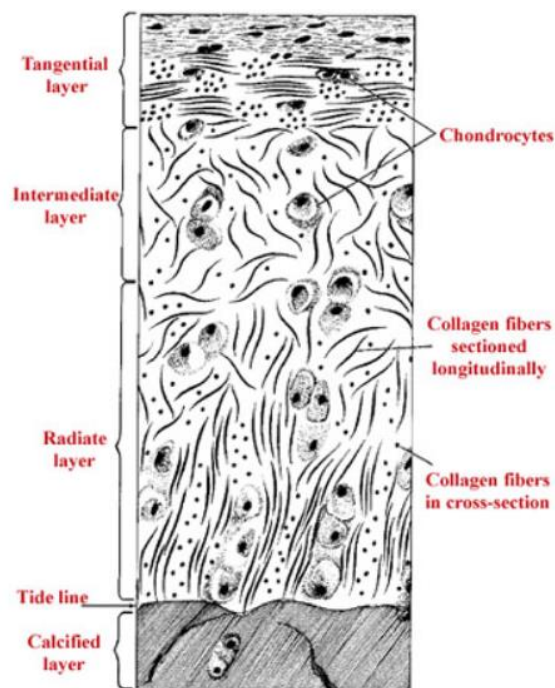
Figure A-7 Diagram of adult articular cartilage showing four layers and arrangement of chondrocytes and collagenous fibres.

Amira HANNOUN/ Thesis in Biomechanics 2020/ INSA Lyon

3.3.   The third body: Synovial fluid

Synovial fluid is a biological viscous liquid produced by the synovial membrane. It's the third body in the tribological triplet, the natural lubricant of the joint. Synovial fluid is a blood filtrate filtered by the synovial membrane and secreted in the articular capsule. It is present in small amounts in the joints, from 0.5 to 4 mL. It is composed of hyaluronic acid (0.5 g/L), proteins (10 to 20 g/L), proteoglycans and phospholipids organized in multilayers against the cartilage and vesicles in the fluid [55]. Synovial fluid has three essential roles: (a) the nutrition of articular cartilage, (b) lubrication, (c) elimination of metabolic products from articular cartilage. Its structure provides these roles.

- Serum proteins, predominantly albumin [56]: they balance intracellular and extracellular osmotic pressures [57] [58]. They help to lubricate cartilage surfaces [59] and maintain synovial osmolarity [60].
- Hyaluronic acid is a glycosaminoglycan molecule with a high molecular weight, which do not penetrate the cartilage [61]. Highly hydrophilic, it increases the viscosity of the fluid and offers to the synovial fluid its gel appearance [62]. It is considered responsible for rheological properties [63].
- There is a high concentration of lipids within the synovial fluid (3 g/L). Due to their biochemical properties, lipids are organized into plane lipid multilayer on the surface of the cartilage [64], or into vesicles containing synovial gel [65] [66].
- The lubricin is a glycoprotein present on the surface of the articular cartilage and the synovial membrane. It protects the joints and avoids their wear. It ensures their structural stability by being a molecular adhesive between collagen fibres, gel and lipid layers [65].

3.3.1. Hyaluronic acid

Naturally, hyaluronic acid is found in many tissues and fluids, but it is more abundant in articular cartilage and synovial fluid. The hyaluronic acid molecule is hydrophilic. It can directly connect 50.000 water molecules or four water molecules per disaccharide unit. Thus, it is responsible for the high viscosity of synovial fluid [67] [68].

Hyaluronic acid is a polysaccharide molecule of the glycosaminoglycan class. The hyaluronic acid in the synovial fluid has a polymeric structure consisting of over 12500 units of disaccharides formed by alternating units of D-glucuronic acid and *N*-acetyl-d-glucosamine (figure 8) [69] [70].

31
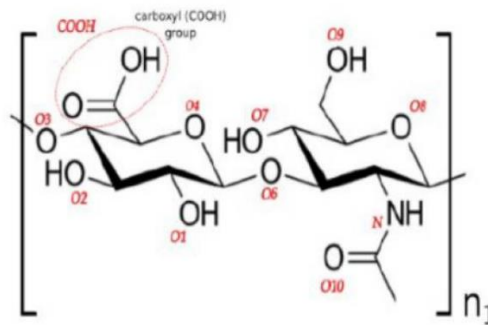
Figure A-8 Chemical structures of the units in hyaluronic acid (figure adapted from [71]*)*

It is found directly at the surface of phospholipid membranes. The chains can be very long, reaching tens of thousands of units or millions of Daltons in weight [70].

Hyaluronic acid is one of the two essential components of the synovial fluid implicated in the lubrication of the joint. Its interaction with the phospholipids participates and modify the lubrication of the joint.

3.3.2. Phospholipids

Phospholipids are among the most common molecules in the human body. There are two distinct parts on the phospholipid structure: a polar and hydrophilic head that contains a phosphorus atom, and two tails, which are hydrophobic fatty acids (Figure 9). The hydrophilic head is composed of three elements that are glycerol, phosphate and a specific group for each type of phospholipid.

Inside the synovial fluid, this group generates three types of phospholipids: phosphatidylcholines (PC) which represent 41% of molecular weight, phosphatidylethanolamines (PE) 27% of the molecular weight and sphingomyelin (Sph) 32% of the molecular weight.
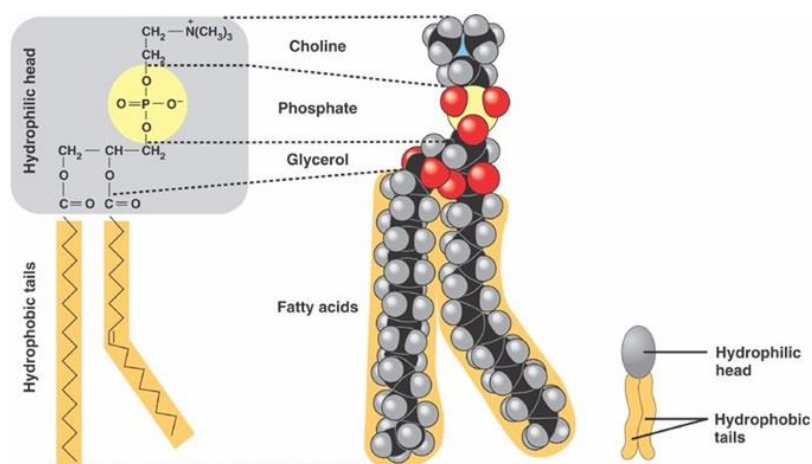
Figure A-9 Structure of phospholipid with a PC head and its symbol (figure taken from ([72]*)*

These two opposing properties allow phospholipids to create 3-dimensional structures in a fluid, where the hydrophobic tails gather to avoid being in contact with the aqueous liquid. The lipids can form

Amira HANNOUN/ Thesis in Biomechanics 2020/ INSA Lyon

multilayers, micelles or vesicles (liposomes), all of which possess a significant role within the organism. For example, the micelle carries fat in the bloodstream, the liposome can carry many different soluble molecules, and the multilayer forms a significant part of the membrane of all cells in the human body (figure 10) [73].

In the synovial fluid, phospholipids are organized in a vesicular structure. Within a joint, the synovial fluid creates a lipid multilayer on opposing sides of the articular cartilage. This particular lipid structure provides the synovial fluid with better lubricating properties, helping to reduce friction within the joint.
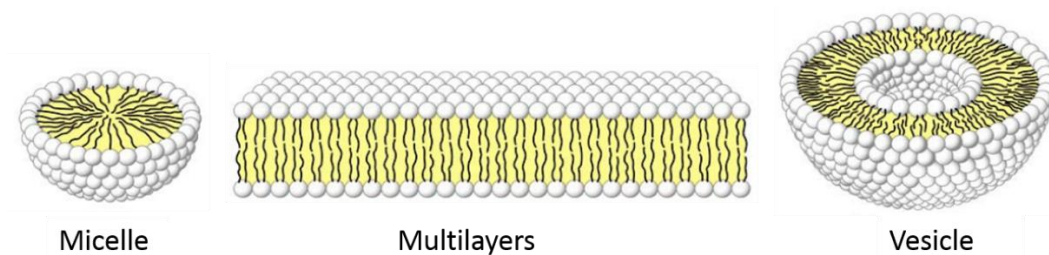
Figure A-10 Lipids formation in a fluid: micelle, lipids multilayer & vesicle [73]

3.3.3. Lubrication

The major synovial joints like hip and knee receive very high mechanical loads. In this case, only boundary lubrication is possible. However, this type of lubrication does not allow the formation of a lubricating film which is thicker than the roughness of the surfaces in contact. Therefore, the contact between the two cartilaginous surfaces is lubricated via a molecular film adsorbed on the surface following the surface topography. The absence of this film accelerates cartilage degradation and wear. Despite this type of lubrication, the coefficient of friction in a synovial joint remains very low [74] [75] [76] [77]. To better understand this low coefficient of friction, several studies have been launched to identify the synovial fluid component promoting boundary lubrication.

Swann and his colleagues extracted the molecular layer of the articular cartilage and characterized it chemically by electrophoresis [78]. They identified a glycoprotein-like molecule, called "superficial zone protein". It is a mucin-like glycoprotein with active and robust surface properties [79] [80] [81] [82]. It is called "surface-active protein" (SAP) afterwards [83] [84].

In 2000, Hills found that synovial fluid samples containing SAP also contain phospholipids molecules called "surface-active phospholipids" (SAPLs) [85]. Consequently, two identified components in synovial fluid may be responsible for the boundary lubrication of the articular surfaces: SAP and SAPLs. Further biochemical characterization of the extracted molecular layer from cartilage indicated the presence of glycoproteins similar to vitronectin and hemopexin (they are abundantly found in serum and extracellular matrix) [80]. The vitronectin gives this layer an adhesive function. It has a strong

affinity to the aggrecan of the articular cartilage matrix and the synovial fluid lipid bilayers [80] [86] [69]. The hemopexin gives this layer antioxidant property [87]. It is protective against the biochemical oxidation of lipids. It prevents their degradation and thus the destruction of the synovial fluid structure, which would affect the tribological joint function.

Also, Batchelor and Stachowiak confirmed that the assemblages of SAPLs and glycoproteins have an essential role in the synovial joints lubrication [88]. This confirmation is supported by Murakami, Forster, Fisher and their colleagues, who proved the lubrication capacity of different synovial fluid components, including SAPLs [89] [90] [91].

SAPLs are transported in the synovial fluid to the cartilage surfaces. They form an interface between cartilage and the volume of synovial fluid thanks to their self-assembly capacity in bilayers [92]. This interface, consisting of lipid multilayers provide boundary lubrication when articular surfaces should typically be "in contact" (figure11) [93]. Therefore, Hills suggests that SAPLs are the essential ingredient of joint lubrication [85].

Besides, recent studies highlighted the role of vesicular lipid interfaces (PC liposomes) in the reduction of friction [94][95]. Not only phospholipids are essential in the lubrication mechanism, but also they interact with the other components of the synovial fluid. Physicochemical studies showed that the combination of the lipids and hyaluronic acid form multilamellar vesicles and tubular structures filled with HA [96]. Interactions between lipid vesicles, HA and proteins of the synovial fluid change the rheology of the lubricating film and affect the bio-lubrication mechanism.
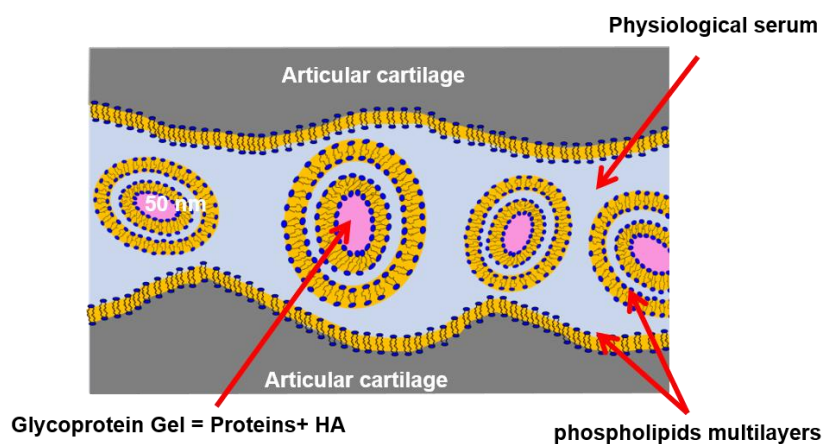
Figure A-11 Assemblages of different synovial fluid components (figure adapted from [93]*)*

The importance of phospholipids in the boundary lubrication of the synovial joint has been established, but is it also the case in the prosthetic joint? The answer is definitely yes.

In 2007, Gale gave proof of the importance of phospholipids in orthopaedic implants. The study aimed to characterise the SAPLs found on retrieved implants. Forty prostheses removed from hip and knee

revision operations were analysed using high-performance liquid chromatography. The analysis identified eight different species of phospholipids [97].

In this context and to continue the investigation on the role of SAPLs in joint bio-lubrication, a biochemical study of the molecular layers adsorbed on retrieved implants is performed and presented in chapter C.

4. The artificial joint: shoulder arthroplasty

4.1. Shoulder anatomy

The shoulder is a complex joint responsible for the articulation of the upper extremities with the trunk. It ensures the positioning and orientation of the hand in the space. Thus, it is a very mobile articulation. The shoulder is ultimately composed of a network of soft tissues overlying the skeleton. The bony anatomy involves three parts, as shown in figure 8 [98] [99]:

- The scapula, a flat, triangular bone is forming the posterior aspect of the shoulder girdle with 17 muscular attachments, with an anterior projection named the glenoid that forms half of the primary shoulder joint.
- The clavicle, or collarbone, serves as a strut connecting the upper extremity skeleton with the axial skeleton anteriorly and articulates with the sternum medially.
- The humerus is the long bone of the upper arm, with a proximal head articulating within the shoulder joint.

It satisfies three degrees of freedom: a sagittal flexion/extension, a frontal abduction/adduction and an internal/external rotation on the horizontal plane.

The shoulder mobility is ensured mainly by muscles and tendons. Superficially, the most prominent muscle is the deltoid, responsible for the contour of the shoulder. The primary function of the deltoid muscle is to abduct the arm, and it functions most efficiently at neutral rotation. As there are anterior and posterior segments, the deltoid also assists with arm flexion and extension.
Besides, the rotator cuff initiates the movement and has a stabilizing role of the head of the humerus. The rotator cuff is a complex structure composed of 4 muscles: anteriorly, the subscapularis, followed by the supraspinatus, infraspinatus, and most posteriorly, the teres minor. These muscles all originate from the scapula and insert at the humerus [98].
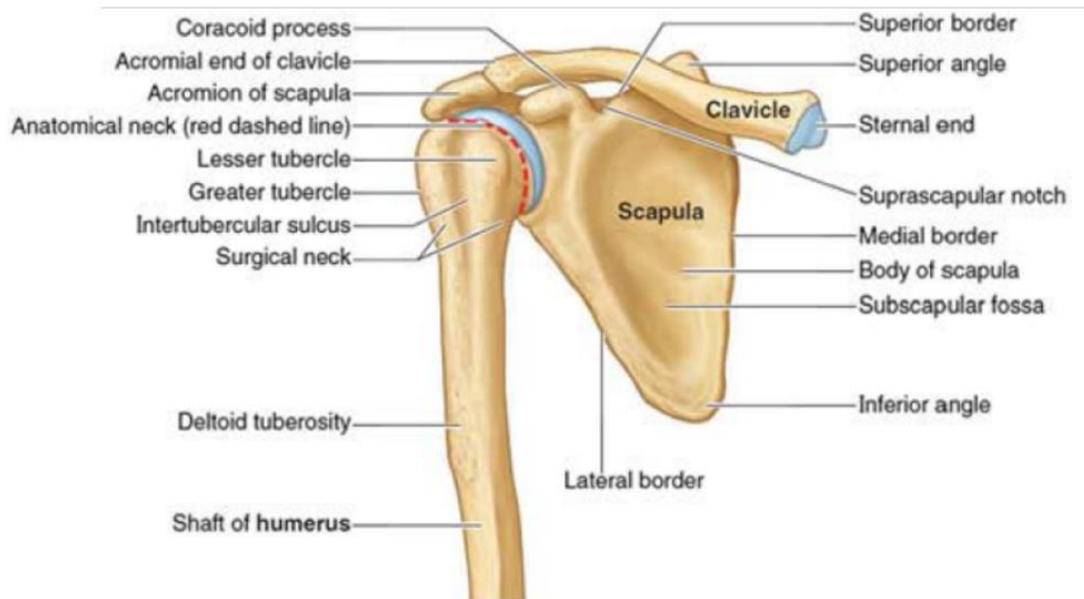
Figure A-12 bony anatomy of the shoulder [98]

4.2. Pathologies of the shoulder

4.2.1. Osteoarthritis is a major joint disease

The synovial joint is considered as a perfect tribological triplet. However, joint performance is modified and affected by joint diseases. They include rheumatoid arthritis, gout, spondyloarthropathies, synovitis and osteoarthritis, among others. In general, degenerative changes and superimposed inflammatory reactions lead to progressive destruction of the joints [100].

Osteoarthritis is the most common among joint diseases. It is an age-related disease that affected about 10 % of the world's population aged more than 60 years [1]. The osteoarthritis involves the whole joint and is associated with focal and progressive articular cartilage loss (figure 13). Soft-tissue structures in and around the joints, including synovial fluid, ligaments, and muscles are also involved [101]. The three main symptoms of the osteoarthritis are a pain, stiffness and a tendency for the affected joint to become immobile.

Osteoarthritis is mainly characterized by cartilage destruction, but in its later stages, bone destruction is included. It is not a disease of inflammatory origin. Still, certain inflammatory events can be observed in the joint as a secondary phenomenon and contribute actively to the maintenance of the disease. Osteoarthritis is the result of an imbalance between the physicochemical properties that give cartilage its resistance and the applied biomechanical forces [102].

Some theories lead to the result that osteoarthritis is not a disease. Still, a failure of the joint, seen as an organ, initially caused by mechanical factors and where the biological changes observed are the consequence. In this perspective, osteoarthritis is the final stage of this failure.

Over the years, the water content of the cartilage decreases as a result of reduced proteoglycan content, thus causing the cartilage to be less resilient. Without the protective effects of the proteoglycans, the collagen fibres from the cartilage can become susceptible to degradation. Inflammation of the surrounding joint capsule can occur as breakdown products from the cartilage are released into the synovial space. This process alters the synovial liquid and exposes the cartilage even more. Without the natural lubricant, the cartilage starts to wear out, exposing the bones. That's why the proposed treatments are often focused on the articular cartilage. However, repairing the articular cartilage remain a difficult task since it is a non-innervated and a non-vascular tissue.
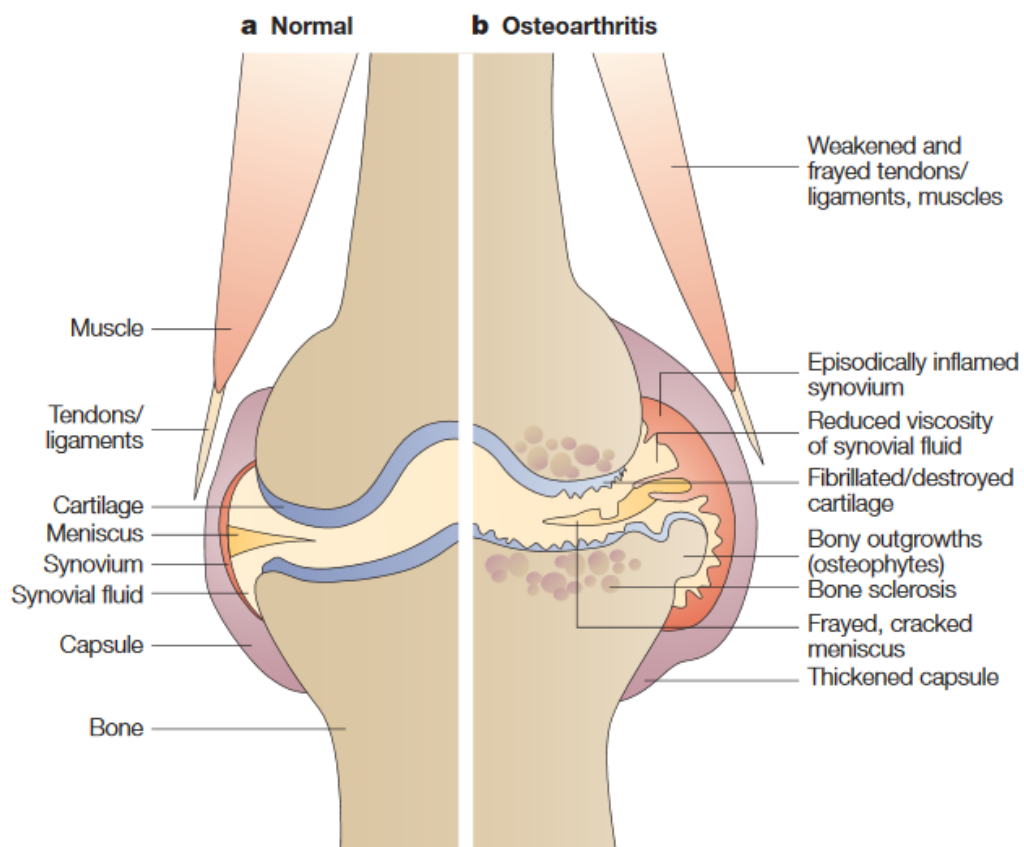
Figure A-13 Articular structures affected by osteoarthritis: a) the healthy synovial joint with normal cartilage, b) the altered joint with an early degenerate lesion of the cartilage [100]

4.2.2. Osteoarthritis in the shoulder joint

Several diseases and pathologies can degrade the bone and muscle structures of the shoulder joint. Clinically, the most common pathologies are osteoarthritis and rheumatoid arthritis [102] [103]. Glenohumeral osteoarthritis represents 50 % of shoulder pathologies. It is a degenerative pathology due to the premature and abnormal wear of the cartilage that covers the articular surfaces: the head of the humerus and the glenoid. As a result, the reduction of the cartilage thickness and the joint space, and therefore contact and friction of bone surfaces, which cause severe pain. Osteoarthritis of the shoulder results in pain with very variable intensity as well as a loss of function [99] [104].

There are two forms of glenohumeral osteoarthritis depending on its origin, primary osteoarthritis which is an initial disease of the cartilage and secondary osteoarthritis when the cartilage wear is caused by another cause, such as the rupture of the rotator cuff, the fracture and the infection.

Various treatments of glenohumeral osteoarthritis are proposed. Non-Surgical management is usually the first used to reduce pain. It includes the use of anti-inflammatories and physical therapy to maintain the shoulder function and to delay the aggravation of the disease [105] [106]. In some cases, and according to the emergency of the patient, surgical management could be considered. It consists of shoulder replacement, and it is used to restore comfort and glenohumeral function and to reproduce normal anatomy [103].

4.3. Treatments of the shoulder diseases: arthroplasty

4.3.1. Overview of osteoarthritis treatments

Several surgical techniques are used to restore the cartilage. However, they are still limited by the problematic implantation and the variability of the patients' response [6] [107] [108] [109] [110]. Among osteoarthritis solutions:

- Lubrication treatment: It is a medical technique consisting of injecting a viscous solution into the joint to lubricate, to absorb the mechanical stresses, to prevent the propagation of cartilage cracks, and to reduce inflammation.

- Traditional surgical treatment: It consists of performing micro-fractures in cartilage/bone junction to stimulate the activity of the stem cells of the subchondral bone. Stem cells could fill the cartilage lesions due to their capacity to regenerate tissue. This technique provides around 70 % of improvements but only for reduced injuries. This technique helps to generate fibrocartilage, which is biomechanically inferior to hyaline cartilage. Thus, the regenerated tissue may deteriorate after 18-24 months [111] [112].

- Surgical repair treatment: it consists of osteochondral transplantation or transplantation of autologous chondrocytes. This treatment is limited in clinical use. Indeed, allografts require donor selection and an efficient sampling system while autologous grafting is indicated for small lesions. The strategy aims to "fill cartilage wear" by stimulating proper cartilaginous extracellular matrix synthesis. Specific pathways of mechanotransduction may be activated by tissue bioengineering [46]. Research in this field is currently focused on the transfer of chondrocytes within support (natural or synthetic biomaterial, having a three-dimensional structure capable of stimulating tissue growth) before implantation to fill the cartilage lesion [46] [113] [114]. Two ways are possible in this approach either to generate entirely *in vitro* a

functional tissue or to implant an immature graft that continues to grow in the implantation environment [115] [46].

- <u>Alternative surgical treatment:</u> The replacement of the joint with a prosthesis (arthroplasty) is recognized as the only valid treatment of OA and to avoid joint immobilization in a long-term perspective. It consists of replacing the defective joint by an artificial one. The arthroplasty industry is a major economic issue: nearly 100,000 total hip prostheses and around 60,000 knee prostheses are implanted each year in France. The cost of osteoarthritis in France reaches more than 12 million euros per year [116]. Despite the success of arthroplasty treatment, some failures are noted for about 25 % of patients, who are not improved or aggravated after a total knee replacement. In addition, with the ageing of the population, approximately 13 % of arthroplasty patients worldwide are re-operated over the next ten years [4].

When the natural joint is affected by any articular problems, the perfect biotribological triplet is disturbed by the pathology. In the same manner, this tribological triplet is modified in case of arthroplasty, as any prosthesis changes the first bodies in contact. Total arthroplasty replaces them by two biomaterials. Hemiarthroplasty keeps a part of the natural first bodies and replaced the other part with the biomaterial of the prosthesis (in many cases metal rubbing against living cartilage). In both cases, the third body is also altered. It is either the synovial fluid with a modified structure due to the disease (inflammation…) or a mixture between the traces of synovial fluid with eventually wear particles of the prosthesis. Contrarily to the total- and hemiarthroplasty, interposition arthroplasty presents a specific contact configuration. Here the implant is in contact on both sides with living tissues.

4.3.2. Focus on shoulder arthroplasty

The first shoulder prosthesis appeared in the 19th century. Although less practised than hip and knee arthroplasty, this one has undergone a steady evolution, and many concepts have been proposed until reaching the current models. To adapt to the type of pathology encountered in the patient, the surgeon has several existing prostheses classified according to two types of arthroplasty. It is a total arthroplasty when the state of the patient allows the setting up of two implants. But sometimes the glenoid wear is too severe to accept an implant, so it is a hemiarthroplasty (Figure 14) [117].

There are two types of total shoulder arthroplasty:

- Total anatomic arthroplasty: it reproduces the normal shoulder anatomy. The prosthesis replaces both joint surfaces in contact by associating a humeral metal implant with a small concave cup glenoid implant made of polyethene. Depending on the model, the stem of the humeral implant is fixed with or without cement. This type of implant requires a functional

rotator cuff to ensure motor skills and articular stability. It could face a permanent subluxation and instability in the short term, which can reproduce in the long-term a loosening of the glenoid implant and loss of bone stock.

- Reverse total arthroplasty: it replaces the humerus with a concave tulip implant and the glenoid with a semi-sphere implant. The centre of the movements of the shoulder will no longer be the same as the regular anatomical centre. This prosthesis is indicated for patients whose cuff is non-functional, hence the interest in changing the centre of rotation of the shoulder. The main problem of this type of implant is the high infection rate compared to the anatomical arthroplasty [8].
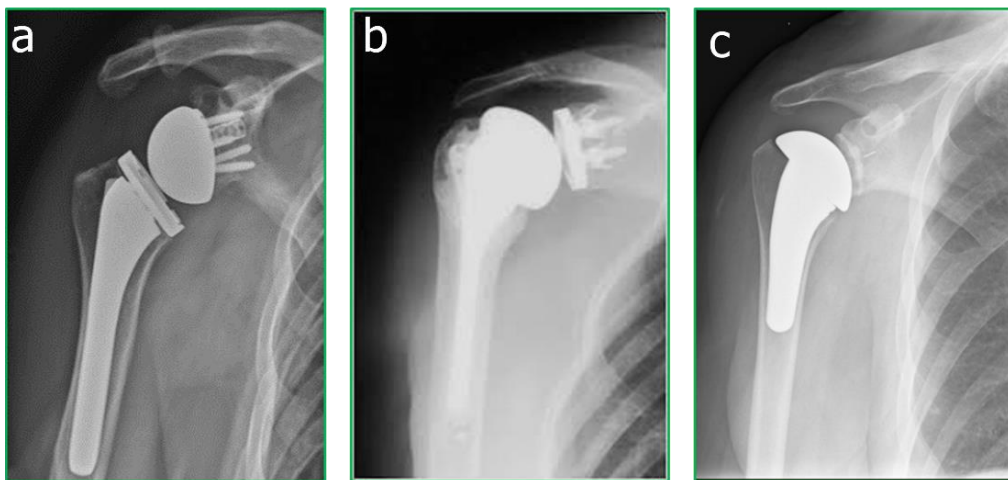
Figure A-14 X-rays of different used shoulder arthroplasty: a) total anatomic arthroplasty, b) Reverse total arthroplasty, c) hemiarthroplasty

In the case of hemiarthroplasty, the humeral part of the shoulder is replaced by either the humeral component of the total anatomic prosthesis or by a cap-shaped implant which is fixed by a very short stem. In both cases, the implant articulates directly against the cartilage of the glenoid. Therefore, hemiarthroplasty is only indicated for patients with a healthy glenoid. Its major risk is the progressive degradation of the cartilaginous or bony surface in contact with the implant [8] [117]. Briefly, depending on the state of the patient, the surgeon could choose among a diversity of available prostheses (figure 15). In some cases, a personalized prosthesis could be conceived to adapt to the specific conditions of the patient.

Figure A-15 Different types of used shoulder prosthesis (the figure is a commercial brochure of the available products of Wright Medical/Tornier)

Despite the successful results of these treatments, they present many complications [118]. Complications of failed shoulder arthroplasty include permanent, or activity-related pain, reduced range of motion, and instability [119]. Causes of pain include problems related to surgical technique, periprosthetic infection, component wear and loosening, rotator cuff degeneration and glenoid erosion.

Because of these inconveniences, a new generation of shoulder implants has been developed for the primary glenohumeral arthritis and patients with limited bone stock: interposition arthroplasty based on a free spherical implant [12] [120]. This new arthroplasty is designed by "Wright Medical / Tornier" and is called "INSPYRE". The implant, designed with a spherical shape, is inserted, without fixation, between the glenoid cartilage and the surgically created humeral metaphyseal cavity. Hence, the spherical implant replaces the anatomical humeral head [13]. The surgeon creates a cavity that reached the metaphysis of the humerus bone with suitable dimensions to place the implant. Then, he puts the implant in the shaped cavity without any fixation and finally, the implant replaces the humeral head as shown in the shoulder x-ray (figure 16).

Contrarily to the existed procedures, the design of this spherical implant is based on the absence of skeletal embedding, the implant mobility and the integrity of the tendons ensuring stabilisation.
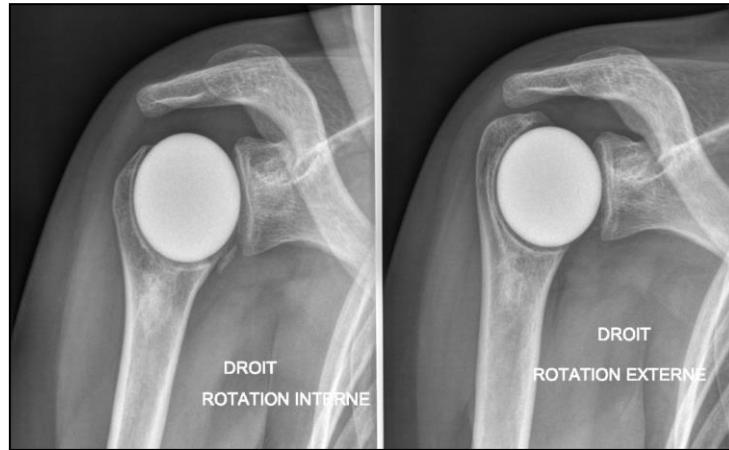
Figure A-16 PyC Humeral Head spacer after 15 months implantation: left internal rotation; right external rotation

Whereas CoCr is the most used biomaterial in shoulder arthroplasty, PyC is selected as the material for the interposition implants [12]. This biomaterial has excellent tissue biocompatibility and good wear properties, as detailed in the following chapter B [14] [15].

Furthermore, PyC tribological properties are different from metals. It can slide against bone and cartilage without causing pain or damage. Also, it has an elastic modulus similar to the elastic modulus of the bone [121] [122]. This type of non-fixed PyC implants has been successfully used as spacers in small joints for more than 20 years (figure 17), in particular, to fix fractures of the proximal pole of the scaphoid [18] but never used in the large joints.
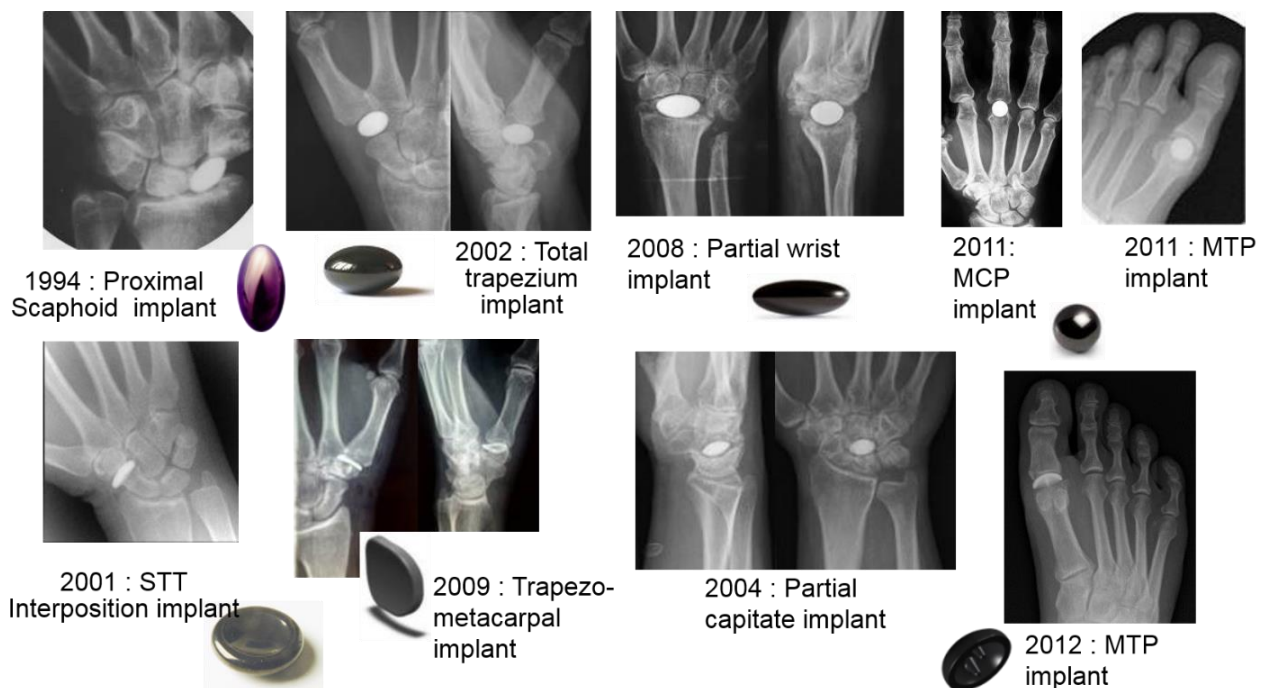
Figure A-17 Wright Medical/ Tornier's spacers for distal extremities since 1994

Amira HANNOUN/ Thesis in Biomechanics 2020/ INSA Lyon

Clinical results of this type of arthroplasty are very satisfying. We wondered if these promising results raised from the use of PyC as a biomaterial: What is the Pyrocarbon? What are its specific properties? What is its performance?

Chapter B

Properties and applications of the Pyrocarbon

B. Chapter B: Properties and applications of the Pyrocarbon

This chapter presents the history of the pyrocarbon from nuclear studies to the arthroplasty. Manufacturing methods, mechanical and biological properties, as well as typical applications, are described, showing that pyrocarbon is a promising material in the orthopaedic field. It presents different uses of the pyrocarbon in particular for shoulder arthroplasty: a newly developed implant is presented with its new concept and its promising results.

1. Pyrocarbon

Carbon is widely used in biomedical applications. It exists in several crystalline structures with different properties and different forms (fibres, composites, thin films). It is tolerated in the biological environment due to its non-toxicity [123]. Among the types of use of carbon, the pyrolytic carbon coating, which is called PyC.

1.1. History: From the nuclear industry to medical application

The first use of the PyC was in the 1960s in the nuclear industry. The main aim of this use was to develop a high-temperature gas-cooled reactor to generate electricity. In this context, researches were focused on finding and developing materials which could be used to coat uranium oxide, to be inserted inside the nuclear reactor.

A collaboration between the American nuclear research centre (General Atomics, San Diego) and the French one (Commissariat à l'Energie Atomique, Grenoble) was made to develop this material. They were focused on some properties as the resistance to the oxidation at high temperature, sealing properties, elasticity… The PyC alloyed with Silicon Carbide (SiC) was the chosen material which is obtained by a particular method of coating, (known as CVD coating: thermal Chemical Vapour Deposition) in a fluidized bed.

Later in the 1970s, PyC started its use in biomedical applications. Researchers from General Atomic with Dr Jack Brokos, and Dr Vincent Gott, a medical researcher at the University of Wisconsin, have tested the PyC in the vena cava of dogs. The results of this study were particularly promising in terms of biocompatibility and non-thrombogenicity [124]. Therefore, PyC implants were made for several biomedical applications.

A few years later, a new company was formed "CarboMedics™" and was specialized in heart valves. Since then, CarboMedics™ developed and manufactured components for all the heart valves, using silicon alloyed PyC (PyCSiC) as shown in figure 1. The satisfactory results of PyC in this application have continued to date; all mechanical heart valves have at least one component made of PyC.

Figure B-1 bileaflet mechanical heart valve made with PyC (figure taken from "FDA Expands Approval of Replacement Heart Valve | DAIC")

In the 1980s the PyC was used in the metacarpophalangeal (MCP) joint as the first use in the orthopaedic field. A MCP prosthesis was made in Mayo clinic by Ascension (Ascension, USA). This prosthesis presented a configuration PyC sliding against PyC (figure 2a) [125] [121]. Then later, in 1990, a scaphoid implant was made by Bioprofile (Bioprofile, Grenoble, France). This implant presents the first use of the PyC in a configuration PyC sliding against living tissue (figure 2b) [126] [18]. From then on, a whole range of hand, wrist and elbow implants were developed, and the use of PyC in the orthopaedic small bones field was extended [127].

From the nuclear industry to the arthroplasty, the PyC shows promising results. Thus, many questions around this biomaterial were raised: What is the composition of PyC? How is it made?
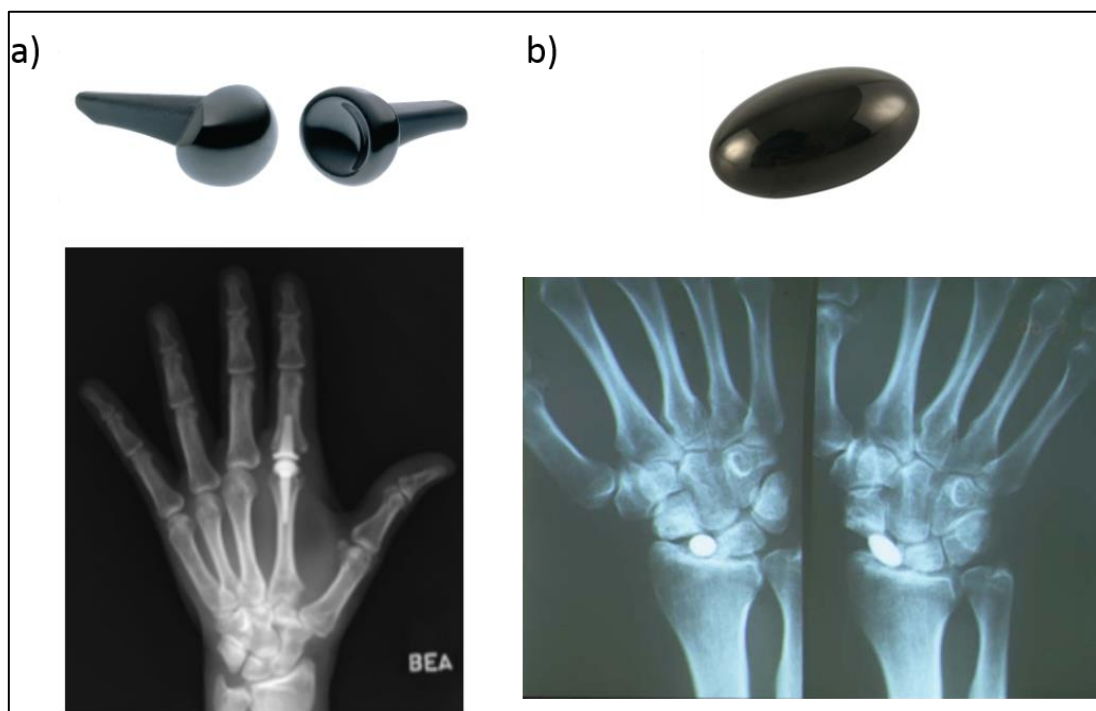
Figure B-2 First prosthesis made with pyrocarbon: a) picture of the PyC metacarpophalangeal prosthesis and its x-ray presenting the configuration PyC sliding against PyC b) Picture of the scaphoid implant made with PyC and its x-ray presenting the configuration PyC sliding against bone [128]

1.2. Pyrocarbon: the material structure and manufacturing

1.2.1. Material structure

PyC is a thin coating on a graphite substrate. The graphite is made of hexagonal arrays of organised Carbon atoms. These organized structures build layers, parallel one to the other. These planes can be long up to an mm. The weak bonding between graphite layers makes graphite material anisotropic and poor in mechanical resistance. Indeed, when submitted to loads, planes move relatively and liberate small debris: this property is used to make pencils: (graphein in the Greek language means writing).

Pyrocarbon structure is similar to graphite at the base, the Carbon atoms organize themselves in the same hexagonal structure, building planes and stacks of planes. But thanks to the shaking of the fluidized bed, the planes cannot grow, and the little stacks orientate randomly with respect to one another. This structure is called a turbostratic. So even if at the scale of the graphite stack, called crystallite, this individual crystallite is very anisotropic, when grouped together and randomly rearranged in aggregate, the crystallite anisotropy appears isotropic (figure 3) [129] [130].

Isotropy is an important parameter when coating substrates with complex shapes. Indeed, when coated with an anisotropic PyC, the complex-shaped substrate could undergo non-uniform dimensional changes during cooling (from 1400°C down to 20°C). These changes could destroy the coating or compromise its mechanical properties.
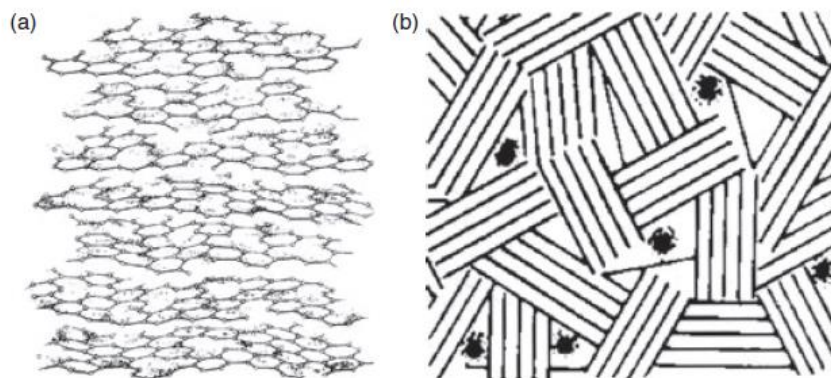
Figure B-3 Isotropic PyC structure [According to Bokros and al (1972)]. A) Turbostatic structure b) crystallite aggregate [129]

1.2.2. Pyrocarbon manufacturing

PyC is a Low-Temperature Isotropic (LTI) carbon coating made by thermal Chemical Vapour Deposition (CVD) in a fluidized bed [131]. It is a thin coating deposited on a graphite substrate. PyC coatings are investigated and studied for the nuclear industry as described previously. They were deposited at a high temperature from 1200 °C to over 3000 °C. The PyC used for biomedical applications was made at only 1500 °C that is why it is called LTI carbon.

PyC is generally a thin coating (up to a millimetre) deposited on a suitable substrate depending on the structure, the heat resistance, the surface topography (figure 4). PyC and the substrate must have a similar Thermal Expansion Coefficient (CTE); otherwise, CTE could limit the coating adherence to the substrate.

Investigations on PyC applications in heart valves and orthopaedic implants have shown that the only adequate substrate for the use of PyC in medical devices is the graphite [132]. Thus, only one type of graphite is used, which has a slightly higher CTE than the PyC.
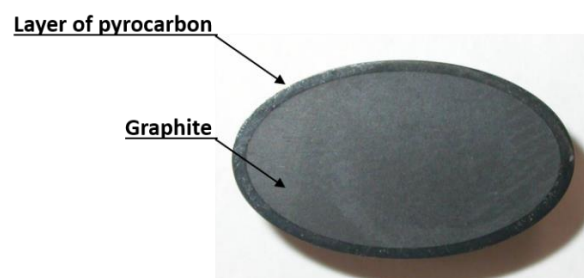
Figure B-4 A graphite substrate coated with pyrocarbon: the light grey core is graphite, and the dark thin film around is pyrocarbon

PyC is produced by the thermal (Pyrolysis) decomposition of a gaseous hydrocarbon (gas with carbon and hydrogen atoms such as propane) in a CVD process. At high temperature, and in the absence of oxygen, the hydrocarbon breaks down to free radicals, which then polymerize into a solid. The hydrogen atoms, detached from carbon, recombine into H_2 gas and are evacuated with a diluent gas (argon or nitrogen).

A fluidized bed is obtained by levitating a volume of particles through the action of a vertical gas flow introduced into a vertical tube from the bottom (figure 5).

The fluidized bed process is ideally suited for producing isotropic PyC. The formation of isotropic carbon structures from the thermal decomposition of a gaseous hydrocarbon (named the precursor gas) is generally thought to be due to the nucleation of planar macromolecules in the gas phase. These macromolecules become supersaturated and are then randomly (because of the fluidized bed) deposited on accessible surfaces, on the walls of the reactor, on the fluidizing particles and the preformed implant graphite substrates [133].

The fluidized bed technology was used to coat uranium oxide particles with carbon and/or other materials such as silicon. It provides a continuous, homogenous and random mixing of the particles that guarantees the isotropic nature of the coating deposited when using appropriate combinations of temperature, total gas flow, gas composition and bed surface area.

In the biomedical preparation of the PyC coating, the historical uranium particles have been replaced by inert, non-radioactive zirconium particles. These inert particles have the same role and provide the means to maintain a random motion of the substrates during coating. The medical implant is obtained after coating [133].
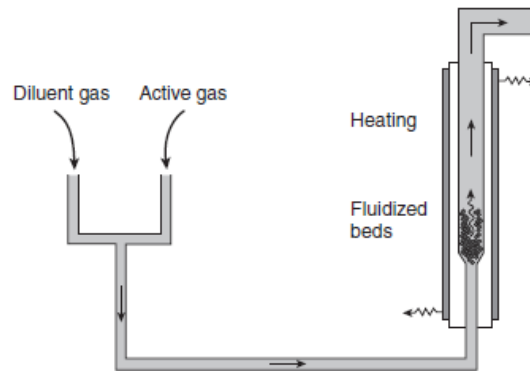
Figure B-5 Principle of particle fluidized bed coating system [129]

During the coating phase (around 3 hours), both particles and substrates are coated, so their surface area and their volume change dramatically. Competition occurs between the surface areas of the substrates. The original nuclear coating system was a batch process. For the long coating times required for biomedical PyC, batch processing has been modified. The new process pilots the injection of new uncoated particles and the withdrawal of coated particles during the coating to maintain the desired bed surface area. The precise control of injection and removal of particles is necessary to ensure the stability of the reaction parameters and thus, the quality of the deposited material (figure 6) [129] [132] [134].
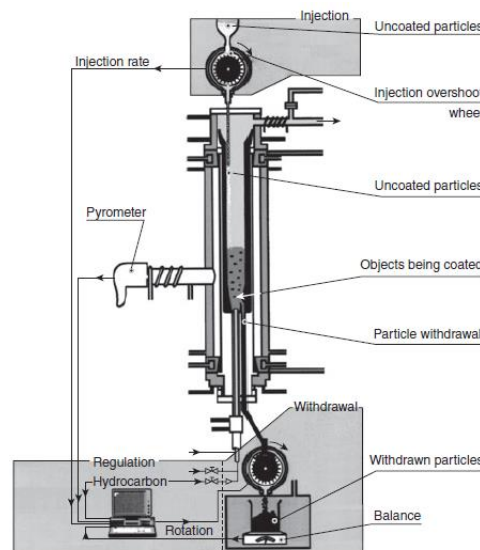
Figure B-6 Principle of particle fluidized bed coating system for biomedical application [127]

A significant drawback of this coating batch is that only a limited number of substrates can be coated in the same batch. This number is affected not only by the size, shape and weight of the substrates but also by the inside diameter of the coater. The typical coaters in use have an inside diameter around 13 centimetres which allows coating 20 heart valve housings or 100 heart valve leaflets in a coating batch. This size could allow only the coating of 4 or 5 hip or shoulder balls at one time. Thus, the cost for coating larger substrates is much higher than the price of heart valve housings coating. Besides, this coating process takes much time. One coating cycle includes a heating phase, a cooling phase and a cleaning and reconditioning phase. Thus, a total of 7 to 9 hours is required to coat only a few large parts!

Since the PyC is not visible by X-rays and is radio-lucent, a radiograph of the PyC coated prosthesis shows only the "substrate" of the prosthesis, which appears smaller than the actual size.
The manufacturing of PyC implant is a long process with four essential steps simplified schematically in figure 7 [132].

- A graphite substrate is machined to the dimensions of the final implant minus the coating thickness. As the coating thickness cannot be predicted, several iterations are performed during the development of the implant to determine the optimal dimensions of the substrate that provides the exact final dimensions after coating. These iterations are necessary to avoid PyC re-machining after coating, which is an expensive process. PyC is only machined with expensive technologies like grinding with diamond tools. When perfect dimensions of the substrate are defined, and when the coating process is mastered, the perfect repeatability from batch to batch provides PyC parts very similar in dimensions, ready to be polished.
- Polishing of the graphite substrates
- Coating of the polished substrates with the CVD process
- Polishing the coated parts to obtain the final medical implant
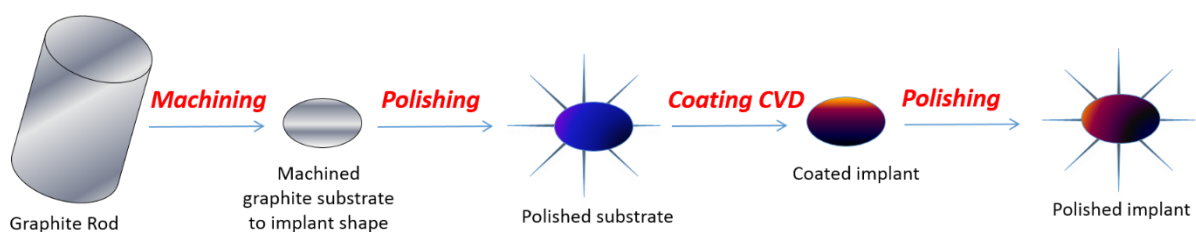
Figure B-7 Schematic of PyC orthopaedic implants manufacturing processing steps

1.3. Different properties of the PyC

1.3.1. Biocompatibility

PyC is well known for its non-toxicity, its biocompatibility and its hemocompatibility. Its extended use on heart valves since 1970, or in contact with cortical bone since 1980 or sliding against tissues since 1990 proved these key features.

Artificial heart valves are the most demanding application for a biomaterial. It must be inert regarding the blood and be able to withstand millions of cycles without degradation, significant wear or fatigue failure.

Over the last thirty years, PyC has been widely used for this application. Thus more than three million heart valves made with PyC were implanted [121]. Many studies have already investigated and proved the compatibility of PyC with blood, tissue and bone [124] [131] [135]. The reason for the PyC hemocompatibility is still under investigations. However, some studies suggested that blood proteins may be adsorbed on PyC surfaces so that cells are unaltered in contact with this protein film [122] [137] [138].

Many other studies tested the PyC in the *in vivo* environment, presenting either clinical studies or animal investigations. Among these studies, Kawalec and colleagues showed that in an adult beagle model, the contact between PyC and full-thickness cartilage defects promotes the neo-synthesis of a cartilage-like tissue [122]. Also, there is more tissue regeneration when using PyC implants than other biomaterials.

1.3.2. Mechanical properties

The isotropic PyC deposited in fluidized beds is the strongest. However, for cardiovascular surgery, in addition to the strength, wear resistance is also an important parameter. Therefore, the wear resistance was improved by the addition of silicon carbide. This improvement was followed by a loss of hemocompatibility and little increase in Young modulus. This process was not needed for orthopaedic application, where the number of cycles is much lower. Consequently, pure PyC has been used in orthopaedics since the late 1980s [132].

1.3.2.1. Elasticity

In orthopaedic application, the implant transmits directly loads to the bone. Therefore, its elasticity is a major criterion. Of interest, PyC has an elastic modulus similar to the elastic modulus of the bone (Table 1). Thus, it transmits loads with the same behaviour as the natural bone without generating stress shielding, bone resorption or pain caused by more rigid materials such as metals (titanium for instance) or ceramics.

Table B-1 Comparison of the elasticity and the density of various materials used in orthopaedic prosthesis [129] [127]

	Bone	Silicon	Polythene	Graphite	PyC	Titanium alloy	CoCr alloy
Elasticity (GPa)	15 to 20	0,004	0,2 to 0,7	11	25 to 30	110	200-240
Density	2,0	1,1	0,9 – 1,1	1.78	1,7 – 2,0	4,5	8,3 – 9,2

In the study of Hassler [129], a finite element analysis simulation was presented. It reported the configuration of bone compression against spherical implant made of various materials. This simulation showed that in the case of ceramic, the bone is overstressed and in the case of polythene, the bone is under-stressed. Furthermore, the overstressed parts (bone, polythene) face the risk of creep and wear. However, since the elastic modulus of PyC and bone are similar, stresses are equally shared.

The mechanical properties of PyC implants are a blend of the properties of the graphite and those of the PyC. Thus, the elastic modulus of each implant depends on the proportion of graphite/PyC. For instance, implant as the trapeziometacarpal implant having in its structure more PyC than graphite has an elasticity approaching of the one of PyC.

1.3.2.2. Resistance in compression and flexion

Despite the excellent biomechanical properties of PyC, which make it an ideal biomaterial for joint replacement, it presents some limitations. As a bearing surface, it can be assimilated to a ceramic with the same restrictions. PyC is a relatively brittle material with low flexural stress compared to metals. Thus, the use of PyC in implants with a shear stress of loaded in flexion is risky and could cause implant fracture. However, the compression resistance of PyC is exceptionally high. Therefore, it is widely used in implant only loaded in compression (hand, wrist…). It is also possible to overpass this limitation by fixing the PyC component on a metal back that supports the load (in shoulder hemiarthroplasty) [129] [135] [139].

1.3.2.3. Wear characteristics

For biomedical applications, PyC is polished to an extremely fine level [140]. The measured surface roughness is around 0.03 µm. This very fine polishing, coupled with a very low friction coefficient, results in impressive little wear results.

PyC wears very little or insignificantly when sliding against itself or a few other materials. Historically, the heart valve application was the most demanding, requiring non-wearable materials. Numerous studies have been performed on heart valve models, showing that the best couple is PyCSiC against PyCSiC (Silicon-Alloyed Pyrolytic Carbon).

The PyCSiC against PyCSiC wears about twenty times less than PyCSiC against metal (titanium or CoCr) [141]. It has been reported that standard valves featuring the PyCSiC/PyCSiC couple, wear less than 1 µm per year (at 40 million cycles/year) as determined by accelerated testing. These laboratory results have been confirmed by patients living with these valves for more than 30 years. Thus PyC can be considered a "nearly non-wearable material" [135] [142]. In the orthopaedic field, the pure PyC against pure PyC couple has been used as a MCP prosthesis for more than 20 years with no wear reported [121]. Using the same couple, an interphalangeal hinged prosthesis was tested *in vitro* under loads that could be expected clinically. Less than 1 µm of wear after 60 million cycles was observed [129] [132] [143]. It is estimated that such prosthesis would experience only 5 million cycles in an average lifetime.

2. Pyrocarbon in arthroplasty

2.1. PyC behaviour in the *in vivo* environment

2.1.1. In the configuration of PyC sliding against PyC

While the superior biocompatibility and exceptional properties of PyC over other materials were demonstrated in cardiovascular application, PyC was not evaluated for orthopaedic applications until the 1980s. As only small components could be coated at that time and because of its low load-carrying capacity, PyC was firstly used for the distal extremities in small prostheses subjected to low loads, such as MCP prosthesis (figure 2a).

Arthroplasty of the MCP joint had been treated for decades using flexible silicone rubber interposition spacers. Silicone rubber implants are effective in reducing joint pain but less effective in re-establishing functional joint motion, functional pinch and grip strength [144]. Then, a PyC MCP prosthesis was developed by Dr Cook in collaboration with Dr Beckenbaugh in the early 1980s.

Even though the design was relatively conventional (stemmed, bi-component), it was the first time PyC stems were introduced into the medullary canal of a long bone without cement and subsequent loosening. Results published in 1999 on a retrospective study on 71 prostheses having around 12 years mean follow-up confirmed that PyC is an appropriate material for this application.

However, the PyC MCP prosthesis and the PyC interphalangeal joint prosthesis faced some limitation concerning the osseointegration or non-integration of the implant by the bone [121]. Indeed, PyC stem surface is insufficiently porous and adequate to allow invasion by bone (osseointegration), so that it does not provide stable anchorage for the prosthesis. The suitable porosity for bone integrity is around 50 to 100 microns, which is similar to the porosity of titanium (approximately 200 microns).

In contrast, PyC surface promotes good "bone-apposition" (no fibrous tissue capsule forms between bone and PyC) which is confirmed by the fact that no load is required to pull out a PyC stem [145]

[146]. Due to this, PyC MCP prosthesis could face some failure caused by the poor fit with the anatomy or the poor positioning [145] [147] [148].

2.1.2. In the configuration of PyC sliding against living tissues

As shown previously, the stemmed PyC had excellent results on long term follow-up. However, with this configuration, the PyC mechanical properties, in particular, its elasticity (similar to the bone) were not exploited. Next, the sliding against living tissue without causing wear was tested. Therefore, a first non-stemmed, non-fixed and a free-floating PyC spacer was developed. It is the partial scaphoid implant (APSI) introduced in 1994 by Pequignot [149] (figure 2b). It replaces the necrotic proximal pole of the scaphoid and is stabilized by the surrounding tissues, bones and ligaments.

This implant restores the natural biomechanics of the joint and fills the space created by the shrinkage of the necrosed bone. PyC excellent surface quality and its performance providing low wear allowed a long-term direct bone-implant contact, without degradation of the implant or surrounding bones and tissues. It also permitted free movement in the inter-osseous free space without adhesion or luxation. No luxation, no wear, no bone erosion and no subsidence of the implant were attested by clinical results reported at 12 years mean follow-up [126] [150] [151].

Gale and colleagues had the idea to investigate the role of the natural lubricant of the joint in implant performances. They tested the interaction between the surface-active phospholipids (SAPL) with PyC. Comparative friction measurements were made using a synthetic SAPL. Friction was reduced by more than 75 % for the polythene/PyC combination, suggesting that phospholipids act as an effective boundary lubricant. This study highlighted the importance of the lubricant and suggested that SAPLs could decrease friction in PyC prosthetic joints [97].

2.2. PyC versus other biomaterials

Over the years and with more than 3 million implanted heart valves, the PyC showed excellent performances. In the orthopaedic field, many other biomaterials are used with promising results. Therefore, researchers were interested in comparing the PyC with other biomaterials.

From 1980, many animal models studies were performed to test the *in vivo* environment. In 1989, Cook and colleagues compared the cartilage degeneration in 45 canine acetabula after implantation of prostheses made with three different biomaterials: PyC, CoCr and titanium for periods from 2 weeks to 18 months. This study showed that cartilage articulating against PyC had lower levels of wear [14]. A few years later, Kawalec and colleagues adapted the same animal model in the knee joint to compare PyC and CoCr. They showed that the contact between PyC and full-thickness cartilage defects, which

continue to the level of the metaphysis, promotes the neo-synthesis of a cartilage-like tissue. Besides, there is more tissue regeneration when using PyC implants than CoCr implants [122].

Later in 2016, the canine model was used again to evaluate the *in vivo* histologic response of PyC and CoCr implants replacing a full-thickness osteochondral defect in the medial femoral condyle of the knee for 52 weeks. Again, this study demonstrated adequate implant fixation and superior *in vivo* response of PyC compared to the CoCr [152]. In addition to the canine model, other models were used. In 2008, a study evaluated the cartilage wear of the tibial plateau after hemiarthroplasty with proximal interphalangeal prostheses in 27 rabbits for three months. The cartilage was histomorphologically examined to compare three different materials: CoCr, PyC, and ceramic. This study indicated less cartilage surface damage in the CoCr group as compared with the ceramic group (p < 0.03).
In contrast, no differences were found between PyC and CoCr or PyC and Ceramic [153]. As already mentioned, titanium implants are mechanically more stable and provide better osseointegration than PyC implants, as shown in another rabbit model [145].

Ex vivo methods were also used to compare PyC to other biomaterials. In the context of scaphoid trapezium joint treatment, PyC implants were compared to zirconia, unalloyed titanium and CoCr. The implants were subjected to wear testing in a joint-motion simulator after articulation against bovine cortical bone. PyC exhibited exceptional performance compared to the other tested materials: bone wear was reduced with an absence of macroscopic material removal. This result is related to the lower elastic modulus of the PyC [154]. Others used a model based on living tissue to investigate the biological response of cartilage articulating against PyC in comparison to CoCr. In this study, the tribological wear behaviour of PyC and CoCr were comparable [155]

In the same context, a few more studies were also performed in the context of the dental application, comparing PyC to ceramic. In 1981, a finite element stress analysis demonstrated that PyC allows a better distribution of the stresses around the implant [156]. However, the implant surface composition and its elastic modulus may have a little apparent effect on the implant performance [157].
Finally, in a clinical survey of Luedemann, mechanisms of direct biological attachment of implants to bone were examined using femoral intramedullary implants made either of PyC or CoCr.
A detailed radiographic examination revealed that all implant systems caused significant remodelling of the femurs. The PyC implants were associated with a higher incidence of fibrous tissue encasement in the proximal cancellous bone region [158].

PyC was widely used for heart valves and small joints replacements. For both applications, it showed excellent performances, and, in many cases, it was more favourable than other biomaterials. In this context, its use was expanded to large joint replacements particularly in shoulder arthroplasty. What

are the different shoulder prostheses? Does PyC keep the same performances in shoulder replacement as it is the case in small joint replacements?

3. Study of retrieved PyC interposition shoulder implants Inspyre: primary results and research hypothesis of this thesis

Clinical evaluations, radiographic outcomes and implant survival of PyC interposition shoulder arthroplasty are assessed at the 2-year follow-up by Garret et al. (2017) and Hudek et al. (2017). Both studies reveal satisfactory clinical results comparable to those of hemiarthroplasty but still inferior to those of total shoulder arthroplasty. Radiographic outcomes suggest that PyC induces minimal bone and cartilage wear and excellent bone remodelling in contact with the implant [12] [16] [159]. Furthermore, in a 5-year follow-up on the glenoid side, no significant erosion was observed with the interposition implant, which seems to confirm the interest of PyC to preserve bone surface as compared to conventional metal Hemi-shoulder arthroplasty.

Until 2018, the interposition implant has been used for different indications. Figure 8 illustrated the various indications for 250 cases.
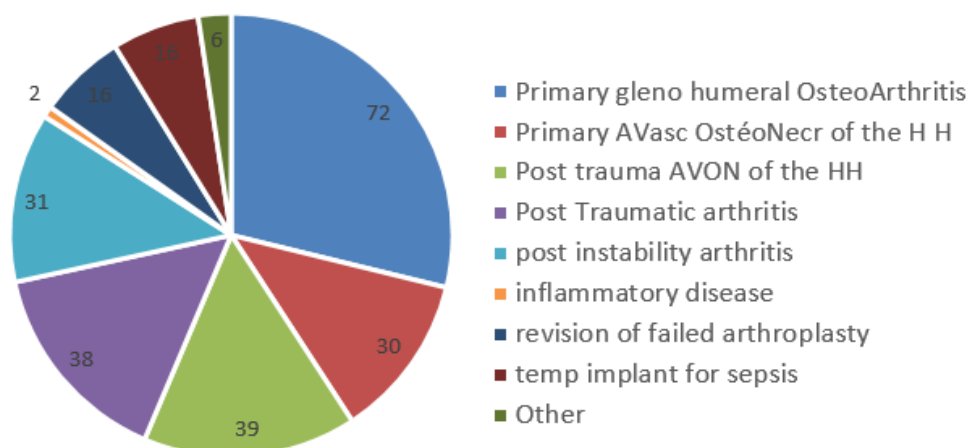
Figure B-8 Different indications for the shoulder interposition prosthesis

Mostly, PyC spherical implants can be used for shoulder arthroplasty either in patients with a variety of osteoarthritic morphologies, where the glenoid cartilage surface is already damaged or in patients with a healthy glenoid. In both cases, glenoid wear is of importance because it may result in pain and functional loss leading to deterioration over time. Thus, the capacity of the implant to preserve cartilage integrity or, at least, to prevent more cartilage degeneration is a source of concern.

A PyC spherical implant also faces the humerus. To insert the shoulder interposition implant, the surgeon creates a cavity in the humeral bone that reaches the metaphyseal zone. This zone contains the mesenchymal stem cells, which promote healing and regeneration, and the growth plate cartilage cells in young patients.

In an ongoing study on human explants, a neosynthesized tissue at the extremity of the humeral metaphyseal cavity in contact with PyC implant is observed. Histological analysis suggests that this new tissue has cartilage-like characteristics (unpublished data from Ghassen Ouenzerfi thesis: Analyse des performances tribologiques du matériau Pyrocarbone dans les applications d'arthroplastie orthopédique). This result is confirmed by the presence of glycosaminoglycans in Safranin O staining and the presence of type II collagen and aggrecan in histological immunolabelling (markers of a cartilaginous tissue) (figure 9). In this study, few analyses were performed using microscopy, environmental scanning electron microscopy and histology [17].

Similarly, Kawalec et al. (1998) showed in an adult beagle model that the contact between PyC and full-thickness cartilage defects, which continue to the level of the metaphysis, promotes the neo-synthesis of a cartilage-like tissue. In the case of spherical implants for shoulder arthroplasty, self-regeneration of the tissue at the site where the humeral bone is machined may be the determinant for clinical outcomes, if only to avoid bone wear. Also, cells behaviour may be affected by the biological and biochemical environment, but also by cell-biomaterial interaction and mechanical solicitations [160]. Thus, surface properties such as micro-roughness and nanostructures can directly affect cell behaviour [161]. Also, since skeletal cells are mechanosensitive, they could react to the tribological stress caused by the non-fixed prosthesis and its spherical shape.
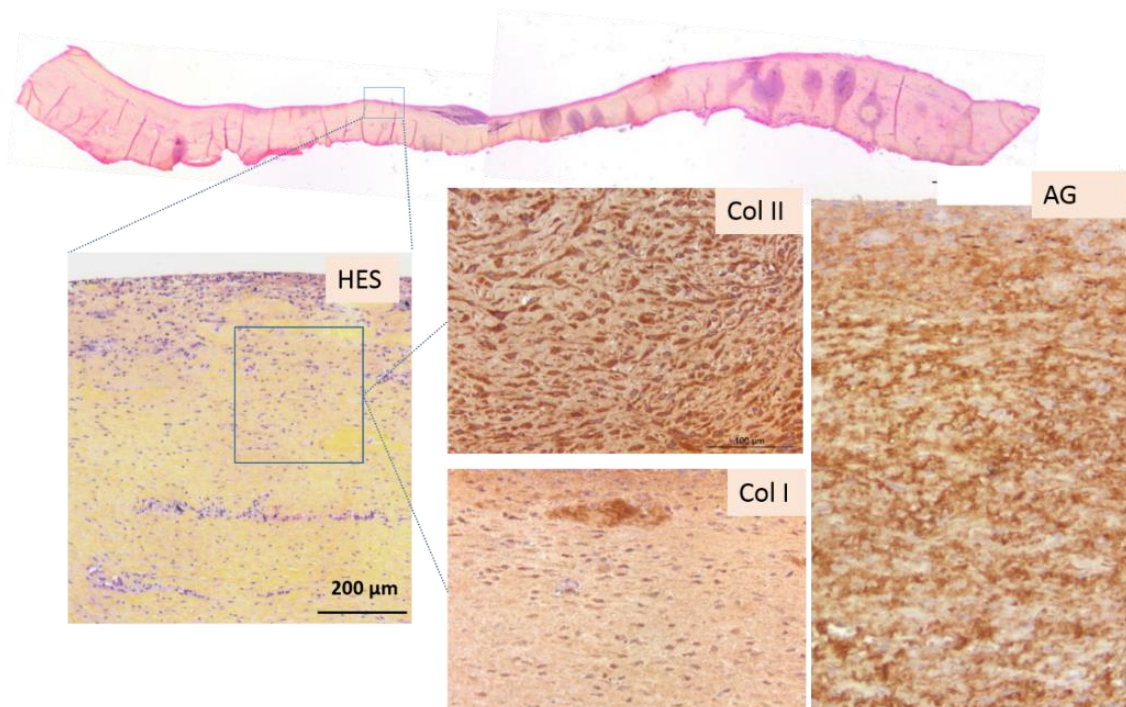
Figure B-9 Matrix biological components of the extracted membrane. Immunolabelling for type I collagen, type II collagen and aggrecan was performed to identify the different elements (Aggrecan presence: Characteristic of articular cartilage)

Amira HANNOUN/ Thesis in Biomechanics 2020/ INSA Lyon

Briefly, many studies showed the different particularities and properties of PyC in the orthopaedic field. Besides, preliminary studies showed a tendency of PyC to favour cartilage-like tissue neo-synthesis. Notably, in the context of shoulder interposition implant, PyC provides minimal bone and cartilage wear and excellent bone remodelling. However, the origin of these results is not yet well understood. Therefore, we are interested to understand and investigate the effect of the biomaterial on the neocartilaginous tissue creation.

Therefore, in this thesis, the PyC is compared to the CoCr, the most used biomaterial in shoulder arthroplasty, regarding the preservation and regeneration of the surrounding tissues. Two significant steps are followed:

1) To carry out three parallel studies to dissociate the role of the biology (cellular response) of the material (PyC vs CoCr) and the transmission of mechanical stresses.
2) To validate the results thus obtained by associating the different aspects in an *in vitro* model based on tissue bioengineering principles.

Understanding the proper functioning of the pyrocarbon: *in vivo* biotribological triplet

C. Chapter C: Understanding the proper functioning of the pyrocarbon: *in vivo* biotribological triplet

We aimed to understand and investigate the effect of PyC biomaterial in the human body. In the context of shoulder surgical replacement, both hemi-prostheses and spherical interposition implant have been developed using PyC [162]. In the case of hemi-prosthesis, the implant articulates directly against the glenoid cartilage, whereas an interposition implant is rubbing against the glenoid cartilage and humeral bone cavity.

In this section, a retrieval analysis for shoulder hemi-prostheses is performed. The hemi-prostheses were selected because they provide a configuration allowing to compare the two biomaterials PyC and CoCr (spherical implants are systematically made with PyC). In addition, clinical studies for shoulder interposition implants showed results similar to shoulder hemi-prostheses [12] [16]. The role of the biomaterial in the bio-lubrication of the joint and its effect on the surrounding tissues are mainly evaluated.

1. Introduction and retrieval analysis background

As already mentioned (Chapter A), glenohumeral osteoarthritis is the most common disease of the shoulder joint, representing 50 % of shoulder pathologies [103]. Premature wear of the cartilaginous surfaces in contact is initially caused by mechanical factors and the biological changes observed are the consequence. Shoulder osteoarthritis results in variable intensity pain and a loss of function [99] [159] [163].

Non-surgical management is usually the first used to reduce pain. However, surgical management (arthroplasty) is considered in some cases, according to the emergency of the patient [103]. Two types of shoulder arthroplasty are used: a total arthroplasty when the state of the patient allows the setting up of two implants and a hemiarthroplasty when the glenoid wear is too severe to accept an implant [117].

This part of the project focused on the hemiarthroplasty type. In this case, the humeral component of the shoulder is replaced by a cap-shaped implant which is fixed by a very short stem. Thus, the implant made either of PyC or CoCr articulates directly against the glenoid cartilage.

Despite the successful results of hemiarthroplasty, it presents many complications, particularly the progressive degradation of the cartilaginous or bony surface in contact with the implant [118] [119]. Consequently, it is revised to total shoulder replacement. Thus, it is possible to obtain retrieved hemi-prostheses of these patients.

Retrieval analysis has long served the orthopaedic community as a tool for understanding implant failure modes. However, what retrieval studies can reveal about the *in vivo* effect of the implant

material on the surrounding tissue remains unknown. In this chapter, we perform a retrieval analysis of shoulder hemi-prostheses made either of PyC or CoCr. This analysis could provide answers regarding the biomaterial effect on cartilage wear and joint lubrication.

As elaborated in chapter A, many studies have already compared different biomaterials articulating against cartilage. In addition to cartilage wear, it is essential to analyse the remodelling of the tissues surrounding the implant. Consequently, for the retrieval analysis, we also collect any tissues around the implant (considered as surgical waste) for histological analysis.

We hypothesize that the key to the implant performance in hemiarthroplasty is its interaction with the biological molecules of synovial liquid, particularly the multilayer phospholipids. Our hypothesis is based on the study of Gale and colleagues. They proved the ability of phospholipids to decrease friction in prosthetic joints by acting as a boundary lubricant and demonstrated the existence of phospholipids on biomaterials surfaces, including PyC [97]. However, PyC was not studied in the configuration of shoulder replacement nor in comparison with the CoCr. As suggested in the same study, the interaction between phospholipids and PyC needs further analysis. Therefore, in addition to the histological examination of the removed surrounding tissues, we extracted the adsorbed molecular layer on the surface of the retrieved implants for lipidomic analysis.

2. Materials and methods

2.1. Specimens

This retrieval analysis was performed in collaboration with orthopaedic surgeons in different hospitals in France and Germany.

All the specimens were provided from revision surgeries of shoulder hemiarthroplasty to total arthroplasty. No specific criterion was selected to include the patients. The retrieval analysis included humeral head prostheses and resurfacing humeral head prosthesis.

This study prospectively included four patients who underwent shoulder hemiarthroplasty using either PyC or CoCr humeral head prosthesis, from December 2015 to Mai 2018. The different implants were revised for various reasons by different surgeons. Two explants are made of PyC, and two explants are made of CoCr.

Three prostheses are manufactured by Wright medical/ Tornier SAS (Montbonnot Saint-Martin, France), and one prosthesis is made by FH ortho (Heimsbrunn, France).

The retrieval study included two women (50 %) and two men (50 %) aged 59.5 ± 8.81 years. Revision surgeries were performed on the right shoulders.

Since the retrieval analysis concerned surgical trash (explant, removed tissues to place the new implant) and is not a clinical trial, some details concerning the patients' cases were not provided. The information was collected from the notes taken during the surgery and from the "complaint investigations and closure" provided by Wright Medical.

Table 1 below summarized the patient information and the details of the retrieved PyC/CoCr prostheses.

Table C-1 Summary of clinical details of the patients and retrieved implants

Case	Date of the surgery	Gender + Age (years)	Lifespan (months)	Type of the implant	Reason for revision	Surgeon
A	12/2015	M 64	10	**Aequalis™ PyC humeral head Ø 48-18** (Wright medical/ Tornier)	Overstuffed prosthesis	Surgeon 1
B	12/2016	M 60	21	**Arrow CoCr humeral head Ø 50-19** (FH orthopaedics)	Misplaced prosthesis	Surgeon 2
C	01/2017	F 67	15	**Aequalis™ PyC humeral head Ø 46-17** (Wright medical/ Tornier)	Lateralized stem	Surgeon 3
D	01/2017	F 47	96	**CoCr resurfacing head Ø 43-16** (Wright medical/ Tornier)	Glenoid erosion	Surgeon 1

2.2.   Procedures

As mentioned above, in this retrieval analysis, we focused on the physicochemical properties of the biomaterials and the effect of the prosthesis on the different surrounding tissues. Therefore, lipidomic and histological examinations were performed.

2.2.1. Lipidomic analysis

2.2.1.1.   Lipid extraction and standards

This analysis aims to identify the lipidic molecules adsorbed on the surface of the biomaterials. Immediately after the surgery, the surface of the explant is washed with saline solution to remove the traces of blood. Then, it is washed with 8 ml of ethanol and chloroform (1:2, v:v) to extract the lipids. The explant A is washed once, but the other explants are washed twice (the second wash is added to make sure that all the adsorbed molecules are extracted). The solution is then conserved in -20 °C until analysis.

The glass tubes used for the assay are specific and resistant to the chloroform. The samples are then vortexed, and the solvent is evaporated under dry nitrogen at room temperature. After total evaporation, 100 µL of the same solvent is added to the tubes and vortexed. The fraction obtained is called the total amount of lipids (TL) afterwards.

Seven internal lipid standards are purchased from Avanti Polar Lipids. They are added in each sample with the following concentrations: sterol esters (ES) (1 µg/µL), triglycerides (TG) (5 mg/mL), phosphatidylcholine (PC) (2 mg/mL), phosphatidylethanolamine (PE) (2 µg/µL), phosphatidylserine (PS) (2 µg/µL), sphingomyelin (Sph) (10 mg/mL), and stigmasterol (5 µg/µL). They are made of heptadecanoic acids (or margaric acids, 17:0) because these fatty acids are only present in trace amounts in animal fats [164].

2.2.1.2. Separation of lipid classes by thin-layer chromatography

90 µL are sampled from the TL fraction and deposited on a thin-layer chromatography plate TLC Silica gel 60 F254 (Merck) with standards for ES, TG, and stigmasterol. The migration solvent is a mixture of n-hexane, diethyl ether and acetic acid (80:25:1, v:v:v). The migration lasts about 90 minutes. Then, the plate is dried under dry nitrogen, and the migration zone of the standards is revealed.
After protection of the migration zone of the samples by aluminium foil, the standards zone is sprayed by 0.02 % dichlorofluorescein and dried under nitrogen. The migration spots are visualized under a UV lamp at 254 nm.

Migration spots of the samples are identified by comparison with the standards. These spots are delineated with a pencil and scraped (figure 1). The phospholipids powder is collected in different new glass tubes and extracted using 2 mL of toluene/methanol (1:2, v:v). The tube is then vortexed and centrifuged 5 min at 2000 RPM. The upper phase of the solution is recovered in a new glass tube. The same procedure is repeated three times. The final solution is evaporated under dry nitrogen.
After total evaporation, 100 µL of toluene/methanol (1:1, v:v) is added to the tube and vortexed. The fraction obtained is called the total amount of phospholipids (TPL) afterwards.
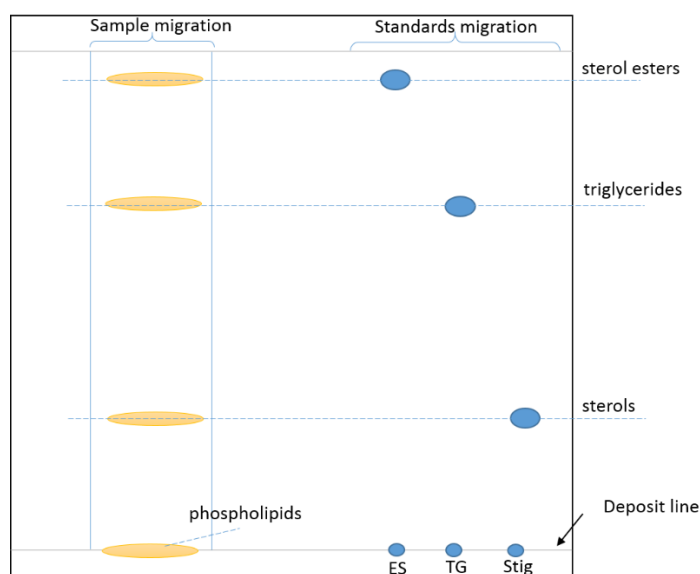
Figure C-1 Reveal of the different standard in the first thin-layer chromatography plate

2.2.1.3. Analysis by gas chromatography (GC)

The resting 10 µL of the TL and TPL fractions are prepared for GC analysis: the solvent is evaporated, and 500 µL of toluene/methanol (1:1, v:v) are added. The tubes are stocked at 4°C until gas chromatography (GC). 500 µL of 14 % of boron-trifluoride (BF3)/ methanol mixture and 500 µL of a mixture of toluene/methanol (1:1, v:v) are added to the samples. Then, the tubes are vortexed and heated at 100 °C for 90 minutes (except for ES and TG tubes, which are heated for 60 minutes) to perform the transesterification of fatty acids. The transesterification separates the fatty acids from their lipid heads. The reaction is stopped by immersing the tubes in ice and adding 1.5 mL of potassium carbonate (K_2CO_3).

The fatty acids are extracted using 2 mL of isooctane. The tubes are then vortexed and centrifuged 5 min at 2000 rpm at 25 °C to obtain a tri-phasic separation. The upper organic phase of each sample solution is recovered in a new glass tube. The same procedure is repeated three times. The final solution is evaporated under dry nitrogen. The lipids are diluted again in 100 µL of isooctane for GC. GC is operated according to the manufacturer's instructions and as previously described in [165][166]. It is used for all samples, comparing the amount of 17:0 fatty acid to the others that can be found in the sample. The amounts of fatty acids are calculated based on the initial quantity of 17:0 and thus the quantities of each lipid class.

As shown previously, the fatty acids are responsible for phospholipids behaviour [97]. Two types of fatty acids are noticed: saturated or unsaturated. Many studies in the literature detected a more significant amount of saturated fatty acids on the surface of the articular cartilage. The unsaturated fatty acids increased in case of pathologies [88] [167].

In a previous study in the laboratory, the lipidomic analysis showed that the healthy synovial fluid contained 60 % of phospholipids with saturated fatty acids compared to 43 % detected in the pathological synovial fluid [91]. During the same study, lipidomic analysis of pathological synovial fluids in comparison to healthy synovial fluid showed that the PC and Sph are more involved in the lubrication (lubricating phospholipids). However, PE and PS are more detected in pathological samples (pathological phospholipids) [91] [168] [169]. Thus the ratio between the two classes could indicate how the biomaterial interacted with the natural lubricant.

2.2.2. Histological analysis

2.2.2.1. Tissue sample collection

During the revision surgery, the surgeon removes the developed tissues on the surrounding of the implant. They are considered clinical waste and are analysed histologically. In total arthroplasty, the glenoid bone is resurfaced by a prosthetic component, which requires some drilling to prepare its anchorage; consequently, a cartilage biopsy is also provided.

For each case, the primary samples provided for the histological analysis are the membrane developed in the friction area between the implant and the glenoid and a cartilage biopsy, as shown in figure 2.

The samples for the histological analysis are detailed in table 2.

Table C-2 Summary of the provided samples for the histological analysis

Case	Type of the implant	Reason for revision	Samples for histology
A	**Aequalis™ PyC humeral head Ø 48-18** (Wright medical/ Tornier)	Overstuffed implant	Tendon, Cartilage, Synovial membrane, Extracted membrane from the stem area
B	**Arrow CoCr humeral head Ø 50-19** (FH orthopaedics)	Misplaced implant	Cartilage biopsy, Extracted membrane from friction area implant/glenoid
C	**Aequalis™ PyC humeral head Ø 46-17** (Wright medical/ Tornier)	Lateralized stem	Cartilage biopsy, Extracted membrane from friction area implant/glenoid
D	**CoCr resurfacing head Ø 43-16** (Wright medical/ Tornier)	Glenoid erosion	Synovial membrane, Cartilage biopsy
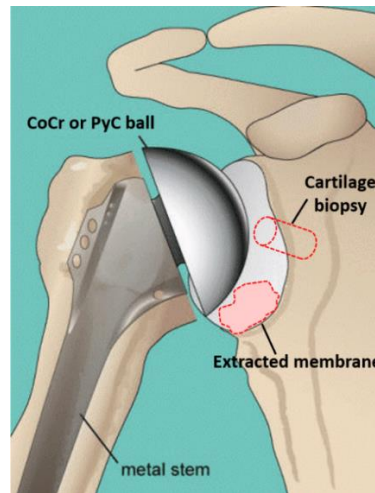
Figure C-2 schema of the shoulder hemiarthroplasty with the potential areas where the membrane and the cartilage biopsy were extracted

2.2.2.2. Histological staining and immunolabelling protocols

All collected samples are analysed by the company Novotec (Bron, France). It is a service provider in tissular analysis and a specialist in the study of the extracellular Matrix.

Samples are fixed in 4 % (v:v) formalin; embedded in paraffin and 5 µm sectioned using a microtome. When needed, the samples received a pre-treatment of decalcification.

Different stainings are performed to evaluate the structure of each sample. Sections are glued with an albumin-glycerol mixture on untreated slides.

- Haematoxylin-Eosin-Saffron staining (HES) allows observing the structure and morphology of the tissue. The cytoplasm is stained pink, nuclei violet-blue and extracellular matrix from yellow to pink. After dewaxing, sections are immersed successively in solutions of Harris haematoxylin, eosin, and saffron.

- Safranin O staining (SO) colours specifically in red the glycosaminoglycans. As already described, GAG is mainly involved in cartilage tissue hydration, but are not specific to that tissue. After dewaxing, sections are stained in SO, and colouration is indicative of glycosaminoglycan presence.

In addition to the different staining, specific immunolabelling are performed to identify the extracellular matrix components, in particular, type I and type II collagen and aggrecan. The sections are glued on treated slides (superfrost plus glass slides are made by a process which electrostatically attracts fresh-frozen and formalin-fixed paraffin-embedded tissue section, binding them to the slide). Hémato Mayer: Diapath C0303, MMFrance, Brignais, France).

- Collagen type I labelling colours in brown the fibres of collagen I which are absent in healthy articular cartilage, but present in almost all other tissues of the body (fibrous tissue, bone…) and healing tissue.
- Collagen type II labelling colours in brown the fibres of collagen II. They are the most abundant protein found in native cartilage.
- Aggrecan labelling colours specifically in brown assemblies of glycosaminoglycan with aggrecan which are specific to articular cartilage.

After dewaxing, antigenic site retrieval is carried out using hyaluronidase 0.5 % solution (Sigma-Aldrich, clone H3506) for matrix labelling. After having incubated sections in the respective antibody solutions overnight at 4 °C (Novotec, 20111, 20211 and 24411), endogenous activity is blocked with 0.5 % hydrogen peroxide. After incubation with peroxidase conjugate antibody Rabbit HRP Envision [DAKO, K4002], antigen-antibody complexes are revealed by tetrahydrochloride diaminobenzidine [DAB, Dako, K3468], and sections are slightly counterstained with Mayer's hematoxylin. Negative controls are carried out with PBS [159] [170].

All observations are made by a light microscope [Leica DM2000], pictures are taken with a digital camera [LAS Version 4] and edited by image analysis software [Adobe, Photoshop CC2015.5].

3. Results

3.1. Case A: Aequalis™ PyC humeral head

3.1.1. Analysis of the mechanism (biotribological triplet)

Case A is a 64 years old man. He had the initial surgery on February 2015 to place an **Aequalis™ PyC** humeral head, combined with an **Aequalis Ascend™ Flex** stem. On December 2015 (10 months of lifespan), he had revision surgery for pain into an **Aequalis™** reversed shoulder combined with the same **Aequalis Ascend™ Flex** stem.

The X-rays showed that the prosthesis was overstuffed, but the patient did not lose mobility. The surgeon declared that the patient had a tough bone difficult to compact so that it was problematic to enter the stem compactor. The decision was to implant the stem even it was not totally entering the humeral shaft.

In revision surgery, no osseointegration was detected. The stem was still not properly seated on the bone. Due to this, the joint was overstuffed, which could be the reason for the pain.

As shown in the X-Ray performed before the revision surgery (figure 3), the prosthesis was overstuffed, the stem was not totally entering. Thus, the mechanical stresses applied to the glenoid were higher compared to the healthy joint [171].

Figure C-3 X-ray of the PyC humeral head performed before the revision surgery

3.1.2. Analysis of the 3rd body (the natural lubricant)

The lipidomic analysis was performed to quantify the adsorbed lipids and particularly phospholipids on the surface of each explant. The performed protocol for the analysis was chosen based on the previous studies on the laboratory [91]. The performed technique allowed to quantify the amount of the total lipids and the phospholipids. Table 3 illustrated different data obtained from the analysis.

Table C-3 Results of the lipidomic analysis of the absorbed molecules on the PyC humeral head from case A

Case A PyC	TL (nmol/mL)	TPL (nmol/mL)	Saturated fatty acids/unsaturated fatty acids	Lubricating phospholipids/pathological phospholipids
	0,069	0,035	0,039	2.048

The adsorbed phospholipids presented around 50 % of the total amount of the adsorbed lipids. The ratio between the saturated and the unsaturated fatty acids indicated the presence of a higher amount of unsaturated fatty acids. Unsaturated fatty acids increase pathologies. Thus the lubrication, in this case, was probably damaged. However, the detailed analysis of the phospholipids classes indicated that the lubricating phospholipids were adsorbed in a higher amount on the surface of the PyC compared to the pathological classes.

3.1.3. Analysis of the 1st bodies (cartilage and membranes biopsies)

The first sample from case A analysed histologically, was a mixture of a synovial membrane with cartilage. The overall structure of the sample was heterogeneous, as showed in figure 4. No signs of an inflammatory reaction were noticed within the sample.

68

It is composed of three zones: (1) a dense and thick fibrous zone with a low cellular density (fibroblasts), (3) a fibrous zone with a cell population of the chondroblastic type and a dense perichondrocytic matrix positive to SO staining and (2) the intermediate area between (1) and (3).

In zone (2), the matrix between the chondrocytes was very fibrous and negative to SO. The cells are rounded and small in size (figure 4). The matrix was lightly coloured with SO, highlighting glycosaminoglycans. At the end of the sample (toward zone (1)), the tissue was only fibrous and very vascular (figure 5). Also, some adipocytes were observed at the periphery (figure 5).
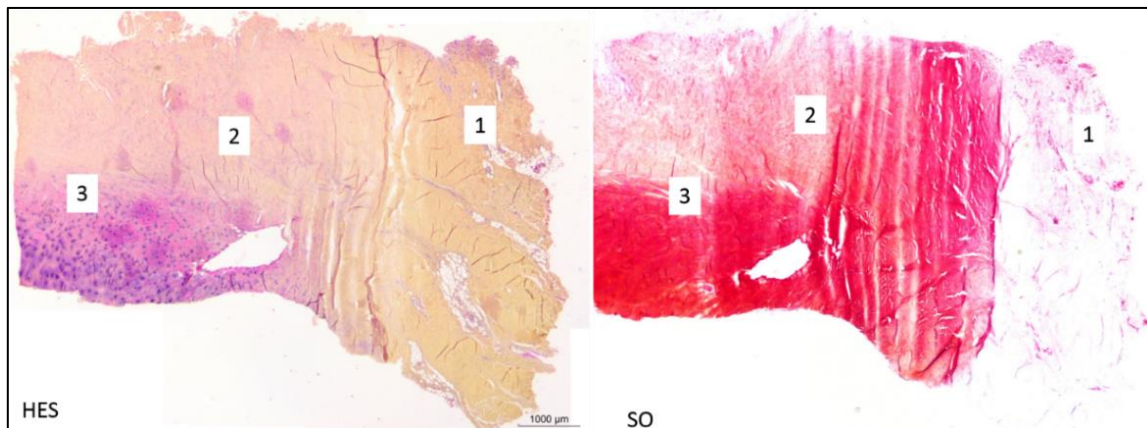
Figure C-4 HES and SO staining for extracted tendon/cartilage following a revision surgery from case A
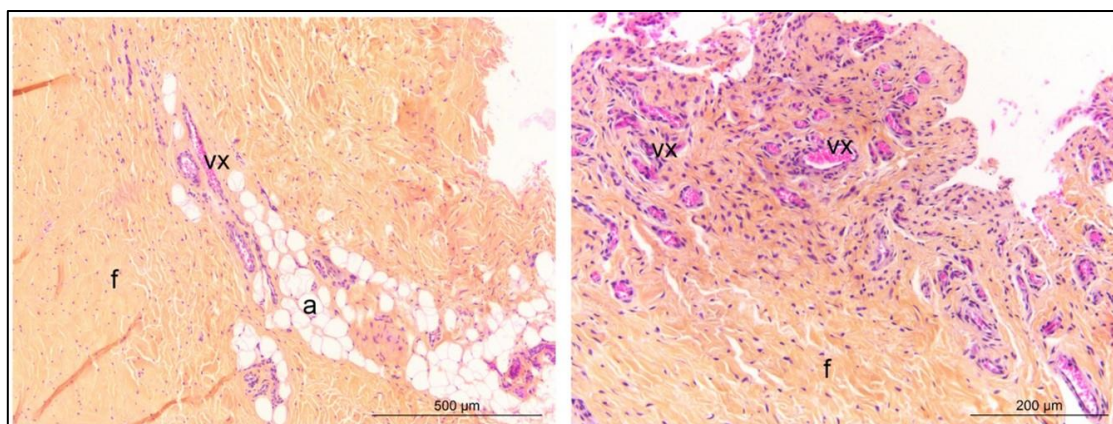
Figure C-5 HES staining for removed synovial membrane following the revision surgery of case A: Vx: vessels, a: adipocytes, f: fibrous tissue

The second extracted sample was a cartilage biopsy (figure 6). However, only a few chondrocytes were observed locally in a fibrous matrix (figure 7a). The sample was composed of dense fibrocartilage area, which was confirmed by the presence of the glycosaminoglycans, highlighted by SO staining (figure 6). The remaining part of the tissue had thick fibres oriented longitudinally (figure 7b), with a compact matrix.
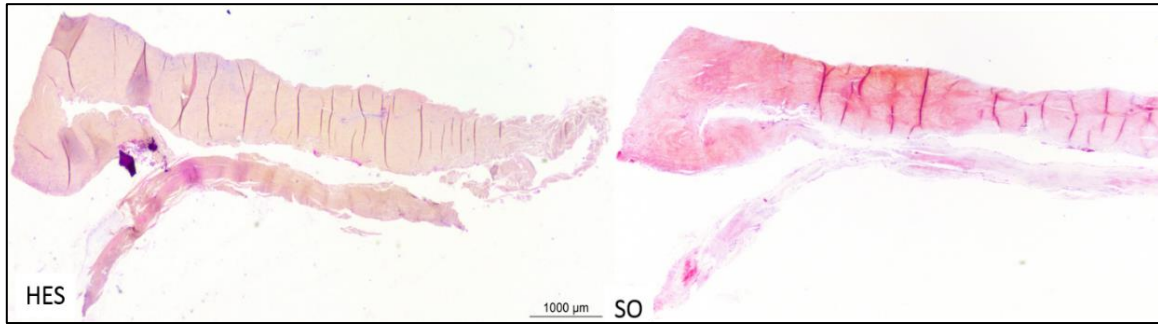
Figure C-6 HES and SO staining for the cartilage biopsy following a revision surgery from case A
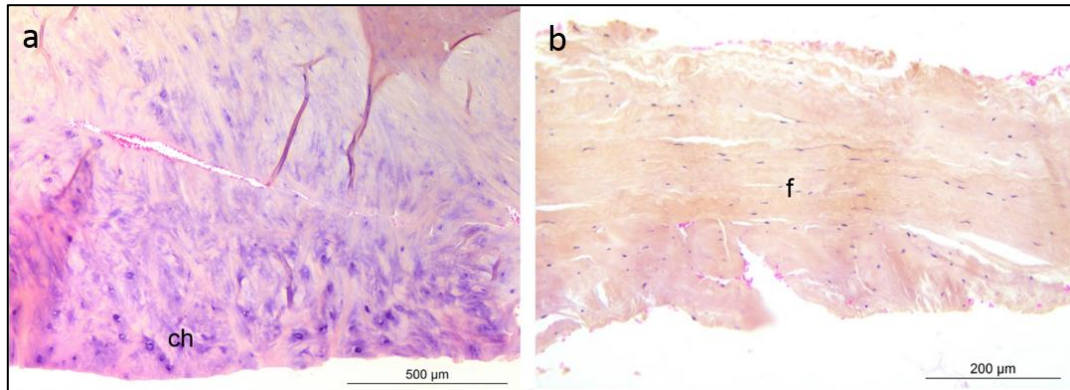
Figure C-7 HES staining for cartilage biopsy following a revision surgery: ch: chondrocyte, f: fibrous tissue

The extracted synovial membrane was well organized, thick and fibrous. No inflammatory reaction was noticed. The matrix fibres were oriented longitudinally (figure 8a). The central area was densified and very compact, almost hyaline (figure 8b). It was stained pink with HES. The more fibrous areas were very vascular (figures 8 b, c). Some macrophages were observed in dense vascular areas (figure 8c). The SO staining highlighted the absence of glycosaminoglycans.

The last sample analysed histologically, in this case, was a membrane extracted from the stem area. Its overall structure was heterogeneous with fibrous tissue characteristics (figure 9a). The tissue had a variable density with very loose areas with thin fibres (figure 9b). The vascular supply was moderate and was mainly present in the deep layers. Some bone fragments were noticed in the central area (figure 9c). Nearby, an inflammatory focus was observed. However, there was no sign of an acute inflammatory reaction. At one extremity, an adipose zone was seen on the surface. It was much vascularized (figure 9d). The SO staining revealed the absence of glycosaminoglycans.
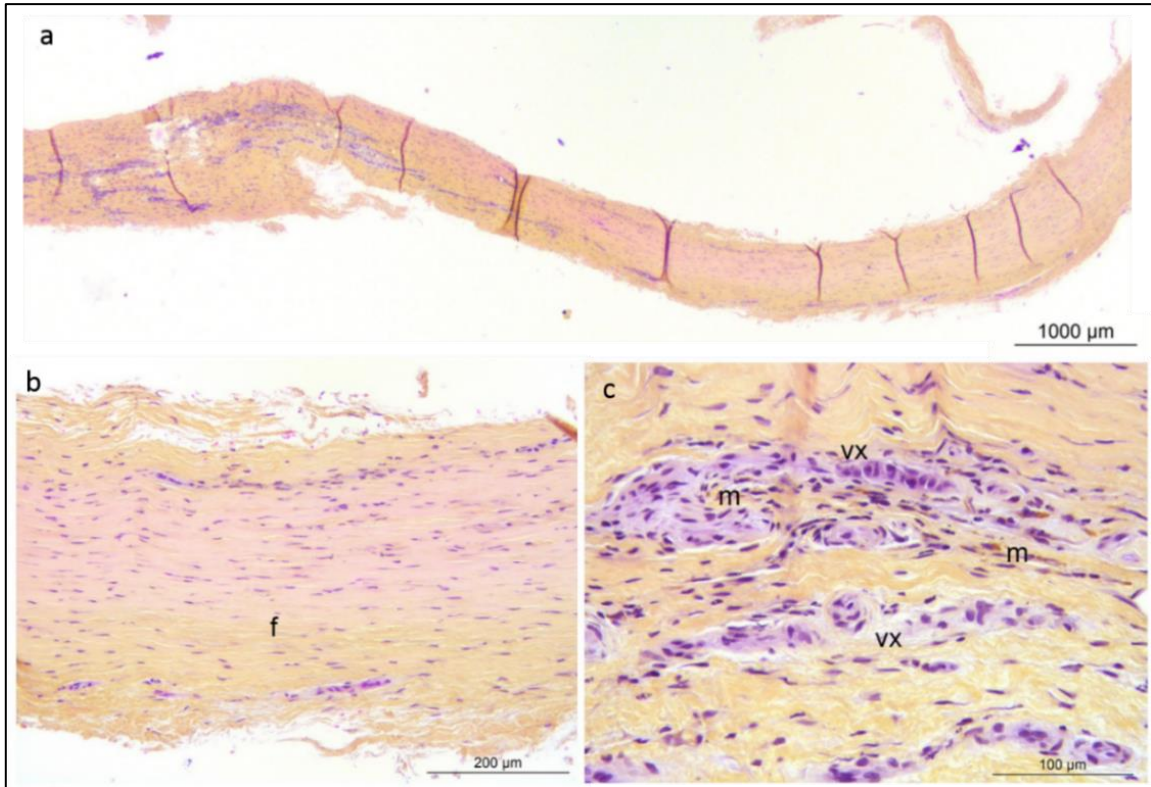
Figure C-8 Histological staining (HES) for synovial membrane following a revision surgery: vx: vessels, m: macrophages, f: fibrous tissue
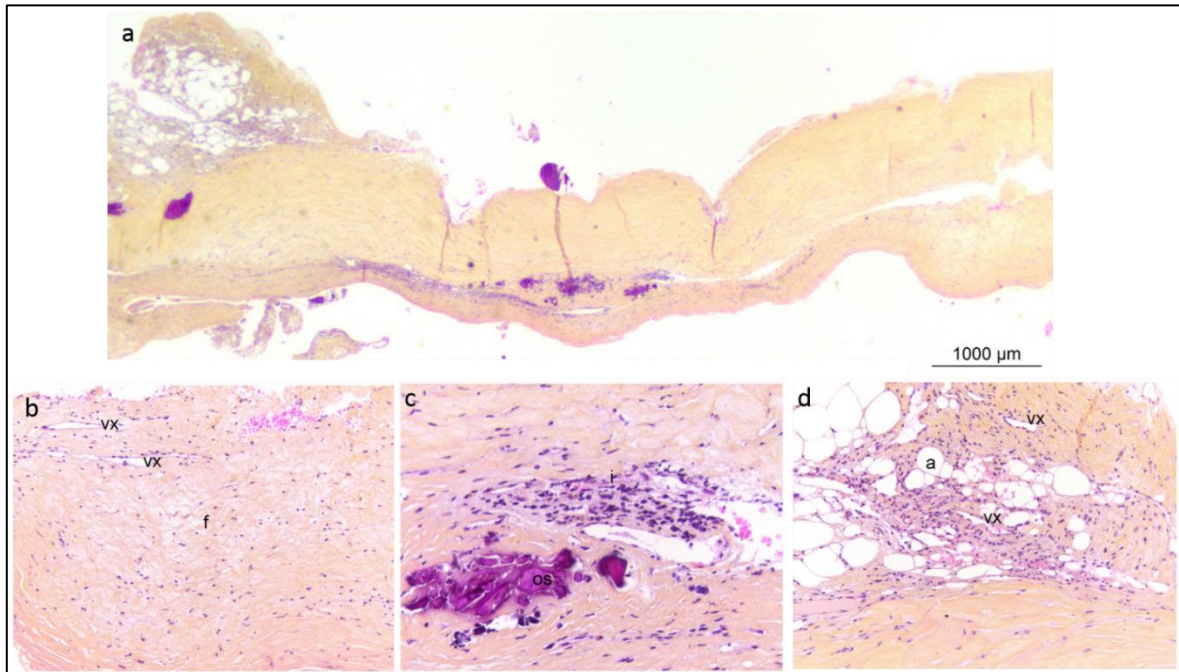
Figure C-9 Histological staining (HES) for the extracted membrane from the stem area following a revision surgery: vx: vessels, a: adipocytes, os: bone, f: fibrous tissue

Amira HANNOUN/ Thesis in Biomechanics 2020/ INSA Lyon

3.1.4. Conclusion

The lipidomic analysis performed on the samples provided after the first revision surgery of this retrieval analysis confirmed the existence of biological molecules originating in the synovial fluid. The adsorbed molecules on the surface of the prosthesis of patient A are mainly phospholipids.

For the histological analysis, only a few macrophages were observed locally in the synovial membrane and a focus in the membrane extracted from the stem side. However, these isolated observations were not indicative of an acute inflammatory reaction.

There were no characteristics of cartilage in the samples. Some fibro-cartilaginous zones were noticed in two of the fragments, with chondrocyte type cells and a very fibrous matrix. The glycosaminoglycans were present locally with very low staining. No exogenous particles were noted. Only HES and SO stainings were performed for this sample.

3.2. Case B: CoCr humeral head

3.2.1. Analysis of the mechanism

Case B is a 60 years old man. He had the first surgery after pain and joint instability. During this surgery, staples were used to stabilize the joint (unknown date for the initial surgery). On March 2015, the patient underwent a second surgery as a result of pain and osteoarthritis of the joint.

On the second surgery, a metallic humeral head made of CoCr was placed. On December 2016 (<u>21 months of lifespan</u>), the case suffered again from pain caused by the lesion of the glenoid cartilage in friction with the metallic head.

It was reported that the implant was misplaced which caused osteophytes without glenoid deviation (figure 10). During this surgery, the arthroplasty was converted into total reverse shoulder arthroplasty.

Figure C-10 X-ray of the CoCr humeral head performed before the revision surgery

Amira HANNOUN/ Thesis in Biomechanics 2020/ INSA Lyon

3.2.2. Analysis of the 3rd body

The lipidomic study showed that the adsorbed phospholipids present around 50 % of the total amount of the adsorbed lipids (Table 4). The ratio between the saturated and the unsaturated fatty acids indicated the presence of a higher amount of the saturated fatty acids compared to the unsaturated fatty acids. Thus the lubrication, in this case, could probably still efficient. However, the detailed analysis of the phospholipids classes indicated a higher amount of pathological phospholipids absorbed on the surface of the prosthesis made of CoCr.

Table C-4 Results of the lipidomic analysis of the absorbed molecules on the CrCo humeral head from case B

Case B CoCr	TL (nmol/mL)	TPL (nmol/mL)	Saturated fatty acids/unsaturated fatty acids	Lubricating phospholipids/pathological phospholipids
	0,074	0,035	4.694	0.153

3.2.3. Analysis of the 1st bodies

In the case, B, the extracted membrane from the friction zone between the glenoid and the misplaced implant presented macroscopically three zones, as shown in figure 11: a scratching zone from the bone, a cartilaginous zone and a fibrous zone.
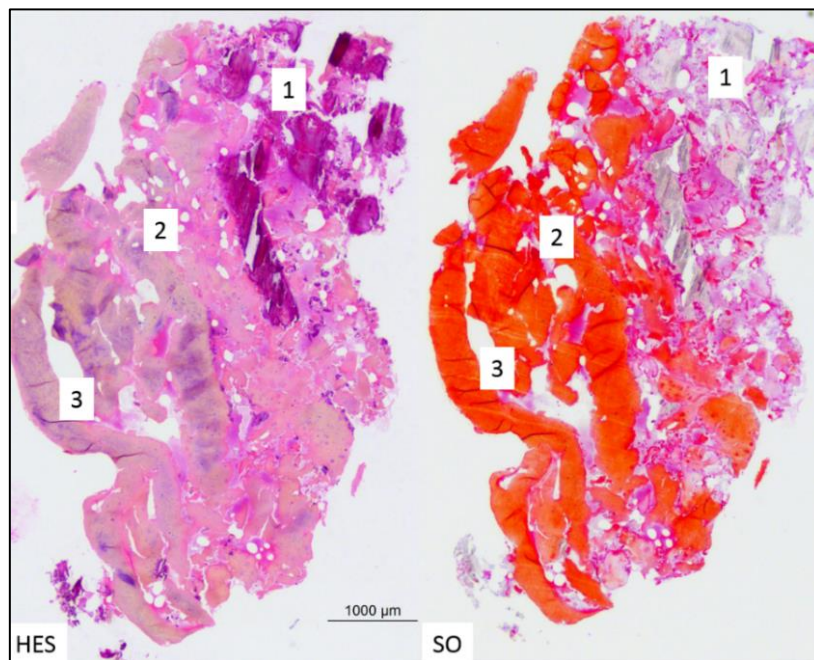
Figure C-11 Histological staining for the extracted membrane following a revision surgery: left: HES staining, right: SO staining.

The first zone (1) (figure 11) contained black granular deposits localized in a haemorrhagic area labelled intensely in type I and type II collagen, as highlighted in figure 12.

Amira HANNOUN/ Thesis in Biomechanics 2020/ INSA Lyon

The cartilaginous zone (2) (figure 12) was characterised by a coexistence of type I and type II collagen with fibro-cartilaginous aspects and some black particles inside the chondrocytes. As shown in figure 12, some chondrocytes and chondrocytes clusters were noticed toward the bone zone.

The fibrous zone (3) (figure 11) was adjacent to the fibro-cartilaginous area. It was more labelled in type I collagen in comparison with the labelling in type II collagen, as shown in figure 12.
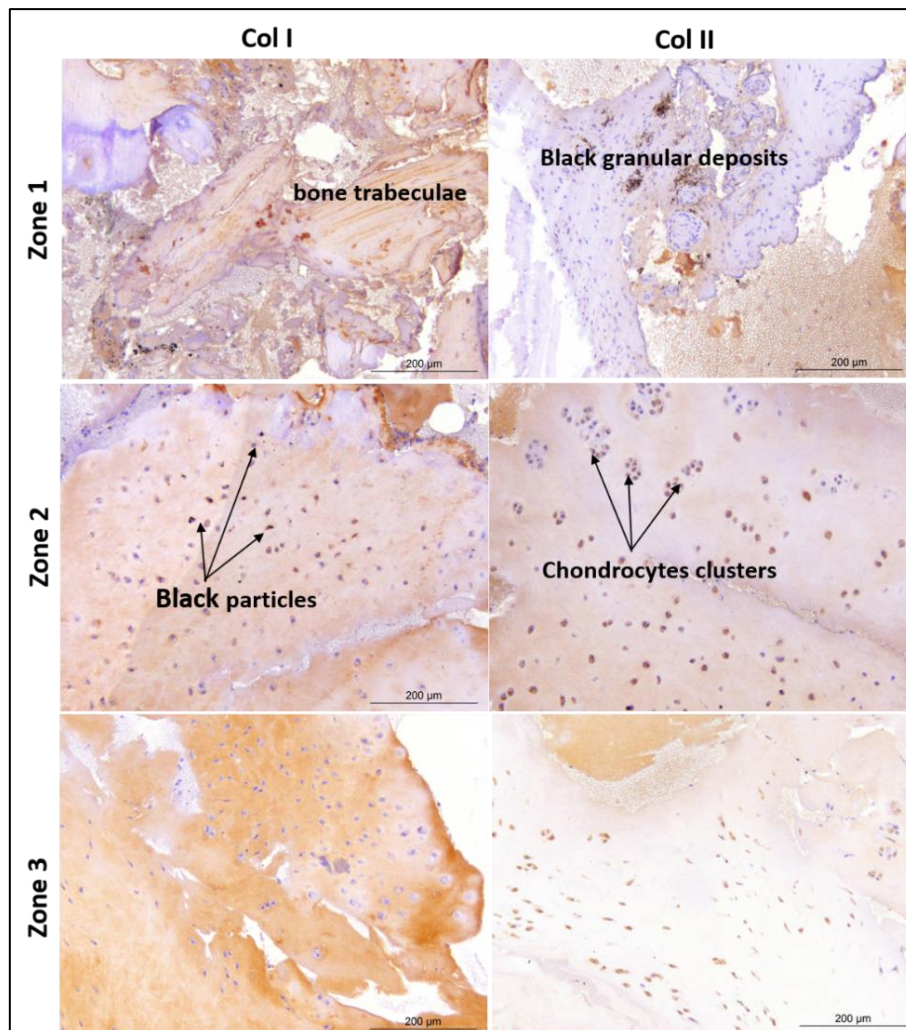
Figure C-12 Specific immunostaining for type I, type II collagen for the different zones of the extracted membrane following a revision surgery

The second sample for the histological analysis was a biopsy from the glenoid. As the first sample, the biopsy presented three zones, as shown in figure 13. The first zone (1) at the implant side had a fibro-cartilaginous aspect, the second zone (2) presented an incomplete development of cortical bone, and the third zone (3) showed an area of bone remodelling.
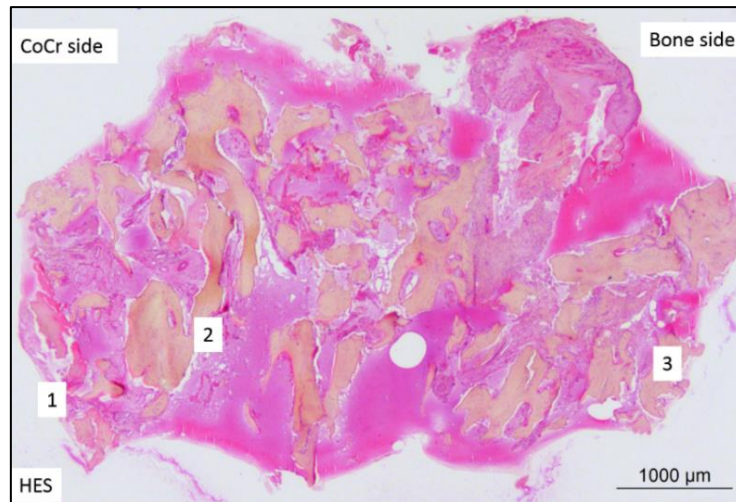
Figure C-13 HES histological staining for the glenoid biopsy following a revision surgery

The first zone was characterised by the presence of chondrogenic cells with the coexistence of type I and type II collagen, as shown in the specific immunolabelling presented in figure 14.

The second zone contained mainly bone trabeculae labelled in type I collagen. The third zone presented an area of spongy bone with several haemorrhagic zones (figure 14).
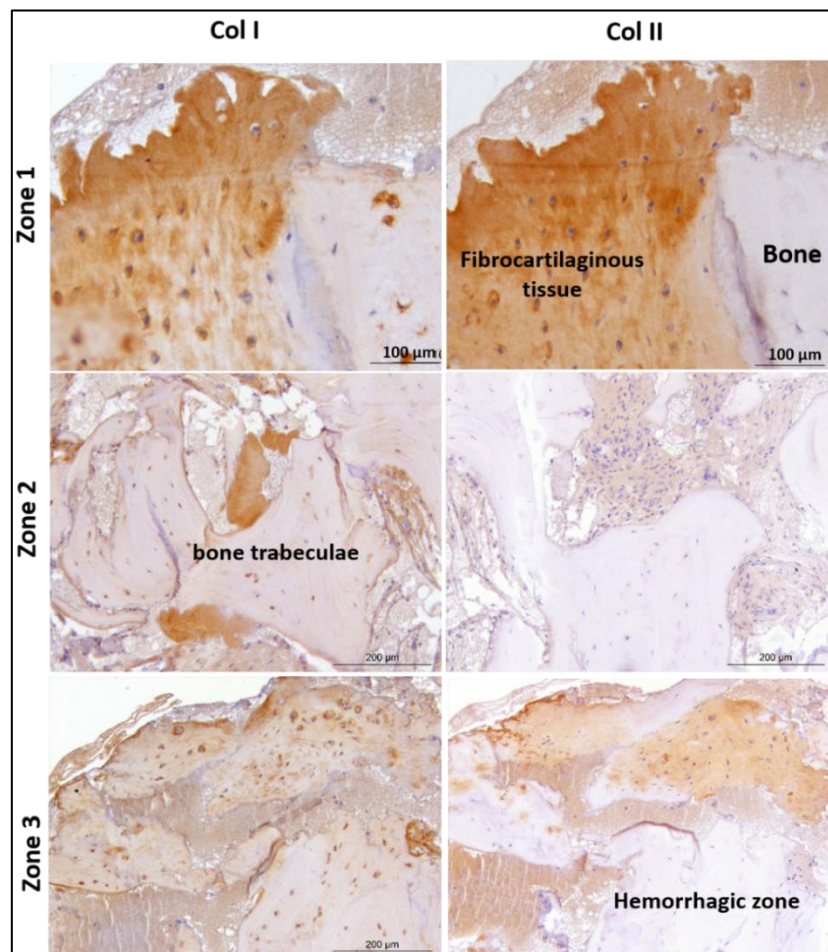
Figure C-14 Specific immunostaining for type I, type II collagen for the different zones of the glenoid biopsy following a revision surgery

3.2.4. Conclusion

Lipidomic analysis of the sample extracted from case B confirmed the absorption of the lipids on the surface of the CoCr as well as the adsorption of the phospholipids.

Overall, the histological analysis showed that the extracted membrane was composed of several tissue fragments with a small mineralised area. The heterogeneity of the membrane structure was noticed due to the folding of the sample. Mainly, haemorrhagic areas were predominant also of little black granular deposits that were locally observed. These deposits could be linked to the metal prosthesis. This membrane consisted of loose fibrous tissue and fibrocartilage. The presence of cartilage areas characterized by hypertrophic chondrocytes (bone differentiation) was highlighted with different labelling. No inflammatory cells were noticed with this sample.

The second sample (the glenoid biopsy) consisted of areas of fibrocartilage visualized by the presence of chondrogenic cells. Some bone areas were characterized by the presence of osteocytes, a sign of recent bone formation. The type I collagen labelling was predominant in the fibrocellular zones with moderate labelling in the bone trabeculae. There was no type II collagen labelling or vascularized area in this sample. This biopsy mainly presents bone tissue with the absence of cartilage and osteolysis activity.

3.3.   Case C: PyC humeral head

3.3.1.   Analysis of the mechanism

The case C is a 67 years old woman. She had trauma in 1991 treated by an osteosynthesis of greater tuberosity fracture. The initial surgery was performed on September 2015 with micro-perforations of the glenoid and placement of an **Aequalis™ Pyrocarbon** humeral head, combined with an **Aequalis Ascend™ Flex** stem.

In the Walch classification, the glenoid appeared as type B2. This classification concerned the morphologic features of the glenoid based on axial cuts of two-dimensional computerized tomography (CT) scans. Type B2 glenoid is characterized by an apparent or obvious erosion of the posterior glenoid, forming a biconcave appearance of the glenoid [172][173].

The primary diagnosis was post-traumatic arthritis. On January 2017 (15 months of lifespan), the patient underwent revision surgery into a reverse configuration with stem retention. The reason for the revision was a pain since the implantation and stiffness.

The surgeon declared that the patient had a malunion following head trauma, which is known as a tricky case to treat since it was difficult to place the stem properly. Accordingly, the stem was too lateralized, as shown in the X-ray (figure 15), generating hypertension of the muscles, which caused the pain and the stiffness.
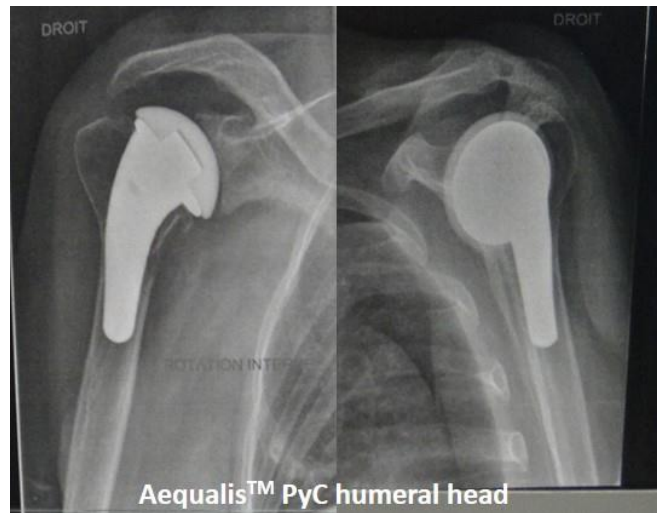
Figure C-15 X-ray of the PyC humeral head performed before the revision surgery

3.3.2. Analysis of the 3rd body

The lipidomic study showed that the adsorbed phospholipids presented around 35 % of the total amount of the adsorbed lipids (Table 5). The amount of the total adsorbed lipids was higher in comparison with the two previous cases. The ratio between the saturated and the unsaturated fatty acids indicated the presence of a higher amount of saturated fatty acids. Thus the lubrication, in this case, could probably still efficient. Furthermore, the detailed analysis of the phospholipids classes indicated that the adsorbed phospholipids on the surface of the prosthesis made of PyC were mostly those responsible for the lubrication.

Table C-5 Results of the lipidomic analysis of the absorbed molecules on the CrCo humeral head from case B

Case C PyC	TL (nmol/mL)	TPL (nmol/mL)	Saturated fatty acids/unsaturated fatty acids	Lubricating phospholipids/pathological phospholipids
	0,355	0,121	3.848	2.155

3.3.3. Analysis of the 1st bodies

Histological analysis, in case C, showed that the membrane extracted from the glenoid was stiffer than the one removed from the previous case (CoCr implant). It was not folded while using the histological solvent, as shown in figure 16, the membrane was more homogeneous and vascularized with a small area of bone fragments due to its scratching. The SO staining highlighted the significant presence of glycosaminoglycans in the cartilaginous and fibrocartilaginous zones.
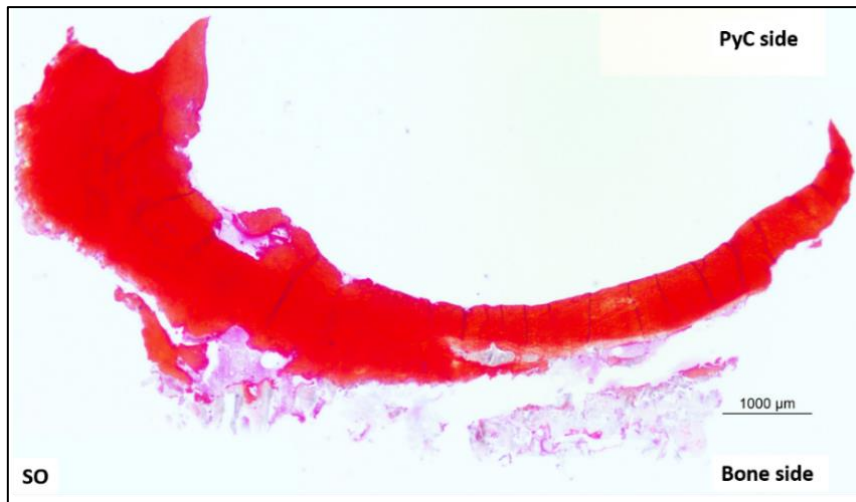
Figure C-16 Safranin O staining of the extracted membrane following revision surgery of the case C

The specific immunostaining showed a predominant type I collagen labelling in the extracellular matrix which confirmed the fibrocartilaginous type of the membrane. However, the cells synthesized type II collagen, which was highlighted in type II collagen labelling presented in figure 17.
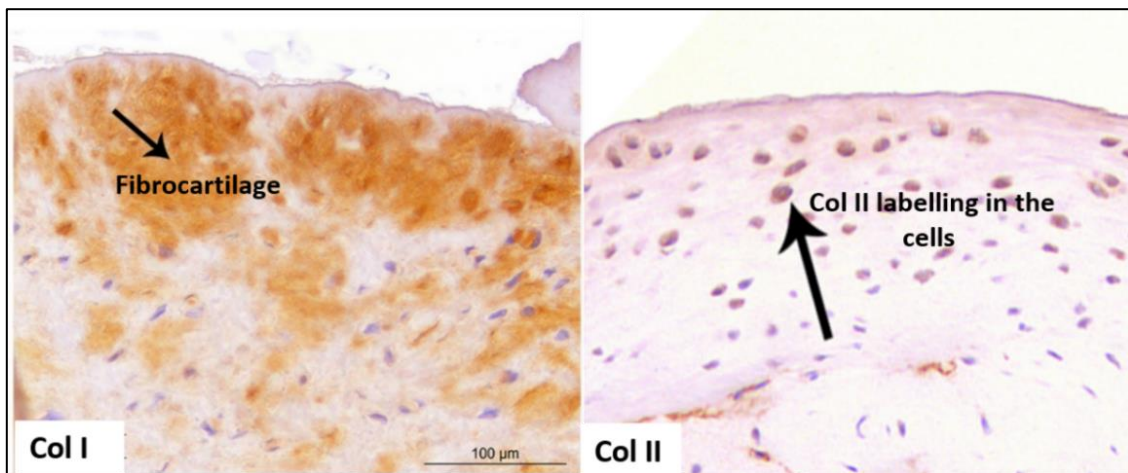
Figure C-17 Specific immunostaining for type I, type II collagen for the extracted membrane following a revision surgery

The second sample was a biopsy of the glenoid. The biopsy, as shown in figure 18, presented two zones: one "corticalized" zone on the implant side and a second "spongy" zone on the bone side. It was composed of a compact bone trabeculae, a vascularized fibrocellular tissue and bone marrow.

Contrarily to the previous case, the specific immunostaining for type I collagen was predominant in the bone trabeculae (figure 19). Type II collagen labelling was noticed only at the vessels. This labelling on the vessels is a sigh of bone remodelling and bone healing which is one of the precursors of hyaline cartilage synthesis.

78
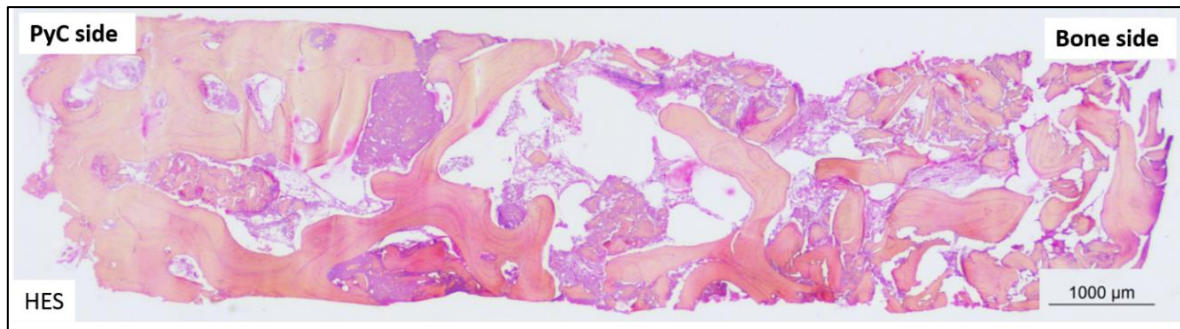
Figure C-18 HES staining of the glenoid biopsy following revision surgery of the case C
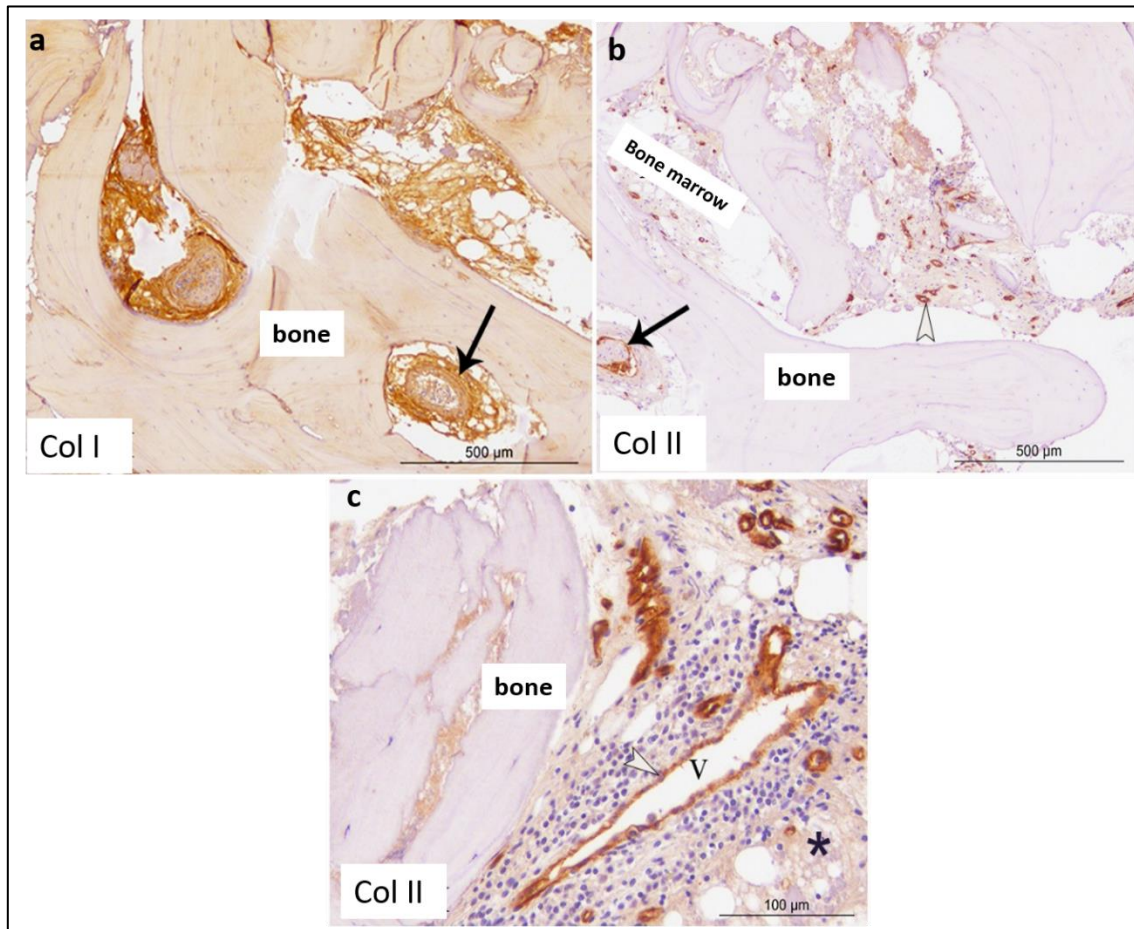
Figure C-19 Specific immunostaining for type I, type II collagen for cartilage biopsy following a revision surgery

3.3.4. Conclusion

The lipidomic analysis revealed higher amounts of the adsorbed lipids and phospholipids on the surface of the PyC humeral head in comparison with the previous cases.

Histological analysis showed that the extracted membrane from the friction area between the glenoid and the PyC implant with the lateralized stem presented mainly a much vascularized fibrocellular tissue with cartilaginous zones.

The membrane was composed of areas with a tendency to synthesize type II collagen and of cartilaginous cells. It had high type II collagen labelling in the vascularized area, which is unusual in fibrous tissue. This vascularization might stimulate the regeneration of cartilaginous tissue.

For the cartilage biopsy, it consisted of bone trabeculae and bone fragments surrounded by bone marrow and fibrocellular tissue. Collagen II was detected at the vessel level.

3.4. Case D: CoCr resurfacing head

3.4.1. Analysis of the mechanism

Case D is a 47 years old woman. On 2009, she underwent the initial surgery on the reason of OA trauma. She received a resurfacing hemiarthroplasty made of CoCr. On January 2017 (<u>96 months of lifespan</u>), revision surgery was performed due to painful glenoid erosion. The implant was converted into reverse shoulder arthroplasty.

Figure 20 illustrated the X-ray performed before the revision surgery.

Figure C-20 X-ray of resurfacing prosthesis performed before the revision surgery

3.4.2. Analysis of the 3rd body

The lipidomic study showed that the adsorbed phospholipids presented around 46 % of the total amount of the adsorbed lipids (Table 6). The ratio between the saturated and the unsaturated fatty acids indicated the presence of both types of fatty acids in comparable amounts. Thus, the synovial

fluid, in this case, had an altered composition. Furthermore, the detailed analysis of the phospholipids classes indicated the presence of both lubricating and pathological phospholipids.

Table C-6 Results of the lipidomic analysis of the absorbed molecules on the CrCo humeral head from case B

Case D CoCr	TL (nmol/mL)	TPL (nmol/mL)	Saturated fatty acids/unsaturated fatty acids	Lubricating phospholipids/pathological phospholipids
	0,233	0,109	1.204	0.902

3.4.3. Analysis of the 1st bodies

The glenoid biopsy of case D consisted of fragments of fibro-cellular tissue, as shown in figure 21a. Numerous mineralised areas surrounding the tissue were detected (*, figures 21 a, c). The presence of the mineralisation caused the tearing of the biopsy (figure 21). The biopsy was composed of dense matrix zones revealed by the HES staining (figures 21 a, c). For the SO staining, there was almost no staining which indicated a limited presence of the glycosaminoglycans (figure 21b).
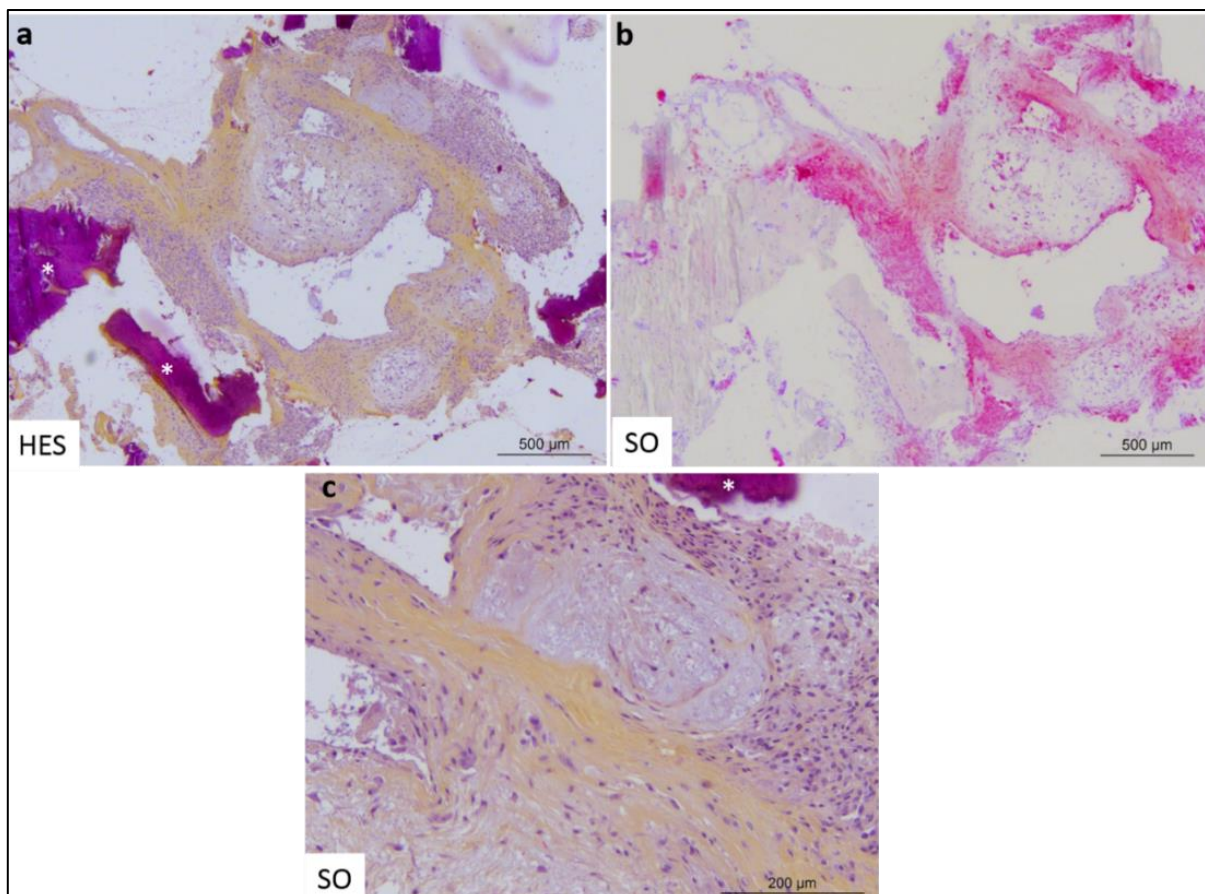
*Figure C-21 Histological staining for a glenoid biopsy following the revision surgery of case D: a, c) HES staining, b) SO staining. *: mineralized area*

The specific immunostainings highlighted a dominant presence of type I collagen and aggrecan with low staining in type II collagen (figures 22 a, b, c). A single small specific area of type II collagen was noticed (Figure 22e). The aggrecan labelling was extensive both in the cartilaginous zones and in certain fibro-cellular zones (figures 22 c, f).

The distribution structure of different specific immunostainings indicated that the biopsy consisted of healing tissue with the absence of cartilage characteristic.
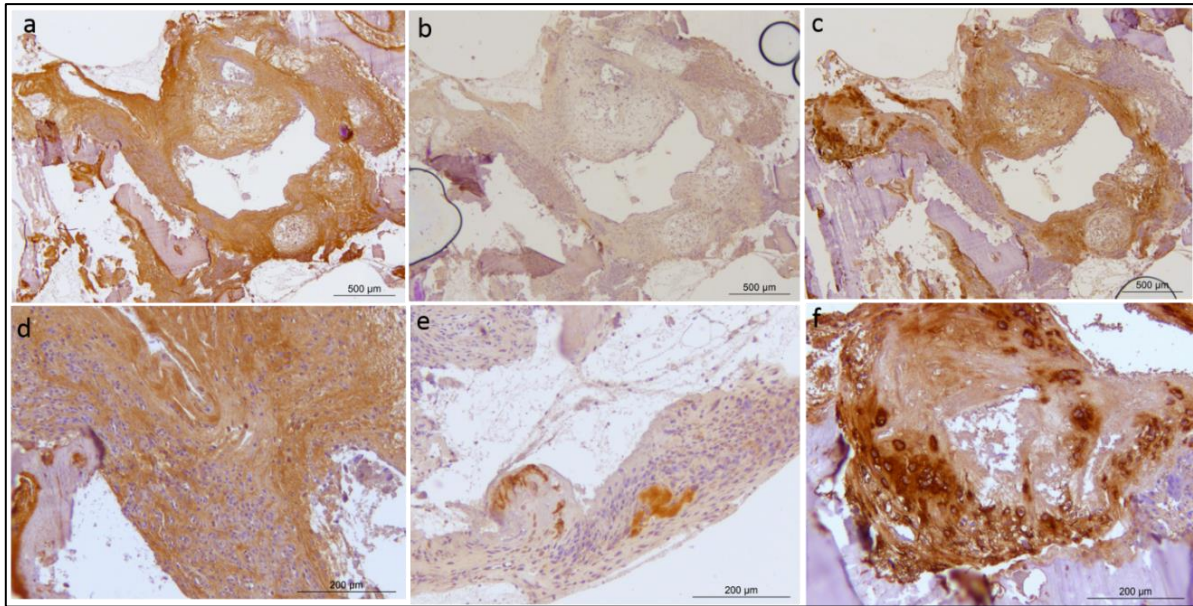
Figure C-22 Specific immunostaining for type I, type II collagen and aggrecan for a glenoid biopsy following the revision surgery of case D: a, d) Type I collagen, b, e) Type II collagen, c, f) Aggrecan.

The extracted synovial membrane during the revision surgery presented many folds, as shown in figure 23. The HES staining revealed a fibrocellular and very vascular structure. Different matrix zones were also detected (figure 23 b). Besides, some area was characterized by the presence of chondrogenic cells (figure 23 c). With this sample, there was no evidence of glycosaminoglycans performing the SO staining.
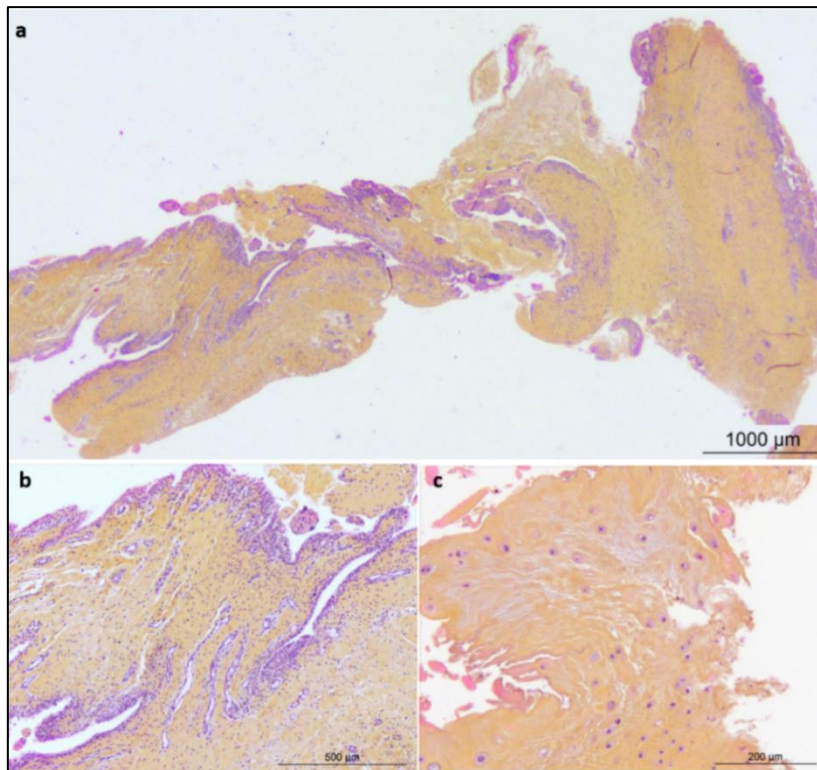
Figure C-23 HES staining for the extracted synovial membrane following the revision surgery from case D

For the specific immunostaining, the type I collagen and aggrecan labelling was predominant with a uniform distribution (figures 24 a, b, c). There was no type II collagen labelling except at the level of the chondrogenic cells (figures 24 b, e). With this sample, non-specific labelling was noticed on the vessels. For the aggrecan labelling, a localization was detected around the same chondrogenic cells labelled in type II collagen (figure 24 f), as well as at the level of certain matrix zones of the fibro-cellular tissue.
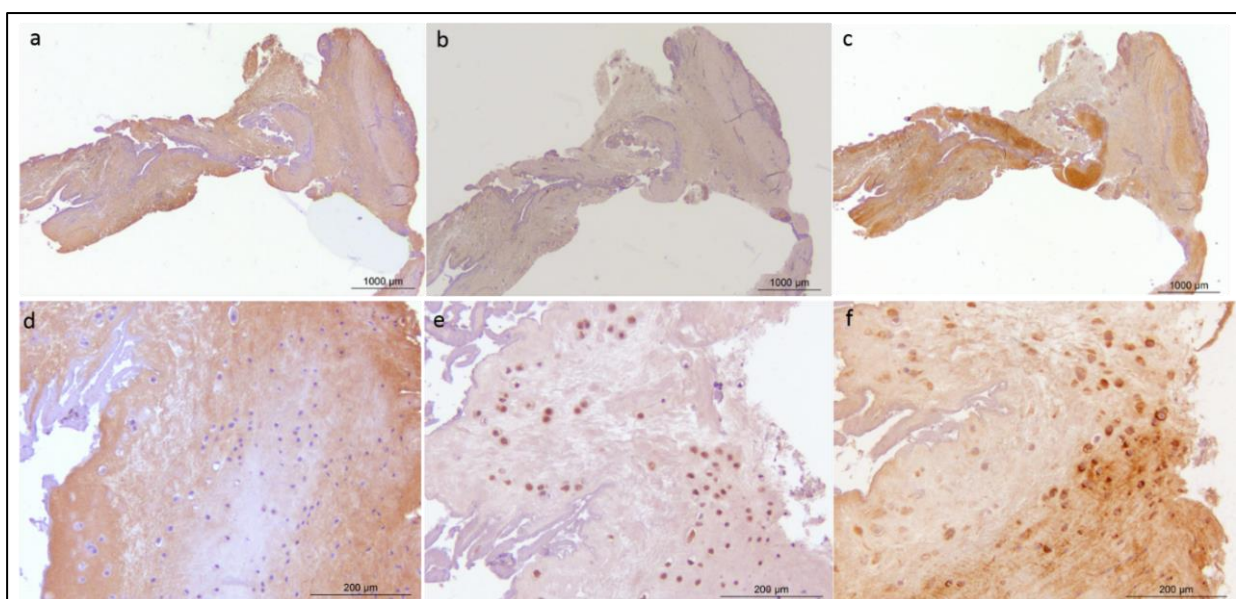
Figure C-24 Specific immunostaining for type I, type II collagen and aggrecan for the synovial membrane following a revision surgery: a, d) Type I collagen, b, e) Type II collagen, c, f) Aggrecan.

83

Amira HANNOUN/ Thesis in Biomechanics 2020/ INSA Lyon

3.4.4. Conclusion

The two samples from the shoulder revision surgery were analysed by histological staining (HES and SO) and by immunostaining (type I, type II collagen and aggrecan). Their structures are very heterogeneous with the presence of a few mineralised zones which made the histological section process complicated. However, specific staining for mineralisation is necessary to confirm this observation.

The glenoid biopsy was mainly fibro-cellular with significant labelling of type I collagen. Some cartilaginous zones were highlighted by aggrecan, but type II collagen labelling was almost absent. The synovial membrane was mainly a vascularized fibro-cellular tissue with an extracellular matrix. Type II collagen was visualized in some chondrogenic cells.

4. Discussion

4.1.   Explants surfaces affect the adsorption of the biological molecules

Overall, the retrieval analysis included 4 shoulder hemi-prostheses revised for different reasons and by different surgeons. The potential adsorbed lipids were extracted from the surfaces of the retrieved implants. Total lipids and phospholipids were separated and analysed by GC (procedure § 2.2.1).

Since the retrieved implants had not the same size, their surfaces were considered in the lipid quantification. The number of retrieved implants did not allow to perform statistical analysis so that each case was presented separately.

The lipid content of case A was particularly low, but the lipids were extracted by washing the biomaterial surface only once with the specific solvent. In comparison with the other retrieved implants, which had been washed twice, we hypothesized that the lipids were not totally extracted. As illustrated in figure 25, the lipidomic analysis of the second wash of the explant from case C showed the existence of the lipids, which confirmed the necessity of the second wash. Consequently, case A was not comparable to case B, C and D and was excluded from the analysis. Still, cases B and D, which are CoCr explants and case D, which is PyC explant, were exploitable.

The total lipid content was different between case B and D, but both are neatly inferior at the total lipid content extracted from the PyC explant. Indeed, the TL quantity adsorbed on the surface of the PyC explant of the case C was 4.7-fold and 1.5-fold higher than the amount adsorbed on respectively the surface of the CoCr explant of the case B and case D. Same as the TL, phospholipids measured quantities were more elevated in case of PyC explant than in the case of CoCr.

Adsorbed TL and TPL on the surface of PyC explant (case C) for the first and second extraction
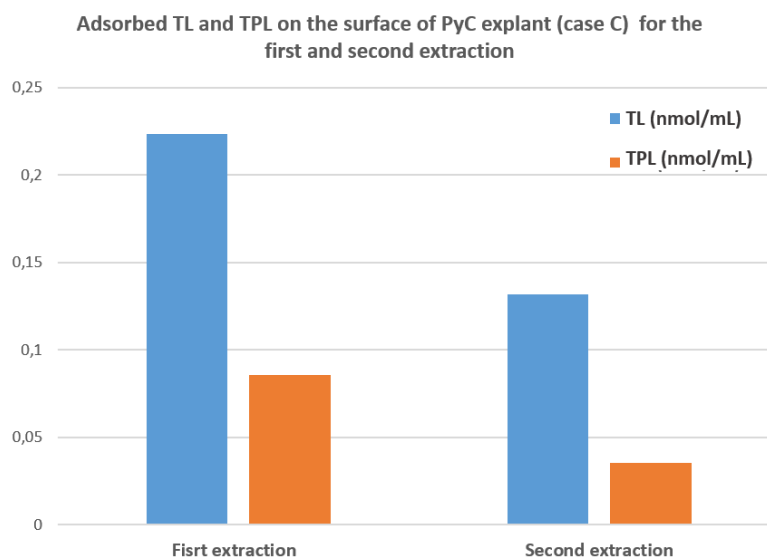
Figure C-25 quantities of the total lipids and phospholipids adsorbed on retrieved PyC implant with the first and the second extraction: the blue represents the total lipids and the orange represent the phospholipids

The diversity of the samples and the different states of the patients made a comparison between cases complicated. The objective of this retrieval analysis was to compare PyC hemi-prosthesis to CoCr hemi-prosthesis. To conclude this comparative analysis, only the explants from case B and case C were chosen (leaving aside cases A and D). The two explants were revised for similar reasons: misplaced implant in the case B and implant with a lateralized stem in the case C. In both cases, the lipid extraction protocol was identical (two washes), and the same samples were provided for the histological analysis which allowed the comparison. Besides, both implants had similar survival period *in vivo*: 21 months in case B and 15 months in case C. Thus, the biology of the joint as well as the interaction between the biomaterial and the biological components of the joint were active for a similar period on both cases B and C.

4.2. PyC had high affinity to the lubricating lipids of the synovial fluid

The comparison between the two cases for lipidomic analysis revealed a 4.8-fold higher quantity of adsorbed lipids on the surface of PyC than on the surface of CoCr (figure 26). Notably, the amount of the adsorbed PL on the surface of PyC was 3.5-fold higher than on the surface of the CoCr. As described previously, the phospholipids are the molecules in the synovial fluid, which ensure proper joint lubrication. The results thus suggest that PyC explant allows better lubrication of its surface than CoCr, thanks to superior adsorption of lipid molecules.

Adsorbed TL and TPL on explants surfaces
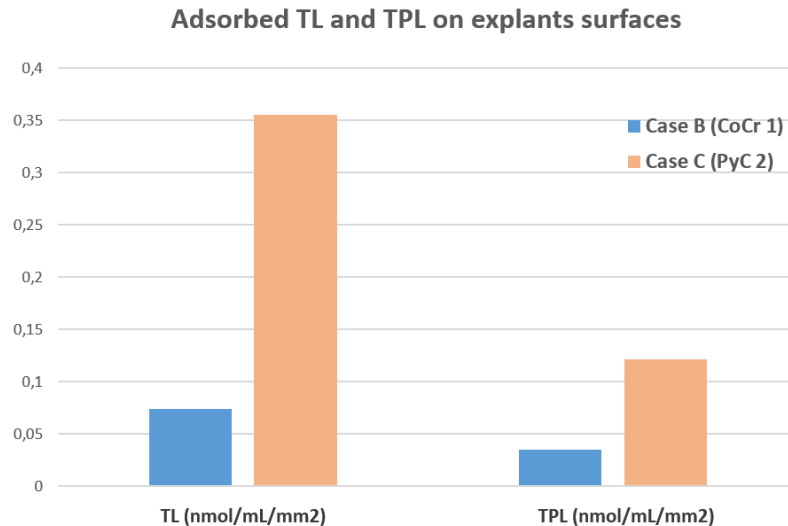
Figure C-26 quantities of the total lipids and phospholipids adsorbed on retrieved implants: the dark and light blue represent the CoCr biomaterial and the dark and bright orange represent the PyC biomaterial

4.3. PyC ensured good tissue remodelling

The histological analysis highlighted differences between the membranes synthesized as a result of the glenoid friction with PyC or with CoCr. Indeed, the membrane in the case of CoCr consisted mainly in healing fibrocartilaginous tissue zones with different amounts of type I, type II collagen and aggrecan. In some sections of the membrane, black deposits were noticed in the tissue (figure 27).

The preliminary hypothesis suggested that the detected deposits are metal ions coming from the prosthesis. The more specific analysis will be performed to confirm the nature of these deposits. The sections will be analysed by energy-dispersive X-ray spectroscopy (EDS) available in the laboratory.

For the PyC implant, the synthesized membrane had components able to synthesize hyaline cartilage with intense type II collagen and aggrecan labelling. Particularly in some histological sections, type II collagen was detected in the vessels, which is an unusual observation in the histological analysis (figure 27).

As a reminder of tissue remodelling, it is activated following a bone fracture or prosthesis replacement. The first step of this remodelling begins by forming a cartilaginous callus. The formed callus contains stem cells which differentiate in the presence of specific factors to proliferating chondrocytes and then to hypertrophic chondrocytes [174].

As a next step, the hypertrophic chondrocytes continue the proliferation into mineralised chondrocytes inducing vasculature invasion in the healing junction. Also, the endothelial cells present in the blood vessels facilitate the mineralisation and preserve the degradation of the cartilage matrix [175].

The role of collagen type II in the healing process is not well explored in the literature; few studies explain this role. It was shown that the collagen II in vessels stimulates the endothelial cells, which induce more blood vessels invasion in the healing junction. Collagen type II in these cells is essential for the stem cells and facilitates their differentiation into chondrocytes [176] [177]. Briefly, collagen type II was detected in the vessels, which is unusual; however, it is favourable for bone remodelling. Therefore, the PyC preserves the vasculature invasion and collagen II expression in the endothelial cells. In conclusion, in this case, the PyC ensures better tissue remodelling than the CoCr.

In conclusion, PyC seems to preserve the vasculature invasion and collagen II expression in the endothelial cells. Thus, PyC could ensure better tissue remodelling than CoCr.

In addition, articular cells are mechanosensitive; therefore, an excellent tissue remodelling is possible when cells receive a suitable mechanical load. In the case of arthroplasty, the mechanical load is transmitted to the cells through the biomaterial. Thus, our results suggest that the PyC provides an adequate transmission of mechanical solicitations.
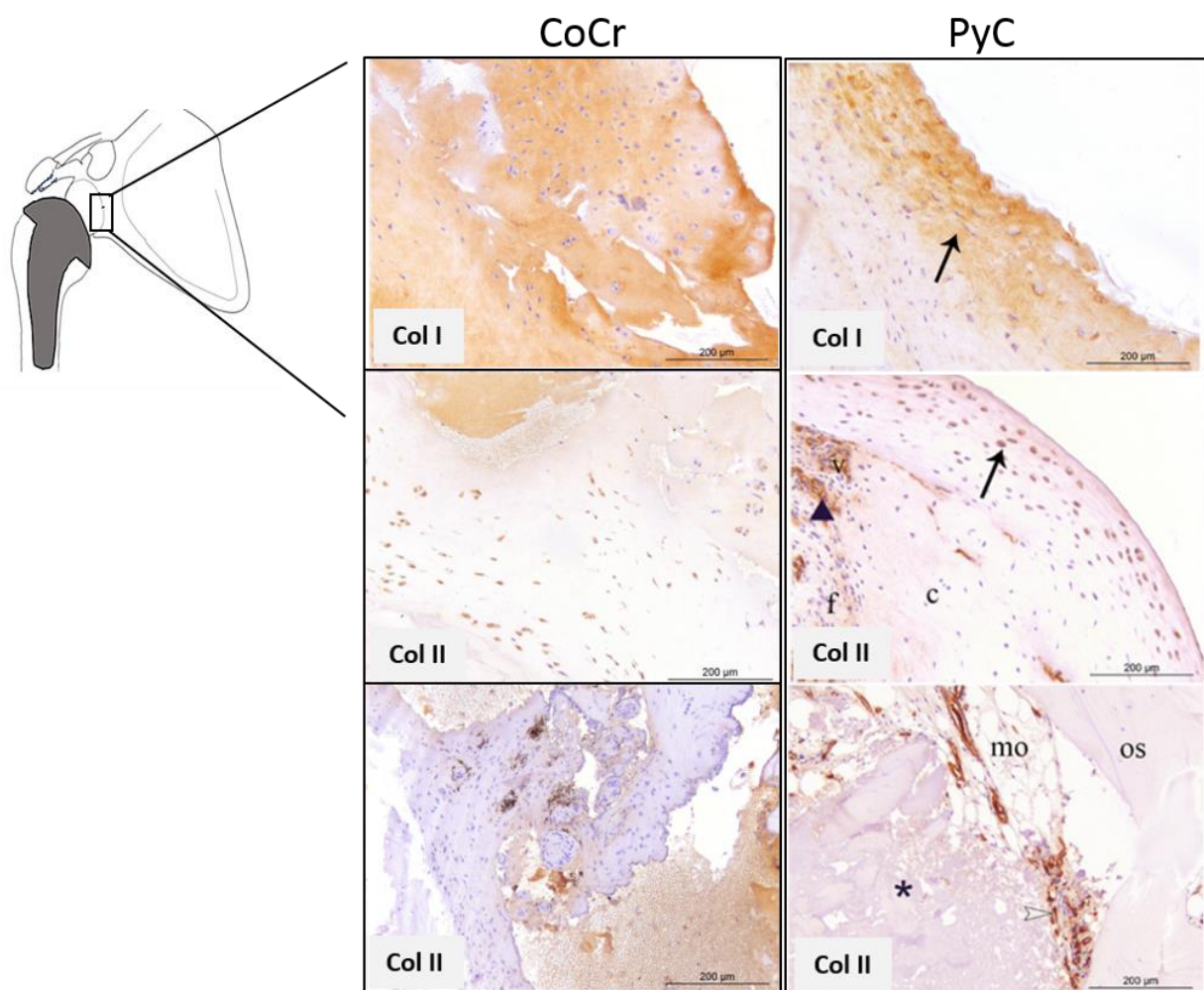
Figure C-27 Immunolabelling of type I and type II collagens performed on the extracted membranes from revision surgeries of CoCr humeral head (case C) and PyC humeral head (case B), scale bar=200 μm

4.4. PyC induced minimal alteration to the glenoid cartilage

For the cartilage biopsies, with the two biomaterials, the samples presented overall healing tissue. However, in the case of PyC, the tissue showed vascular periphery with higher amounts of type II collagen and aggrecan indicating that the cells in this biopsy conserve their ability to synthesize extracellular matrix with cartilage characteristics.

The synthesis of the different extracellular matrix component could be affected by the biomaterial and the geometry of the implant and its placement. All these parameters affect the transmission of mechanical solicitations to the mechanosensitive skeletal cells.

Consequently, the misplaced implant and the implant with the lateralized stem in the two cases induced higher mechanical solicitations than the natural joint. The difference between the biomaterial could be related to the way each biomaterial transmits these solicitations. Due to this, the synthesis of cartilage components in the case of PyC may be ensured first by its spherical shape and second by the favourable transmission of the mechanical solicitations through its structure.

4.5. Conclusions and limitations

Overall, previous studies and the present results suggest that in the case of hemiarthroplasty, the PyC would preserve the cartilage components and would ensure an adequate tissue remodelling better than the CoCr.

Despite the information provided by performing the retrieval analysis, it had some limitations. The limited number of the explants indicates a successful orthopaedic treatment; however, it did not allow an accurate statistical analysis. Also, the diversity of the patients' cases and their states did not allow as well an extensive comparison. Therefore, it is interesting to launch a clinical analysis with specific criteria for including patients. However, with particular criteria, the clinical study will last longer. The cases of shoulder arthroplasty are still fewer in comparison with the hip or knee arthroplasties.

Nevertheless, our analysis gave some answers regarding the effect of the biomaterial *in vivo* through the expertise of the live biotribological triplet. It showed that:

- PyC induced minimal wear to the glenoid cartilage (effect on the 1st bodies).
- PyC ensured good tissue remodelling through a suitable transmission of the mechanical solicitations (effect on the mechanism).
- PyC had an affinity to the phospholipids which are the lubricating molecules in the synovial fluid (effect on the 3rd body).

The thesis aims to understand the origin of tissue remodelling on the bone and cartilage side using PyC as a replacement biomaterial. This section allowed to identify the *in vivo* effect of the PyC biomaterial

on the components of the live biotribological triplet. Therefore, in the following sections, our strategy is to dissociate *in vitro* the role of the biology (cellular response), of the lubricant, and the transmission of mechanical stresses.

The next chapter presents the first approach to study the effect of the biomaterials in contact with articular cells, particularly chondrocytes (impact of the biomaterial on the 1st bodies).

Chapter D

Understanding the proper functioning of the pyrocarbon *in vitro*: effect on the 1st bodies

D. Chapter D: Understanding the proper functioning of the pyrocarbon *in vitro*: effect on the 1ˢᵗ bodies

In the previous chapter, a retrieval analysis of shoulder hemi-prostheses was performed to evaluate the effect of the PyC biomaterial on the live biotribological triplet in comparison with the CoCr. The study showed the impact of the biomaterials on each component of the triplet *in vivo*. To better understand this effect, our strategy is to carry out three parallel studies *in vitro* to dissociate the role of the biology (cellular response), of the lubricant and the transmission of mechanical stresses.

This section focuses on the biology aspect. To insert the interposition implant, the surgeon creates a cavity in the humeral bone that reaches the metaphyseal zone. This zone is characterized by containing the mesenchymal stem cells and growth plate cartilage cells (proliferative chondrocytes) that facilitate bone elongation but also promote its healing and regeneration. Owing to this surgical process, the implant is in direct contact with healing bone which usually develops a fibrous tissue and then a bony structure. However, in this case, the contact between the biomaterial and the cells leads to the development of cartilaginous tissue.

Cells behaviour is easily affected by the biological and biochemical context, but also by cell-biomaterial interaction [160]. Therefore, in this chapter, the effect of PyC biomaterial on chondrocyte behaviour is analysed *in vitro* in two conditions mimicking either bone-like conditions (as a model for the humeral surgical cavity - implant interface) or cartilage-like conditions (for the glenoid cartilage - implant interface) in comparison to CoCr biomaterial.

1. Healing bone process

Bone is a complex live structure, presenting about 15 % of human body mass. It ensures various functions, including organs protection, muscles attachment, and blood cells generation for immuno-protection.

The bone structure in the human body consists of 80 % of cortical bone and 20 % of cancellous/ spongy bone. The cortical bone has 10 % porosity while the cancellous bone is 90 % porous, which makes its mechanical properties lower than those of the cortical bone.

The long bone, such as the humerus, is divided into two main physiological parts (figure 1). The diaphysis is the tubular shaft that runs between the proximal and distal ends of the bone. The hollow region in the diaphysis is called the medullary cavity, which is filled with yellow marrow. The walls of the diaphysis are composed of dense and hard compact bone [160][178].

The wider section at each end of the bone is the epiphysis. It is filled internally with cancellous bone. In long bones, the red marrow fills the spaces between the cancellous bones. The zone where the

epiphysis meets the diaphysis is the metaphysis. This zone contains the epiphyseal plate, the site of bone elongation [178].
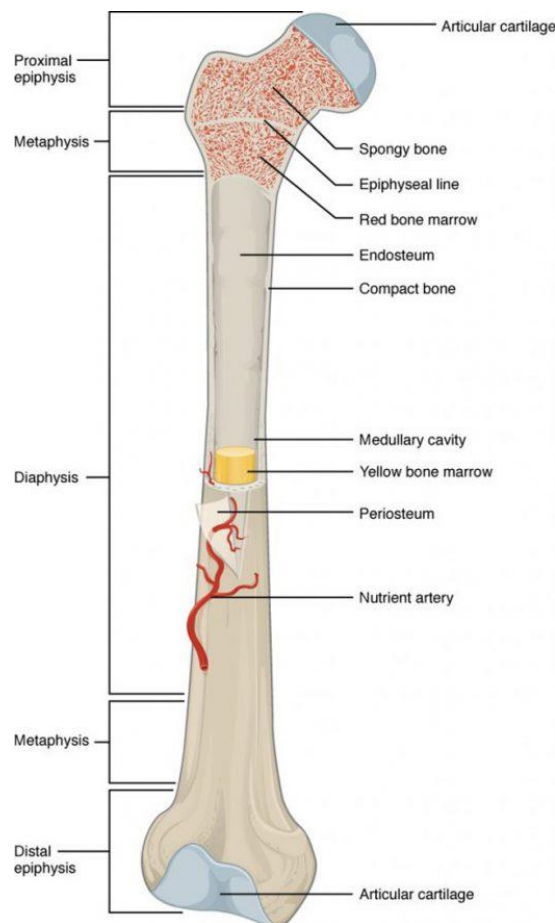
Figure D-1 Anatomy of a Long Bone: A typical long bone showing gross anatomical features. [178]

The human bone faced much stress during the lifetime. It can be affected by fracture, arthritis or surgical procedure to place a prosthesis. As a response to these stresses and changes, a process called bone healing begins when the bone is affected. It is adapted to the event that affected the bone. The healing process is not the same in the case of the fracture, as in the case of arthroplasty.

In the case of fracture, bone healing is essentially a bone remodelling by resident bone cells (osteoblasts and osteoclasts). The process is similar to the endochondral bone formation as the broken bones form cartilaginous callus before creating the new bone. The bone healing from a fracture flows three main steps (figure 2):

1) Blood released from broken vessels in the periosteum and/or medullary cavity clots into a fracture hematoma which promotes an increase in nutrient delivery to the affected site and around the fracture.

2) Stem cells from the endosteum of the bone differentiate into chondrocytes to generate a fibrocartilaginous tissue between the two ends of the fracture. After several days/weeks, this

92

tissue unites the opposite ends of the fracture into a soft internal callus to stabilize the fracture.

3) Bone cells become finally active. Osteoclasts resorb dead parts of the bone and osteoblasts produce new bony tissue. The cartilage of the soft callus is now destructed and replaced by the new bone to form the hard-bony callus. In response to mechanical stress, this callus is transformed into a spongy bone then into a compact one to reach a healed fracture finally.
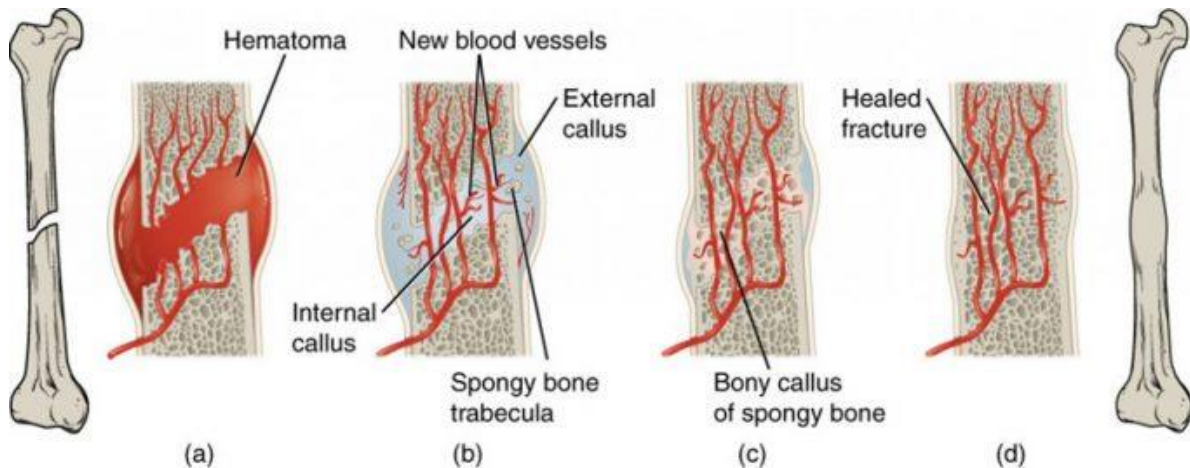
*Figure D-2 **Stages in Fracture Repair:** The healing of a bone fracture follows a series of progressive steps: (a) broken blood vessels leak blood that clots into a fracture hematoma. (b) Internal and external calluses form made of cartilage and bone. (c) The cartilage of the calluses is gradually eroded and replaced by trabecular bone, forming the hard callus. (d) Remodelling occurs to replace the immature bone with mature bone. [178]*

During the arthroplasty, the bone is machined to either put a stem or to create a placement for the implant. Here, bone healing involves a variety of biological events to ensure the stability of the implant. This healing process follows different steps [161]:

1) As soon as the implant is placed in the human body, adsorption of proteins and lipids from the blood starts on its surface. Thus, some interactions of the proteins with the implant surface can take place, sometimes presenting an inflammatory reaction. Due to this, platelets form fibrin clots to fill the voids and facilitate the transfer of the different cells, including stem cells to the implant surface.

2) Stem cells differentiate to promote bone healing and tissue regeneration. They secrete a cartilaginous matrix to form the soft internal callus. This differentiation depends mostly on the biological environment and the surface properties of the implant.

3) In the case of bone implants (placing a stem in the femur for the hip arthroplasty), the healing continues until the formation of the hard-bony callus. In other cases, the healing process and

93

the soft callus evolution depend on the biomaterial properties and the biological/ physicochemical environment of the joint [160].

Therefore, interactions between different cells and the implanted material are essential to predict the implant effect in the human body and the type of synthesized tissue.

2. Cell cultures in the presence of biomaterials

The reaction of the human body facing a new implant is different depending on the surgical procedure, on the biomaterial properties but mainly on the interaction between the cells and the implant. In the literature, many studies have been conducted to improve arthroplasties results. Most of these studies presented *in vivo* experiments on animal models [179] but *in vitro* experiments of cell cultures reproducing the same *in vivo* conditions are limited.

Such experiments are mainly launched to either develop biological paths to improve the biomaterial performances or to evaluate the inflammatory response and the viability of cells in the presence of a biomaterial [180][181]. Several cell types have been used, such as macrophage or specific cell lines. We rather focus on how the interactions between resident cells and the implanted material could affect the type of synthesized tissue around the prosthesis.

A study has already been conducted to evaluate bone cell behaviour in contact with silk fibroin films and different polymers. The study aimed to assess whether or not the used biomaterials supported the growth and the differentiation of cultured murine osteoblasts and osteoclasts. The tested materials did not affect cells growth, but fibroin degradation and surface changes in the polymers were detected due to cellular activities [182]. Cells adhesion on biomaterials is another parameter to be taken into account. The interaction between cells and materials are quite complex and mainly involve the cell-surface proteins [183].

Furthermore, it was shown that the surface chemistry and the roughness of biomaterials affect cell culture of joint cells. Chondrocytes behaviour changed depending on the support of the cell culture. Consequently, optimization of biomaterials structure and their surface chemistry is necessary [184].

Besides, wear is a major problem in arthroplasty. The generated particles from wear may interact with the surrounding tissues causing, in some cases, the implant loosening. Nine and colleagues presented a review of the biological effect of some wear particles. They summarized the biological response of different types of human cells in the presence of various particles as detailed in Table 1 [185].

Table D-1 Biological response of human cells in the presence of implant particles

Biomaterial	Source	Cells type	Biological response	
			Realised test	**Result**
Aluminium	Commercial powder	Osteoblasts	Tissue Non-specific Alkaline Phosphatase	Active for low concentrations
Titanium	Commercial powder	Osteoblasts	Tissue Non-specific Alkaline Phosphatase	Non-active
CoCr alloy	tribometre	Fibroblasts	Toxicity	Non-toxic
Metallic Alloy FeAlCr	Commercial powder	Osteoblasts	Viability	No alteration the first day
Titanium alloy	Commercial powder	Osteoblasts	Proliferation	Only good the first day
Polyethene UHMWPE	Commercial powder	Blood cells	Viability	No alteration

In this chapter, we aim to evaluate the direct contact between cells and implant biomaterials to understand the cellular behaviour that may lead to cartilaginous tissue regeneration. The effect of CoCr or PyC contact on chondrocytes is analysed *in vitro*. Murine primary chondrocytes are selected for their ability to synthesize a cartilaginous extracellular matrix or to differentiate into bone-forming cells. Also, primary cultures are widely used to mimic human cells. These cells are grown on discs of PyC or CoCr using two culture media to mimic either cartilage-like conditions (CLC) or bone-like conditions (BLC). Different characterisation tests (biological and mechanical tests) are performed to evaluate the behaviour of the cells in the presence of both biomaterials and to assess the type of the synthesized extracellular matrix.

3. Study Model

3.1. Biomaterials

Samples made of PyC and CoCr are supplied by Wright Medical/Tornier (France) with similar surface conditions as the medical implants used in shoulder arthroplasty. They are disc-shaped with the following dimensions:

For PyC: 20 mm diameter, 2 mm thickness.

For CoCr: 22 mm diameter, 2 mm thickness.

The difference between the biomaterials dimensions is related to the manufacturing process. Before the test the roughness of the sample (R_a) is assessed by classic topographies with the available profilometer in the laboratory Altisurf 500: $Ra_{Pyc}= (16.9 \pm 1.9)$ nm; $Ra_{CoCr}= (12.0 \pm 2.8)$ nm

Amira HANNOUN/ Thesis in Biomechanics 2020/ INSA Lyon

The biomaterials are unusual supports for cell culture, so it is considered to include a regular cell culture support as a control. In this case, wells of the culture plates (Corning) without biomaterial (Polystyrene 35 mm diameter) are used as a reference to control cell behaviour.

3.2. Murine primary chondrocytes: cell culture conditions

Dissection of new-born mice (4 to 6 days-old) is performed to obtain murine chondrocytes. Cartilage is recovered from femoral heads and knees of the hind legs. Then, cells are obtained by sequential enzymatic digestions [186]. The cells obtained this way are proliferative chondrocytes at the beginning of the culture period. Approximately 1.5 million cells per mice were obtained and seeded at a density of 12,500 cells per cm² in 6-well culture plates.

Implant samples are placed in a culture plate with phosphate-buffered saline (PBS) to be hydrated overnight before seeding cells. Due to their sizes, samples did not recover the entire surface of the well-culture plate. The seeded cells grew on the biomaterial discs but also the underlying polystyrene [159].

The standard conditions for chondrocytes culture are respected. Chondrocytes are cultured at 37 °C in the presence of 5 % CO_2 in a saturated water atmosphere. Each cell culture lasts 17 days with specific days for testing (Table 2). To maintain the decent conditions for the cell culture, each culture well received 4ml of the culture medium. The culture medium is regularly changed, as shown in Table 2.

Three types of cell culture medium were mainly used.

- An amplification culture medium composed of Dulbecco's Modified Eagle Medium (DMEM) containing 20 mM L-glutamine, 1 g/L glucose, 100 U/mL penicillin and 100 µg/mL streptomycin, 10 % Foetal Bovine Serum (FBS, v:v).
- CLC medium composed of DMEM, 4.5 g/L glucose, 100 mM HEPES and 10% FBS (v:v) (still containing L-glutamine, penicillin and streptomycin)
- BLC medium composed of CLC medium in which ascorbic acid (50 µg/mL) and β-glycerophosphate (10 mM) were added to stimulate the mineralisation of the cells.

	Tests	Cartilage-like conditions (CLC)	Bone-like conditions (BLC)
Day 0		Dissection Biomaterial hydration in PBS	Dissection Biomaterial hydration in PBS
Day 1		Cell seeding in amplification medium	Cell seeding in amplification medium
Day 3		Changing the amplification medium	Changing the amplification medium
Day 6		Changing for CLC medium	Changing for CLC medium
Day 7			Changing for BLC medium
Day 10		Changing CLC medium	Changing BLC medium
	Test at day 10	Viability and toxicity tests	
Day 13		Changing CLC medium	Changing BLC medium
Day 16		Changing CLC medium	Changing BLC medium
	Test at day 17	Mineralisation and calcium tests Samples collection for mechanical and histological tests	

3.3.   Biological characterisation

3.3.1. Viability test by MTT assay and cytotoxicity test by LDH assay

To evaluate the effect of different biomaterials on chondrocytes behaviour, viability test is performed on day 10 by the MTT assay. The living and metabolically active cells transform the MTT (3-(4,5-dimethylthiazol-2-yl)-2,5-diphenyltetrazolium bromide) to form violet formazan crystals. The formazan crystals are solubilised in dimethyl sulfoxide (DMSO) and measured at 570 nm [187].

At day 10, cells from the culture plate intended for viability test are incubated at 37 °C for 4 hours with 0.125 mg/mL of MTT. Then, the cell culture medium containing the MTT is removed, and formazan crystals are solubilised by 4 mL DMSO per well. As already mentioned, the samples did not recover the entire plastic-well. Therefore, samples are translocated in new plates, and the 4 mL of DMSO is equally shared between cells grown on the disc and those grown on the underlying plastic.
Briefly, 4 mL of DMSO is added in control wells (without biomaterial), 2 mL is added in the well of the biomaterial after removing it, and 2 ml is added in the new well containing the biomaterial. The measured absorbance indicates cell viability on the biomaterial surface. The sum of the two absorbances is compared to the control without biomaterial, which considered as 100 % viability.

In addition to the viability test, cytotoxicity test is performed on the same day by LDH assay. The lactate dehydrogenase (LDH) is a cytosolic enzyme released into the culture medium in the case of cell damage. Before pouring the MTT in the wells to test the viability, 200 µL of the cell medium in each well is recovered. Extracellular LDH is detected on the recovered mediums using a LDH kit (LDH Cytotoxicity Assay Kit, Pierce). For this assay, two control wells are used: a negative control presenting

0 % of cytotoxicity and a positive control presenting 100 % cytotoxicity. For positive control, 10 % of triton X100 (v:v) is added to the cells to induce full LDH release.

3.3.2. Mineralisation test by Alizarin red staining

The mineralisation test is performed on day 17 (at the end of the culture period). To determine the presence of calcium deposits in the extracellular matrix of the chondrocytes and to evaluate the degree of mineralisation, the dye "Alizarin red" (3,4-dihydroxy-9,10-dioxo-2-anthracenesulfonate sodium) is used [188].

The culture medium is removed from wells of the plate intended for this test. Then, cells are washed with PBS. Same as the MTT assay, the biomaterials are translocated in another plate to evaluate the cells grown on the discs and those grown on the plastic. To fix cells, 2 mL of ethanol 70 % (v:v) are added in all the wells for 20 min at room temperature. The ethanol is removed, and the wells are washed with water for 5 min. Then, the plates are incubated for 20 min at room temperature with 2 mL/well of 2 % (v:v) Alizarin red, pH 4.2. After three washes with water, 2 mL/well of cetylpyridinium chloride (100 mM) is added to solubilize the Alizarin red. All the plates are then incubated for overnight under gentle stirring before measuring the absorbance at 570 nm.

3.3.3. Specific calcified deposits and Tissue Non-specific Alkaline Phosphatase (TNAP) assays

The assessment of the mineralisation of the extracellular matrix in the presence of different biomaterials by alizarin red staining is not a quantitative evaluation. Therefore, it is completed by the quantification of calcified deposits and by the Tissue Non-specific Alkaline Phosphatase (TNAP) assay. Both assays are performed on day 17.

The calcium determination is based on the reaction of calcium with o-cresolphthalein complexone in alkaline solution, which yields to a violet coloured complex [189]. To perform calcium quantification, cell medium is removed from all the wells, and 2 mL of HCl 0.6 M is poured in each well and left to overnight incubation to extract calcium. 20 µL of samples are mixed to 100 µL of the reagent. The absorbance is measured at 570 nm after plate incubation of 5 min at room temperature [190]. Calcium quantities are standardized by the protein content. Bicinchoninic acid protein assay is performed using the Pierce BCA Protein Assay kit (Thermo Scientific).

TNAP is an enzyme present in the cells to ensure the mineralisation process. It can hydrolyse the inorganic pyrophosphate, which is the primary inhibitor of the cell's mineralisation. Therefore, TNAP activity is used as a marker of mineralizing cells. It is measured based on the cleavage of a synthetic

substrate (para-nitrophenyl phosphate) into a yellow compound, the para-nitrophenol [191]. An important TNAP activity usually reflects a high rate of mineralisation.

Briefly, 400 μL/well of Nonidet P40 0.2 % (v:v) (octyl phenoxy poly (ethyleneoxy) ethanol) and 20 seconds of sonication are used to extract TNAP from cells. 20 μL of samples are mixed to 180 μL of the reagent [191]. The absorbance is measured kinetically on a 96-wells plate for 5 min at 405 nm with the controlled temperature at 37 °C. To evaluate the TNAP activity, a standardization by protein assay is also necessary. BCA protein assay is performed to calculated TNAP specific activity. Results are calculated as μmol of para nitrophenol (pNP) produced/min/mg protein [159].

3.3.4. Histology

On day 17 of culture, a tissue-like is developed on each sample surface. This tissue-like is called in this project "tissue-like cell-membrane". Thus, tissue-like cell-membranes are removed carefully from biomaterials for histological analyses to identify their structure and components.

Samples are fixed in 4 % (v:v) formalin; embedded in paraffin and 5 μm sectioned using a microtome, then glued with an albumin-glycerol mixture on untreated slides. Different stainings are performed to evaluate the structure of each tissue-like cell-membrane as detailed in chapter C: HES, Safranin O and Von Kossa.

Von Kossa staining colours in black the mineralisation zones. Samples are fixed in 4 % formalin for 15 min and washed twice with distilled water. After fixation, they are incubated with 5 % silver nitrate solution for 30 min under ultraviolet light then rinsed three times with distilled water. After complete drying, dehydrated sections are mounted between slide and coverslip using Entellan®.

In addition to the different staining, specific immunolabelling are performed to identify the extracellular matrix components: type I and type II collagen and aggrecan.

All observations are made by a light microscope [Leica DM2000], pictures are taken with a digital camera [LAS Version 4] and edited by image analysis software [Adobe, Photoshop CC2015.5].

3.4. Mechanical characterisation

A new device "Tribo-bioreactor" is developed in the laboratory (LaMCoS) for cell culture and mechanical characterisation. Thus, it is used in this section to perform rheological tests. The conception of the new device and its functions are detailed in chapter G.

Briefly, it is composed of two parallel circular trays: a Plexiglas tray for samples visualization during the mechanical test and a stainless-steel tray for the application of mechanical stress. Different parameters are modifiable such as the gap between the two plates, the type of the mechanical solicitation

(compression or shear), its value, its frequency. The device allows measuring the normal dynamic force needed to evaluate the mechanical properties of the samples.

The tissue-like cell-membranes formed in the surface of the biomaterials are characterised mechanically. Thus, a dynamic mechanical analysis (DMA) is performed. It is a non-destructive technique to characterize the viscoelastic properties of different samples [192]. By imposing sinusoidal stress or deformation, mechanical properties of samples are evaluated.

Removed tissue-like cell-membranes are placed between the two trays of the device to evaluate their rheological behaviour. The gap is fixed according to the volume of the cell-membranes obtained for each cell culture (between 500 μm and 700 μm). Then, a dynamic displacement (100 μm, 2Hz or 4 Hz) is applied. For each sample, two signals are obtained for the applied displacement and the measured force. The elastic modulus is calculated as previously described in [159] and later in chapter G.

3.5.   Statistical analysis

The results of different biological tests are analysed using the software "Prism" (GraphPad). Bars represent the mean and standard error (SEM) of at least three independent experiments (the exact number of experiment *n* is indicated on the figures). Effects of the different biomaterials on cells are compared to controls, using Student T-test.

Significant results are represented in the figures by an asterisk (*) if the *p-value* is lower than 0.05, two asterisks (**) if the *p-value* is lower than 0.01 and three asterisks (***) if the *p-value* is lower than 0.001.

For the Immunohistological analysis, the results were assessed by a semi-quantitative approach to summarize the observations of each parameter, as shown in Table 3 [159].

Table D-3 Semi-quantitative evaluation of histological and Immunohistological analyses

Score	For the chondrocyte clustering (HES staining) and the mineralisation areas (Von Kossa staining)	For the collagen I, collagen II and aggrecan labelling (matricial and cellular)
0	no cluster / no mineralisation	no specific staining/labelling
1	Few clusters / few mineralized areas (≤10%)	Slight specific staining/labelling (≤10%)
2	Moderate number of clusters / mineralized areas (10-50%)	Moderate specific staining/labelling (10-50%)
3	Numerous clusters / mineralized areas (≥50%)	Strong specific staining/labelling (≥50%)

4. Results

4.1. Chondrocytes did grow on PyC and CoCr biomaterials without alteration of cell viability

Murine chondrocytes are cultured on discs made of PyC, or CoCr or on plastic culture plates (the control without biomaterial). To assess the biomaterials effect on cells, MTT test is used comparing both biomaterials to the control conditions. The overall cell population was equivalent with PyC or CoCr discs and in control wells (Figure 3).

After 4 hours incubation with the MTT, purple colour is noticed at the surface of the discs which confirm the cells adhesion to the biomaterial's surfaces and the creation of a tissue-like cell-membrane on different support (Figure 3C). Thus, MTT staining that was assessed for cells grown on the biomaterial discs (without considering those grown on the underlying plastic) demonstrated the attachment of the cells to the different biomaterials (Figure 3D). Absorbance scores were normalized to the area of the disc to compare cell adherence on PyC, CoCr or plastic. Both crude observations of the picture and MTT analysis showed that chondrocytes adhered on PyC as well as on plastic control, whereas cell adherence was lower on CoCr (Figures 3C, 3D). The difference in cell attachment between both biomaterials could be explained by the difference in the roughness. So, the poorer cell attachment on CoCr (-28 %) is related to its lower roughness compared to PyC (-35 %).

For LDH assay, a property of less than 5 % of cytotoxicity is considered negligible. Consequently, no cytotoxicity is detected with the tested biomaterials (Figure 3B). The presence of PyC or CoCr did not alter cell viability [159].
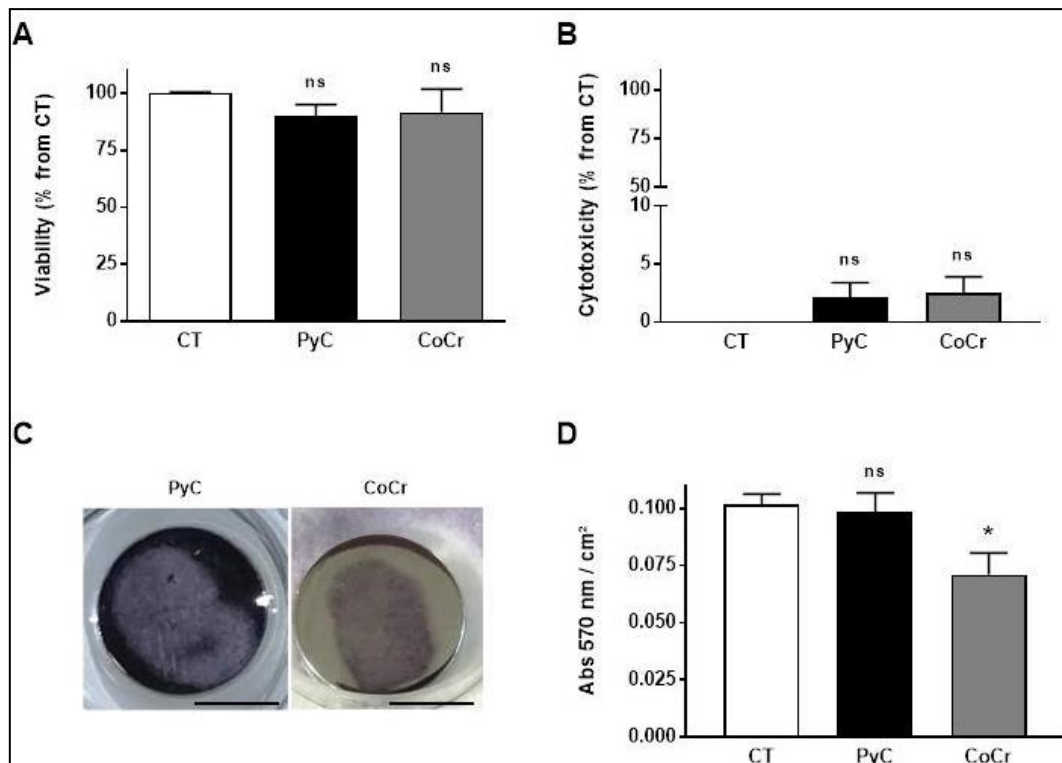
Figure D-3 Growth of chondrocytes onto PyC and CoCr biomaterials without significant alteration of cell viability. Cell viability was measured by MTT assay (A) and biomaterial cytotoxicity on cells by LDH assay (B) and compared with plastic control (CT). (C) Pictures of MTT-stained tissue-like cell-membranes grown on the biomaterials (scale bars: 10 mm). (D) Absorbance measured at 570 nm for MTT assay from cell area on the biomaterial surface. Bars indicate mean ± SEM of 4 independent experiments. ns: no statistical difference, * p<0.05 [159]

4.2. PyC promoted the creation of a homogenous tissue-like cell-membrane of chondrocytes in bone-like conditions (BLC)

Various tests are performed to evaluate the capacity of mineralisation of cultured chondrocytes in BLC. First, cells mineralisation is assessed through biological assays. Secondly, the mechanical properties of the tissue-like cell-membrane developed in biomaterial surface are evaluated. Finally, the tissue-like cell-membrane structure and matrix biological components are analysed histologically.

4.2.1. The capacity of mineralisation of chondrocytes is affected by the presence of the biomaterials

Alizarin red assay is performed to stain calcified deposits from the extracellular matrix. The results of this assay highlighted a diminution of around 60 % of the staining in the presence of both biomaterials compared to the plastic control condition (Figure 4B). Moreover, mineralisation was significantly more significant in the presence of PyC than in the presence of CoCr (1.4 folds). The results of the alizarin red assay are confirmed by the quantitative measurement. Specific calcified deposits assay showed a reduction of about 60 % in both biomaterials comparing to the plastic control (Figure 4C). The difference between PyC and CoCr is not significant.

The obtained results from previous assays corroborate the analysis of TNAP activity. As expected, a decrease of this enzymatic activity in cultured chondrocytes is observed on both PyC and CoCr biomaterials in comparison to the control (Figure 4A). TNAP activity detected in cells grown on PyC is higher than in cells grown on CoCr (2.2 folds) [159].
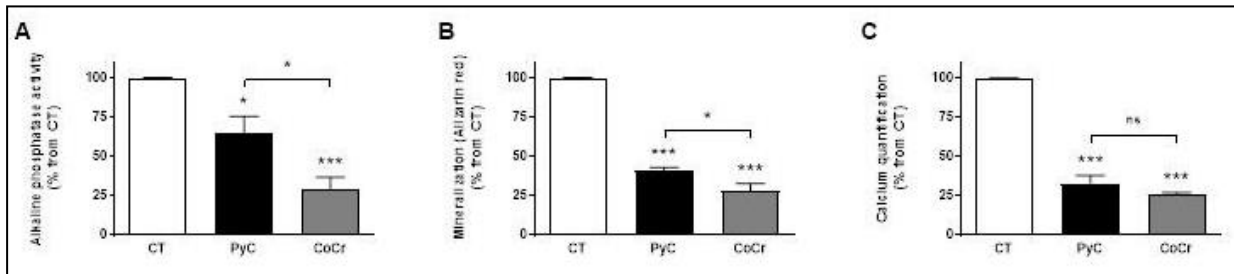
Figure D-4 Mineralisation capacity of chondrocytes grown on PyC and CoCr biomaterials. (A) TNAP enzymatic activity BLC (day 17). (B) Mineralisation (Alizarin red) and (C) calcified deposits quantification. Bars indicate mean ± SEM of 4 or 5 independent experiments. ns: no statistical difference, * p<0.05, *** p<0.001

4.2.2. The mechanical properties of the tissue-like cell-membranes are affected by the presence of biomaterials

The tissue-like cell-membranes developed on both biomaterials are extracted at the end of the cell culture and placed between the two plates of the "tribo-bioreactor" for DMA. For each sample, the complex modulus (G*) is calculated. Three independent experiments are done. The calculation of the elastic modulus G' is performed twice with a displacement frequency of 2 and 4 Hz. This calculation gave acceptable accuracy and reproducible results. The calculated viscous modulus G" and thus the Viscosity η_0 are very variable (Table 4). Therefore, no difference is observed between PyC and CoCr in terms of viscosity. For a better standardisation, results are paired (Figure 5).

The elastic modulus G' of the cell-membrane grown on PyC surface is found 1.8 ± 0.3-fold higher than the one grown on CoCr surface. The DMA results corroborate the previously different behaviour of chondrocytes cultured in BLC on PyC or CoCr. In the presence of PyC the samples were more elastic or more resistant than in the presence of CoCr (both at 2 and 4 Hz; $p = 0.046$ and $p = 0.052$, respectively; $n = 3$; Figure 5).

Table D-4 DMA analysis of chondrocytes cultured under BLC on PyC or CoCr [159]

	Tissue-like cell-membrane on CoCr		Tissue-like cell-membrane on PyC	
Frequency of displacement	2 Hz	4 Hz	2 Hz	4 Hz
Elasticity G' (N/m*m)	1024 ± 399	1092 ± 411	1822 ± 722	1880 ± 660
Viscosity η_0 (Pa.s)	185 ± 116	115 ± 100	170 ± 94	86 ± 47
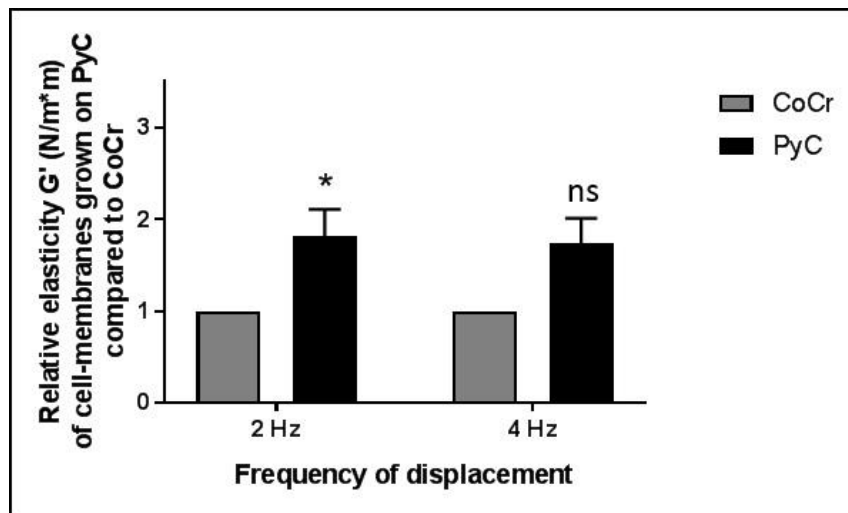
*Figure D-5 Mechanical properties of chondrocytes cultured under BLC on PyC or CoCr. The elastic modulus of the PyC samples was compared to CoCr samples r. * p < 0.05, ns: no statistical difference*

4.2.3. Matrix biological components of the tissue-like cell-membranes

The structure of the tissue-like cell-membrane is analysed histologically. HES staining showed a tissue-like with a large amount of extracellular matrix joining cells together (Figures 6A, 6B, 6C). The overall structure revealed a little difference between control and both PyC and CoCr biomaterials. Many cell clusters are observed in all cell culture support. Numerous clustered hypertrophic chondrocytes are noticed and identified by their large diameter.

In BLC, cultured chondrocytes on plastic control have a heterogeneous size and morphology. They have a round shape and a large nucleus (Figure 6). Cells grown on CoCr surface are very similar to the control, whereas cells grown on PyC surface are more homogeneous (Figure 6B).

Matrix mineralisation is assessed histologically by Von Kossa staining (Figures 6D, 6E, 6F). This analysis confirms our previous assays using alizarin red and calcium assay: more mineralized zones are detected on cell-membranes grown on control than on both biomaterials, and more on the PyC discs than on the CoCr discs. Overall, in BLC, the tissue-like cell-membranes grown on PyC are more mineralized and more homogenous than those grown on other supports (CoCr, control) [159].

Furthermore, the biological components of the extracellular matrix of each tissue-like cell-membranes are analysed. Specific immunolabelling is performed to detect type I and type II collagen and aggrecan. Safranin O staining is used to identify glycosaminoglycans (Figure 7). The major components of the cartilage tissue matrix are type II collagen and glycosaminoglycans attached to aggrecan protein. Type I collagen is present in most body tissue, particularly in healing tissues. However, it is absent in healthy cartilage.
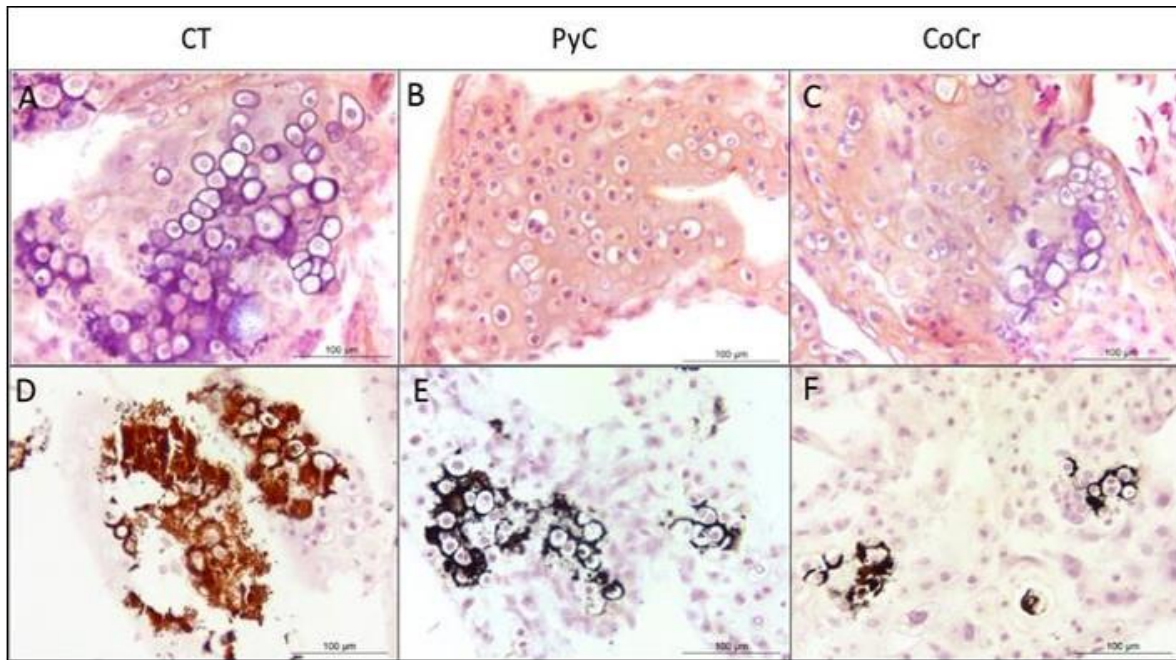
Figure D-6 Histological analysis of chondrocytes cultured under BLC. HES staining (A, B, C) and von Kossa staining (D, E, F) were Histological analysis of chondrocytes cultured under BLC. Hematoxylin-Eosin-Saffron staining (A, B, C) and von Kossa staining (D, E, F) were performed on the tissue-like cell-membranes grown on plastic control (A, D), on PyC discs (B, E) or on CoCr discs (C, F)

In BLC, type I collagen is used as a marker of bone-like tissue matrix. The immunohistological analysis confirmed the tissue-like organization that was suggested by HES staining (Figure 7).

Tissue-like cell-membrane extracted from the plastic control is characterised by a homogeneous extracellular matrix with various amounts of type I and type II collagen and aggrecan (Figures 7A, 7D, 7G). Safranin O staining revealed numerous synthetic zones of glycosaminoglycans, located within hypertrophic chondrocyte clusters, at the periphery of the cells (Figures 7J, 7K, 7L)

The matrix of the cell-membranes grown on both PyC and CoCr biomaterials are more heterogeneous. However, all the studied markers are detected in large amounts, suggesting that matrix compositions are quite similar (Figure 7). The only significant difference between the 3 supports is identified for type II collagen immunolabelling, which is more evident on cell-membranes grown on PyC surface (Figures 7D, 7E, 7F).

Briefly, in BLC, the cultured chondrocytes on PyC biomaterial generate a dense extracellular matrix with cartilage-specific components but also type I collagen.
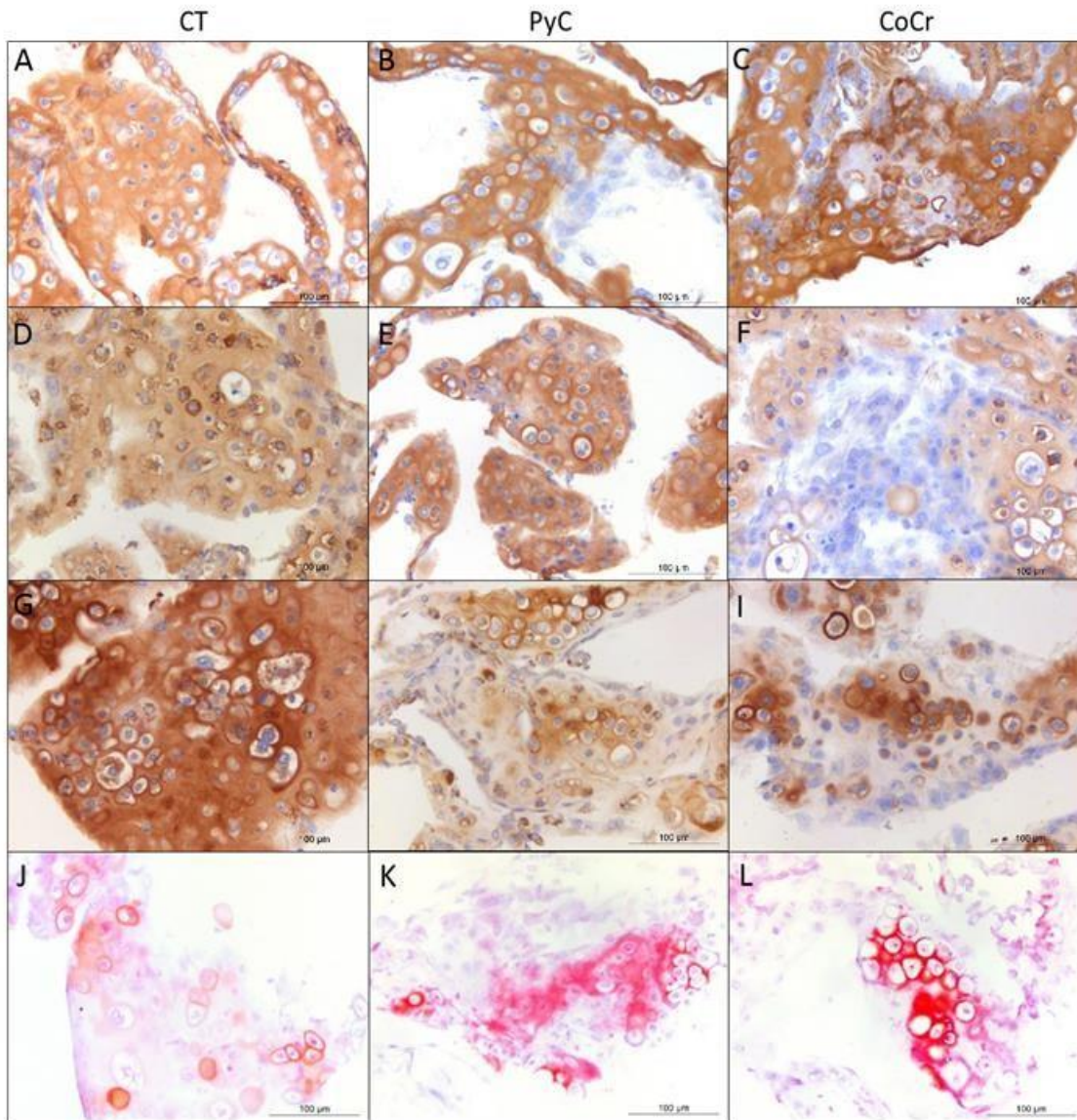
Figure D-7 matrix biological components of the tissue-like cell-membranes grown under BLC. Immunolabelling for type I collagen (A, B, C), type II collagen (D, E, F) and aggrecan (G, H, I) and safranin O staining (J, K, L) were performed on the tissue-like cell-membranes grown on plastic control (A, D, G, J), on PyC surface (B, E, H, K) or CoCr surface (C, F, I, L)

4.3. PyC promoted the creation of a cartilage-like membrane from chondrocytes cultured in cartilage-like conditions (CLC)

The same as BLC, structure and biological components of tissue-like cell-membrane developed in CLC are analysed at the end of the culture period. HES staining reveals a similar tissue-like organization in plastic control and both biomaterials PyC and CoCr (Figures 8A, 8B, 8C).

The cultured chondrocytes in CLC have heterogeneous size and morphology. They are often arranged in clusters (Table 5). In particular, no mineralisation zones are detected, and fewer amounts of clusters of hypertrophic chondrocytes are noticed in these conditions comparing to the BLC (Figure 7, Figure 8). Glycosaminoglycans stained by Safranin O are located within these hypertrophic chondrocytes'

clusters (Figures 8D, 8E, 8F). For the structure, no difference is observed between control and both biomaterials PyC and CoCr (Table 5).
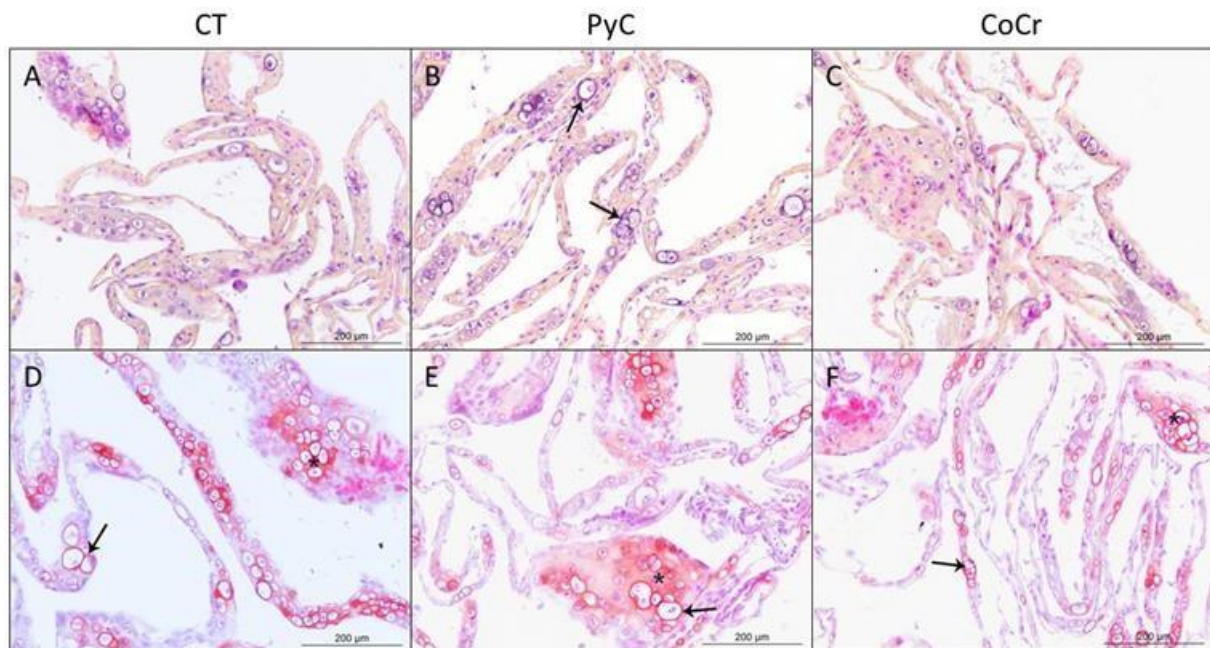
*Figure D-8 Histological analysis of chondrocytes cultured under CLC. Hematoxylin-Eosin-Saffron staining (A, B, C) and Safranin O staining (D, E, F) were performed on the tissue-like cell-membranes grown on plastic control (A, D), on PyC surface (B, E) or CoCr surface (C, F). Arrows indicate hypertrophic chondrocytes and * indicate zones with high glycosaminoglycan content*

However, results of the specific immunolabelling are different depending on the cell culture support. The intensity and the distribution of type I, type II collagen and aggrecan labelling are different between control, PyC and CoCr samples (Figure 9, Tables 5, 3).

In control, the tissue-like cell-membrane is mainly characterized by the presence of type I collagen (Figure 9A) and aggrecan (particularly in the pericellular zone) (Figure 9C). Type II collagen is weakly detectable in the matrix but more visible intracellularly (Figure 9B).

For CoCr samples, type I collagen and aggrecan (Figure 9I) are detectable in the extracellular matrix, same as the control. Thus, a little amount of type II collagen is detected; it appears granular around some hypertrophic cells (Figure 9F).

For PyC samples, aggrecan labelling is similar to the control (Figure 9H) but type I collagen labelling is less intense (Figure 9B). More importantly, the matrix is neatly enriched in type II collagen, which was also detected intracellularly (Figure 9E).

Overall in these conditions, the cultured chondrocytes on PyC generate a tissue-like cell-membrane with a cartilage-like characteristic: more type II and less type I collagen. These matrix components distinguish the PyC from the control and the CoCr [159].

	CT	PyC	CoCr
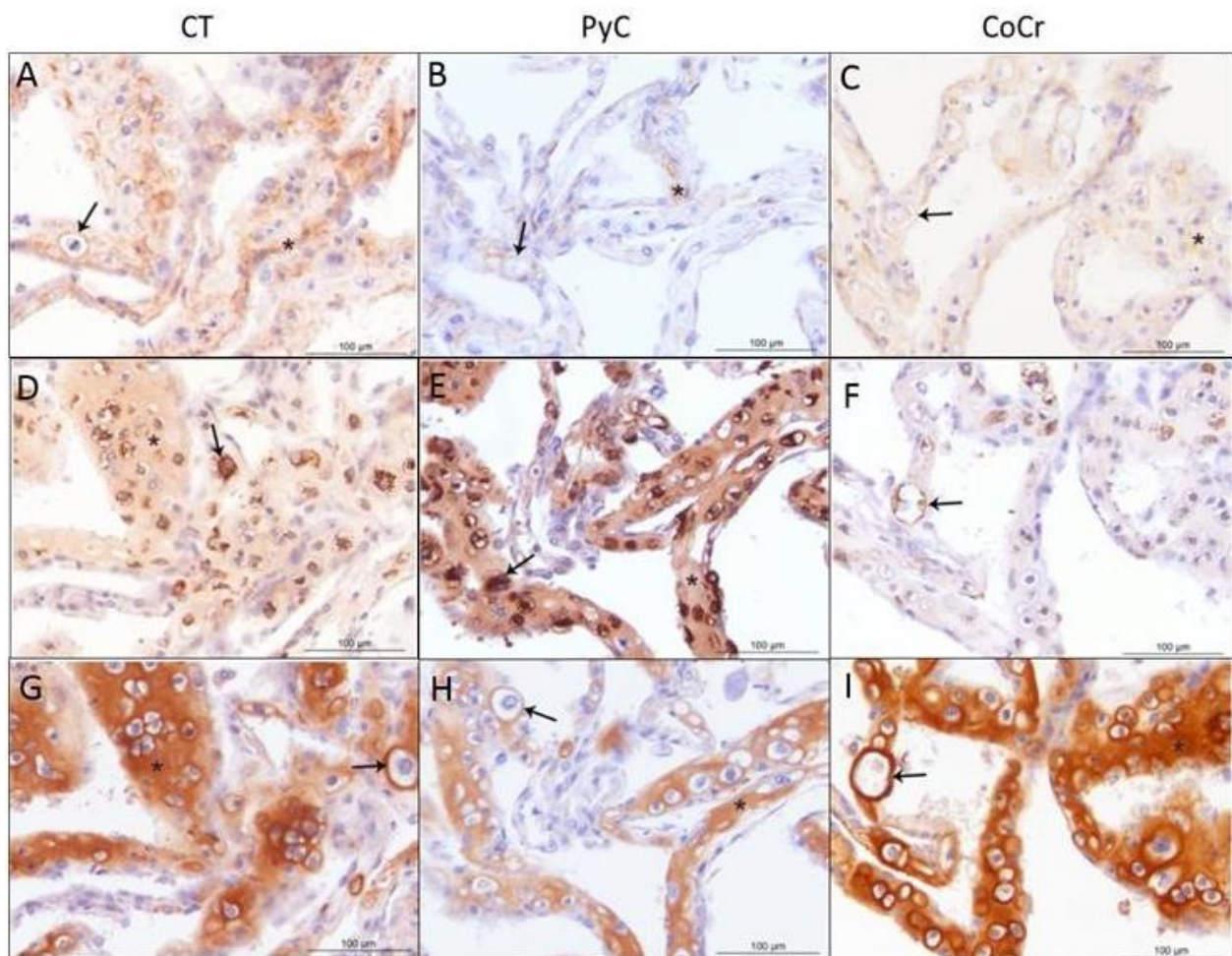
Figure D-9 Matrix biological components of the tissue-like cell-membranes grown under CLC. Immunolabellings for type I collagen (A, B, C), type II collagen (D, E, F) and aggrecan (G, H, I) were performed on the tissue-like cell-membranes grown on plastic control (A, D, G), on PyC surface (B, E, H) or CoCr surface (C, F, I). Arrows indicate hypertrophic chondrocytes and * indicate zones with high specific staining

Table D-5 Histological analysis of chondrocytes cultured under CLC on plastic, PyC or CoCr [159]

	control cell membranes	cell membranes on PyC	cell membranes on CoCr
Chondrocytes clusters	2	2	2
Collagen I	1	0 a,b	1 b
Collagen II	2	3 a,b	1 a,b
Aggrecan	3	2 a,b	3 b

a indicates a difference in comparison to plastic control; b indicates a difference between PyC and CoCr biomaterials (Results are obtained based on table D-3 from § 4.2.2)

5. Discussion

To investigate the biological response to the joint prosthesis, most studies examine the osseointegration (bone growth), the osteoinduction (stimulation of osteogenesis) and the vascularization in the surrounding bone tissue to improve the mechanical stability of the implant [193]. However, the new design of the PyC spherical interposition implant allows overriding this problematic

108

as it is placed in the shoulder without fixation. Due to the surgical procedure to place the interposition implant, the PyC is in contact with chondrocytes which are the critical elements of the first bodies in this configuration. Therefore, our experiments are designed to study the effect of PyC and CoCr in contact with chondrocytes [159].

The results of these experiments, particularly the MTT and LDH tests, proved that both tested biomaterials are innocuous for chondrocytes, which is expected since PyC and CoCr are already used for medical applications. In addition, cell adherence was higher on PyC than on CoCr, which depend on which molecules adsorbed at the biomaterial surface. For instance, osteoblast *in vitro* adhesion to common polystyrene culture plates need the adsorption of extracellular matrix proteins synthesized by bone cells or proteins from the serum used in the culture medium [163] [183] [194]. Our experiments confirmed that surface chemistry and roughness of biomaterials are essential parameters for chondrocytes behaviour [159] [161] [184].

In our experimental model, two conditions are tested: BLC and CLC. The osteogenic potential of the BLC culture media containing ascorbic acid and β-glycerophosphate is already validated in plastic control conditions in previous studies. In BLC, chondrocytes produced lots of extracellular matrix forming tissue-like cell-membranes with mixed characteristics of bone and cartilage. The cells developed a mineralized extracellular matrix and behaved differently on the contact with the PyC or the CoCr. In the presence of PyC, more calcified deposits are observed with higher TNAP activity; thus, the mineralisation capacity is more significant than in the presence of CoCr. Concerning the matrix biological components of the tissue-like cell-membranes, little difference is detected. In these conditions, the PyC surface appears more favourable for type II collagen synthesis, characteristic of cartilage extracellular matrix.

Furthermore, the variations in matrix composition and mineralisation affected the mechanical properties of the tissue-like cell-membranes. For DMA, the calculation of the elastic modulus (G') gave acceptable accuracy. However, the calculation of the viscous modulus (G'') was very variable, which is probably related to the different amounts of medium stuck around the tissue-like cell-membrane for each experiment [159]. The elasticity of the tissue-like was higher in contact with PyC than with CoCr. Thus, more stiffness for the tissue-like cell-membranes developed on PyC surface. This result is explained by the higher level of mineralisation which may contribute to the extracellular matrix stiffening. In BLC, all the experiments ascertain that PyC promotes the creation of stiff well-formed tissue-like membrane [159].

Some studies already evaluate the bone attachment to PyC with controversial results. They suggested that PyC enhances bone ingrowth with a high degree of mineralisation [195]. However, studies in a

rabbit model showed no osseointegration or implant stability for PyC material (chapter B) [145]. The results of our model suggest that in BLC, PyC promotes the formation of a well-organized, well-mineralized and resistant tissue-like cell-membrane.

In CLC conditions, the culture medium is used without adding ascorbic acid and β-glycerophosphate. In the absence of those two components, TNAP activity and Alizarin red staining are maintained at basal level in the culture conditions. At the end of the culture period, tissue-like cell-membranes are identified with much extracellular matrix but no mineralisation. Immunohistological analysis of this matrix revealed a different distribution of the type I and type II collagen and aggrecan between plastic control, PyC and CoCr samples. Importantly, the matrix of chondrocytes grown on PyC contains less type I collagen and is neatly enriched in type II collagen. Consequently, the tissue-like cell-membrane developed on PyC biomaterial in chondrogenic conditions presents characteristics very similar to cartilage [159].

Overall, cell culture experiments demonstrated that in adequate conditions, the PyC could promote cartilage-like tissue growth better than CoCr, with an extracellular matrix enriched in type II collagen. Thus, PyC may be a suitable biomaterial to preserve the glenoid cartilage at the interface with the implant. Our experiments investigated the effect of the PyC on cultured chondrocytes. They are considered as a first study to understand the impact of the PyC on the 1st bodies and to explain the synthesis of the neocartilaginous tissue in the humeral side of the interposition implant.

Also, we show in this section that the chondrocytes adhered differently to the surfaces of PyC and CoCr. Cells attachment was explained by the difference in surface chemistry and roughness. Cell adherence may also be modulated by the molecules adsorbed at the biomaterial surface. Indeed, we already mentioned that the PyC had a particularly high affinity to the phospholipids. Overall, the cell culture experiments could partly explain the *in vivo* results presented in chapter C. In the next chapter, the effect of the PyC on the 3rd body (the lubricant) is investigated *in vitro*.

Understanding the proper functioning of the pyrocarbon *in vitro*: effect on the 3rd body

E. Chapter E: Understanding the proper functioning of the pyrocarbon *in vitro*: effect on the 3rd body

In the previous chapters, the performed experiments compared the PyC to the CoCr. It was showed that the PyC favours the synthesis of type II collagen in murine chondrocytes cultured *in vitro*. Also, it had a high affinity to the phospholipids *in vivo*. Both biomaterials are widely used in direct contact with the articular cartilage, that's why maintaining a viable tissue state in their presence is a common challenge. Despite many efforts to improve the existent implants, their *in vivo* lifespan is still very disappointing compared to that extrapolated from *ex vivo* tribological simulations.

This discrepancy is mainly attributed to the tribological conditions of the *ex vivo* test, insufficiently realistic regards the mechanical and physicochemical particularities of the biological environment.

Notably, the biological liquid in which the joint is immersed (the synovial fluid) is a complex molecular medium. It can represent a good or a bad lubricant for implant surfaces decreasing or increasing their wear.

During pathologies, the synovial fluid undergoes some physicochemical modifications, which reduce the tribological performance of the contacts. Therefore, the optimization of the implants requires a realistic tribological analysis which includes a suitable lubricant (the 3rd body in the biotribological triplet). Here, a new lubricant has been developed for *ex vivo* biotribological simulations with similar lubricating properties as the synovial fluid.

1. The study background

Wear testing of articular cartilage continues being under improvement until today. Experimental devices must maintain a viable tissue state and monitor the wear rates continuously over time. It is challenging to keep the chondrocytes within the cartilage metabolically active. The solution was to reproduce an accurate reproduction of *in vivo* conditions regarding temperature, CO_2, humidity, load and cell viability.

A protocol has been previously suggested by Wimmer and colleagues using a new motion simulator. They used a protocol for polythene and CoCr materials that reflected clinical experience regarding cartilage wear [196]. Different CoCr and PE balls were used. The balls articulated against live cartilage discs with complex trajectories for three days (3 hours per day). The simulator is housed in an incubator to ensure cell viability. After testing, the wear of the cartilage discs was assessed by the proteoglycan/glycosaminoglycans release (DMMB assay). The protocol was validated as the cell viability was maintained throughout wear testing. Comparing both groups, the cartilage surfaces articulating against CoCr stayed intact, and tissue degradation was considerably higher for the cartilage

articulated against polythene. The results agreed with clinical observation [197], where it was found that polythene is not suitable for movable weight-bearing prostheses articulating against cartilage.

In this context, in 2010, a collaboration between Wright Medical/Tornier and the tribology laboratory of the department of orthopaedic surgery at Rush University Medical Centre (RUMC) (Chicago, Illinois) resulted in the development of a similar protocol to compare PyC with CoCr balls articulating against live cartilage. Wright Medical/Tornier is specialized in the manufacture of medical devices for the extremities and of biologics, and the RUMC tribology laboratory is specialized in the study of the friction, the lubrication and the wear of joints, using data from *in vivo* and *in vitro* experiments.

2. Wear testing of PyC vs CoCr using standard lubricant

The bioreactor used in RUMC reproduces similar articular motions as the natural shoulder joint. Thus, for this study, it was considered as a "shoulder simulator". The technical consideration and details of this simulator are presented later in chapter F.

Ex vivo simulations were performed to compare PyC with CoCr articulating against live cartilage using the "shoulder simulator" with biochemical and histological endpoints. The main objectives were:

- Evaluation of wear and tissue integrity after articulating against PyC and CoCr.
- Assessment of cell viability and metabolism of the cartilage discs.
- Assessment of the microscopic tissue morphology.

2.1. Set up for the ex vivo simulations

2.1.1. Loading protocol and standard lubricant

Oval-shaped cartilage explants are obtained from bovine joints. The protocol for explants procurement is detailed in the next chapter F. They are washed three times with fresh PBS then transformed to 12-well culture plate with culture medium for a five-day-long preculture period. The medium is changed every day.

The standard lubricant adopted in the tribology laboratory of RUMC for the *ex vivo* simulations is the classical culture medium for cartilage explant culture. The lubricant is composed of 125 mL of Dulbecco's Modified Eagle Medium with high glucose concentration, L-glutamine and phenol red, 120 mL of Ham's F12 solution (a nutrient mixture), 2.5 mL Mini ITS (Insulin-transferrin-sodium selenite), 2.5 mL of PSF antibiotics, and 250 µL of gentamicin. PSF antibiotics and gentamicin are added to prevent bacterial and fungal contamination. The solution is then filtered using a 0.22 µm vacuum filter for sterilization. The standard lubricant allows preserving the cartilage viability during tribological testing.

After the preculture, four randomly cartilage explants are selected. Each explant is transformed into one station of the simulator. Wear testing was performed to compare PyC and CoCr using the "shoulder simulator" which is housed in an incubator (95 % humidity, 5 % CO_2, and 37 °C) for cartilage survival. Thus, cartilage sample in each station is loaded with a ∅ 28 mm ball of either CoCr or PyC, for 3 hours per day, for 10 days, followed by 2 resting days.

The balls are pressed with 40 N onto cartilage explants. The wear testing followed a specific trajectory. The biomaterials balls oscillated ± 30° sinusoidal movement at 0.5 Hz movement and the sample holders' oscillated ± 15° with a 10 mm offset to generate a migrating contact area. The remaining cartilage explants served as free-swelling controls. They were cultured in the presence of the standard lubricant in the same conditions without articulation against a biomaterial.

Morning and afternoon shifts (two sets) are conducted per day in the presence of the standard lubricant. Then, the used mediums in each station and in control are individually collected and refreshed at the end of the three-hour test. All media samples were stocked for further analysis. Upon test/rest completion, all cartilage explants were also collected.

2.1.2. Analysis of tissue integrity

All media samples are pooled for days 1, 4, 7, and 10 of testing and analysed for evaluation of wear after articulating against PyC and CoCr. The collected mediums are analysed for proteoglycan and hydroxyproline (a marker for collagen) release [198].

As shown in chapter A, proteoglycans are responsible for the swelling properties of cartilage, allowing them to support compressive loading. The cartilage releases proteoglycan due to loading and friction during wear testing. Therefore, proteoglycan is considered biomarkers for cartilage wear. By analysing the concentration of proteoglycan and glycosaminoglycans in the bathing solution before and after wear, it is possible to estimate the amount of wear in cartilage explants.

The Dimethylmethylene Blue Assay (DMMB) assay is used to measure this marker and to study the difference in wear on articular cartilage in the two different lubricants [199]. Hydroxyproline was measured using a hydroxyproline assay kit (Sigma-Aldrich) following the manufacturer's instructions and as already described in [200].

Upon test/rest completion, all cartilage explants are dissected in half, parallel to the wear track path to perform cell viability with live/dead assay and histological appearance (SO staining as previously described in chapter C).

For live/dead assay, a solution of 25 mL of PBS, combined with 4 µL of Calcein AM (Fluorescent marker for live cells) and 8 µL of Ethidium homodimer (a fluorescent marker for dead cells) was prepared. Cartilage punches were cut in half and placed in 1 ml of the prepared solution. Then, they were placed

in the incubator for 45 minutes. After incubation, the explants are imaged at the face where they were cut, to observe a cross-section. Live cells are stained green and dead cells are stained red.

2.2. Results of the *ex vivo* simulations in standard lubricant

The overall results of the simulations showed a layer of dead cells in the upper zone of cartilage explants articulating against both biomaterials. Cell viability was similar for both materials (data not shown). Regarding wear rates, the release of PGs and hydroxyproline into the media during the test was comparable for PyC and CoCr but was significantly higher than the free swelling controls (figure 1).

The extracellular matrix of the cartilage tissue was thus affected by the load so that some molecules were detached from the tissue and released in the standard lubricant. Cartilage tissue degradation was confirmed by histological staining. Indeed, SO staining revealed wear at the surface of the explant with empty cellular lacuna in cartilage discs articulating against CoCr (data not shown).

The result suggests that CoCr may be histologically more damaging than PyC [155] [198]. Overall, our *ex vivo* simulations protocol shows no significant difference between the biomaterials, which is in opposition with the previous conclusions based on the *in vivo* retrieval analysis and the *in vitro* chondrocytes cell cultures approaches.
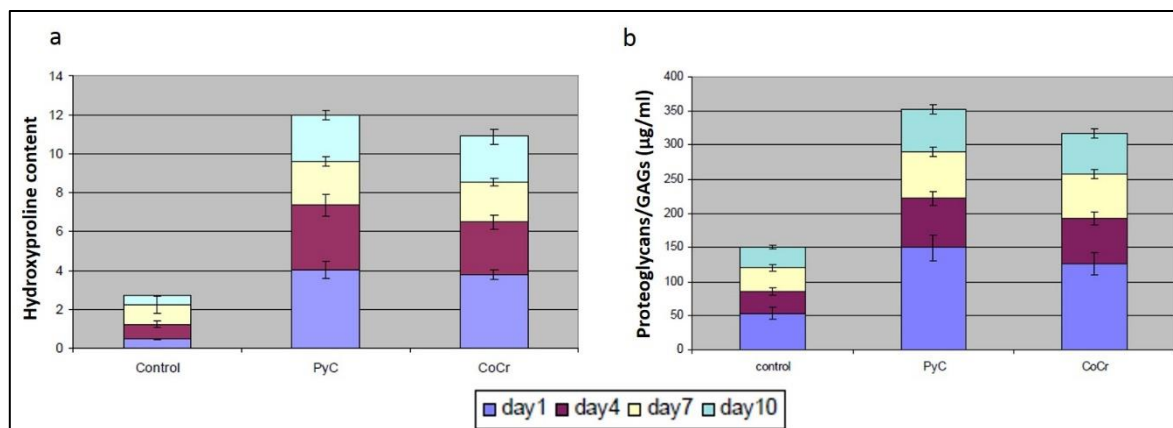
Figure E-1 a) Hydroxyproline content in 1ml aliquots of pooled samples (average ± SEM), b) Proteoglycans/GAGs detected in pooled media samples (average ± SEM) [155].

2.3. The possible reasons behind the difference between *in vivo* observations and *ex vivo* simulations

The present study presented *ex vivo* simulations to compare between PyC and CoCr behaviour articulating against live cartilage. The overall result suggested no significant difference between the tested biomaterials as if PyC irritated the superficial layer of the tested cartilage similarly than CoCr. This result is contradictory with previous analysis and clinical studies; hence the study model should be revised.

The limitations of the study are related to the dimensions of the biomaterials and the used lubricant. First, the used balls were 28 mm in diameter, whereas the simulator was designed to test 32 mm diameter balls, which requires additional adjustments. Second, the tests were conducted in a cell culture medium that maintains the cartilage metabolic activity without containing lubricating proteins. The PyC disrupted the superficial zone of the cartilage similar to the CoCr. However, in the case of PyC, although the superficial area is damaged, the remaining tissue appeared healthier.

In chapter C, the retrieval analysis of different hemi-prostheses showed that the adsorption of the lubricant molecules on the biomaterials surfaces is different between PyC and CoCr. PyC showed an affinity for the phospholipids existing in the natural synovial fluid, which are also important in the natural lubrication process. Hence, *ex vivo* testing in a lubricant such as synovial fluid or similar lubricant could better maintain the integrity of the superficial zone of the cartilage than the culture medium used here. Therefore, it is essential to develop a suitable lubricant for the *ex vivo* simulations to get closer to the results from *in vivo* studies.

3. Development of a new biomimetic lubricant for the *ex vivo* biotribological simulations

In this framework, an experimental lubricant is developed in the research laboratory (LaMCoS). It is called the "serum+" and is consisted of a biomimetic synovial fluid containing the characteristics of the synovial fluid without considering the components ensuring cell viability. Thus, it is used only to conduct *ex vivo* simulations of the contact between biomaterials (total arthroplasty configuration). In the newly developed serum, the importance of phospholipids and hyaluronic acid is mainly considered.

3.1. Production of the first generation of biomimetic lubricants "serum+"

Even though the concentration of the phospholipids in the volume of the synovial fluid is smaller than the other components, they have amphiphilic structures requiring a very low concentration to form interfaces structures as the vesicles [201]. Two variety of phospholipids can be used in the "serum+": either DOPC (Dioleoyl phosphatidylcholine) or DPPC (Dipalmitoyl phosphatidylcholine). In a previous study using a homemade bio-tribometer allowing the measurement of friction coefficient and the *in situ* visualization of contact surfaces by fluorescence microscopy simultaneously, it was showed that the use of DPPC provides a stable coefficient of friction with a very reproductive value in comparison with the DOPC [169]. Besides, the presence of the DPPC in the lubricant reduces the coefficient of friction more than the presence of the DOPC [169]. Consequently, the DPPC is selected to compose the biomimetic synovial fluid, in addition to the hyaluronic acid, which is considered as a major lubricating component in the natural synovial fluid.

Corneci and colleagues have estimated the concentrations of the phospholipids and the hyaluronic acid within the total synovial lipid about respectively 0.1–0.3 mg/ml and 2.42 mg/mL [168]. Based on this study, the mixture of the "serum+" is composed of only bovine serum in which DPPC and hyaluronic acid powders are added with the concentrations 0.3 mg/mL and 2.42 mg/mL.

As showed in chapter A, the phospholipids are organized in a vesicular structure in the synovial fluid, which provides its lubricating properties [202]. To mimic the synovial fluid behaviour, a hyaluronic acid-phospholipid solution is developed, ensuring that the phospholipids form large spherical vesicles [93] [168].

For this study, two biomimetic synovial fluids were synthesized with different structures:

- A Gel-OUT structure where the phospholipid (DPPC) vesicles are surrounded by a glycoprotein gel (hyaluronic acid)

- A Gel-IN structure where the DPPC vesicles are filled with a glycoprotein gel serum.

3.2.   Tribological properties of the "serum+" lubricants

Tribological studies are performed to compare the behaviour of the two developed serums to healthy natural synovial fluid [96]. The healthy synovial fluid was collected from two equine carpal joints. Friction test was performed using a homemade bio-tribometer to reproduce the boundary lubrication regime, with the 3 media: "serum+ gel-in", "serum+ gel-out" and natural synovial fluid. The coefficient of friction was measured between a soft hydrophilic lens HEMA (to mimic the cartilage) and a flat glass plate.

The overall results of the study showed that the healthy synovial fluid and the biomimetic synovial fluid with the Gel-IN structure had a comparable tribological behaviour. They ensured a low and stable friction coefficient. The study suggested that the tribological behaviour is provided by the vesicular structures that included the glycoprotein gel [96]. Consequently, for the new lubricant "serum+" the Gel-IN structure was selected for the further tribological simulations performed in the laboratory.

The "serum+" has a similar tribological behaviour as the synovial fluid; however, it is not adequate for the use with biological tissues or live cartilage. Thus, it could not replace the standard serum used in wear testing with live cartilage. Therefore, we aimed to develop a new serum/lubricant which nourishes the cells and contains similar lubricating proteins as the synovial fluid.

3.3.   Optimization of the biomimetic lubricant for the use with biological samples

As showed above (§ 2) a current limitation in the tribological testing of live cartilage in RUMC involved the use of cell-culture media as a standard lubricant. However, it was not possible to use the "serum+" in the testing since it did not ensure cell viability. Consequently, we aimed to develop another lubricant

for tribological testing using live cartilage. Our strategy was to associate the biological components of the standard lubricant (cell-culture media) with the lubricating ingredients of the "serum+" (Gel-IN structure with DPPC and hyaluronic acid). We hypothesized that a cell culture medium supplemented with DPPC vesicles and hyaluronic acid would improve cell viability and ensure lower friction.

Briefly, DPPC (0.3 mg/mL) and hyaluronic acid (2.42 mg/mL) were added to the cell culture medium To create liposomes within the medium, the DPPC powder is dissolved in chloroform. 15 µL of the fluorescent marker is added immediately.

Using a rotary evaporator, the solvent is evaporated from the mixture, causing the lipids suspension against the side of the round bottom flask. The transition temperature of DPPC (41 °C) is respected, allowing the lipids to create a multilayer against the wall of the flask (figure 3). The dissolution and the evaporation steps are repeated five times to ensure enough layers of lipids had formed.

The last round of evaporation lasts several hours, to remove all chloroform traces since it is toxic for the cells. Then, 100 mL of the control medium is heated and added to the lipids for hydration. This solution is agitated for 10 min until DPPC dissolution. Powdered hyaluronic acid is then added. The new solution called "HA–phospholipid medium" is rotated until the hyaluronic acid dissolution respecting at 47 °C. The reagents used in this protocol are detailed in figure 2 [203].

Hyaluronic acid sodium salt from *Streptococcus equi*
■ Purity ≤ 1% protein
■ Sigma Aldrich (St. Louis, MO, USA)
■ Molecular weight ~1.5–1.8 × 10^6 Da
■ Cat No. 53747
16:0 PC (DPPC) 1,2-dipalmitoyl-*sn*-glycero-3-phosphocholine
■ Avanti Polar Lipids, Inc. (Alabaster, AL, USA)
■ Molecular weight 734.039
■ Purity > 99%
■ Cat No. 850355C
Ethyl Alcohol 200 Proof
■ Pharmco-Aaper (Brookfield, CT, USA)
■ Absolute, Anhydrous
■ Cat No. 111000200
Chloroform
■ Sigma-Aldrich
■ 0.5–1.0% ethanol as stabilizer
■ Purity ≥ 99.8%
■ Cat No. 439142
14:0–06:0 NBD PC Fluorescent Marker
■ Avanti Polar Lipids
■ Cat No. 810122

Figure E-2 Materials for the preparation of Phospholipid Medium [203]

Amira HANNOUN/ Thesis in Biomechanics 2020/ INSA Lyon
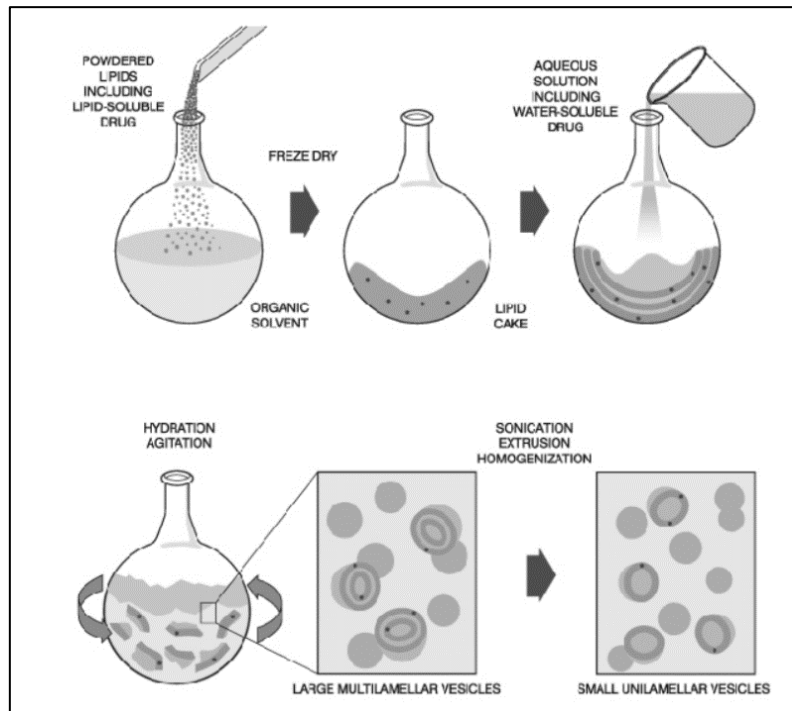
Figure E-3 Protocol for the formation of the liposomes (From the technical support- Avanti Polar Lipids)

3.4. Biological innocuousness of the new HA-phospholipids medium

3.4.1. Physicochemical properties

First, the HA-phospholipids medium structure was verified by the fluorescent images. The addition of the NBD PC fluorescent marker in the medium allowed the visualization of the formed vesicles within the lubricant. It contained many liposomes throughout the solution ranged from 0.1 to 50 µm, as shown in figure 4. Besides, its rheological properties were tested by Veselack and colleagues using a rheometer with plate-on-plate configuration [203].

A shear strain rate of 20.000 s^{-1} was applied to 0.5 ml of the lubricant. The measurement revealed better rheological properties of the HA-phospholipids medium in comparison with the standard cell-culture medium (figure 5): the viscosity was increased by 5 folds (3.92 ± 0.07 mPa, 0.73 ±0.01 mPa, p < 0.001) [203].
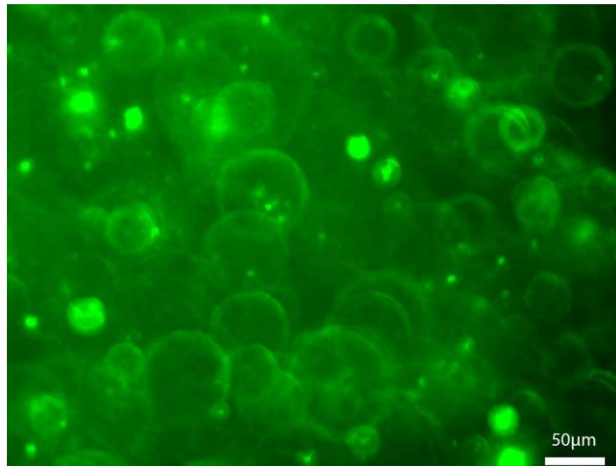
Figure E-4 Fluorescent image of liposomes (20X) [203]
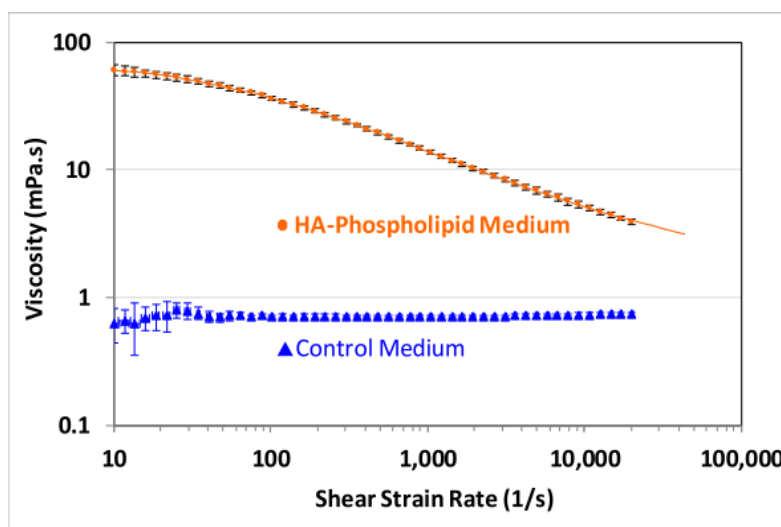
Figure E-5 Viscosity curves for the HA–phospholipid and control media. The error bars denote the 95% confidence intervals; the curve has been extended beyond the measurement range for visibility [203]

3.4.2. Biocompatibility with cartilage explants

The HA-phospholipids medium was evaluated for cell viability in comparison to the standard cell culture medium. Biopsy punches (3 mm x 2 mm) were obtained from bovine stifle joints. The punches were cultured randomly in either HA–phospholipid medium or the standard medium. Cells viability was tested after 7 days of culture using live/dead imaging (§ 2.1.2).

Amira HANNOUN/ Thesis in Biomechanics 2020/ INSA Lyon
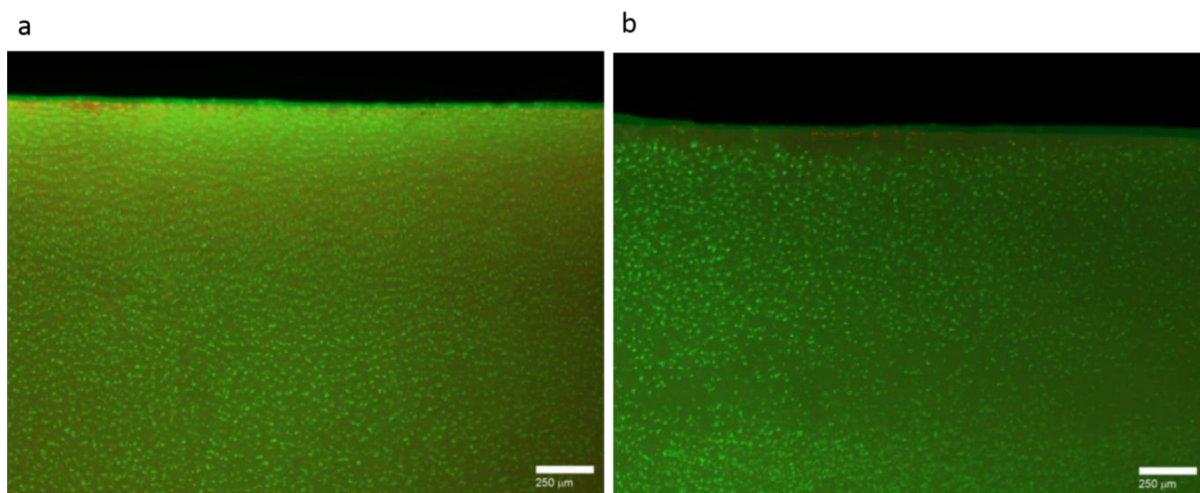
Figure E-6 Histological sections of a tangential layer of cartilage biopsy punch cultured in standard serum (a) and HA-phospholipids serum (b) [204]

The performed viability test revealed a significant difference between both lubricants: the HA-phospholipids one showed better cell viability (figure 6) [203] [204]. Living cells (stained in green) are homogeneously distributed throughout the explant, even in the superficial areas. On the contrary, no living cells are observed in the upper 100 µm of the explant with the standard lubricant. Thus, the HA-phospholipids is considered innocuous for cartilage explants and could be used for tribological simulations.

3.4.3. Innocuousness for cultured chondrocytes

We aim to confirm the nontoxicity that was observed on cartilage explants on cultured chondrocytes. The chondrocytes in the explants obtained from bovine joints presented a mature state; they are already embedded in their extracellular matrix and are metabolically stable. Therefore, cell culture of murine chondrocytes is performed in the presence of either the HA-phospholipids serum or the culture medium (CLC) (chapter D, §3.2). The only difference between the standard medium and the CLC medium is the use of the Mini ITS for the explants instead of the FBS for the cultured chondrocytes.

First, the cell viability was assessed by MTT assay. During the test, it was noticed that the viscosity of the new lubricant did not allow the penetration of the MTT inside the developed tissue-like cell-membrane. The results were thus exploitable. Hence, the effect of both lubricants was evaluated histologically. At the end of cell culture, tissue-like cell-membrane grown in either CLC medium or HA-phospholipids medium is removed from the culture plate and fixed in 4 % (v:v) formalin. Different stainings are performed to evaluate the structure of each sample, as previously described in chapter C: HES, SO. In addition, specific immunolabelling are performed to identify the extracellular matrix components type I and type II collagen and aggrecan.
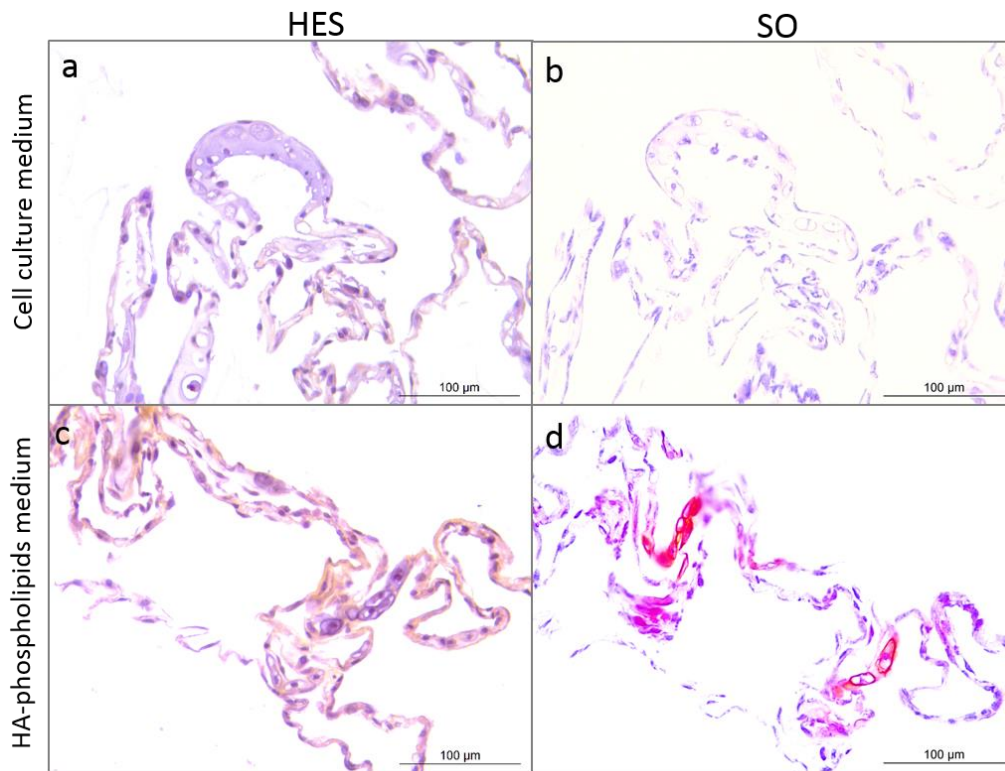
Figure E-7 Histological analysis of chondrocytes cultured with CLC medium and HA-phospholipids medium HES staining (a, b) and SO staining (c, d)

The HES staining highlighted a similar structure between the samples (figure 7a, c). No significant difference was noticed. In both samples, cells were large with a rounded shape attesting their chondrogenic phenotype. However, the SO staining was more abundant in the presence of HA-phospholipids, indicating the presence of more glycosaminoglycans (figure 7b, d). SO staining is not an indicator for cell viability; however, it highlights the synthesis of the glycosaminoglycans, which indicates the presence of active cells. Thus, the use of the HA-phospholipids medium does not alter cell viability.

The specific immunolabelling suggested that the chondrocytes were metabolically active and synthesized an extracellular matrix with a chondrogenic phenotype in the presence of HA-phospholipids medium (figure 8). Aggrecan labelling was intense in both samples (figures 8c, f); however, slight differences were noticed with type I and type II collagen labellings. The collagen type I was negative for the tissue-like cell-membrane developed in the presence of both mediums: HA-phospholipids medium and CLC (figures a, d). Under CLC, collagen type II labelling was localized essentially on some chondrocytes cells with heterogeneous distribution (figure 8b). Using the HA-phospholipids medium, the collagen type II was restricted on the extracellular matrix.

Overall, histological analyses confirmed the benefits of using the HA-phospholipids medium in comparison with the standard cell culture medium. The viscosity of the lubricant is highly improved

while being innocuous for cultured chondrocytes. Second, it contributed to the synthesis of an extracellular matrix with cartilage characteristics. Based on these analyses, the HA-phospholipids medium is adopted for future tribological simulations.
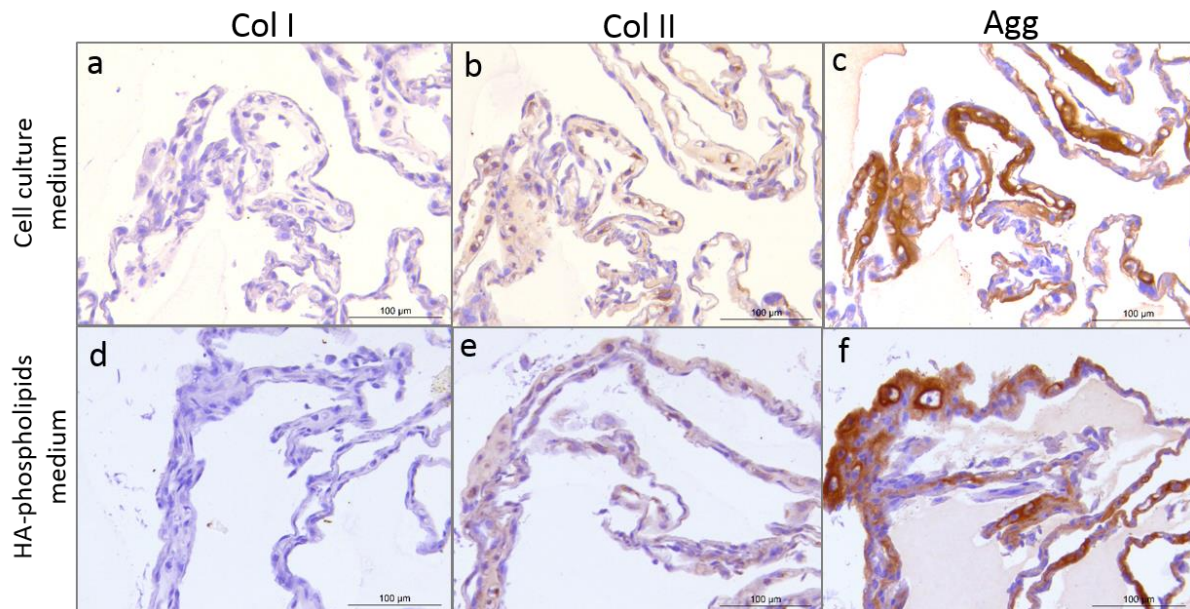
Figure E-8 matrix biological components of the tissue-like cell-membranes grown under CLC (a, b, c) and in the presence of HA-phospholipids medium (d, e, f). Immunolabelling for type I collagen (a, d), type II collagen (b, e) and aggrecan (c, f) were performed on the developed tissue-like cell-membrane.

3.5.   Revised protocol for the synthesis of the HA-phospholipids medium

As continuity for testing the biomaterials behaviour articulating against live cartilage, this part of the project was realized in the tribology laboratory of RUMC to use the available "shoulder simulator" with the HA-phospholipids medium. However, the protocol elaborated to synthesize this lubricant (§ 3.3) was challenging to reproduce. In particular, no rotary evaporator was available in the RUMC laboratory. Here, we aimed to validate a new protocol of the medium fabrication and to test its effect using wear and friction tests.

The lipids supplier (Avanti) confirmed the ability of the provided DPPC powder to dissolve without using an evaporation step. Accordingly, a new protocol was considered. It consists of heating the culture medium at 47 °C and then adding the HA and DPPC powders respecting the previous concentrations (2.42 mg/ml for HA and 0.3 mg/ml for the DPPC) and vortex vigorously The obtained solution is let in rotation during a minimum of 2 hours at 47 °C.

Since the fluorescent marker is provided in chloroform solution (toxic for the cells), it is used only to evaluate the structure of the new HA-phospholipids serum using fluorescent microscopy. Observations showed the overall structure of the new serum, which contains vesicles (figure 9). Thus, the liposomes were well-formed with the new protocol. However, in comparison with the first protocol (figure 9), it

Amira HANNOUN/ Thesis in Biomechanics 2020/ INSA Lyon

seemed that some lipids were sequestered in the deposit and did not form vesicles. Furthermore, the previous serum contained more prominent vesicles with Gel-In structure. Microscopic visualisation of the new serum showed the presence of vesicles with a mixture of Gel-IN and Gel-OUT structures. Probably, the DPPC powder was not able to dissolve totally in the solution.
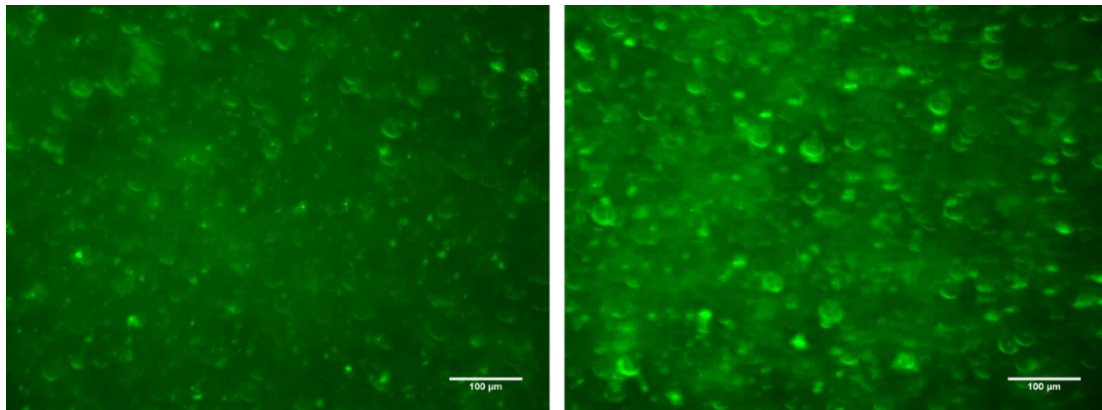
Figure E-9 Fluorescent images of liposomes in the serum synthesised with the new protocol

As presented previously, the protocol for HA-phospholipids medium fabrication was updated to reduce the time of its synthesis and to simplify the used materials and the methods. However, with the updated protocol, there were some doubts about the serum structure and whether it contains Gel-IN vesicles or a mixture between Gel-IN and Gel-OUT vesicles. As presented previously, with the Gel-IN structure, the medium has better lubrication contribution [96]. Besides, with the first protocol, microscopic observation revealed a Gel-IN structure with bigger vesicles within the serum in comparison with the updated protocol.

Neither tribological nor biological properties of this last generation of lubricant have been tested to date. However, the lubricant still contains the ingredients ensuring cell viability and those providing the lubrication. That's why we assumed that the different structure between the two protocols would not affect the tribological simulations.

4. Conclusion

This part of the project overrides the limitations of the previous tribological testing by providing a new biomimetic lubricant. As mentioned before, the natural 3rd body is a complex molecular medium which could affect the tribological performances of the joint implant. Thus, the developed 3rd body combines the lubrication properties and the structure of the natural synovial fluid and the biological considerations to respect the cell viability. For the next step, it is necessary to test the HA-phospholipids lubricant with biotribological simulations and to evaluate the effect of the mechanism in the case of the biomaterials articulating against living cartilage. The objective of the *in vitro* biotribological simulations always being to improve existing prostheses.

Amira HANNOUN/ Thesis in Biomechanics 2020/ INSA Lyon

Cette thèse est accessible à l'adresse : http://theses.insa-lyon.fr/publication/2020LYSEI025/these.pdf
© [A. Hannoun], [2020], INSA Lyon, tous droits réservés

Understanding the proper functioning of the pyrocarbon *in vitro*: effect on the mechanism

F. Chapter F: Understanding the proper functioning of the pyrocarbon *in vitro*: effect on the mechanism

In the previous chapters, the experiments on the live biotribological triplet showed that the PyC was a favourable biomaterial for joint replacement *in vivo*. Indeed, the PyC preserve the 1st body (cartilage) by inducing minimal wear. *In vitro*, it favours the synthesis of type II collagen in murine chondrocytes, so probably the remodelling of the surrounding tissues after implantation. Also, it showed an affinity to the phospholipids that facilitate the sliding of the surface. To perform proper *ex vivo* tribological tests, a new biomimetic lubricant has been developed. Thus, the effect of the PyC on the 1st body and 3rd body was particularly explored. In addition, the performance of the biomaterial replacement could be affected by the *in vivo* mechanism, i.e. the mechanical system containing the 1st bodies, which is the last actor of the tribological triplet.

In chapter C, the histological analysis suggested that the PyC implants provide proper mechanical transmission, which in turn favours a benefic bone remodelling. Furthermore, it was showed that the mechanical stresses applied in the implant could affect the synthesis of the different components of the extracellular matrix, which are responsible for its mechanical properties.

Here, we focus on the effect of different mechanisms on the biomaterials behaviour articulating against live cartilage. Again, PyC was compared to CoCr, both being widely used in the prosthesis in direct contact with cartilage. First, the friction test is performed to compare the coefficient of friction between the biomaterials in the presence of the HA-phospholipids lubricant. Second, a joint motion simulator is used to examine the effect of PyC and CoCr in realistic physicochemical and mechanical conditions. We hypothesized that in suitable conditions, the PyC might cause less damage to the articular surfaces than the CoCr.

1. Cartilage explants used in the biotribological simulations

Bovine stifle joints of 24-26 week-old animals, recently slaughtered, are obtained from a local abattoir. In a sterile hood, the bovine stifle joint is exposed carefully by stripping the tissue from the bone without cutting or damaging the trochlea cartilage. The exposed trochlea is then cleaned gently with PBS to remove any blood. The exposed joint is then covered with wet gauzes to keep it hydrated until cutting the cartilage explant.

To obtain cartilage explants, healthy plane area of the middle region of trochlea cartilage are identified. Then, with a scalpel, the edges of the trochlea are cut along. The explants are cut out with an oval-shaped punch (Maximum length= 20 mm, Diameter= 14 mm) (figure 1). The length of the explant is parallel to the range of motion the cartilage is exposed to in the knee. The bottom surface of explant

is trimmed using a scaffold block. The explant is then placed into a sterile 12-well culture plate with PBS and thoroughly identified (animal and joint side: right, left).
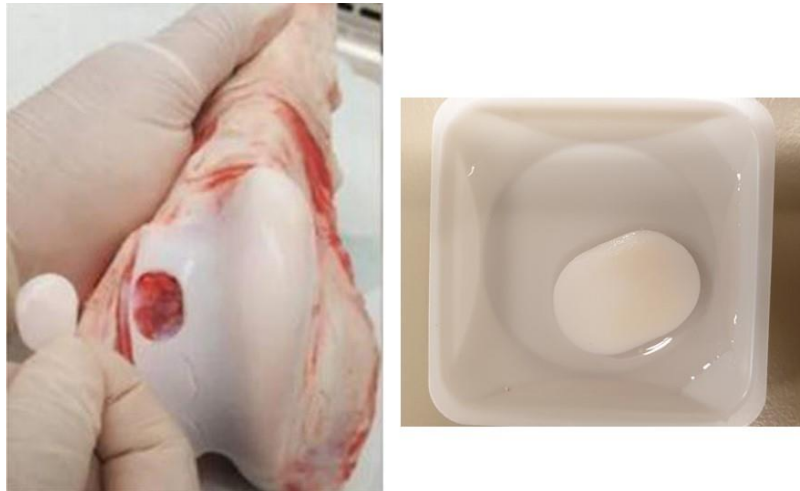
Figure F-1 Cartilage explant from the trochlear groove

2. Effect of the biomaterials in friction against live cartilage discs

2.1. The testing set up

This test aims to compare the coefficient of friction (COF) (or friction factor) between PyC and CoCr articulating against bovine cartilage in two different lubricants: Standard medium and HA-phospholipids medium. As presented in chapter E, there are two protocols for HA-phospholipids medium fabrication. In this test, the lubricant was obtained with the second method. The experiment was performed in the tribology laboratory of RUMC, on a wheel on flat (WOF) device (figure 2). Only CoCr and PyC balls and not wheels were available to perform the test. Consequently, a ball holder was conceived to support the sample during the test.

Thus, friction is measured using a ball-on-flat configuration in which ball made of CoCr or PyC provided by Wright Medical/Tornier is articulated against a flat confined bovine articular cartilage disc immersed in a lubricant (figure 3b, c). The COF of both biomaterials is compared to the COF of cartilage articulating against cartilage (figure 3a). To provide a cartilage counter-face for the cartilage-on-cartilage testing, cartilage strip (45 mm length x 8 mm width x 3 mm height) is removed with a scalpel from the trochlear rim as previously detailed in [205]. The strip was adapted with a specific holder to replace the ball in cartilage/cartilage configuration (figure 3). The tested explants are obtained from different animals and randomized for the test.

The device is equipped with different hydraulic actuators. For the friction test, only the horizontal actuator is used. Its displacement caused the translation of the cartilage holder. The tangential force is measured with a load cell.

The WOF Set-up

Fixture for the ball/strip holder

PE scaffold
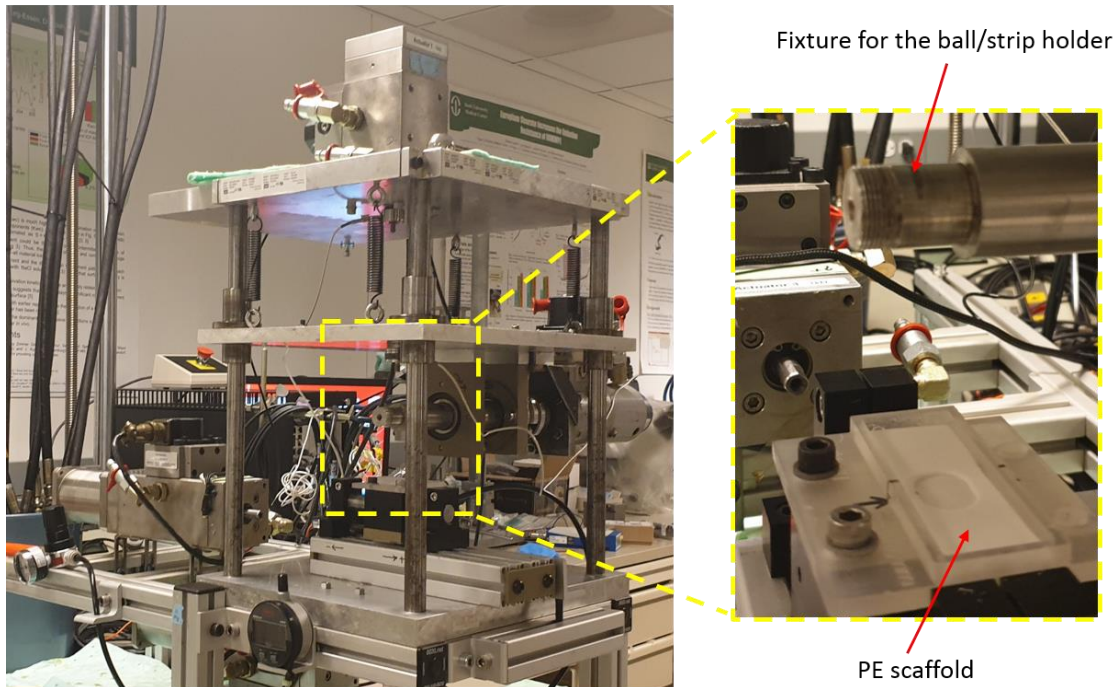
Figure F-2 the friction test set-up

The stationary ball is pressed on cartilage disc with 40 N normal load. The sliding distance of the ball against the cartilage is 6 mm. The friction test is performed with three different velocities for one hour each: 10 mm/s, 20 mm/s and 40 mm/s (figure 4). For each biomaterial (CoCr, PyC or cartilage) and each lubricant (standard or HA-phospholipids medium), three different tests are performed with fresh medium, and fresh cartilage explant (figures 3, 4) and the frictional (or tangential) force is measured (in N). Then, the COF is computed by dividing the average measured force (for one minute) by the normal force.
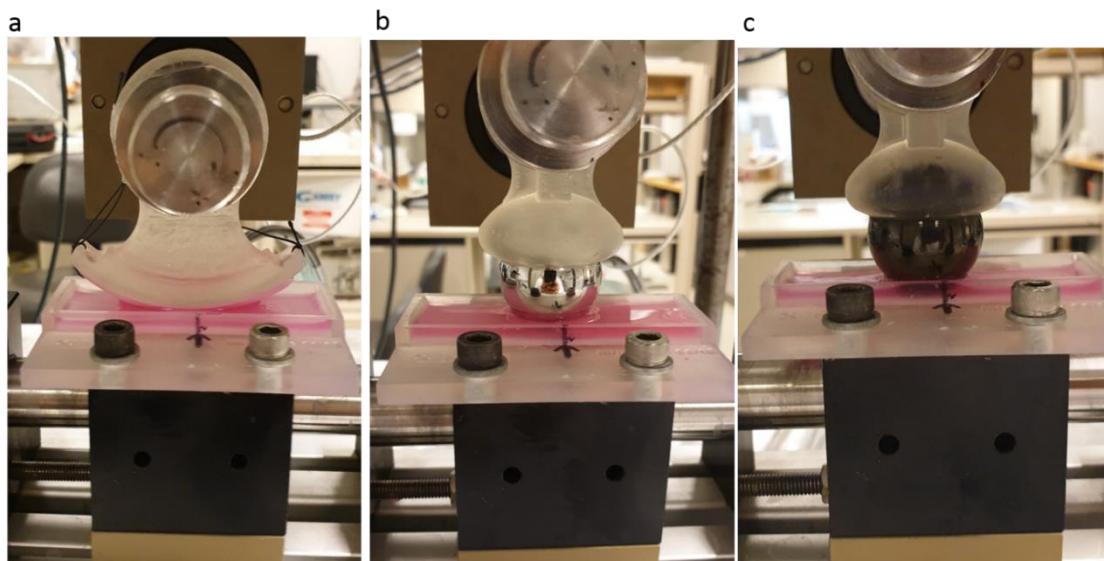
Figure F-3 Different configurations for the friction test: a) Cartilage articulating against cartilage b) CoCr ball articulating against cartilage, and c) PyC ball articulating against cartilage

Amira HANNOUN/ Thesis in Biomechanics 2020/ INSA Lyon
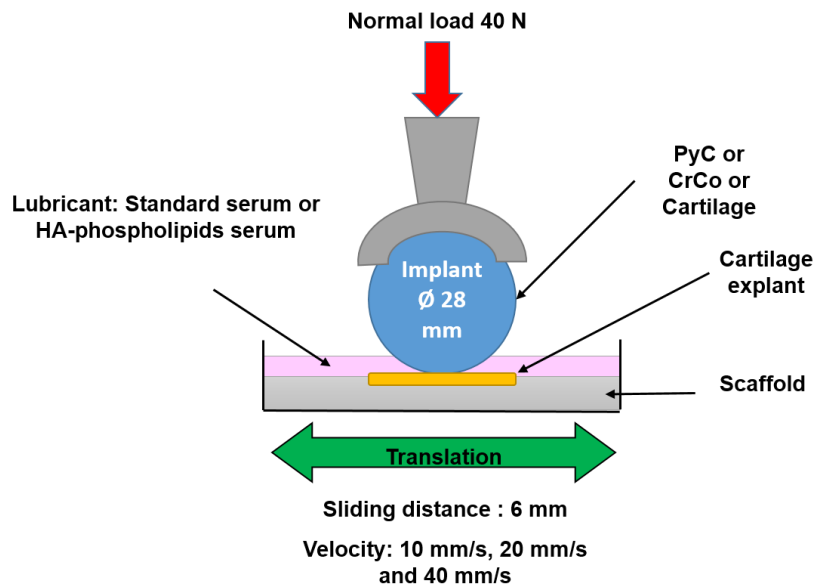
Figure F-4 schema of the friction test set-up

2.2. The biomaterials affect the cartilage explants differently in friction testing

For all tests, starting at the 10-min time point, the curves of the COFs start to plateau to a steady-state. Independently of the tested velocities, the used lubricants and cartilage explants, the friction factors COFs were higher in the case of both biomaterials in comparison with the cartilage/cartilage configuration. The highest COFs were noticed with CoCr balls articulating against cartilage. To further analyse the results, tests using cartilage explants obtained from the same animal were considered. Indeed, due to experimental constraints, tested cartilage explants were obtained from different animals which could cause the variability of the results. Many factors could affect the cartilage explants state: the animal age, the explantation zone…

2.2.1. Effect of the lubricant on the COF

The impact of the lubricant on the COF of cartilage articulating against cartilage was first evaluated (Figure 5). In this configuration, the COF of cartilage/cartilage increased ≈2.7-fold when using the HA-phospholipids medium in comparison to the standard medium. The difference between the COF was statistically significant. This observation is counterintuitive as one would expect an easier cartilage/cartilage sliding with a better lubricant. However, this result could be caused by the higher viscosity of the HA-phospholipids lubricant (figure E-5) [203]. Also, hyaluronic acid and phospholipids of the medium could cause the swelling of the cartilage on both sides of the contact and affect the measure.

As presented in chapter E, the HA-phospholipids medium provided better cell viability and contributed to a better extracellular matrix synthesis than the cell culture medium (figures E-6, E-8). The difference

in COF between the two lubricants may reflect the difference in the healthiness of the cartilage explants.
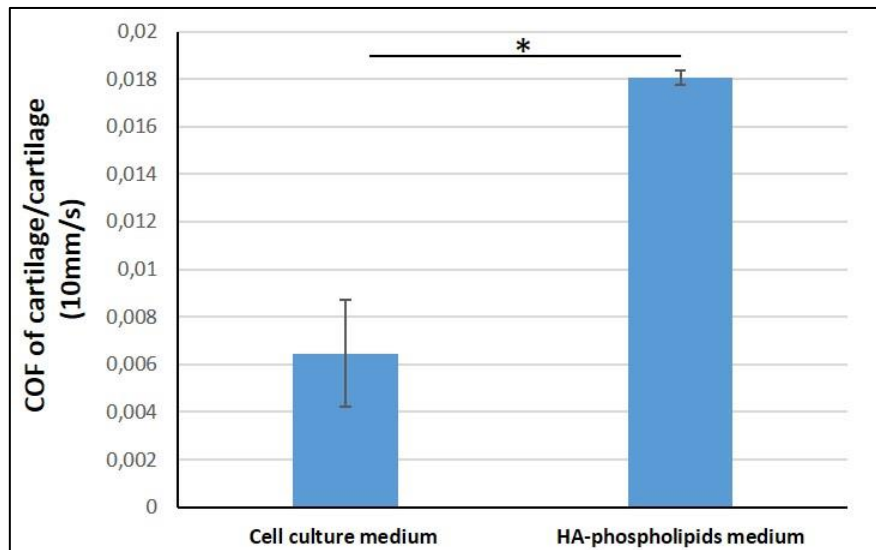
*Figure F-5 the effect of the lubricant in the friction tests (velocity 10 mm/s). The bars present the COFs of the cartilage/cartilage configuration measured using either the standard lubricant or the HA-phospholipids lubricant (Bars indicate mean ± SEM, * p <0.05)*

The effect of the lubricant on the COF of biomaterial articulating against cartilage was then evaluated. For these tests, contrarily to the cartilage/cartilage, the COF of the tested biomaterial decreased when using the HA-phospholipids medium: 53% lowering for the PyC and 63 % lowering for the CoCr.

These results confirmed our previous hypothesis about the importance of the used lubricant in tribological simulations. The same observations were made using the two protocols for the HA-phospholipids medium fabrication. The test was performed with another setup, and it showed a 20 % lowering of the COF of CoCr articulating against live cartilage in comparison with the standard lubricant [203].

2.2.2. Effect of the biomaterial on the COF

To compare the effect of the biomaterials and for better standardisation, results were paired: the COFs obtained with the PyC were compared to those obtained with the CoCr in the same lubricant (Figure 6). The three configurations (Cartilage/cartilage, PyC/cartilage and CoCr/cartilage) were tested with cartilage explants obtained from the same animal. The ratio between the COF of the biomaterial and the COF of the cartilage (control) was calculated.

Friction test in the presence of the standard lubricant showed that the COF of the CoCr was 3.2-fold higher than the COF of the PyC, while in the presence of the HA-phospholipids the COF of CoCr was 2.2-fold higher than the COF of the PyC. Thus, with the two lubricants, both biomaterials showed the same behaviour: in any case, the COF of CoCr is statistically higher than the COF of PyC. This result

corroborates our previous data by demonstrating that the PyC allow better lubrication and an easier sliding of the cartilage against the biomaterial. The expected consequences would be reduced wear and better preservation of the tissue facing the implant.
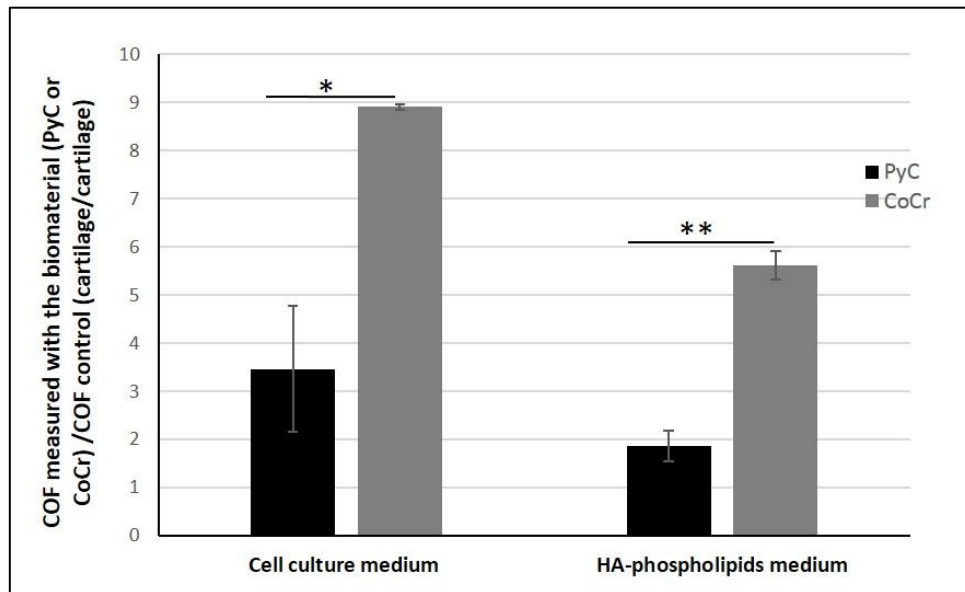
*Figure F-6 the effect of the tested biomaterial in the friction test. The bars present the ratio between the COF of the tested biomaterial and the COF of the control (cartilage) measured using same lubricant (Bars indicate mean ± SEM; * p< 0.05, ** p< 0.01)*

2.2.3. Conclusions and limits of the friction test

As hypothesised previously, the presence of DPPC and hyaluronic acid affected the tribological behaviour of the tested biomaterials. Of interest, a difference between the PyC and the CoCr was observed using the new lubricant in the friction tests. However, the friction factor alone could not be considered as a critical parameter of wear behaviour. The friction test presented only one movement and could not offer the natural mechanism of the joint. Therefore, it is still needed to evaluate the cartilage wear articulating against the biomaterials with adequate movements. Consequently, we decided to repeat the wear testing presented previously in chapter E and in [198] to compare PyC to CoCr using the newly developed lubricant (HA-Phospholipids medium) in the shoulder simulator.

3. *In vitro* wear testing of living cartilage against PyC and CoCr

3.1. The mechanical simulator

3.1.1. History and optimization of the device

In 2004, Wimmer and his team developed a new simulator respecting the articular motion. The developed prototype ensures the rotation of a scaffold with a sample of cartilage against a rotating ball made with the biomaterial to be tested. The cartilage sample is pressed orthogonally against the

ball. The generated compression force is controlled with a load sensor. The rotation of the ball and the scaffold is ensured by two-step-motors (figure 7a). The concept of the simulator is detailed in [206]. The prototype was validated comparing the free-swelling configuration and a compression-loaded sample using nasal cartilage. The simulator was initially designed with one station. It is later improved to include four individual stations to ensure test reproducibility in the same conditions (figure 7b) and thus facilitates the investigations of the mechanical solicitations at the contacting surfaces. The prototype respects the tribological considerations, and it allows to create complex shear force patterns on the surface of the cartilage.

This simulator was used in 2010 to evaluate the cartilage wear articulating against PyC and CoCr balls [198]. The limitations of this study were the dimensions of the biomaterials balls, which require some adjustments on the simulator and the used lubricant. Indeed, the used balls were 28 mm in diameter, whereas the bioreactor was designed to test 32 mm diameter balls. Since 2009, Wright Medical/ Tornier manufactured shoulder interposition prostheses made of PyC (Inspyre) with various diameters (from 36 mm to 44 mm). Thus, 32 mm diameter PyC and CoCr balls were provided for the testing. Besides, an adequate lubricant was developed: HA-phospholipids medium. Consequently, the limitations of the previous study are overridden.
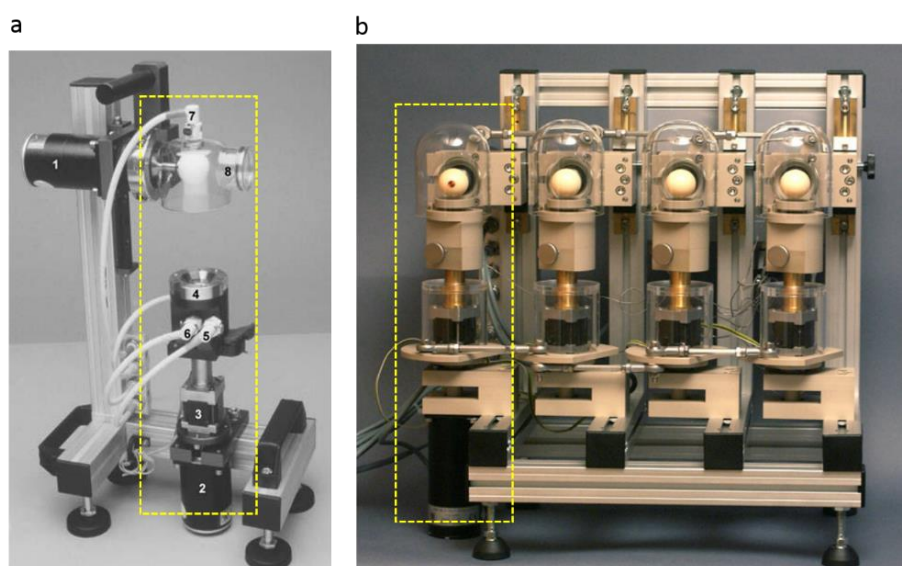
Figure F-7 a) One station configuration of the simulator: (1 and 2) step engines providing reciprocating motion for scaffold and of the ball, (3) actuator providing the compression, (4) cartilage sample holder. (Figure is taken from [206]*), b) the final four-station set-up of the simulator*

3.1.2. Experimental design

Here, wear testing was performed to compare PyC and CoCr balls articulating against live cartilage explants in the presence of either standard medium or HA-phospholipids medium. In this test, the HA-phospholipids lubricant was obtained with the second method (chapter E, § 3.5). The PyC and CoCr balls were manufactured and sterilized by Wright Medical/Tornier. Specific fixtures were provided and

attached to the simulator to support the balls. The biomaterials balls had similar surface conditions as the medical implants used in shoulder arthroplasty.

Cartilage explants were obtained as previously described (§1). Before launching the test, they were precultured for three days in either standard medium or HA-phospholipids medium. After the preculture, four randomly selected cartilage explants were inserted into sterile scaffolds (sterilized porous polythene, figure 8a). The cartilage explant should fit the scaffold only by pushing on the bottom surface without touching the articular surface. The scaffold containing the cartilage explant was then introduced into a sample holder (sterile PEEK (Polyether ether ketone) cup, figure 8b) with the explant face up (figure 8d). Then 3 ml of the lubricant was added to the cup (figure 8c).

Finally, the sample is ready for the simulator test (figure 9). The remaining cartilage explants served as free-swelling controls. The tested conditions in the simulator are summarized in table 1.

Table F-1 diagram of the 6 experimental conditions for the wear testing using the 4-station stimulator

Biomaterial / Lubricant	Ø (control)	PyC	CoCr
standard	**Control 1**	**Station 3**	**Station 1**
HA-phospholipids	**Control 2**	**Station 4**	**Station 2**
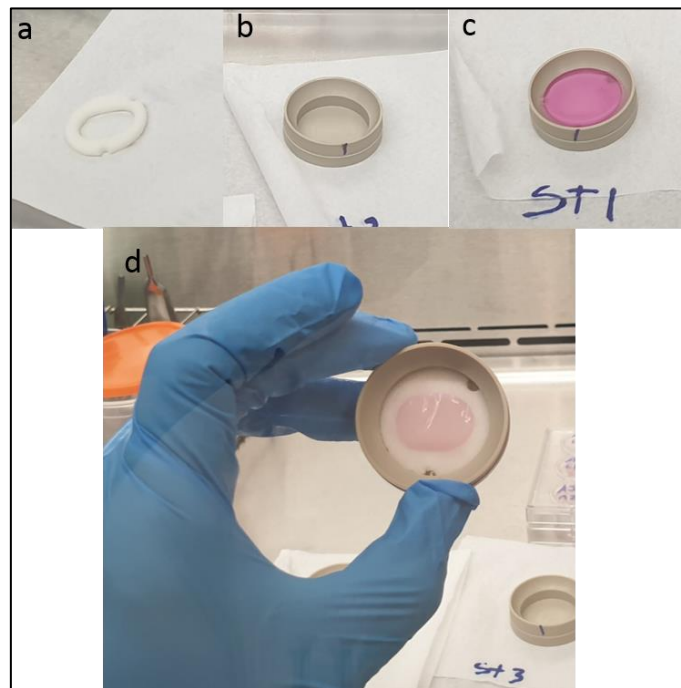
Figure F-8 Cartilage procurement for wear testing. a) Porous PE scaffold, b) PEEK cup: the explant holder, c) the sample holder with the lubricant before placing in the simulator, d) the cartilage explant placed in the scaffold transferred in the PEEK cup.

For the test, the balls oscillated at 0.5 Hz with ± 30° sinusoidal movement and were loaded against cartilage explants with 40 N load (2 MPa contact pressure). Simultaneously, the samples holders' oscillated at ± 15° with a 10 mm offset.

The wear testing was performed 3 hours per day for three days with two shifts (morning, afternoon). The experiment was performed twice. For each set, the stations were randomized (figure 9).

At the end of testing, the viability was assessed. The viability test is performed using the live/dead test, as described previously (chapter E, § 2.1.2). At the end of each 3-hour testing period, the mediums are individually collected. We planned to estimate the wear and the tissue integrity by measuring extracellular matrix breakdown using the release of proteoglycan/glycosaminoglycans as previously described [155] [198] (chapter E § 2.1.2). However, some experimental limitations did not allow to perform this analysis. It was not possible to override these problems during the period of the internship in RUMC.
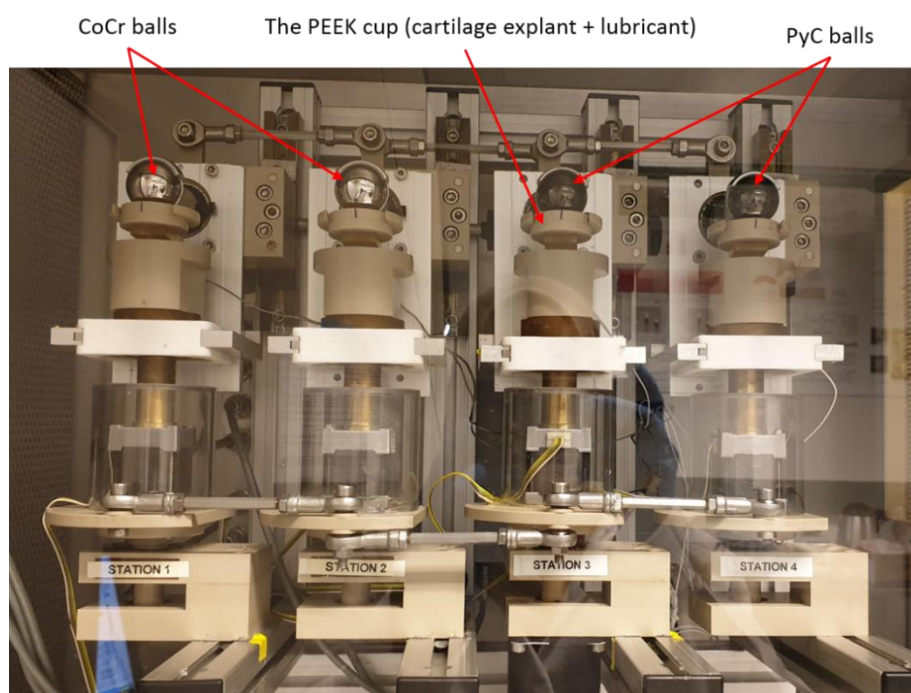
Figure F-9 the simulator set-up with CoCr and PyC balls housed in a controlled incubator (95 % humidity, 5 % CO₂, 37 °C)

3.2. Effects of the lubricant and the biomaterial on cell viability during the wear testing

Wear testing was performed twice comparing CoCr and PyC behaviour articulating against living cartilage using both lubricants. The test allowed us to evaluate the biomaterials' tribological behaviours with intricate movements, similar to the natural movements of the joint and the role of the new lubricant.

In the present test, the cell viability was approximately similar with the HA-phospholipids or with the standard cell culture medium (figures 10). As a reminder, the previous findings comparing the cultured cartilage explants in either HA-phospholipids medium or the CLC medium (presented in chapter E,

figure E-6) showed that the cell viability on cartilage explants was improved by changing the standard lubricant into the HA-phospholipids serum.

Regarding the effect of the biomaterial, the dead/live cells assay neatly showed better cell viability in the presence of PyC in comparison to the CoCr (figure 10). However, during tribological simulations, a loss of viability was noticed with both biomaterials in comparison with the free-swelling control (Figure 10). Compared to PyC, a thicker area at the superficial zone of the cartilage explant articulating against CoCr was coloured in red, indicating dead cells, using both lubricants (figures 10 c, f). Thus, the microscopic observations suggested that the CoCr alters the superficial zone of the cartilage more than the PyC. This region could be damaged even if the remaining tissue appeared healthy (stained green). We can speculate that the wear of the cartilage explant is more severe in this case, with probably more cartilaginous matrix degradation. Because of technical limitations (§ 3.1.2), this hypothesis could not be confirmed by a post-test media analysis. Nevertheless, the present wear testing globally attests that the PyC biomaterial better preserves the cartilage than the CoCr.
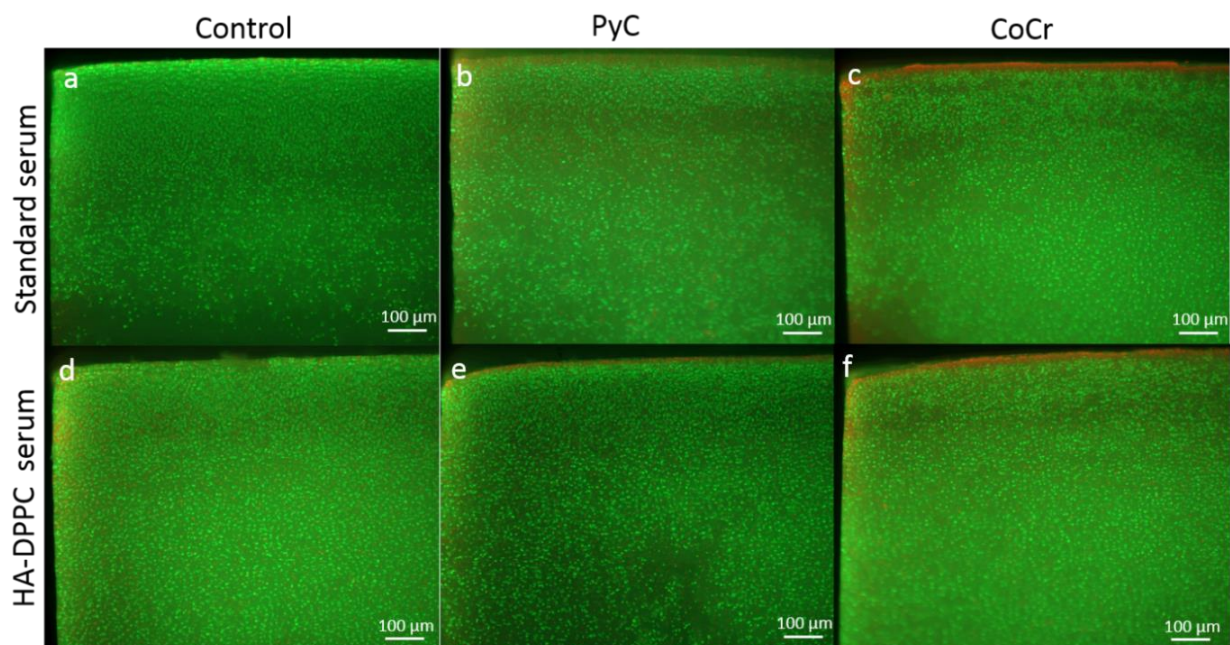
Figure F-10 Cell viability of cartilage articulated against PyC (b, e) and CoCr (c, f), and of the free swelling control (a, d), in the presence of the standard serum (a, b, c) or the presence of HA-phospholipids serum (d, e, f). The cross-sections of the articulated cartilage are from the centre of the wear region. Live cells are stained green and dead cells are stained red.

4. Towards a better understanding of the biomaterials effect on the mechanism

4.1. Conclusions

In this section, the effects of two biomaterials – CoCr and PyC – on cartilage explants were evaluated, in the presence of two different lubricants – standard and HA-Phospholipids media –, using two different mechanisms for the *in vitro* biotribological simulations – friction and wear tests –.

The first tested mechanism was through friction tests. Biomaterials balls were pressed onto cartilage explants and displaced tangentially on the cartilage surface with different velocities. The results indicated that the HA–phospholipids medium is superior to the control cell culture medium in mimicking the lubricative properties of synovial fluid and decreasing the coefficient of friction of the biomaterials.

The wear testing using the "shoulder simulator" allowed to evaluate the effect of the biomaterial and the lubricant with a natural joint movement. In this case, cell viability at the surface of the cartilage explant was similar between the two lubricants. Besides, friction tests showed that the PyC better preserve the cartilage than the CoCr by providing a lower COF. Furthermore, testing the contacts with a complex tribological mechanism using the "shoulder simulator" showed that the PyC was able to improve cell viability compared to the CoCr. However, the system is still perfectible. Indeed, cell viability decreased after mechanical solicitations using both biomaterials in comparison with the free-swelling control. In addition, for both biomaterials, the friction factors were higher than the cartilage/cartilage configuration that mimics a natural joint. Therefore, the mechanism is an important parameter to assess the cartilage wear articulating against different biomaterials.

In the presence of complex tribological solicitations, the superiority of PyC could be due to more efficient transmission of mechanical stresses through its structure and properties. Anyhow, it is essential to combine a suitable lubricant and an adequate simulator for the *in vitro* biotribological simulations.

4.2. Perspectives

To continue the investigation on the PyC and CoCr behaviour articulating against live cartilage, it is essential to perform additional wear testing in the HA-phospholipids medium. Therefore, the perspectives for this part are:

- Characterizing the wear by assessing proteoglycan/glycosaminoglycans and Hydroxyproline release
- Re-evaluating of the biomaterial behaviour by cell viability test and a lipidomic assay of the adsorbed molecules on the biomaterials surfaces.
- Changing of HA-phospholipids medium synthesis for the alternative protocol (chapter E, § 3.3)

For a reminder, the HA-phospholipids medium that was tested in this part was obtained from a quicker protocol, which did not ensure a proper Gel-IN structure with large vesicles (Figure E.4). It would be more relevant to use the first tested protocol that guarantees these properties. Such a synthesis is achievable in LaMCoS laboratory (available material in the laboratory), in sterile conditions (in a

cleanroom ISO Cleanliness Class 5). It could then be sent to Rush university medical centre to perform the wear testing.

- Modifying the mounting timing: we hypothesized that keeping the cartilage explants and the biomaterials mounted during the total testing period will be more efficient.
- Extending the period of testing: we believe that a 15-day-long test (5 days preculture + 10 days of testing 3h/day) could be more significant and comparable to the first performed test.

With this configuration, the test may give more answers about the advantages of the PyC articulating against cartilage compared to the CoCr as previously suggested by Cook and colleagues [14].

Development of a realistic *in vitro* model to reproduce the *in vivo* contact

G. Development of a realistic *in vitro* model to reproduce the *in vivo* contact

In all previous experiments, the PyC showed some advantages compared to the CoCr, which could be the reason of the neocartilage synthesis facing the interposition shoulder implants. After identifying the effect of the biotribological triplet components separately, it is necessary to validate the results in an *in vitro* model associating the different aspects. This chapter presents the design and the use and the validation of an *in vitro* model based on tissue bioengineering principles. This simulator allows combining the biological, physicochemical and tribological results obtained previously.

1. General principles of bioreactors for tissue bioengineering

During the healthy development of living tissue, cells modify their biological behaviour according to the mechanical stress they receive. Each received mechanical stimulation results in a physiological response, which define the mechanotransduction [47]. It is considered as an essential pillar of tissue bioengineering. In addition to mechanical considerations, the process of the tissue bioengineering combines the use of biomaterial support seeded with cells and the inclusion of growth factors allowing cells to differentiate and to regenerate a specific tissue [207] [208].
Altogether, it requires choosing the ideal support, controlling the cells' differentiation and introducing the mechanical constraints concerning the tissue-type desired [209] [210]. Therefore, bioreactors are used as devices in which biological and biochemical process is developed under a controlled environment (pH, temperature, mechanical solicitations…). All of these parameters are specific to the type of the developing tissue.

We aim to develop a simulator for cartilage testing, that combines the biological constraints (biomaterial support and growth factors), the physicochemical constraints (compatible with an incubator, easy to sterilize and permeable to CO_2) and the mechanical constraints (application of different mechanical stresses).

With regard to favourable mechanical parameters for cartilage culture, three main types of mechanical solicitations have been integrated: direct compression, hydrostatic pressure and shear stress [27] [211] [212] [213]. Different reviews proved the efficiency of the dynamic compression in comparison to static compression [214] [215] [216]. Moreover, other studies demonstrated the importance of the shear stresses induced by the flow of the cell media inside the biomaterial.
In brief, the most promising results for the cartilage matrix synthesis are obtained using devices able to combine dynamic shear and axial dynamic compression [217] [218] [219]. However, the value of the transmitted solicitation to the cellular level is still unknown and uncontrollable, which contributes to the variability of the results [216] [217] [219]. Accordingly, in this section, we developed a new

bioreactor with bi-axial load able to follow *in situ* the transmitted stresses and the new tissue formation. Particular attention was paid to integrate the measurement of the constraints.

2. The developed simulator

2.1. Technical consideration, concept and design

The new device represented by figure 1 solicits separately or simultaneously in compression or shear cell/organ cultures with the possibility of microscopic observation. These cultures are immersed in a specific culture medium to maintain physiological conditions. The medium flow is regulated with a peristaltic pump (Masterflex L/S).

The dimensions of the device are fixed respecting the aspects of the incubator to control the cell culture conditions (CO_2 level, hygrometry, and temperature) and the design of the available microscope in the laboratory (Microscope Zeiss Axio Examiner) equipped with a confocal head LSM700. As it is respecting the tribology and the biology conditions, the new device is called in this project the "tribo-bioreactor". Its concept is based on the configuration of parallel-plate rheometer to perform parallelism with micrometric resolution (the same device used in chapter D).
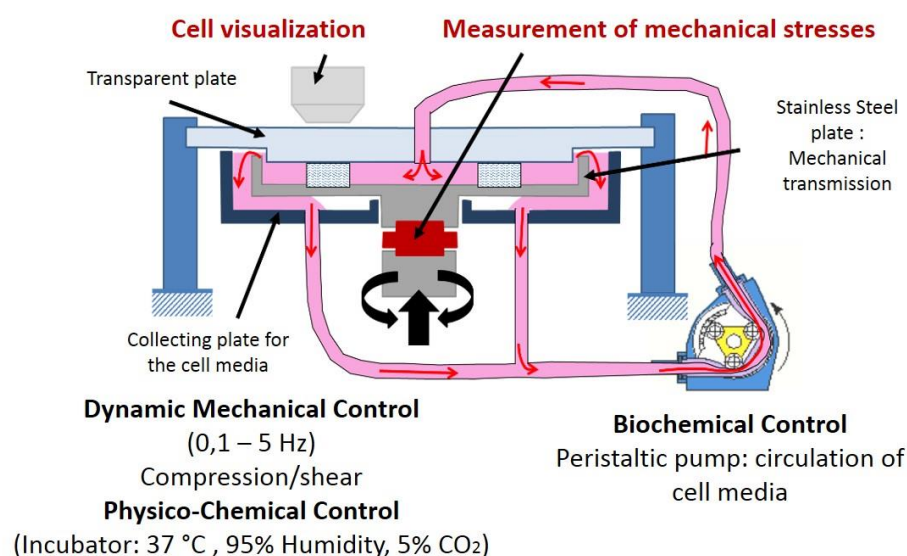
Figure G-1 Global diagram of the new "tribo-bioreactor". It allows applying mechanical solicitations with microscopic observation under biochemical and physicochemical control

The culture room of the "tribo-bioreactor" is composed by two parallel circular plates as shown in figure 2: a transparent Plexiglas® plate which facilitates the visualization of samples (made from polymethyl methacrylate (PMMA) which is sterilisable and thermoplastic) and a stainless steel plate which facilitates the application of mechanical stress.

140

The two plates were made with the same diameter, 50 mm. The gap between them is modifiable by a lifting table in which the stainless steel plate is clamped.

To ensure the biological reproducibility, three locations were made in the stainless steel plate to hold the samples. They were positioned 20 mm from the plate centre and with a 120° equal angular distance between them. Other stainless steel plates are conceived to hold different samples (number, dimensions).
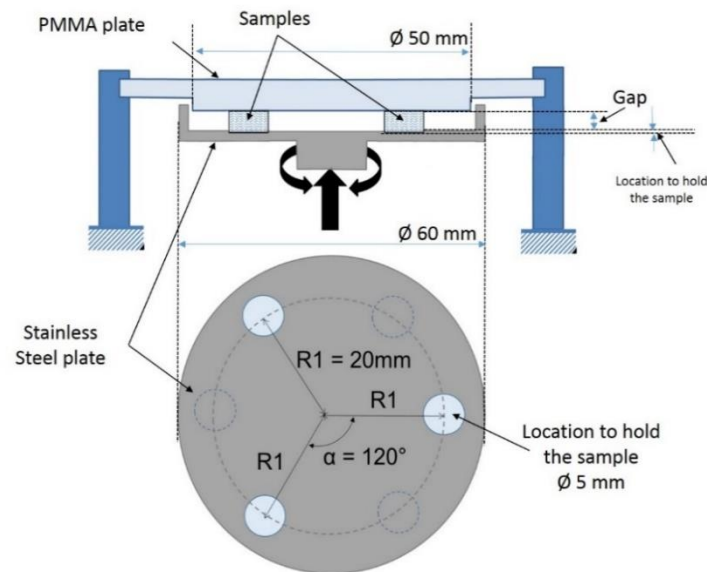
Figure G-2 Contact configuration: the two parallel plates allowed forming a cell culture chamber where the sample is placed

An extra inferior plate made from polyvinyl chloride (PVC) is added to recover the culture medium (called "the collecting plate" in figures 1 & 3). A peristaltic pump is used to renew the cell culture medium. It is connected to both sides of the culture room (up and down) through a system of pipes. Thus, the Plexiglas® plate was designed with a 3 mm central hole for the medium supply, and the PVC plate was designed with two holes (3 mm) for the medium evacuation (figures 1, 3).
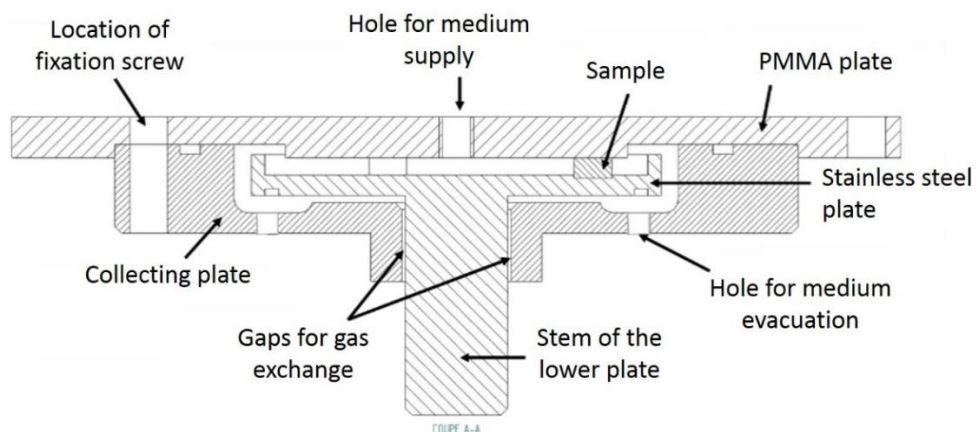
Figure G-3 Cross-Section of the different plates of the "tribo-bioreactor" showing the holes for the pipes system

Amira HANNOUN/ Thesis in Biomechanics 2020/ INSA Lyon

Piezoelectric actuators "Amplified Piezo Actuators (APA)" (Cedrat Technologies, Grenoble, France) are selected to apply the different mechanical stresses. The compression is applied by the vertical displacement of an APA. The horizontal displacement of another APA applies the shear after being transformed into rotation by an elastic system (Figure 4). Strain gauges measure both movements. A piezoelectric sensor with 2-Component Force Reaction Torque Link (KISTLER, France) measures the normal dynamic force and the torque.

The APA actuators are selected for the use of a mechanical amplifier to preload the stack of multilayer piezoelectric components and to mechanically amplify the displacement. Therefore, they provide a significant stiffness for the system and increase generated efforts.

The chosen elastic system is a bending bearing with flat, internal, crossed springs encapsulated in a cylindrical housing to provide precise rotation and to avoid friction losses. This bearing offers a significant lifespan when used under nominal load and rotation conditions. The rotation of the bearing is facilitated by the bending of the flat springs on which the segments are supported. The vertical translation link is ensured by an elastic link (rod).

The piezoelectric sensor (KISTLER Type 9345B) was chosen for its characteristics, offering a sensitivity of 0.001N for the measurement of normal force and 0.001 N.m for the measurement of torque.

The "tribo-bioreactor" is monitored by a developed LabVIEW interface (National Instruments, France) to adjust the needed load: type (compression or/and shear), the value of the APA displacement and the frequency.
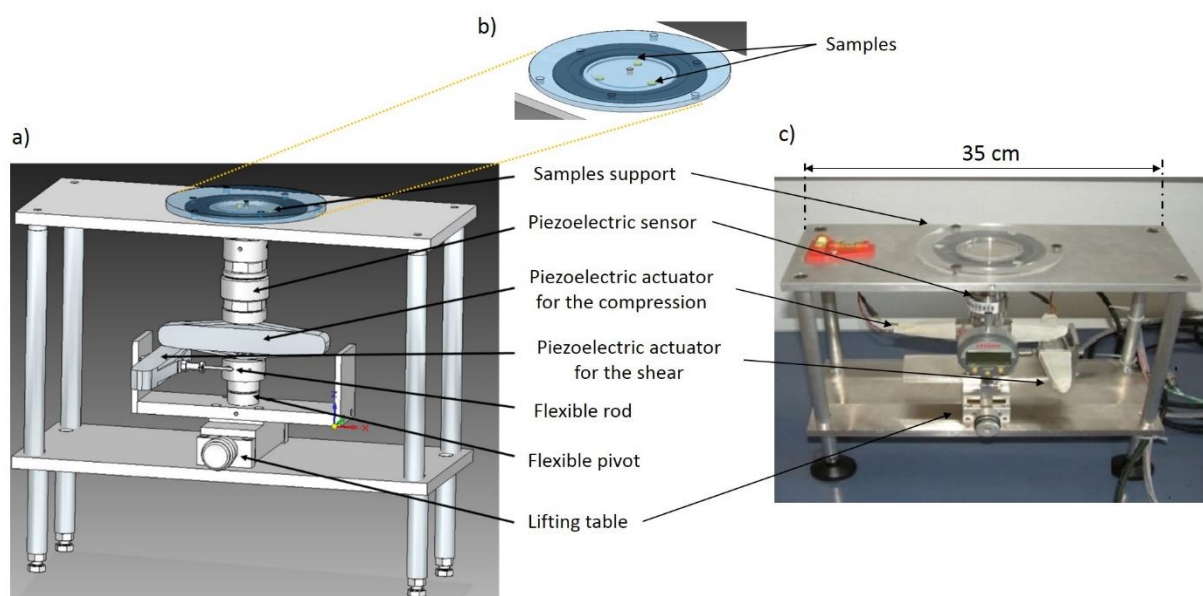
Figure G-4 the prototype of "tribo-bioreactor". a) Design with the specific components. b) Cell culture chamber composed of the two plates. c) Final prototype

142

The new device can be used for three different main applications, as detailed hereafter: mechanical characterization, cell visualization under mechanical stress, and cartilage-tissue bioengineering. First, different tests are performed to validate each function.

2.2. Experiment I: experimental strategy for mechanical characterization

2.2.1. Principle of dynamic mechanical analysis

Thanks to its design, the "tribo-bioreactor" makes it possible to characterise the samples inserted in the cell culture chamber mechanically. The combination of the applied dynamic stresses (APA) and the measured force (Piezoelectric sensor) supports the application of the principle of the dynamic mechanical analysis (DMA). The DMA is a non-destructive technique used to characterize the viscoelastic properties of different samples [192]. These properties are studied by imposing dynamic stress to the sample (Chapter D). To validate the "tribo-bioreactor" for this application, its results are compared to those obtained by a classic rheometer.

For the validation experiment, various viscoelastic parameters are measured as follows. For elastic and viscoelastic samples, the DMA allows calculating the complex modulus (G*) and thus the elastic modulus (G'), the viscous modulus (G") and the viscosity (η) as described in [159] and based on the equations (1), (2) and (3).

$$G^* = \frac{\sigma_0}{\varepsilon_0} \cos \varphi + i \frac{\sigma_0}{\varepsilon_0} \sin\varphi = G' + iG" \quad (1)$$

$$G' = \frac{\sigma_0}{\varepsilon_0} \cos\varphi \quad (2)$$

$$G'' = \frac{\sigma_0}{\varepsilon_0} \sin\varphi \quad (3)$$

The following equations (4) (5) describe how to calculate the stress (σ) and strain (ε) in DMA:

$$\sigma(t) = \sigma_0 \cos(2 * \pi * f * t + \varphi) \, ; \, \sigma_0 = \frac{A_{force}}{S} \quad (4)$$

$$\varepsilon(t) = \varepsilon_0 \cos(\omega t) \, ; \, \varepsilon_0 = \frac{A_{displacement}}{gap} \quad (5)$$

σ_0 and ε_0 are the values of the stress and the strain, φ the phase shift between the two signals, f the frequency, '$A_{displacement}$' the measured vertical displacement, 'A_{force}' the measured force and S the contact area.

For viscous samples, the viscosity calculation is based on Stefan formula described by (4). It consists of squeezing a fluid between two parallel plates [220].

$$A_{force} = \frac{3\pi\omega\eta R^4 A_{displacement}}{2*gap^3} \quad (4)$$

R is the plate radius, $A_{displacement}$ and A_{force} are the values of the imposed displacement and the measured normal force.

2.2.2. Samples and settings for the validation experiment

Two different types of samples are tested using the "tribo-bioreactor": the bee-honey for the viscous behaviour and the hydrogel discs for elastic behaviour.

Hydrogels based on Poly(hydroxyethyl methacrylate) p(HEMA) are prepared by mixing HEMA monomer (Sigma-Aldrich) with 25 % by weight of acrylic acid monomer (Sigma-Aldrich). Then, hydrogel discs (HEMA discs) are synthesized by radical cross-linked polymerization as described in [221]. HEMA discs have similar elastic properties as the articular cartilage; that is why they were selected for the tests [221].

The test parameters are 50 µm for the dynamic displacement, 3 Hz for the frequency and 1 mm for the gap between the two plates. These parameters are presented as (displacement, frequency, gap) and are adjusted depending on the type of the sample and its volume.

2.3. Experiment II: Fluorescence analysis of cell displacement under mechanical stress

2.3.1. Principle of cell tracking under mechanical stress

The fluorescence analysis is used to ensure the transmission of the mechanical stress throughout the biomaterials support for cells culture and up to the cells (Figure 5). It identifies the local displacement of the cells during mechanical stress. The biomaterial has to be clear to allow the visualization of fluorescent cells. Alternatively, fluorescent beads can be used to mimic living cells.

While a dynamic compression is applied to the sample, a stack of images on Z position is taken with confocal microscopy. The succession of the images allows following the displacement of the beads. Therefore, a compromise between the duration of the mechanical stress and the time of the camera's acquisition is necessary. The parameters for the compression (displacement, frequency, gap) is dependent on the tested biomaterial.
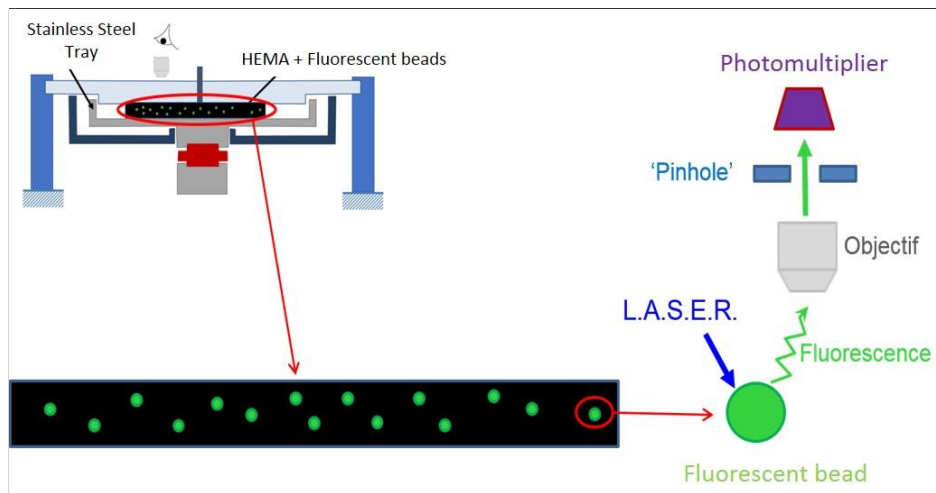
Figure G-5 Fluorescence analysis principle using the "tribo-bioreactor" and the confocal microscopy

2.3.2. Samples and settings for the validation experiment

Two different biomaterials are selected to adjust this technique: HEMA discs and agarose hydrogel discs. HEMA discs are prepared as described previously in [221] with the addition of 15 µm polystyrene fluorescent beads (FluoSpheres TM Polystyrene Microspheres, ThermoFisher Scientific).

For agarose discs, 2 % agarose hydrogels (Sigma Agarose IX-A) are prepared. Briefly, the appropriate amount of the hydrogel powder is mixed with PBS in a beaker between 70 °C and 80 °C with stirring for ten minutes to obtain an initial concentration of 2.5 %. Then, the solution is autoclaved [222]. Cells or fluorescent beads are suspended in the agarose solution with a density of 2000 cells or beads per mL to reach a final 2 % concentration. 700 µL of the mixture is poured into 24 wells-culture plates. Agarose constructs are allowed to gel at the room temperature. Then, they are punched to obtain cylindrical plugs (13-mm diameter and 3-mm height).

The cells were human chondrocytes obtained, as described in (§2.4.1). They were fluorescently labelled using "CellTracker Red" (ThermoFisher Scientific) as detailed by the manufacturer.

For HEMA discs testing, the parameters for the "tribo-bioreactor" displacement are fixed as (200 µm, 0.05 Hz, 1 mm). Once validated for HEMA discs, this analysis is performed with agarose hydrogel discs containing either fluorescent beads or fluorescently labelled chondrocytes. The parameters are adapted respecting the maximum load the hydrogel could undergo without cracking (150 µm, 0.05 Hz, 3 mm). The agarose hydrogel is tested on compression; the discs cracked when the displacement reached 175 µm.

2.4.   Experiment III: "Tribo-bioreactor" is a bioreactor for chondrocytes 3D culture

The "Tribo-bioreactor" is tested for cell culture by the use of human chondrocytes. Two biomaterials support are tested: collagen sponges and agarose hydrogels.

145

2.4.1. Culture of human articular chondrocytes

Human articular chondrocytes (HACs) are isolated from macroscopically healthy zones of hip joints obtained from donors undergoing total joint replacement (n= 4; 51-79 years). The study is performed in full accordance with local ethics guidelines, national and European Union legislation regarding human sample collection, manipulation and personal data protection (Ethics Committee for research with human samples, CODECOH: DC-2014-2325). Cartilage samples are collected after written informed consent of the donors. Chondrocytes are extracted as described by Hautier and colleagues [223].

Pieces of cartilage finely cut are rinsed with PBS. Then, cells are obtained by two enzymatic digestions with 1 mg/mL trypsin (Sigma; ref T4799) followed by 0.06 % bacterial collagenase A (Roche Applied Science; ref 10103586001). Chondrocytes are filtered through a 70 μm sieve and then centrifuged in control medium composed of the 1:1 mixture of DMEM with Glutamax and HamF12 supplemented with L-glutamine, 10 % of foetal bovine serum, 50 μg/mL of gentamycin (Panpharma) and 2 μg/mL of amphotericin B (Bristol Myers Squibb). The chondrocytes are seeded at the density of 1.5×10^4 cells/cm^2 on culture dishes and cultured in the same medium. At this time, the cells are designated as P0. The medium is changed and completed with 5 ng/mL of FGF-2 (fibroblastic growth factor) and 5 μg/mL insulin, 36 hours after seeding. The medium is replaced three times per week until the cells reach confluence. The chondrocytes are then detached by the action of trypsin-ethylenediaminetetraacetic acid (EDTA) (Sigma) and again seeded at the same density [224][225].

2.4.2. Testing the culture of HACs in collagen sponges in the "tribo- bioreactor."

2.4.2.1. Culture of HACs in collagen sponges

Collagen sponges are provided by Symatese Biomaterials (Chaponost, France). They are composed of native bovine type I (90-95 %) and type III (5-10 %) collagen, derived from the extraction of American calf dermis. These sponges are cross-linked with glutaraldehyde to increase their stability and are beta-irradiated to ensure sterility. Sponges are then cut with a skin biopsy punch (Laboratories Stiefel) in discs with a 5 mm diameter and 3 mm thick to fit the locations made in the "Tribo-bioreactor" stainless steel plate. The pore size is about 100 μm.

The chondrocytes-collagen sponges' constructs are prepared as previously described [225] (figure 6). Briefly, chondrocytes are seeded onto the sponges at the density of 13×10^6 cells/cm^3, and the sponges are incubated at 37 °C for 2 hours to allow cells adhesion. Culture medium containing 10 % of New-born Calf Serum and supplemented with 50 μg/mL of ascorbic acid (sodium salt, Fluka) is then added

to the wells in the presence or not of 200 ng/mL of (BMP)-2 (bone morphogenetic protein), 5 µg/mL insulin (Umulin, Lilly), and 100 nM thyroxine T3 (Sigma).

The culture medium is changed every two days. Chondrocytes-collagen sponges are cultured several days or weeks *in vitro* before the "Tribo-bioreactor" test to allow cells fixation and extracellular matrix production. This period is designated as a pre-culture period. The medium circulation and mechanical constraints could cause cell detachment from the sponges. A decent pre-culture period avoids this phenomenon.
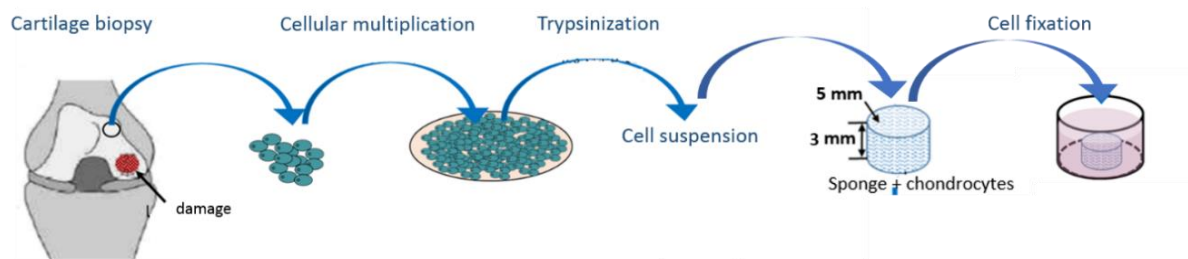
Figure G-6 Different steps to obtain collagen sponges with seeded chondrocytes

2.4.2.2. Settings for the validation experiment

Several tests are performed to adjust the convenient parameters for the cell culture (presented in table 1). For each experiment, a reference sponge "REF" without mechanical stresses, cultured *in vitro* is considered. The "REF" sponge helps to compare chondrocytes response without ("REF") and under mechanical solicitations ("TriboR"). The period of cell culture is similar for the "REF" and "TriboR" sponges.

For the compression, a displacement of 10 % of the sponge thickness is applied (300 µm). For the shear, a displacement of 5 % of the sponge circumference is applied. Based on Waldman study, both mechanical solicitations are employed with a frequency of 0.5 Hz [219]. The flow rate of the media circulation is slow enough not to induce hydrostatic pressure and shear effects on the samples (8 mL/min). Collagen sponges without cells are used as the controls (WC). They are tested under and without mechanical solicitations.

Table G-1 Tests performed using the «tribo-bioreactor» with different parameters for the duration of pre-culture and mechanical solicitations

	Test 1 : Dynamic compression & shear		Test 2 : Dynamic compression & shear		Test 3 : Static compression	
Pre-culture period	3 weeks		4 days		2 days	
Cell culture period in the "Tribo-bioreactor"	4 weeks		5 weeks		3 weeks	
Tests	«REF»	«TriboR»	«REF»	«TriboR»	«REF»	«TriboR»
Solicitation **Parameters**	none	Compression (a) Shear (b) Freq: 0.5 Hz	none	Compression (a) Shear (b) Freq: 0.5 Hz	none	Compression (a)

(a) *10% of the sponge thickness*

(b) *5 % of the sponge circumference*

2.4.2.3. Analysed parameters, post-test

Mechanical characterization of different sponges ("REF", "TriboR") is performed with the rheometer to avoid additional stresses due to the cell media circulation, as described in [226]. Therefore, 30 % of compression is applied to the sponges with a 0.002 N preload followed by a relaxation period. Elastic modulus E is calculated based on Hooke's law. It is given by the slope of the straight line obtained in the curve of the stress (σ = F/S) as a function of the strain (ε).

Also, fluorescence recovery after photo-bleaching (FRAP) is performed using the confocal microscope to evaluate the physicochemical properties of the collagen sponges. Collagen sponges from "Test 1" are recovered and immersed in a solution of 70 kDa dextran labelled with neutral fluorescein (Sigma) at 0.1 mg/mL in PBS at 4°C for at least 1 hour. Photo-bleaching is performed with an argon laser at 70 % laser power and 100 % transmission and imaging with the same laser at 15 % transmission. We reproduced the same measurement and the same parameters as described by Bougault and collaborators [226] for nine samples (3 sponges without cells maintained in static conditions "WC", 3 "REF" and 3 "TriboR"). Diffusion data acquisition and the diffusion coefficient calculation are based on the methodology described by Axelrod [227] and by Bougault [226].

At the end of the cell culture period, collagen sponges on each condition were fixed in 4% (v:v) formalin and embedded in paraffin for histological analysis. HES staining was performed to evaluate the structure of each sample. Also, specific immunolabelling was made for collagen type II to identify the extracellular matrix components as previously detailed (chapter C § 2.2.2).

2.4.3. Testing the culture of HACs in agarose hydrogel in the "tribo-bioreactor"

2.4.3.1. Culture of HACs agarose hydrogel

For chondrocytes culture using hydrogel agarose as a scaffold, two types of constructs are prepared: discs of randomly seeded cells and discs with aligned cells using 3D printing.

Discs of agarose hydrogel seeded with chondrocytes are prepared with a density of 2×10^6 cells/mL as previously described (§2.3.2). Constructs were then punched to obtain discs of randomly-seeded chondrocytes in agarose gels with the same dimensions as collagen sponges [228].

Since chondrocytes are organized as aligned cells *in vivo* [208], 3D printing is used to make constructs of agarose hydrogel with aligned chondrocytes [229]. Discs of 3D-printed constructs of agarose and chondrocytes are composed of three layers, as shown in figure 7. Each layer is formed of agarose hydrogel printed by inkjet process and chondrocytes printed by 3D printing assisted by laser.
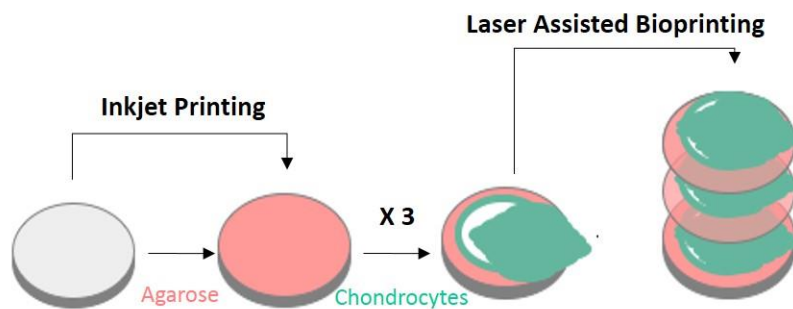
Figure G-7 3D printing technique of cartilage discs. The agarose is printed by inkjet and once the gelled agarose layer, the chondrocytes are printed by laser on top. The process is repeated three times

2.4.3.2. Validation of the 3D printing protocol

The inkjet printing process is launched when overpressure is generated to flow the sample (hydrogel agarose) through a hole. Then the sample droplet formation and propagation begin until the impact with the receiver (wells of the culture plates Corning Ref 10578911). The receiver is warmed in the incubator at 37 ° C for a few minutes to prevent the appearance of irregularities and to ensure several layers of printed agarose in a cohesive set.

The used bioprinting process is a "Laser-Induced Forward Transfer" (LIFT). It uses laser pulses to generate and inject drops of liquid with cells. It is controlled by the interaction between the laser and the material. Consequently, different parameters are involved in the printing process. The device fixes some parameters (wavelength), and other parameters are controlled by the operator depending on

the printing conditions (laser energy). The printing assisted by laser allows the creation of patterns with a resolution from tens to hundreds of micrometres [230].

The combination of inkjet and 3D printing is already validated with the fibroblasts. Different pressures are tested to specify the convenient parameters to print a homogeneous layer of agarose. The fibroblasts spots are separated by 300 µm in grid spacing. As shown in figure 8, using fibroblasts labelled with a green fluorochrome, there is a clear distinction between the cells within each spot. Thus, this technique is validated, and it is used for human chondrocytes.
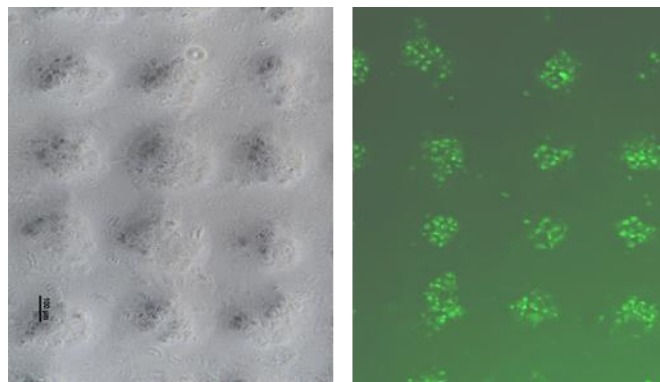
Figure G-8 Visualization of fibroblasts printing on printed agarose layer

2.4.3.3. Settings and analysis of the validation experiment

Cell culture of the 3D printed chondrocytes-agarose constructs is performed during three weeks under dynamic compression (150 µm, 0.5 Hz). Agarose constructs with printed cells are characterised mechanically with the "Tribo-Bioreactor" using the parameters (100 µm, 2 Hz, 1 mm).

Furthermore, histological analysis was performed to characterise the chondrocytes cultured in the tested conditions. At the end of the cell culture period, agarose discs were fixed in 4% (v:v) formalin. HES staining was performed to evaluate the structure of each sample. Also, specific immunolabelling was made for collagen type II to identify the extracellular matrix components as previously detailed (chapter C § 2.2.2).

3. Results of the three different experiments

The different results are analysed statistically. The rheological tests are analysed using the software OriginPro of at least four measurements. Bars represent the mean and standard error of the mean (SEM). Effects of the mechanical solicitations on the collagen sponges are compared to the "REF" sponges, using the Student's t-test. In tables 2 and 3, the results are presented as mean ± standard deviation (SD). Significant results are represented as * $p < 0.05$, ** $p < 0.01$ and *** $p < 0.001$. Non-significant results are represented as ns $p > 0.05$.

3.1. Experiment I: The "Tribo-bioreactor" as a simulator for mechanical characterization

The "tribo-bioreactor" is compared to a classic rheometer. The bee-honey is first tested with cone-plate configuration. The rheometer measurement led to a viscosity value of 4.6 Pa x s (table 2) and a phase shift value of π/2 between displacement and force signals. Using the "tribo-bioreactor", the obtained phase shift was π/2, thus confirming the viscous behaviour of the sample (figure 9a). A viscosity of 4.7 Pa x s is calculated (based on Stefan formula). Thus, the viscosity measurements obtained with both devices are quite similar; hence the new prototype is considered as a rheometer for this type of sample. While testing the bee-honey with the "Tribo-bioreactor", sliding effect between the sample and the plates appeared causing deformation in the force signal. After numerous tests, the problem is resolved by sticking removable sandpapers on both plates.

For the synthetic HEMA, the two signals are in the same phase, which approves the elastic behaviour of the sample, as shown in figure 9b. The measurements of the elastic modulus with the "tribo-bioreactor" are equivalent to those made with the rheometer, as shown in table 2. Thus, the "tribo-bioreactor" is considered as a rheometer for elastic samples. The results of the mechanical characterization are detailed in table 2.

Table G-2 Mechanical characterization of bee-honey and synthetic HEMA using both rheometer and "tribo-bioreactor."

	Rheometer	**"tribo-bioreactor"**
Bee-honey: Viscosity η (Pa x s)	4.635 ± 0.017	4.712 ± 0.018
Synthetic HEMA: Elasticity G' (MPa)	0.2 ± 0.05 [221]	0.220 ± 0.001
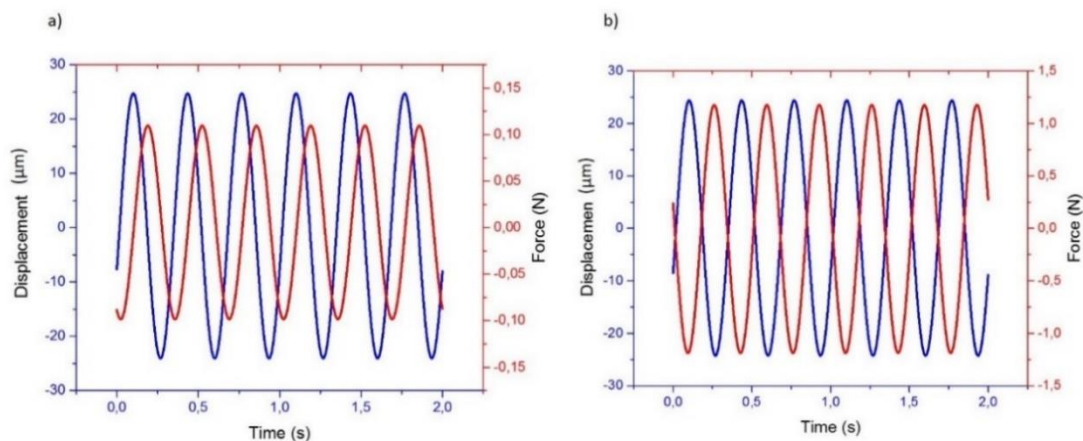
Figure G-9 Obtained signals with a displacement of 50 μm and a frequency of 3 Hz: a) Applied displacement and obtained force-displacement signals of the bee-honey, phase shift π/2 b) applied displacement and obtained force signals of the synthetic HEMA, phase shift π

In conclusion, the comparison with a rheometer confirmed the performance of the new prototype as a simulator for the DMA. It allows evaluating the mechanical properties of different samples with

151

different rheological behaviours. Accordingly, the "Tribo-bioreactor" is used in various research projects in the laboratory. It is used to evaluate the rheological properties of prostate cancer cell lines to detect the evolution of cancer and to predict its stages [231]. Also, it was used to characterize the mechanical properties of different tissue-like cell-membranes developed in the surface of orthopaedics biomaterials, as shown in chapter D [159]. Likewise, it was used to characterize the mechanical properties of human cartilage samples and samples of atheroma.

3.2. Experiment II: Fluorescence analysis of cell displacement under mechanical stress

The first cell tracking experiments is conducted using fluorescent beads included in HEMA discs. The movement of the beads embedded in the biomaterial is followed in Z position by making 200 μm thick images stacks for 9 seconds. Before applying any mechanical stress to the sample, the initial position of some fluorescent beads inside the HEMA is identified at the location 150.7 μm from the total thickness of the sample. After applying a displacement of 200 μm, the same beads are located at position 0 μm. Consequently, we conclude that only 75 % of the imposed load is received by the fluorescent beads inside the synthetic HEMA (figure 10).
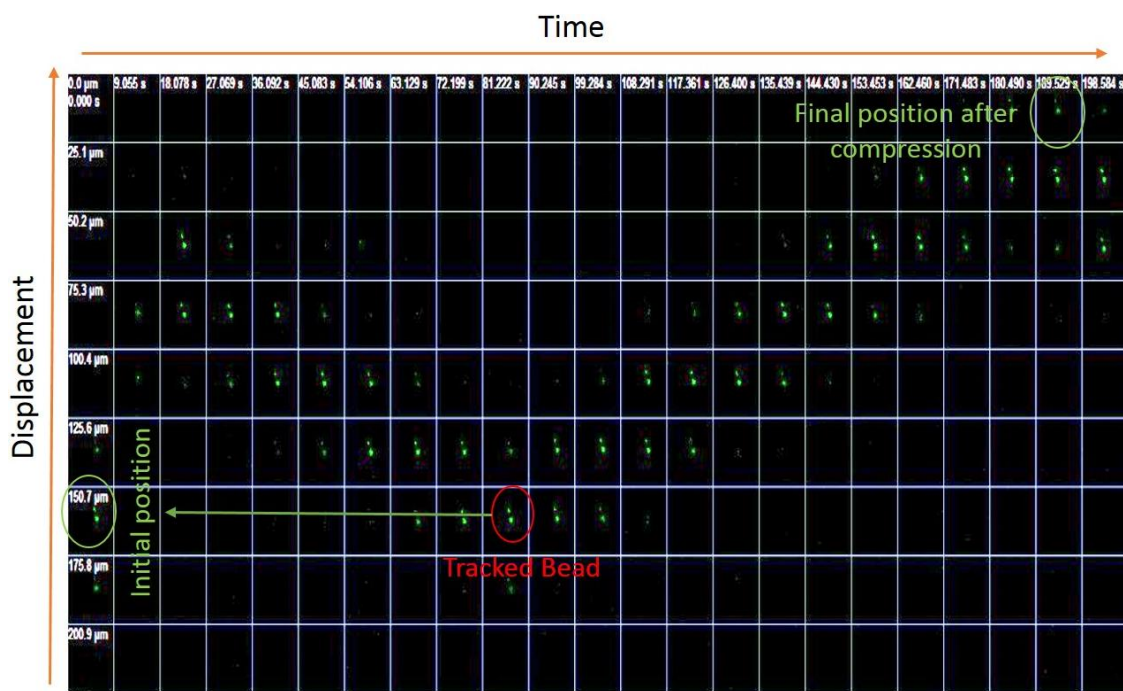
Figure G-10 Bread displacement during compression

The second experiment was performed in the same conditions, but the fluorescent beads were embedded in agarose hydrogel. They received only a movement of 100 μm, with an imposed 150 μm displacement. Thus, they received only 67 % of the imposed displacement by the "Tribo-bioreactor".

Based on these results, the transmission of the mechanical stresses is different, whether it is inside the HEMA discs or the agarose hydrogel. This difference could be caused by the stiffness of the material support. In addition, the stiffness of the beads may affect the transmission of the load.

Consequently, it is considered to test the mechanical stress transmission throughout the biomaterial support for the living cells instead of fluorescent beads, as a third step. Accordingly, fluorescence analysis is performed using the hydrogel agarose with fluorescently labelled chondrocytes. In this configuration, cells received only 45 % of the imposed displacement (150 μm).

This result suggested that the rheological properties of the agarose hydrogel are different depending on whether it contains beads or cells. Thus, the agarose hydrogel elasticity containing either cells or beads is evaluated using the "Tribo-bioreactor" (DMA with the parameters: (100 μm, 2 Hz, 1mm)). The DMA results detailed in table 3 corroborate this hypothesis. The discs of agarose hydrogel containing chondrocytes are approximately two times stiffer than the discs of agarose hydrogel without cells.

Table G-3 Mechanical characterization of agarose hydrogels using the "tribo-bioreactor."

	Agarose hydrogel without cells	Agarose hydrogel with chondrocytes
Elasticity G' (MPa)	0,0034 ± 0.001	0,0066 ± 0.001

To conclude, using the "Tribo-bioreactor" and the confocal microscope allowed the application of the fluorescence analysis. This analysis permitted controlling the transmission of the applied mechanical stress inside the tested biomaterial and up to the cellular level. This analysis is essential for accurate management of mechanotransduction conditions and can be a game-changer in the cartilage bioengineering tests.

When performing the fluorescence analysis, we are sure that even within a biomaterial, the cells still be subjected to mechanical constraints. Besides, it is possible to identify the exact level of mechanical constraints transmitted locally to the cells compared to those applied theoretically. Then, the used parameters can be adapted according to the received load by the cells during cells culture. Many bioreactors with bi-axial load apply different solicitations, but to date, none evaluates the received load in the cellular level.

3.3. Experiment III: Use of the "Tribo-bioreactor" for chondrocytes 3D culture

3.3.1. Chondrocytes 3D culture in collagen sponges

In that configuration, the main challenge for 3D culture with the "Tribo-bioreactor" is to keep the cells inside the collagen sponges. Therefore, three tests with different pre-culture periods are performed to find the appropriate time for a better cellular attachment to the collagen sponges.

A good cellularization of the sponges is observed at the end of each pre-culture period, irrespective of the pre-culture period, as shown by HES staining (figure 11).

Test 1   Test 2   Test 3
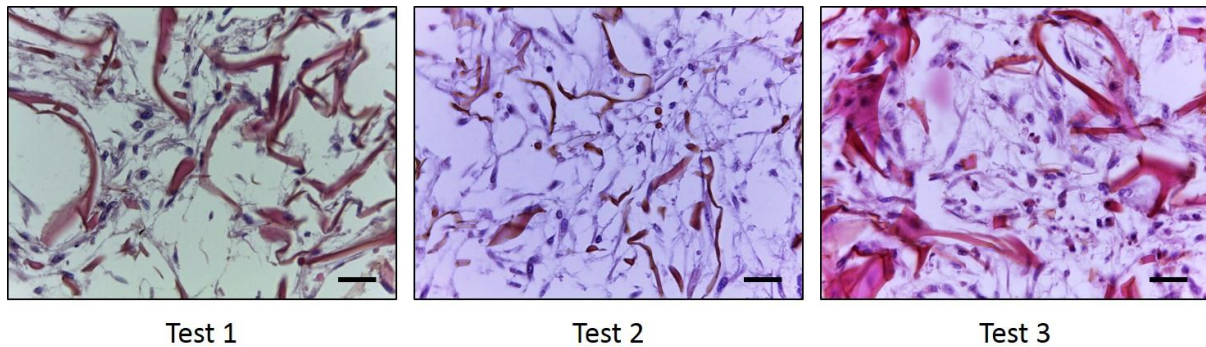
Figure G-11 HES staining of "TriboR sponge". Collagen sponges were seeded with articular chondrocytes, pre-cultured for three weeks (test 1), four days (test 2) or two days (test 3) before placement in the "tribo-bioreactor" and compression. Scale bar = 50 µm

Moreover, the chondrocytes submitted to mechanical constraints synthesized a more abundant cartilaginous matrix compared to "REF" condition (without mechanical solicitation). Indeed, immunostaining revealed an accumulation of type II collagen, the most abundant protein found in native cartilage, for collagen sponges cultured in the "Tribo-bioreactor" under mechanical solicitations (Figure 12). Of note, the staining was more intense at the periphery of the sponge.

« REF » sponge   « TriboR » sponge
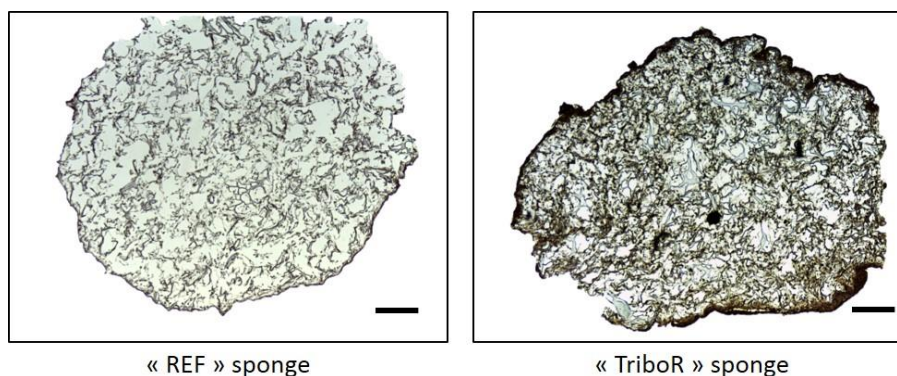
Figure G-12 Type II collagen immunostaining of "REF" sponge compared to "TriboR sponge". Collagen sponges were seeded with articular chondrocytes, pre-cultured before placement in the "tribo-bioreactor" and submitted ("TriboR sponge") or not ("REF" sponge) to mechanical constraints. Scale bar = 500 µm

For the mechanical characterization, different sponges were placed into the rheometer for DMA. For each sample, the elastic modulus E was calculated. Three independent experiments were performed, and the calculation of the elastic modulus E gave acceptable accuracy (Figure 13).

For a better standardization, results were paired: data obtained with "REF" sponges were compared to "TriboR" sponges. As expected, the DMA confirmed the importance of mechanical solicitations. Indeed, the "TriboR" sponges were more elastic or more resistant than "REF" sponges, except for "Test 2", where no difference was detected (figure 13). Collagen sponges without cells ("WC") were also used to assess the elastic modulus of the support alone.
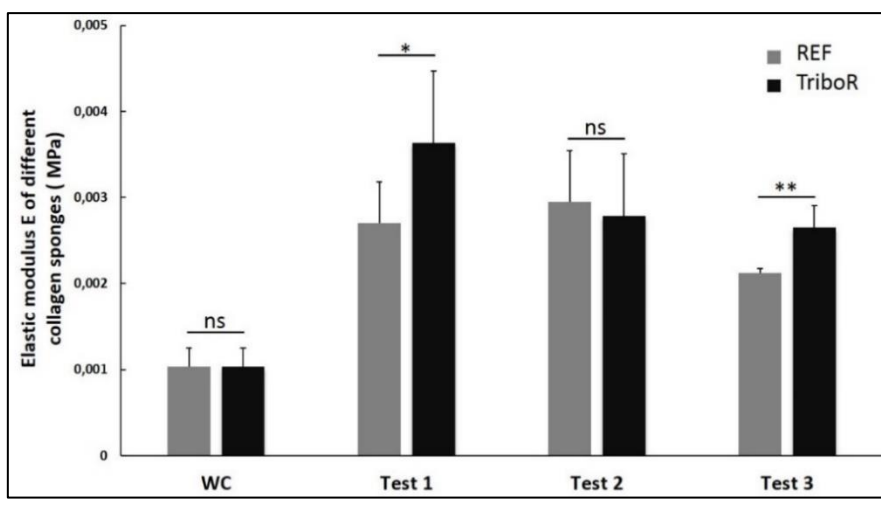
*Figure G-13 Mechanical properties of collagen sponges without cells (WC) or with chondrocytes cultured under mechanical solicitations or without solicitations. Rheological tests on the sponges were performed with a rheometer, and the elastic modulus E was calculated. The elasticity of the "REF" sponges was compared with "TriboR" sponges. * p < 0.05, ** p < 0.01, ns: no statistical difference.*

FRAP experiments were performed on "TriboR" sponges and compared to the "REF" and "WC" controls. The diffusion coefficient was $20.23 \pm 1.35 \ \mu m^2/s$ in "WC" sponges, $10.98 \pm 0.90 \ \mu m^2/s$ in "REF" sponges and $15.60 \pm 2.05 \ \mu m^2/s$ in "TriboR" sponges. Thus, the diffusion properties of the collagen sponges containing chondrocytes changed in the presence of the mechanical solicitations (figure 14). The difference in the diffusion properties is probably the consequence of the difference between the extracellular matrixes synthesised by the cells.
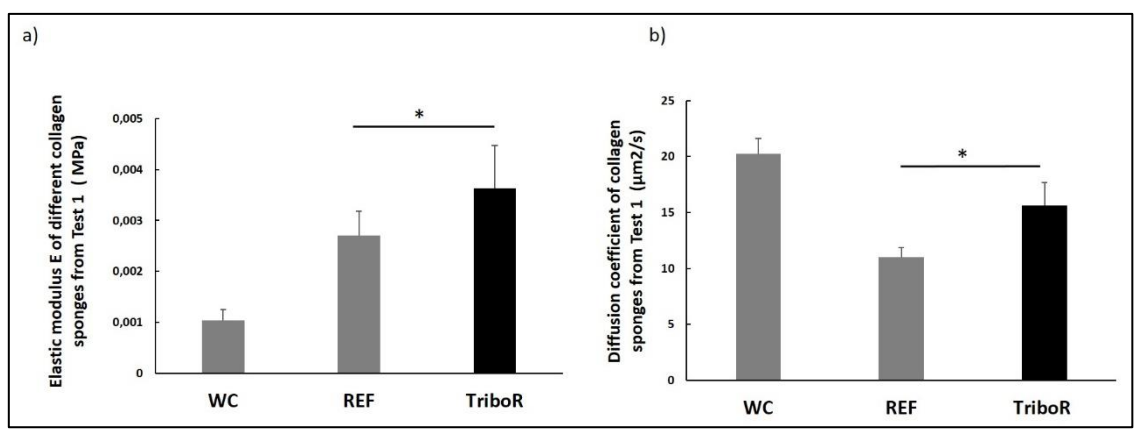
*Figure G-14 Mechanical measurements for collagen sponges seeded with chondrocytes and cultured following conditions of Test 1 (cf. Table 1). a) Elastic modulus of sponges under mechanical solicitations and without solicitations. b) Diffusion coefficient of fluorescein-dextran 70 KDa through different sponges. The diffusion coefficient of the "REF" sponges was compared to "TriboR" sponges. * p < 0.05.*

Overall, these results confirmed the role of mechanical stresses in the synthesis of the cartilage-like extracellular matrix and the capacity of the new device to handle a cell culture for four weeks without any contamination. These cell cultures presented an experimental validation of the "Tribo-bioreactor" as a cell culture bioreactor. However, the stiffness of the collagen sponges was not adequate for a convenient mechanical stress transmission. Consequently, most of the synthesis of the cartilaginous

155

matrix was at the periphery of the sponge. Therefore, it was considered to change the biomaterial scaffold. Due to this, we continued the experiments with agarose hydrogel.

3.3.2. Agarose hydrogel allowed a cellular development for aligned chondrocytes

First, the mechanical properties of the two type of agarose hydrogel constructs were compared. The agarose hydrogel containing the cells aligned by 3D bioprinting had a higher elastic modulus and were more resistant than the agarose hydrogel containing randomly seeded chondrocytes and without cells (figure 15).
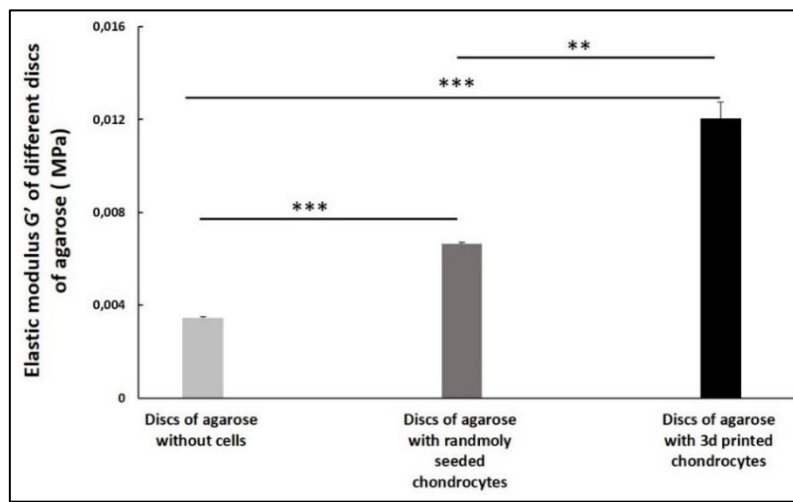
*Figure G-15 Mechanical properties of 3D-printing agarose discs with and without chondrocytes. Rheological tests were performed with the "tribo-bioreactor" and the elastic modulus G' was calculated. *** p < 0.001, ** p < 0.01.*

Also, data analysis showed that the elastic modulus of agarose discs reconstructed by 3D printing decreased as their viscosity increased during the compression (Table 4). The sliding effect between agarose layers causes this result. Indeed, the printed agarose discs were too large (1 cm in diameter) to fit the locations in the "Tribo-bioreactor" plate. Consequently, they were punched, which could cause the separation between agarose layers and the sliding effect between them. It's a parameter to work on to improve the 3D bioprinting process further.

Table G-4: Mechanical characterisation of 3D printed agarose constructs performed with the "Tribo-Bioreactor."

	Day 0	Day 3	Day 5
$G'(\frac{N}{m^2})$	136,72	115,78	102,94
$\eta\,(Pa.s)$	2,75	4,49	8,36
Phase shift (°)	3.62	6.94	14.32

Amira HANNOUN/ Thesis in Biomechanics 2020/ INSA Lyon

The first tests with agarose hydrogel were performed with human nasal chondrocytes. Nasal chondrocytes are more accessible than articular ones while being very similar (hyaline cartilage) [232] [233]. After applying the usual amplification protocol for nasal chondrocytes for two weeks on plastic in the presence of multiplication medium, randomly seeded chondrocytes in agarose hydrogel were differentiating and producing a cartilage matrix as shown in the histological sections in figure 16.

This result indicates that the cell culture in hydrogel agarose is convenient for bioengineering and confirms the possibility of producing cartilage from human chondrocytes seeded in agarose.
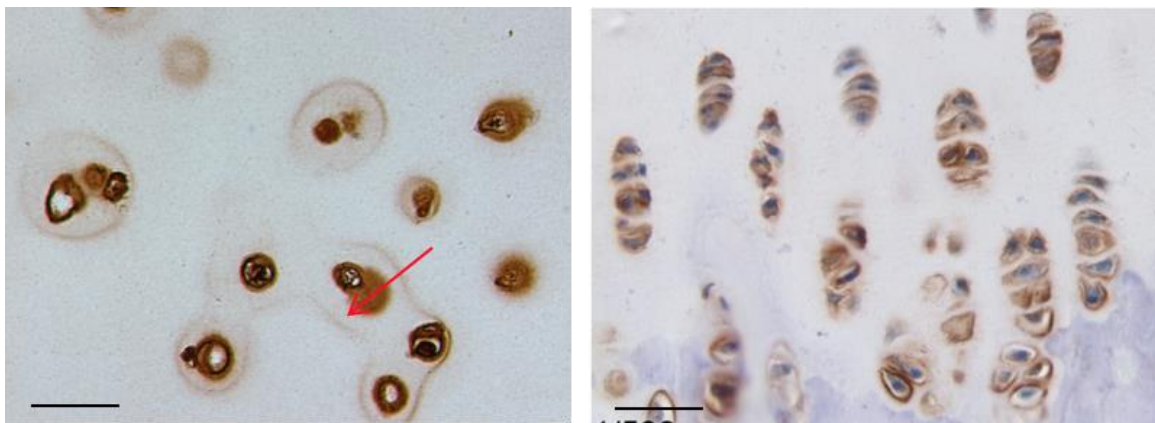
Figure G-16 Left: histological section of an agarose gel randomly seeded with human nasal chondrocytes. The section was immunostained (brown) with type II anti-collagen antibody, the major cartilage protein. The cells pool their neo-synthesized matrix (arrow), forming first tissue units that develop over time within the hydrogel.
Right: histological section at the level of articular cartilage with the same immunostaining. The chondrocytes also share their extracellular matrix, but the cells, in this case, are aligned along a principal vertical axis (axis of the long bone).
Scale bar = 50 μm

The effect of the 3D printing on chondrocytes was analysed too. 3D printed constructs were included in paraffin for histological analysis, to visualize the printed cells topography. The observations clearly showed the printed layers of chondrocytes on the vertical axis (y); however, cells spots were not well separated from each other on the horizontal axis (Figure 17).

Immunohistological analysis was also performed after 21 days of cell culture. These analyses showed that cells still metabolically active by producing type II collagen, as shown in figure 18.
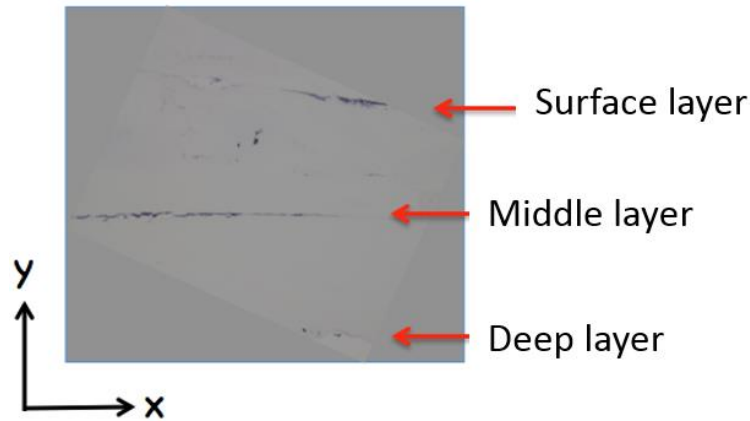
Figure G-17 HES staining shows the successive layers of cells printed on three layers of agarose (After the 3D printing process)
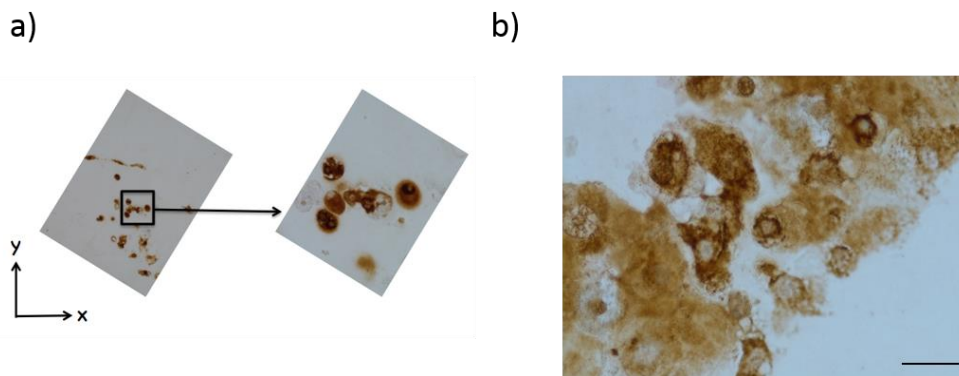
Figure G-18 a) Cross-section of agarose disc, immunostained with anti-collagen II antibody, b) Accumulation of cartilage produced by laser-printed human chondrocytes grown for 21 days in agarose hydrogel. The histological section was labelled with an anti-collagen II antibody Scale bar = 50 µm

In accordance with our results, different studies have already shown that the 3D bioprinting technique is innocuous for chondrocytes [229] [230]. Thus, the present test highlighted the interest of the combination of chondrocytes alignment and mechanical solicitations. However, the available and used 3D bioprinting technique needed more improvement to avoid the separation between agarose layers and to provide better mechanical transmission. Consequently, 3D bioprinting was not considered for future tests.

3.3.3.   Conclusions on the use of the "Tribo-bioreactor" for chondrocytes 3D culture

Overall, different tests of cell culture using the "Tribo-bioreactor" confirmed the importance of the mechanical solicitations in cartilage matrix synthesis. Our new prototype allowed us to apply various mechanical solicitations to different constructs combining different biomaterials and chondrocytes. Therefore, the "Tribo-bioreactor" is considered a suitable bioreactor for cartilage-cell culture. There was no contamination, and no cell death detected in the different performed cell culture. In this

context, it can be used to continue the investigation on the synthesis of the neocartilage in the presence of the PyC.

4. Association of the PyC with the mechanical solicitations in murine chondrocytes culture

The "Tribo-bioreactor" applies tribological solicitations to 3D cell cultures with the possibility of microscopic observation. It is developed to investigate the principles of tissue bioengineering for cartilage research. We tested its capacity to hold and perform a cell culture applying mechanical solicitations without affecting cell viability. We validated our "Tribo-bioreactor" prototype as a suitable bioreactor for cartilage-cell culture so that it is considered to continue our investigation on the PyC effect using this new device. We also highlighted the importance of mechanical solicitations to improve cartilage matrix deposition. By fluorescence analysis, we showed that the transmission of mechanical stress is affected by the rheological properties of the used biomaterial support. Thus, the choice of the cell culture support is crucial. Consequently, many challenges were encountered for the 3D cell culture in the presence of the PyC:

- How to seed cells on the surface of the PyC biomaterial?
- What scaffold should be used?
- How to place the cell-seeded PyC support in the "Tribo-bioreactor"?
- What is the decent configuration for cell culture and for how long?

4.1. Cultured chondrocytes with PyC support

To perform the chondrocyte culture in the presence of PyC, it was necessary to figure out the possible configurations for the test. We look for a 3D structure suitable for insertion in the "Tribo-bioreactor", which allows the cell-contact with PyC biomaterial. Two configurations are tested: either the use of beads or discs.

4.1.1. Cultured chondrocytes with PyC beads

4.1.1.1. Principle and settings

The first proposed configuration was to use PyC beads to form a 3D structure, including cells, as shown in figure 19. The hypothesis is that the culture period in the "Tribo-bioreactor" would favour extracellular matrix deposition, which would embed both the chondrocytes and the PyC beads to form a tissue-like sample.
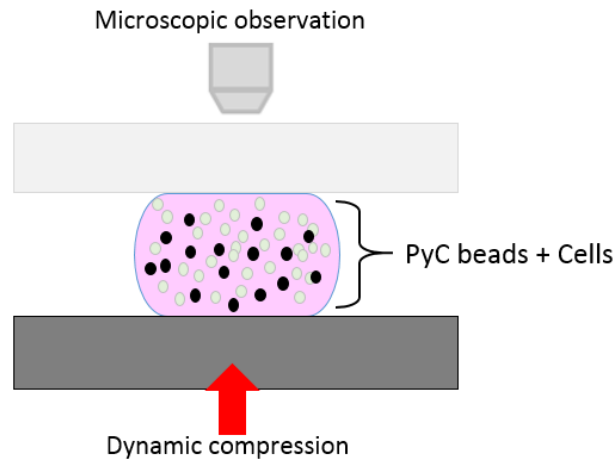
Figure G-19: Possible configuration of chondrocytes cultured in the presence of PyC beads

As a first step to test this configuration, standard cell cultures of primary murine chondrocytes (chapter D § 3.2) in the presence of PyC beads are performed. Two configurations were considered for the cell culture: either to seed chondrocytes before placing the beads in the culture plate or after. Culture of murine chondrocytes is launched in the presence of beads of PyC with different sizes (the same cell culture protocol presented in chapter D).

The biomaterial samples used in this test are made of PyC, supplied by Wright Medical (Tornier) and sterilised in the LaMCoS. The samples are polished beads with two different sizes:

- "S1" ≈ Ø 1000-1120 µm diameter
- "S2" ≈ Ø 1400-1600 µm diameter

The effect of PyC beads on chondrocytes was analysed *in vitro* by MTT and LDH assays for viability and cytotoxicity (as described chapter D §3.3.1), in comparison to the control (without beads). Primary murine chondrocytes were cultured for 17 days in CLC medium (cartilage-like conditions, chapter D §3.2) in the presence of PyC beads.

4.1.1.2. Results regarding the cytotoxicity of PyC beads

MTT test showed that the beads dramatically affected cell viability independently of their size or the selected configuration (figures 20a, b). Cell viability was altered by at least 50 % in the presence of PyC beads. In correlation, up to 20 % of cytotoxicity was detected by LDH assay (cytotoxicity is negligible only when it is less than 5%) (data are not shown). Given the extent of the cell loss, the experiment was performed only once (for the configuration "beads placed after the cells") or twice (for "beads before cells"). Based on these results, it was not suitable to continue the test with PyC beads for viability and cytotoxicity issues.
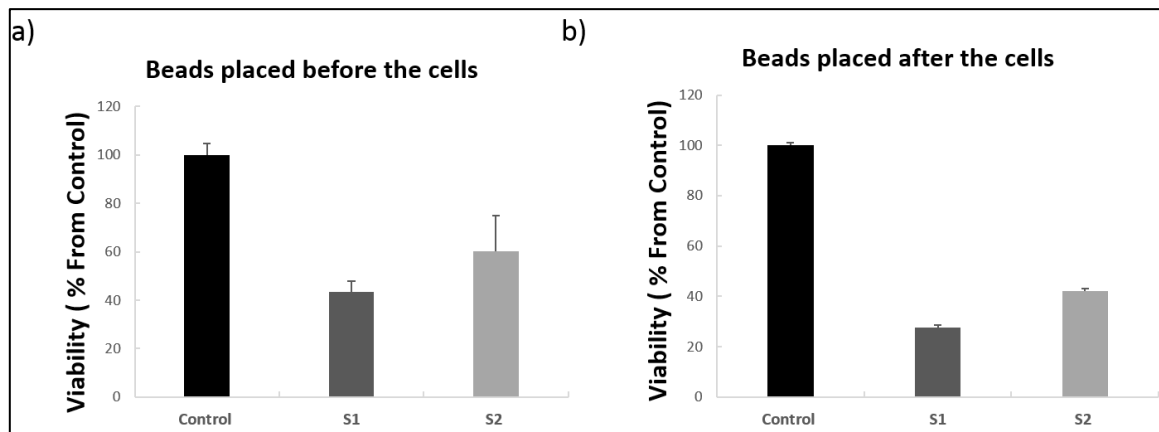
Figure G-20 Growth of murine chondrocytes in the presence of PyC beads. MTT assay (a, b). Bars indicate mean ±SEM of 2 independent experiments.

4.1.2. Cultured chondrocytes on the surface of PyC disks in the presence of mechanical solicitations

4.1.2.1. Experimental design

The second proposed configuration was to obtain a cell pellet which was placed directly in a PyC disc. Consequently, the culture on the surface of PyC is considered as a 3D-cell culture in comparison with the standard chondrocytes 2D-cell culture performed in the culture plate (figure 21). The hypothesis is that the culture period in the "Tribo-bioreactor" would favour extracellular matrix deposition, which would reinforce the cohesion of the cell pellet that would form a tissue-like cell-membrane on the surface of the PyC support. Therefore, cell culture of primary murine chondrocytes was conducted in the "Tribo-bioreactor" with the presence of PyC for 17 days.

The chondrocytes were fluorescently labelled to evaluate their behaviour during the period of the culture in the "tribo-bioreactor". As mentioned before, the "tribo-bioreactor" allows performing a cell culture with the application of mechanical solicitation, while following the cell comportment by the fluorescence analysis.

Three different conditions were tested:

- Control "CT": standard 2D chondrocytes cultured in the cell culture plate without cell labelling and biomaterial in CLC medium.
- Static control "SCT": 3D cell culture of labelled chondrocytes in specific support in the presence of PyC without mechanical solicitations, gap = 500 μm.
- Dynamic culture "DC": 3D cell culture of labelled chondrocytes in the presence of PyC with applied mechanical solicitations using the "Tribo-bioreactor", gap = 500 μm.

161

Amira HANNOUN/ Thesis in Biomechanics 2020/ INSA Lyon
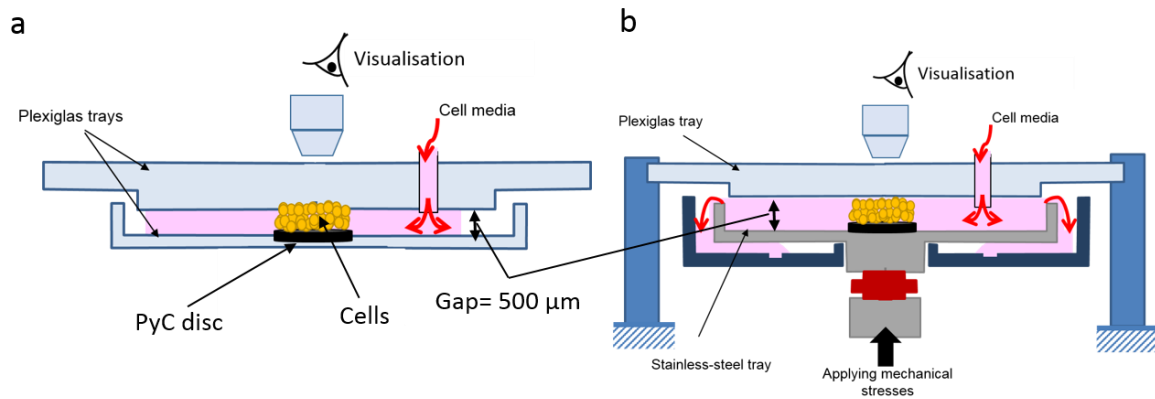
Figure G-21 Schema of the SCT and DC tests: a) the two conceived plates for the static conditions with 500 μm gap b) the bioreactor test

4.1.2.2. Protocol and settings

Primary murine chondrocytes were used as cell model as previously described (chapter D §3). They were chondrocytes fluorescently labelled using a lipophilic membrane marker (dialkyl aminostyryl dye: Dil, Thermofisher) marked in orange-red (λ_{ex}= 549 nm and λ_{em}= 565 nm). The membrane labelling did not affect cell viability, development, or basic physiological properties. After dissection, the cells were washed with PBS, incubated with 5 μL of the marker diluted in 6 ml of CLC media for 15 min, and washed with PBS, as described by the manufacturer. After labelling, cells were centrifuged and divided in suspensions of 125 μL, each containing 1 million cells.

The obtained cell pellet was then placed directly in the PyC disc. Since no biomaterial support or scaffold was used for the cell culture, the cell pellet was let rest for 2 hours to allow cell cohesion before insertion into the "tribo-bioreactor".

The samples of the PyC were disc-shaped with 20 mm diameter and 2 mm thickness supplied by Wright Medical/Tornier, with the same surface conditions as the medical implants used in shoulder arthroplasty. They were sterilised in the LaMCoS research laboratory.

To evaluate the impact of mechanical solicitations, a new cell culture room was conceived from the existing plastic one for the static conditions (figure 21). It consisted of two plates separated by a gap of 500 μm. For the static and dynamic conditions, a PyC disc was glued in the inferior plate with two-component all-purpose glue, made with an epoxide-resin base "Araldite® Rapid". After the 2-hour-long rest of the labelled chondrocytes, both superior plates of the plastic support and the "tribo-bioreactor" were put back, and a CLC media was added. In the "DC" condition, a dynamic compression (50 μm and 0.5 Hz) was applied.

Cell growth on the discs of PyC was assessed and followed *in situ* by visualization using an optical light and vertical fluorescence microscope (Zeiss Axio Examiner Z1, Leica DMLM). The microscope is

equipped with a CCD camera (Leica DC350F) and with two laser lines (488 and 555 nm) coupled to a fluorescence camera (Axio Camera 60 N-C). Fluorescence microscopy imaging was performed *in situ* during the cell culture in the same days of changing the medium as presented in table 5 (the same culture conditions and planning described in chapter D).

Table G-5 Planning of chondrocyte culture

	Chondrocytes cultured under CLC
Day 0	Dissection Biomaterial hydration in PBS
Day 1	Cell seeding in CLC medium
Day 3	Changing CLC medium
Day 6	Changing for CLC medium
Day 7	Changing CLC medium + adding vitamin C
Day 10	Changing CLC medium + adding vitamin C
Day 14	Changing CLC medium + adding vitamin C
Day 17	Samples collection for histological tests

The cell culture was performed in an incubator (T: 37°C; 95% humidity; 5% CO_2) placed in a clean room (ISO Cleanliness Class 5) located in LaMCoS. The environment maintained a level of cleanliness equivalent to ISO Cleanliness Class 5, less than 100,000 particles with the size of 0.1 µm or larger per m^3, or less than 832 particles with the size of 1 µm or larger per m^3. The main parameters that control the environmental performance of a cleanroom are the air flows and pressure difference. By adjusting the air flows, positive differential pressure can be created to prevent the introduction of potential contaminants from the surrounding cleanroom. The temperature, humidity, and cleanliness were also controlled [234].

After cell culture, the tissue-like cell-membranes developed in either PyC surface in SCT and DC conditions or the plastic control were carefully removed for histological analysis. Different staining and immunolabelling (HES, SO, type I collagen, type II collagen, aggrecan) were performed as described previously in chapter C and in [159].

4.1.2.3. The dynamic compression affected chondrocytes growth on the surface of PyC

Microscopic observations assessed the cellular growth on the surface of the PyC discs throughout the culture period (until day 17) both without (SCT) and with dynamic (DC) mechanical solicitation (figure 22). The chondrocytes cultured under mechanical solicitations exhibited a better cell development than the static conditions. In the SCT condition, the chondrocytes were spaced and seemed to synthesize a limited amount extracellular matrix (limited diffusion of the fluorescence).

In fact, at the end of the cell culture, the cells were separated and stretched, which represented an unusual shape for chondrocytes. In these conditions, chondrocytes had probably lost the ability to

synthesis a suitable extracellular matrix, which could affect the cell cohesion and cause the observed decrease in cell number (figure 22).

On the contrary, in the presence of dynamic compression, chondrocytes clusters were observed with a probable extracellular matrix deposition. In that DC condition, cell aggregates affected the adjustment of the contrast with the microscope. During the cell culture, the cultured chondrocytes in DC conserved a safe behaviour and their ability to synthesize the extracellular matrix.

Again, our observations corroborate the importance of mechanical solicitations. However, they did not allow to conclude the effect of the PyC on cellular behaviour. Therefore, histological analysis was performed to provide more information about the biomaterial effect separately or in combination with mechanical solicitations.
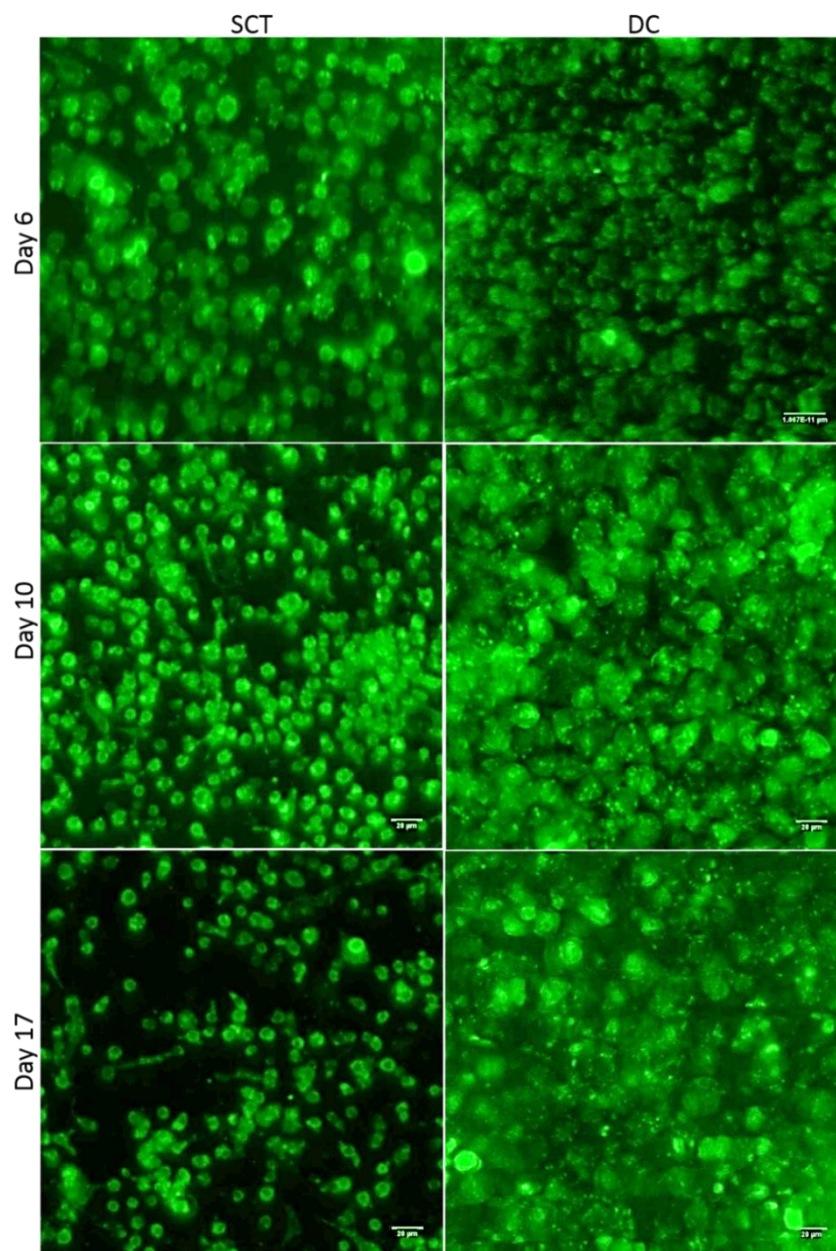
Figure G-22 Fluorescence observations of chondrocytes cultured on PyC discs during 17 days in dynamic conditions (DC) or static conditions (SCT), scale bar=20 µm

Amira HANNOUN/ Thesis in Biomechanics 2020/ INSA Lyon

4.1.3. 3D-culture on PyC disc promoted the creation of cartilaginous tissue-like in the presence of mechanical solicitations

After cell culture, the tissue-like cell-membranes developed in either PyC surface in SCT and DC conditions or the plastic control (CT) were analysed by histochemistry. Overall, the HES staining highlighted dissimilar structures between the samples cultured in the three different conditions (figure 23). The tissue-like cell-membranes developed in CT has already been observed previously (figures E7, E8). No significant difference was noticed due to the labelling of the cells.

The SCT sample was distinguished by many small round cells. As suggested by the fluorescence analysis, at the end of the culture period, the cells do not show a chondrocyte-like phenotype anymore. On the contrary, the cells cultured with dynamic solicitation (DC) were larger with a rounded shape which indicates a proper chondrogenic phenotype. Besides, cell density was also higher in DC than in CT condition, suggesting an enhanced cell proliferation throughout the culture period.

SO staining is used to detect glycosaminoglycans which are considered among the major components of the cartilage tissue matrix. More SO staining was detected in chondrocytes cultured on PyC discs (DC and SCT) in comparison with the chondrocytes cultures under CT condition (figures 23e, f). This result confirmed that the PyC discs favoured the synthesis of cartilage components, as shown in chapter D (figure D9, CLC+PyC). Moreover, the red staining was intense at the level of cellular condensations in SCT conditions, while it was restricted around the chondrocytes in DC conditions. Thus, the application of the dynamic compression could allow a better extracellular matrix development.
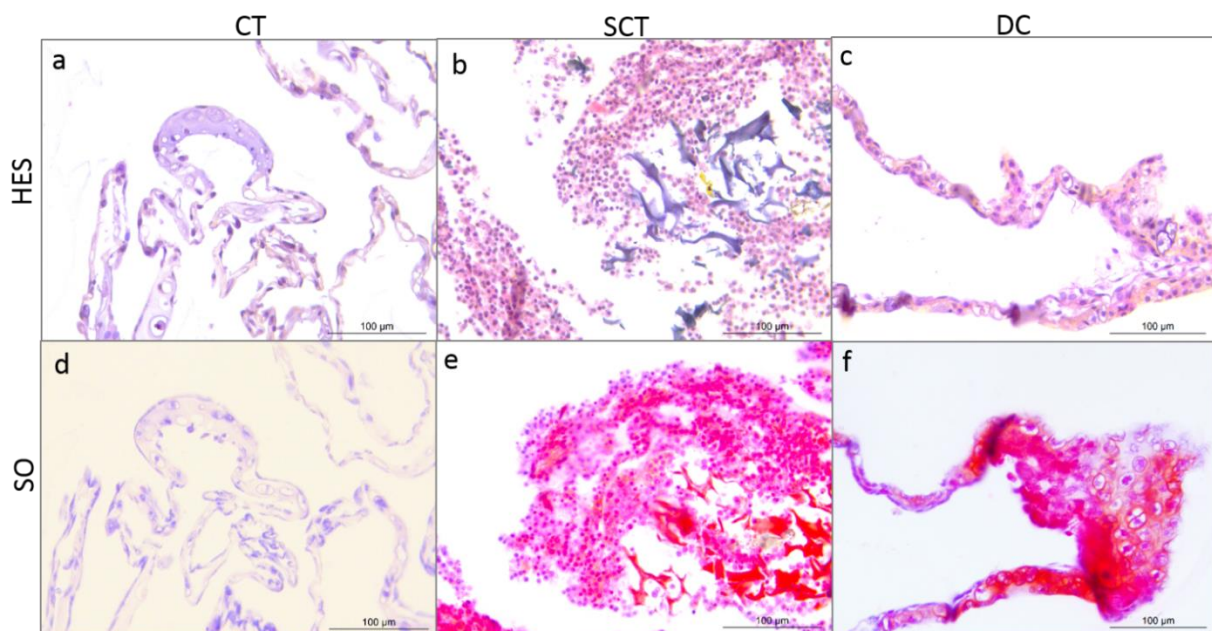
Figure G-23 Histological analysis of chondrocytes cultured under CT, SCT and DC. HES staining (a, b, c) and SO (d, e, f). HES and SO were performed on the tissue-like cell-membranes grown on plastic control or PyC discs.

165
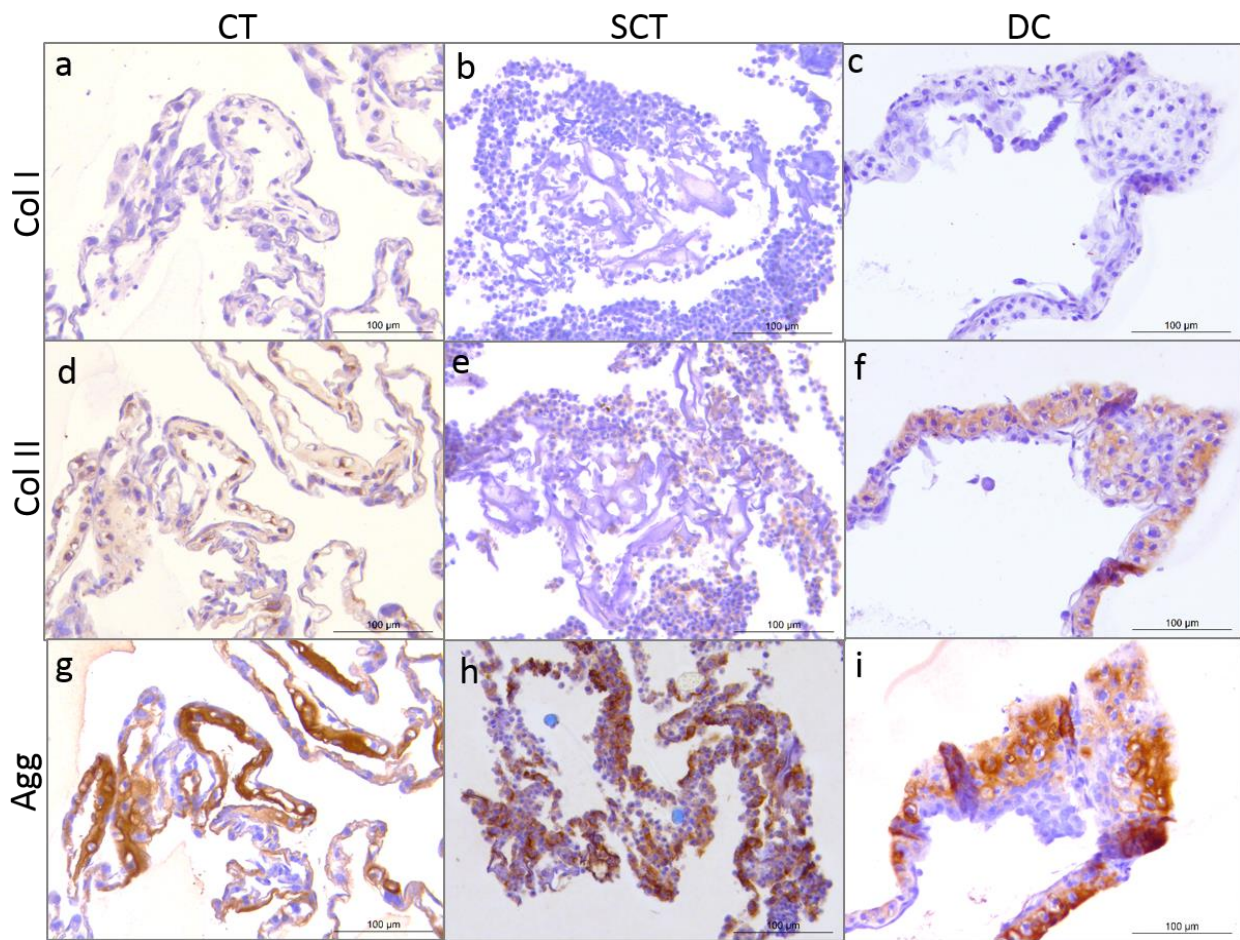
Figure G-24 matrix biological components of the tissue-like cell-membranes grown under CT, SCT and DC. Immunolabelling for type I collagen (a, b, c), type II collagen (d, e, f) and aggrecan (g, h, i) were performed on the tissue-like cell-membranes grown on plastic control and PyC discs.

Type I collagen specific immunolabelling was quasi-negative for all tissue-like cell membranes (figure 24). In opposition, the aggrecan labelling was intense for the three samples. However, differences were noticed regarding type II collagen labelling. In the CT group, type II collagen labelling presented a heterogeneous distribution. For tissue-like cell-membranes developed on PyC disc (SCT and DC groups), the distribution was more homogenous in the extracellular matrix. Notably, the type II collagen staining appeared enhanced in DC conditions and localized in the same zones where the aggrecan labelling was intense.

Overall, the comparison between the CT group and (SCT and DC) group highlights the importance of the PyC biomaterial in the synthesis of extracellular matrix with cartilage characteristics. Furthermore, the difference between SCT and DC brings out the necessity of applying dynamic solicitations in cell culture.

5. Conclusion on the development of a realistic *in vitro* model and perspectives

The "tribo-bioreactor" presented in this chapter achieved its objectives. The device can be used for mechanical characterization, cell visualization under mechanical stress, and cartilage-tissue

Amira HANNOUN/ Thesis in Biomechanics 2020/ INSA Lyon

Cette thèse est accessible à l'adresse : http://theses.insa-lyon.fr/publication/2020LYSEI025/these.pdf
© [A. Hannoun], [2020], INSA Lyon, tous droits réservés

bioengineering, separately or at the same time. It allows applying various mechanical solicitations to different constructs combining different biomaterials and chondrocytes in several configurations. It has proven its flexibility by allowing the mechanical stimulation of cells embedded in collagen sponges or agarose hydrogels or cells in 3D-pellet in interaction with PyC disks. All the tests confirmed the importance of the mechanical solicitations to favour cartilage matrix synthesis.

Based on our previous results revealing the importance of the HA-phospholipids medium for proper lubrication and force transmission (presented in chapter E) (figures E-7, E-8), it will be interesting to combine this element to the "tribo-bioreactor" optimization. A more extended cell culture period could also be envisaged to cumulate more matrix-deposition and obtain an even more cartilage-like sample at the end of the experiment. Therefore, the next suggested step would be to perform murine primary chondrocytes cultured in the presence of the PyC with mechanical solicitations, applied by the "tribo-bioreactor", using the cell culture medium with adding HA-phospholipids mixture.

To be continued…

Conclusions and perspectives

The impact of osteoarthritis in terms of public health is significant. It is ranked between the 15 most reported chronic diseases in Europe. Notably, in France, it affected around 50 % of the population aged more than 65 years old (according to the Health and Social Protection Survey 2017) [4]. This pathology is sometimes consecutive to trauma and is characterized by cartilaginous tissue wear inducing severe disability.

Due to the difficulty in detecting early the first symptoms of cartilage degradation, there is no current treatment allowing its total repair. Two leading therapeutic solutions are still very promising: either the joint replacement by a prosthesis (arthroplasty) or restoring the cartilage structure using bioengineered grafts.

At present, the arthroplasty presents the only valid treatment in the long term. However, failures have been recorded. The reported rate of complications could reach 62 % with 12 % of revision surgeries in the case of shoulder arthroplasty (data from a review including more than 4000 prostheses [235]). Medical problems as inflammation or rejection of the implant appear during the *in vivo* operation, which caused this high rate of revision surgeries. Therefore, improving the existent prostheses and their *in vivo* lifespan remains a big challenge.

Because of the limits in the resolution of *in vivo* investigation techniques, the implant optimization requires realistic *ex vivo* models. In this view, *ex vivo* tribological simulations are considered. However, there is no biotribological model with a sufficiently realistic representation of the living tribological triplet. The conditions of these simulations are unsatisfactory regarding the mechanical and physicochemical particularities of the biological environment. Thus, the *in vivo* lifespan of different prostheses is still very disappointing compared to that extrapolated from the *ex vivo* simulations.

For the shoulder joint, degenerative pathologies are currently treated by total arthroplasty or hemiarthroplasty. The complication rate of total arthroplasty reaches 22 % due to the complexity of this joint mechanics and the limited bone stock [11][12][16][159]. Failures include constant or activity-related pain reduced range of motion and instability. In this context, for patients with complications arising from limited bone stock and with primary glenohumeral arthritis, a new generation of interposition implant has been developed. The implant has a unique concept; it is a free spherical implant. It is designed to be inserted between the glenoid cartilage and a surgically created humeral bone cavity. Hence, the spherical implant replaces the anatomical humeral head [13].

Whereas cobalt-chromium (CoCr) is the most used biomaterial in shoulder arthroplasty, pyrocarbon (PyC) was selected for the new implant for its elastic modulus similar to that of bones and its excellent tissue biocompatibility (Chapter B). Clinical studies revealed satisfactory results comparable to those

of hemiarthroplasty but still inferior to those of total arthroplasty [12] [16]. Notably, short-term clinical results showed minimal bone and cartilage wear and good bone remodelling in contact with the implant. However, the origin of these results is not yet well understood.

In this framework, in a recent study on human explants (a previous PhD work in the laboratory), a neosynthesized tissue at the extremity of the humeral metaphyseal cavity in contact with the PyC implant has been observed. Usually, following the arthroplasty procedure, a fibrocartilaginous tissue is developed due to the healing of the joint [160]. However, in the case of the spherical implant, the histological analysis suggested that the formed tissue had cartilage-like characteristics. This result remains the most promising advantages of the new implant confirming that the proper functioning of the prosthesis is related to the "biological adaptability" of the surrounding tissues, which helps the creation of a non-painful biological tissue in contact with the implant. In addition, this result partly explains the favourable clinical outcomes. However, the clinical findings are more controversial on the scapula side, including cartilage erosion [11][12][12] [12] [16]. Therefore, the role of PyC and the geometry of the implant on the remodelling of the surrounding tissues need further investigation. Thus, this thesis aims to understand the origin of tissue remodelling on the bone and cartilage side.

For all the performed experiments, the PyC was compared to the CoCr, which is the most used biomaterial in shoulder arthroplasty. The first step of our strategy is conducting a retrieval analysis to identify *in vivo* the effect of the PyC on each component of the living tribological triplet. The second step is to carry out three parallel studies, based on the identified effects of the PyC *in vivo,* to dissociate the role of the biology (cellular response of the first bodies) of the lubricant (third body) and the transmission of mechanical stresses (third body and mechanism). Finally, our strategy aims to validate the results thus obtained by associating the different aspects in a developed *in vitro*-model based on tissue bioengineering principles. Consequently, as illustrated by the diagram below (figure 0.1), our methodology is based on:

①	The expertise of retrieved explants (histological and lipidomic analyses) (Chapter C)

②	The analysis of murine primary chondrocytes cultures in contact with PyC and CoCr (Chapter D)

③	The development of a biomimetic lubricant (Chapter E)

④	The *in vitro* biotribological simulations (Chapter F)

⑤	The design and validation of a 'tribo-bioreactor' which allowed to combine the biological, physicochemical and tribological results obtained previously (Chapter G)
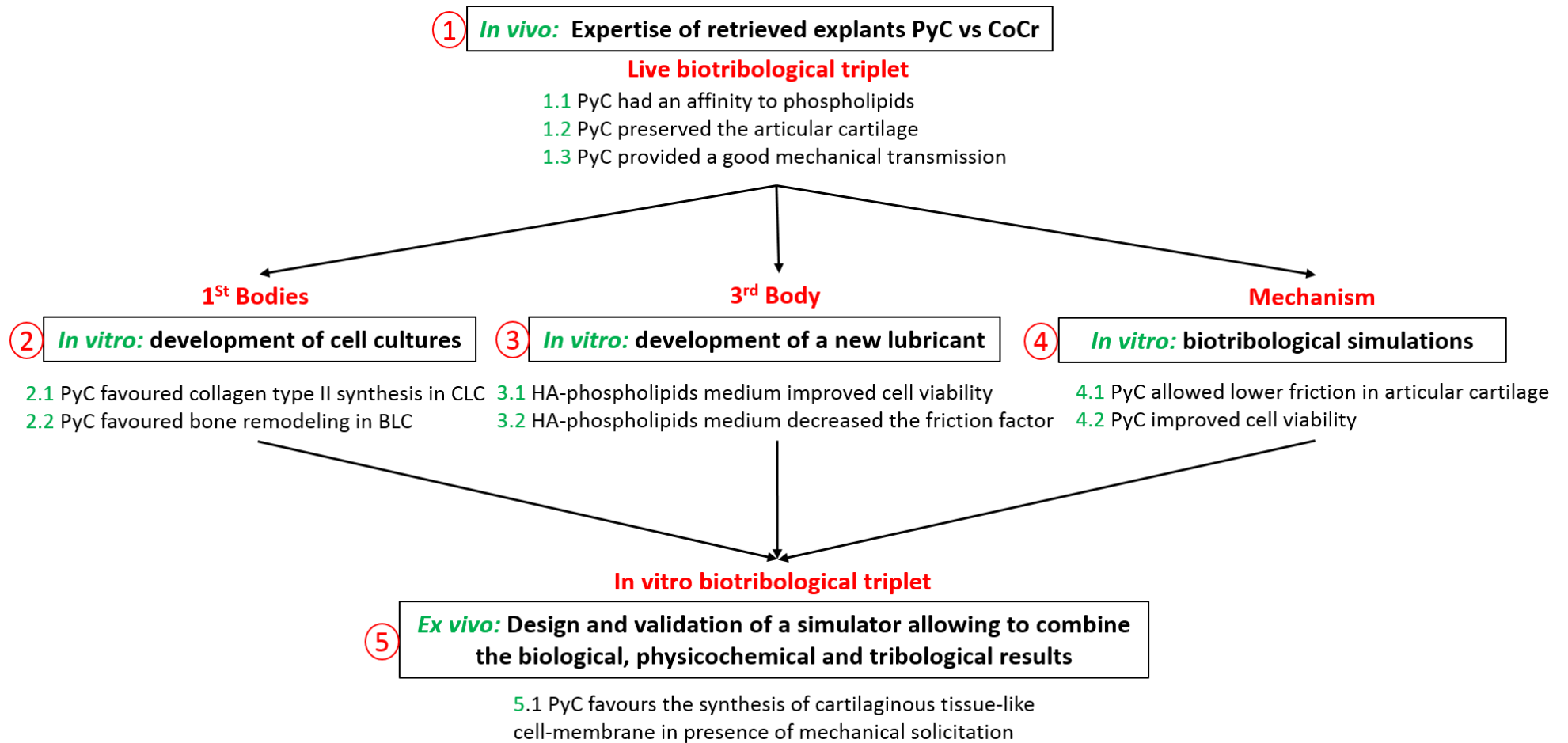
Figure 0-1 the followed strategy during the thesis illustrating the main findings for each part

Amira HANNOUN/ Thesis in Biomechanics 2020/ INSA Lyon

Hereafter are resumed the major results of this thesis (the numbers in red and green colour in the text below are referred to figure 0.1):

① The effect of the PyC on the living biotribological triplet was identified through a retrieval analysis of shoulder hemi-prostheses. It was showed that the PyC induce minimal wear to the first bodies (cartilage) and favours a good bone remodelling (1.2). An excellent tissue remodelling is only possible when the cells receive suitable mechanical solicitations. Thus, the PyC provided an outstanding transmission of the mechanical stresses through its surface properties and structure (1.3).

The PyC was used for more than 3 million implantations in heart valves. It showed excellent results in this application which corroborates the findings of this project. Our study model emphasizes the particularities of this biomaterial in the biological environment. Compared to the CoCr, the PyC had a particular affinity to the phospholipids, which were adsorbed on its surface (1.1). Phospholipids are the lubricating molecules in the synovial fluid.

This first part of the work identified the *in vivo* effect of the PyC in comparison with the CoCr. After that, three parallel studies were carried out to study the impact of the PyC on each component of the live biotribological triplet *in vitro*.

② To study the impact of the PyC on the 1st bodies of the live biotribological triplet, an *in vitro* biological approach was considered. The effect of the biomaterials on chondrocytes was analysed *in vitro*. Murine primary chondrocytes were grown on discs made of PyC or CoCr using two culture media to mimic either the cartilage-like conditions (CLC) or the bone-like conditions (BLC). The study showed that the chondrocytes did grow on the biomaterials without alteration in cell viability or manifestation of cytotoxicity. Histological analysis suggested that under CLC, the PyC promotes type II collagen expression in chondrocytes, generating more cartilage-like matrix than samples grown on both CoCr and plastic control (2.1). In BLC, the tissue-like cell membranes grown on PyC were more mineralised and homogenous. Also, the elastic modulus of the tissue-like cell membranes developed on the PyC surface was higher, indicating more stiffness (2.2).

Overall, the cellular results suggested that PyC could present some benefits for interposition shoulder arthroplasty, promoting more cartilage-like characteristics synthesis than the CoCr. The findings of this part were published in European Cells and Materials DOI: 10.22203/eCM.v037a01 and deserve further clinical investigations.

③ A physicochemical approach was next elaborated to investigate the 3rd body of the live biotribological triplet. It was related to the fact that the biological medium of the joint, called the synovial fluid, is a complex molecular mix that can be a good or a bad lubricant for implant surfaces. It can either decrease or increase their wear. Its composition is modified during pathologies generating

several variations in the physicochemical parameters. These modifications affect the living biotribological triplet and reduce its performance. Therefore, a new biomimetic lubricant was developed for the biotribological simulations. The optimal lubricant that we obtained was a mixture of cell culture medium with hyaluronic acid and phospholipids. The HA-phospholipids medium was tested *in vitro* with live cartilage explants. It improved cell viability during the testing (3.1).

④ Then, a tribological approach was elaborated to explore the impact of the PyC on the mechanism of the live biotribological triplet. First, friction tests analysed the effect of PyC articulating against live bovine cartilage compared to the CoCr. The testing was performed using the new developed HA-phospholipids lubricant. Experiments showed a lower coefficient of friction using the PyC in comparison with the CoCr (4.1) and using the newly developed lubricant in contrast with the standard cell culture medium (3.2). Second, the same contacts were analysed through wear testing to evaluate the effect of a more complicated movement. Wear testing was performed using a "shoulder simulator" developed in the tribology laboratory of RUMC (Chicago, USA) (as a part of an internship). The performed experiments showed that the PyC was able to improve cell viability compared to the CoCr. Thus, PyC preserves the cartilage better than the CoCr (4.2).

⑤ Overall, the three performed approaches (points 2, 3 and 4) dissociated the role of the biology (cellular response), of the lubricant and the transmission of mechanical stresses. To validate these results, the different aspects were associated in an *in vitro* model based on tissue bioengineering principles.

A simulator "Tribo-bioreactor" was conceived and validated to perform cell culture of murine primary chondrocytes on PyC discs in the presence of mechanical solicitations. This final part of the project aimed to provide a realistic model to perform the biotribological simulations respecting the identified roles of each component of the living tribological triplet.

Preliminary results proved the importance of mechanical solicitations in chondrocytes 3D culture. Indeed, microscopic observations showed that cellular development was better under the dynamic mechanical conditions compared to the static conditions or no mechanical solicitations. The histological analysis corroborated these observations as the extracellular matrix development was enhanced and more cartilage-like in the presence of dynamic compression. The immunostainings showed a higher type II collagen staining in cells cultured on PyC discs and in the presence of mechanical solicitations. Thus, PyC further favoured the synthesis of cartilaginous tissue-like cell-membrane in the presence of mechanical solicitation.

Our new device represents a global approach to gather the biomaterial, the cells and the adequate lubricant in the presence of the mechanical solicitations. Since a suitable HA-phospholipids lubricant

had been developed and validated, it will be essential in the future experiments using the "tribo-bioreactor".

To conclude, the results of this thesis allowed to develop a realistic *in vitro* model to investigate the biomaterial effect on cellular development to optimise the existing orthopaedic prostheses. The overall finding of the project showed better chondrogenic and osteogenic cell activity in the case of PyC compared to CoCr. These results were correlated on the one hand with better adsorption of the lubricating molecules, phospholipids, on the surface of PyC and the other hand with an optimal transmission of the mechanical stress due to its properties. Whether the crucial properties are its particular structure, its surface properties, its roughness, its porosity… remains to be explored.

The *in vivo* control of the transmission of mechanical stresses is essential to guarantee good results of the prosthesis in the long term. Therefore, this thesis opens up fresh perspectives on the control of this transmission through biomaterials and their geometries to regenerate the cartilage. In particular, the following opportunities could be considered:

1) Performing cell culture on the PyC surface using the "Tribo-bioreactor" with cells obtained directly from patients to decipher the in vitro mechanotransduction better.
2) Improving the existing PyC implants and their designs to provide better mechanical transmission *in vivo*.
3) Taking advantages of the bio lubrication quality of PyC to develop not only the orthopaedic implants but also new heart valves.

References

[1] M. L. Tiku and H. E. Sabaawy, "Cartilage regeneration for treatment of osteoarthritis: A paradigm for nonsurgical intervention," *Therapeutic Advances in Musculoskeletal Disease*, vol. 7, no. 3. pp. 76–87, 2015.

[2] M. C. Hochberg *et al.*, "Osteoarthritis: a story of close relationship between bone and cartilage," *Medicographia*, vol. 35, no. 2, pp. 139–254, 2013.

[3] A. J. Sophia Fox, A. Bedi, and S. A. Rodeo, "The basic science of articular cartilage: Structure, composition, and function," *Sports Health*, vol. 1, no. 6, pp. 461–468, 2009.

[4] N. Célant and T. Rochereau, "L'Enquête santé européenne - Enquête santé et protection sociale (EHIS-ESPS) 2014," 2014.

[5] N. Fourcade and F. von Lennep, "L'état de santé de la population en France," 2017.

[6] J. Mika, T. O. Clanton, C. G. Ambrose, and R. W. Kinne, "Surgical Preparation for Articular Cartilage Regeneration in the Osteoarthritic Knee Joint," *Cartilage*, 2017.

[7] D. L. Kerboull, "Fiche D'Information Securite De L'arthroplastie totale de la hannche Approvisionnement," pp. 1–14, 2012.

[8] C. Lévigne, P. Lacroix, and J. Garret, "La proth??se d'??paule en 2010: Proth??se anatomique ou proth??se invers??e? Indications et contre-indications," *Rev. du Rhum. Monogr.*, vol. 77, no. 3, pp. 195–200, 2010.

[9] M. J. Wiater and M. H. Fabing, "Shoulder arthroplasty: prosthetic options and indications," *J. Am. Acad. Orthop. Surg.*, vol. 17, no. 7, pp. 415–425, 2009.

[10] Tc. Ozturk, O. Guneysel, and H. Akoglu, "Anterior shoulder dislocation reduction managed either with midazolam or propofol in combination with fentanyl," *Hong Kong J. Emerg. Med.*, vol. 21, no. 6, p. 346, 2014.

[11] J.-F. Gonzalez, G. B. Alami, F. Baque, G. Walch, and P. Boileau, "Complications of unconstrained shoulder prostheses," *J. shoulder Elb. Surg.*, vol. 20, no. 4, pp. 666–682, 2011.

[12] J. Garret *et al.*, "Pyrocarbon interposition shoulder arthroplasty: preliminary results from a prospective multicenter study at 2 years of follow-up," *J. Shoulder Elb. Surg.*, no. 2003, pp. 1–9, 2017.

[13] Y. Allieu, "Le concet d'arthroplastie par interposition avec implant libre en pyrocarbone," *Arthroplast. radiocarpiennes. Actual. thérapeutiques. Montpellier, Fr. Sauramps Médical*, pp. 51–57, 2012.

[14] S. D. Cook, K. A. Thomas, and M. A. Kester, "Wear characteristics of the canine acetabulum against different femoral prostheses.," *J. Bone Joint Surg. Br.*, vol. 71, no. 2, pp. 189–97, 1989.

[15] M. O. Gauci, M. Winter, C. Dumontier, N. Bronsard, and Y. Allieu, "Clinical and radiologic outcomes of pyrocarbon radial head prosthesis: Midterm results," *J. Shoulder Elb. Surg.*, vol. 25, no. 1, pp. 98–104, 2016.

[16] F. G. R.Hudek, B.Werner, A.F.Abdelkawi, "Pyrocarbon interposition shoulder arthroplasty in advanced collapse of the humeral head," *Orthopade*, vol. 46, no. 12, pp. 1034–1044, 2017.

[17] G. Ouenzerfi, M. Hassler, A. Trunfio-Sfarghiu, A. Nallet, and Y. Berthier, "Tribological behavior of Pyrolytic carbon against bone promotes cartilage regeneration?," in *Proceedings of the 42th Leeds-Lyon Symposium on Tribology September 7-9, 2015, Lyon, France*, 2015.

[18] M. Gras, A. L. Wahegaonkar, and C. Mathoulin, "Treatment of avascular necrosis of the proximal pole of the scaphoid by arthroscopic resection and prosthetic semireplacement arthroplasty using the pyrocarbon adaptive proximal scaphoid implant (APSI): long-term functional outcomes," *J. Wrist Surg.*, vol. 1, no. 02, pp. 159–164, 2012.

[19] M. Godet, "The third-body approach: A mechanical view of wear," *Wear*, vol. 100, no. 1–3, pp. 437–452, Dec. 1984.

[20] Y. Berthier, "Experimental evidence for friction and wear modelling," *Wear*, vol. 139, no. 1, pp. 77–92, Jul. 1990.

[21] V. Linck, "Modélisation numérique temporelle d'un contact frottant. Mise en évidence d'instabilités locales de contact - Conséquences tribologiques," *http://www.theses.fr*, Jan. 2005.

[22] H. Fay, "films lubrifiants supramoléculaires organisés : de la microsctructure aux propriétés tribologiqes," 2011.

[23] D. Dowson and A. Neville, "Bio-tribology and bio-mimetics in the operating environment," *Proc. Inst. Mech. Eng. Part J J. Eng. Tribol.*, vol. 220, no. 3, pp. 109–123, Mar. 2006.

[24] A. Unsworth, "Tribology of Human and Artificial Joints," *Proc. Inst. Mech. Eng. Part H J. Eng. Med.*, vol. 205, no. 3, pp. 163–172, Sep. 1991.

[25] A. Neville, A. Morina, T. Liskiewicz, and Y. Yan, "Synovial joint lubrication — does nature teach more effective engineering lubrication strategies?," *Proc. Inst. Mech. Eng. Part C J. Mech. Eng. Sci.*, vol. 221, no. 10, pp. 1223–1230, Oct. 2007.

[26] J. Katta, S. S. Pawaskar, Z. M. Jin, E. Ingham, and J. Fisher, "Effect of load variation on the friction properties of articular cartilage," *Proc. Inst. Mech. Eng. Part J J. Eng. Tribol.*, vol. 221, no. 3, pp. 175–181, Mar. 2007.

[27] R. M. Schulz and A. Bader, "Cartilage tissue engineering and bioreactor systems for the cultivation and stimulation of chondrocytes," *Eur. Biophys. J.*, vol. 36, no. 4–5, pp. 539–568, Apr. 2007.

[28] A. C. Osborne, K. J. Lamb, J. C. Lewthwaite, G. P. Dowthwaite, and A. A. Pitsillides, "Short-term rigid and flaccid paralyses diminish growth of embryonic chick limbs and abrogate joint cavity formation but differentially preserve pre-cavitated joints.," *J. Musculoskelet. Neuronal Interact.*, vol. 2, no. 5, pp. 448–56, Sep. 2002.

[29] M. Pacifici *et al.*, "Cellular and molecular mechanisms of synovial joint and articular cartilage formation," in *Annals of the New York Academy of Sciences*, 2006, vol. 1068, no. 1, pp. 74–86.

[30] M. Wong and D. R. Carter, "Theoretical stress analysis of organ culture osteogenesis," *Bone*, vol. 11, no. 2, pp. 127–131, Jan. 1990.

[31] M. Wong and D. Carter, "A theoretical model of endochondral ossification and bone architectural construction in long bone ontogeny," *Anat. Embryol. (Berl).*, vol. 181, no. 6, pp. 523–532, Jul. 1990.

[32] R. Meller *et al.*, "Postnatal maturation of tendon, cruciate ligament, meniscus and articular cartilage: A histological study in sheep," *Ann. Anat. - Anat. Anzeiger*, vol. 191, no. 6, pp. 575–585, Nov. 2009.

[33] C. Muehleman and K. E. Kuettner, "Distribution of cartilage thickness on the head of the human first metatarsal bone," *J. Anat.*, vol. 197, no. 4, pp. 687–691, Nov. 2000.

[34] J. J. Crisco, J. Blume, E. Teeple, B. C. Fleming, and G. D. Jay, "Assuming exponential decay by incorporating viscous damping improves the prediction of the coeffcient of friction in pendulum tests of whole articular joints," *Proc. Inst. Mech. Eng. Part H J. Eng. Med.*, vol. 221, no. 3, pp. 325–333, Mar. 2007.

[35] R. Forsey, J. FISHER, J. THOMPSON, M. STONE, C. BELL, and E. INGHAM, "The effect of hyaluronic acid and phospholipid based lubricants on friction within a human cartilage damage model," *Biomaterials*, vol. 27, no. 26, pp. 4581–4590, Sep. 2006.

[36] B. Abernethy, V. Kippers, S. Hanrahan, and M. Pandy, "Biophysical foundations of human movement," 2013.

[37] A. Johansson *et al.*, "Spectroscopic measurement of cartilage thickness in arthroscopy: Ex vivo validation in human knee condyles," *Arthrosc. - J. Arthrosc. Relat. Surg.*, 2012.

[38] D. R. Eyre, M. A. Weis, and J.-J. Wu, "Articular cartilage collagen: an irreplaceable framework?," *Eur. Cell. Mater.*, vol. 12, pp. 57–63, Nov. 2006.

[39] A. Mobasheri, R. Mobasheri, M. J. Francis, E. Trujillo, D. Alvarez de la Rosa, and P. Martín-Vasallo, "Ion transport in chondrocytes: membrane transporters involved in intracellular ion homeostasis and the regulation of cell volume, free [Ca2+] and pH.," *Histol. Histopathol.*, vol. 13, no. 3, pp. 893–910, 1998.

[40] A. Mobasheri, "Correlation between [Na+], [glycosaminoglycan] and Na+/K+ pump density in the extracellular matrix of bovine articular cartilage.," *Physiol. Res.*, vol. 47, no. 1, pp. 47–52, 1998.

[41] C. S. Mow, S. T. Woolson, S. G. Ngarmukos, E. H. Park, and H. P. Lorenz, "Comparison of Scars from Total Hip Replacements Done with a Standard or a Mini-incision," *Clin. Orthop. Relat. Res.*, vol. 441, no. NA;, pp. 80–85, Dec. 2005.

[42] L. Ng, A. J. Grodzinsky, P. Patwari, J. Sandy, A. Plaas, and C. Ortiz, "Individual cartilage aggrecan macromolecules and their constituent glycosaminoglycans visualized via atomic force microscopy.," *J. Struct. Biol.*, vol. 143, no. 3, pp. 242–57, Sep. 2003.

[43] Y. Krishnan and A. J. Grodzinsky, "Cartilage diseases," *Matrix Biol.*, May 2018.

[44] E. Gibon, L. Lu, and S. B. Goodman, "Aging, inflammation, stem cells, and bone healing," *Stem Cell Res. Ther.*, vol. 7, no. 1, p. 44, 2016.

[45] J. Z. Wu and W. Herzog, "Elastic anisotropy of articular cartilage is associated with the microstructures of collagen fibers and chondrocytes.," *J. Biomech.*, vol. 35, no. 7, pp. 931–42, Jul. 2002.

[46] A. R. Armiento, M. J. Stoddart, M. Alini, and D. Eglin, "Biomaterials for articular cartilage tissue engineering: Learning from biology," *Acta Biomater.*, vol. 65, pp. 1–20, 2018.

[47] F. J. Alenghat and D. E. Ingber, "Mechanotransduction: all signals point to cytoskeleton, matrix, and integrins.," *Sci. STKE*, vol. 2002, no. 119, p. pe6, Feb. 2002.

[48] D. E. Ingber, "Cellular mechanotransduction: putting all the pieces together again.," *FASEB J.*, vol. 20, no. 7, pp. 811–27, May 2006.

[49] S. Sukharev and D. P. Corey, "Mechanosensitive channels: multiplicity of families and gating paradigms.," *Sci. STKE*, vol. 2004, no. 219, p. re4, Feb. 2004.

[50] S. Khan and M. P. Sheetz, "Force effects on biochemical kinetics.," *Annu. Rev. Biochem.*, vol. 66, no. 1, pp. 785–805, Jun. 1997.

[51] M. Wong, M. Siegrist, and K. Goodwin, "Cyclic tensile strain and cyclic hydrostatic pressure differentially regulate expression of hypertrophic markers in primary chondrocytes.," *Bone*, vol. 33, no. 4, pp. 685–93, Oct. 2003.

[52] C. Herberhold *et al.*, "In situ measurement of articular cartilage deformation in intact femoropatellar joints under static loading.," *J. Biomech.*, vol. 32, no. 12, pp. 1287–95, Dec. 1999.

[53] "Collagen organization in articular cartilage, determined by X-ray diffraction, and its relationship to tissue function," *Proc. R. Soc. London. Ser. B. Biol. Sci.*, vol. 212, no. 1188, pp. 299–304, Jul. 1981.

[54] J. Dunham, D. R. Shackleton, M. E. Billingham, L. Bitensky, J. Chayen, and I. H. Muir, "A reappraisal of the structure of normal canine articular cartilage.," *J. Anat.*, vol. 157, pp. 89–99, Apr. 1988.

[55] A.-M. Mustonen *et al.*, "First in vivo detection and characterization of hyaluronan-coated extracellular vesicles in human synovial fluid," *J. Orthop. Res.*, vol. 34, no. 11, pp. 1960–1968, Nov. 2016.

[56] A. Weinberger and P. A. Simkin, "Plasma proteins in synovial fluids of normal human joints," *Semin. Arthritis Rheum.*, vol. 19, no. 1, pp. 66–76, Aug. 1989.

[57] P. Knox, J. R. Levick, and J. N. McDonald, "SYNOVIAL FLUID - ITS MASS, MACROMOLECULAR CONTENT AND PRESSURE IN MAJOR LIMB JOINTS OF THE RABBIT," *Q. J. Exp. Physiol.*, vol. 73, no. 1, pp. 33–45, Jan. 1988.

[58] J. Hankins, "The role of albumin in fluid and electrolyte balance," *Journal of Infusion Nursing*, vol. 29, no. 5. pp. 260–265, 2006.

[59] H. W. Fang, M. C. Hsieh, H. T. Huang, C. Y. Tsai, and M. H. Chang, "Conformational and adsorptive characteristics of albumin affect interfacial protein boundary lubrication: From experimental to molecular dynamics simulation approaches," *Colloids Surfaces B Biointerfaces*, vol. 68, no. 2, pp. 171–177, Feb. 2009.

[60] D. Scott, P. J. Coleman, R. M. Mason, and J. R. Levick, "Interaction of intraarticular hyaluronan and albumin in the attenuation of fluid drainage from joints," *Arthritis Rheum.*, vol. 43, no. 5, pp. 1175–1182, May 2000.

[61] T. Nishimoto, "[Changes in the visco-elastic properties of the articular cartilage incubated in various kinds of liquid].," *Nihon Seikeigeka Gakkai Zasshi*, vol. 69, no. 9, pp. 776–87, Sep. 1995.

[62] O. Schmut and H. Hofmann, "Preparation of gels from hyaluronate solutions," *Graefe's Arch. Clin. Exp. Ophthalmol.*, vol. 218, no. 6, pp. 311–314, Jun. 1982.

[63] I. Anadere, H. Chmiel, and W. Laschner, "Viscoelasticity of "normal" and pathological synovial fluid.," *Biorheology*, vol. 16, no. 3, pp. 179–84, 1979.

[64] B. A. Hills and R. W. Crawford, "Normal and prosthetic synovial joints are lubricated by surface-active phospholipid: a hypothesis.," *J. Arthroplasty*, vol. 18, no. 4, pp. 499–505, Jun. 2003.

[65] I. M. Schwarz and B. A. Hills, "Surface-active phospholipid as the lubricating component of lubricin.," *Br. J. Rheumatol.*, vol. 37, no. 1, pp. 21–6, Jan. 1998.

[66] D. Mazzucco and M. Spector, "The John Charnley Award Paper. The role of joint fluid in the tribology of total joint arthroplasty.," *Clin. Orthop. Relat. Res.*, no. 429, pp. 17–32, Dec. 2004.

[67] R. C. Gupta, R. Lall, A. Srivastava, and A. Sinha, "Hyaluronic Acid: Molecular Mechanisms and Therapeutic Trajectory.," *Front. Vet. Sci.*, vol. 6, p. 192, 2019.

[68] S. G. Cook *et al.*, "Dynamics of Synovial Fluid Aggregation under Shear," *Langmuir*, p. acs.langmuir.9b02028, Oct. 2019.

[69] M. D. Alexandru, "NANOPHYSICAL ANALYSIS TO STUDY EVOLUTION OF VASCULAR AND ARTICULAR INFLAMMATORY," Université Claude Bernard Lyon-1, 2011.

[70] P. Bełdowski, S. Yuvan, A. Dėdinaitė, P. M. Claesson, and T. Pöschel, "Interactions of a short hyaluronan chain with a phospholipid membrane," *Colloids Surfaces B Biointerfaces*, vol. 184, p. 110539, Dec. 2019.

[71] P. Bełdowski, A. Mazurkiewicz, T. Topoliński, and T. Małek, "Hydrogen and Water Bonding between Glycosaminoglycans and Phospholipids in the Synovial Fluid: Molecular Dynamics Study.," *Mater. (Basel, Switzerland)*, vol. 12, no. 13, Jun. 2019.

[72] L. Rodriguez-Berdini and G. Ferrero, "A Technique for the Measurement of in vitro Phospholipid Synthesis via Radioactive Labeling," *BIO-PROTOCOL*, vol. 6, no. 2, 2016.

[73] P. Sautot, "Propriétés d'auto-assemblage de phospholipides riches en acides gras polyinsaturés : caractérisation physico-chimique et simulation de bicouches par dynamique moléculaire To cite this version : HAL Id : tel-01749542 soutenance et mis à disposition de l'," 2018.

[74] W. H. Briscoe, S. Titmuss, F. Tiberg, R. K. Thomas, D. J. McGillivray, and J. Klein, "Boundary lubrication under water," *Nature*, vol. 444, no. 7116, pp. 191–194, Nov. 2006.

[75] H. Forster and J. Fisher, "The Influence of Loading Time and Lubricant on the Friction of Articular Cartilage," *Proc. Inst. Mech. Eng. Part H J. Eng. Med.*, vol. 210, no. 2, pp. 109–119, Jun. 1996.

[76] B. A. Hills, "Oligolamellar lubrication of joints by surface active phospholipid.," *J. Rheumatol.*, vol. 16, no. 1, pp. 82–91, Jan. 1989.

[77] A. M. Trunfio, Y. Berthier, M. H. Meurisse, and J. P. Rieu, "Analysis of the tribological role of molecular assemblies of synovial fluid in the operation of healthy joints and articular joint prostheses," *Comput. Methods Biomech. Biomed. Engin.*, vol. 10, no. sup1, pp. 173–174, Jan. 2007.

[78] D. A. Swann and E. L. Radin, "The molecular basis of articular lubrication. I. Purification and properties of a lubricating fraction from bovine synovial fluid.," *J. Biol. Chem.*, vol. 247, no. 24, pp. 8069–73, Dec. 1972.

[79] G. D. Jay, "Lubricin and surfacing of articular joints," *Current Opinion in Orthopaedics*. 2004.

[80] D. K. Rhee *et al.*, "The secreted glycoprotein lubricin protects cartilage surfaces and inhibits synovial cell overgrowth," *J. Clin. Invest.*, 2005.

[81] D. A. Swann, F. H. Silver, H. S. Slayter, W. Stafford, and E. Shore, "The molecular structure and lubricating activity of lubricin isolated from bovine and human synovial fluids," *Biochem. J.*, 1985.

[82] A. A. Young *et al.*, "Proteoglycan 4 downregulation in a sheep meniscectomy model of early osteoarthritis," *Arthritis Res. Ther.*, 2006.

[83] D. A. Swann, S. Sotman, M. Dixon, and C. Brooks, "The isolation and partial characterization of the major glycoprotein (LGP-I) from the articular lubricating fraction from bovine synovial

fluid," *Biochem. J.*, 1977.

[84] T. MURAKAMI, "The lubrication in natural synovial joints and joint prostheses.," *JSME Int. journal. Ser. 3, Vib. Control Eng. Eng. Ind.*, 1990.

[85] B. A. Hills, "Boundary lubrication in vivo," *Proc. Inst. Mech. Eng. Part H J. Eng. Med.*, vol. 214, no. 1, pp. 83–94, Jan. 2000.

[86] I. Schvartz, D. Seger, and S. Shaltiel, "Molecules in focus: Vitronectin," *Int. J. Biochem. Cell Biol.*, 1999.

[87] E. Tolosano and F. Altruda, "Hemopexin: Structure, Function, and Regulation," *DNA Cell Biol.*, vol. 21, no. 4, pp. 297–306, Apr. 2002.

[88] A. W. Batchelor and G. W. Stachowiak, "Arthritis and the interacting mechanisms of synovial joint lubrication. Part II: Joint lubrication and its relation to arthritis," *Journal of Orthopaedic Rheumatology*. 1996.

[89] T. Murakami, H. Higaki, Y. Sawae, N. Ohtsuki, S. Moriyama, and Y. Nakanishi, "Adaptive multimode lubrication in natural synovial joints and artificial joints," *Proc. Inst. Mech. Eng. Part H J. Eng. Med.*, 1998.

[90] H. Forster and J. Fisher, "The influence of continuous sliding and subsequent surface wear on the friction of articular cartilage," *Proc. Inst. Mech. Eng. Part H J. Eng. Med.*, 1999.

[91] M. Corneci, "Fonctionnement tribologique des articulations synoviales pathologiques : rôle des interfaces phospholipidiques," Sep. 2012.

[92] C. Tanford, "The hydrophobic effect: formation of micelles and biological membranes 2d ed," 1980.

[93] A.-M. Trunfio, "MODELE BIO-TRIBOLOGIQUE DES ARTICULATIONS. ROLE MECANIQUE ET PHYSICOCHIMIQUE DES ASSEMBLAGES MOLECULAIRES DU FLUIDE SYNOVIAL.," Dec. 2002.

[94] A. Gaisinskaya *et al.*, "Hydration lubrication: exploring a new paradigm," *Faraday Discuss.*, vol. 156, no. 0, p. 217, Jul. 2012.

[95] R. Goldberg, A. Schroeder, Y. Barenholz, and J. Klein, "Interactions between adsorbed hydrogenated soy phosphatidylcholine (HSPC) vesicles at physiologically high pressures and salt concentrations," *Biophys. J.*, 2011.

[96] M.-M. Sava *et al.*, "Structural and tribological study of healthy and biomimetic SF," *Comput. Methods Biomech. Biomed. Engin.*, vol. 16, no. sup1, pp. 216–218, Jul. 2013.

[97] L. R. Gale, R. Coller, D. J. Hargreaves, B. A. Hills, and R. Crawford, "The role of SAPL as a boundary lubricant in prosthetic joints," *Tribol. Int.*, vol. 40, no. 4, pp. 601–606, 2007.

[98] M. Wajeeh Bakhsh, MD and Gregg Nicandri, "Anatomy and Physical Examination of the Stallion," *Equine Breed. Manag. Artif. Insemin.*, vol. 26, no. 3, pp. 1–16, 2018.

[99] J. Pandya, T. Johnson, and A. K. Low, "Shoulder replacement for osteoarthritis: A review of surgical management," *Maturitas*, vol. 108. Elsevier, pp. 71–76, 01-Feb-2018.

[100] H. A. Wieland, M. Michaelis, B. J. Kirschbaum, and K. A. Rudolphi, "Osteoarthritis — an untreatable disease?," *Nat. Rev. Drug Discov.*, vol. 4, no. 4, pp. 331–344, Apr. 2005.

[101] S. B. Abramson and M. Attur, "Developments in the scientific understanding of osteoarthritis," *Arthritis Research and Therapy*, vol. 11, no. 3. BioMed Central, p. 227, 2009.

[102] A. Farron, "Les prothèses d'épaule," *Forum Med Suisse*. pp. 53–58, 2006.

[103] V. Astier, "UN MODELE ELEMENTS FINIS DE L'EPAULE : DU TRAUMATISME A LA REHABILITATION," 2010.

[104] A. Hannoun, "Caractérisation multi physique des cultures cellulaires en contact avec différents biomatériaux des implants orthopédiques: Application de l'arthroplastie d'épaule," 2016.

[105] J. J. Guo *et al.*, "Three-Year Follow-up of Conservative Treatments of Shoulder Osteoarthritis in Older Patients," *Orthopedics*, vol. 39, no. 4, pp. e634–e641, Jul. 2016.

[106] T. J. Menge, R. E. Boykin, I. R. Byram, and B. D. Bushnell, "A Comprehensive Approach to Glenohumeral Arthritis," *South. Med. J.*, vol. 107, no. 9, pp. 567–573, Sep. 2014.

[107] H. Mistry *et al.*, "HEALTH TECHNOLOGY ASSESSMENT Autologous chondrocyte implantation in the knee: systematic review and economic evaluation," *Health Technol. Assess. (Rockv).*, vol. 21, no. 6, 2017.

[108] L. Constantinou, T. K. Cobb, and A. L. Walden, "Long-term follow-up of osteochondral autologous transplantation in the metacarpophalangeal joints," *Hand*, vol. 9, no. 3, pp. 335–339, 2014.

[109] D. J. Ruta, A. D. Villarreal, and D. R. Richardson, "Orthopedic Surgical Options for Joint Cartilage Repair and Restoration," *Phys. Med. Rehabil. Clin. N. Am.*, 2016.

[110] H. Schenker *et al.*, "Aktuelle Übersicht knorpelregenerativer Verfahren," *Orthopade*, vol. 46, no. 11. pp. 907–913, 2017.

[111] R. Karuppal, "Current concepts in the articular cartilage repair and regeneration," *Journal of Orthopaedics*. 2017.

[112] Y. Nam, Y. A. Rim, J. Lee, and J. H. Ju, "Current therapeutic strategies for stem cell-based cartilage regeneration," *Stem Cells International*. 2018.

[113] B. A. Ayodele, M. Mirams, C. N. Pagel, and E. J. Mackie, "The vacuolar H + ATPase V 0 subunit d 2 is associated with chondrocyte hypertrophy and supports chondrocyte differentiation," *Bone Reports*, vol. 7, pp. 98–107, 2017.

[114] S. Peng, C.-W. Wu, J.-Y. Lin, C.-Y. Yang, M.-H. Cheng, and I.-M. Chu, "Promoting chondrocyte cell clustering through tuning of a poly(ethylene glycol)-poly(peptide) thermosensitive hydrogel with distinctive microarchitecture," *Mater. Sci. Eng. C*, vol. 76, pp. 181–189, 2017.

[115] C. Vilela, C. Correia, J. M. Oliveira, R. A. Sousa, J. Espregueira-Mendes, and R. L. Reis, "Cartilage repair using hydrogels: a critical review of in vivo experimental designs," *ACS Biomater. Sci. Eng.*, p. 150813111234008, 2015.

[116] N. Célant, S. Guillaume, and T. Rochereau, *Enquête sur la santé et la protection sociale 2012*. 2012.

[117] O. Levy and S. a Copeland, "Cementless surface replacement arthroplasty of the shoulder. 5- to 10-year results with the Copeland mark-2 prosthesis.," *J. Bone Joint Surg. Br.*, vol. 83, no. 2, pp. 213–221, 2001.

[118] P. Y. K. Chin, J. W. Sperling, R. H. Cofield, and C. Schleck, "Complications of total shoulder arthroplasty: Are they fewer or different?," *J. Shoulder Elb. Surg.*, vol. 15, no. 1, pp. 19–22, 2006.

[119] B. P. Wiater, J. E. Moravek, and J. M. Wiater, "The evaluation of the failed shoulder

arthroplasty," *J. shoulder Elb. Surg.*, vol. 23, no. 5, pp. 745–758, 2014.

[120] J. Garret, A. Godenèche, S. Grosclaude, and C. Lévigne, "Innovations au Membre supérieur / for the upper member Does the non-fixed Pyrocarbon Interposition Shoulder Arthroplasty allow to avoid glenoïd complications for the treatment of primaray osteoarthritis ?," no. 8, pp. 27–29, 2013.

[121] S. D. Cook, R. D. Beckenbaugh, J. Redondo, L. S. Popich, J. J. Klawitter, and R. L. Linscheid, "Long-term follow-up of pyrolytic carbon metacarpophalangeal implants.," *J. Bone Joint Surg. Am.*, vol. 81, pp. 635–648, 1999.

[122] J. S. Kawalec, V. J. Hetherington, T. C. Melillo, and N. Corbin, "Evaluation of fibrocartilage regeneration and bone response at full-thickness cartilage defects in articulation with pyrolytic carbon or cobalt-chromium alloy hemiarthroplasties.," *J. Biomed. Mater. Res.*, vol. 41, no. 4, pp. 534–40, 1998.

[123] J. C. Bokros, "Carbon in medical devices," *Ceramics International*, vol. 9, no. 1. Elsevier, pp. 3–7, 01-Jan-1983.

[124] Bokros, Lagrange, and Shoen, "Control of structure of carbon for use in bioengineering." 1972.

[125] S. D. Cook, R. D. Beckenbaugh, A. M. Weinstein, and J. J. Klawitter, "Pyrolite carbon implants in the metacarpophalangeal joint of baboons," *Orthopedics*, vol. 6, 1983.

[126] J-P.Pequignot; B.Lussiez; Y.Allieu, "Implant adaptatif du scaphoid proximal." 2000.

[127] P. Bellemère, "Pyrocarbon implants for the hand and wrist," *Hand Surg. Rehabil.*, vol. 37, no. 3, pp. 129–154, Jun. 2018.

[128] J. J. Srnec, E. R. Wagner, and M. Rizzo, "Implant Arthroplasty for Proximal Interphalangeal, Metacarpophalangeal, and Trapeziometacarpal Joint Degeneration.," *J. Hand Surg. Am.*, vol. 42, no. 10, pp. 817–825, Oct. 2017.

[129] M. Hassler, "Other commonly used biomedical coatings: pyrolytic carbon coatings," *Coatings Biomed. Appl.*, pp. 75–105, Jan. 2012.

[130] J. Pelissier and L. Lombard, "Contribution a l'étude de la perméabilité des pyrocarbones isotropes de basse temperature," *J. Nucl. Mater.*, vol. 78, no. 1, pp. 33–42, Nov. 1978.

[131] J. C. Bokros, "Carbon biomedical devices," *Carbon N. Y.*, vol. 15, no. 6, pp. 353–371, Jan. 1977.

[132] M. Hassler, S. Rambaud, R. Ranc, and C. Real, "Medical applications of carbonaceous materials," vol. 1989, no. 1, pp. 1–13, 1989.

[133] B. P. Sharma, "Nuclear Reactors: Moderator and Reflector Materials," in *Encyclopedia of Materials: Science and Technology*, 2001.

[134] T. Neuberger, B. Schöpf, H. Hofmann, M. Hofmann, and B. von Rechenberg, "Superparamagnetic nanoparticles for biomedical applications: Possibilities and limitations of a new drug delivery system," *J. Magn. Magn. Mater.*, vol. 293, no. 1, pp. 483–496, May 2005.

[135] A. D. Haubold, "On the durability of pyrolytic carbon in vivo.," *Medical progress through technology*, vol. 20, no. 3–4. pp. 201–8, 1994.

[136] L. Feng and J. D. Andrade, "Protein adsorption on low temperature isotropic carbon: V. How is it related to its blood compatibility?," *J. Biomater. Sci. Polym. Ed.*, vol. 7, no. 5, pp. 439–52, 1995.

[137] T. H. Chiu, E. Nyilas, and D. M. Lederman, "Thermodynamics of native protein/foreign surface

interactions. IV. Calorimetric and microelectrophoretic study of human fibrinogen sorption onto glass and LTI-carbon.," *Trans. Am. Soc. Artif. Intern. Organs*, vol. 22, pp. 498–513, 1976.

[138] S. L. Goodman, "Sheep, pig, and human platelet-material interactions with model cardiovascular biomaterials," *J. Biomed. Mater. Res.*, vol. 45, no. 3, pp. 240–250, 1999.

[139] M. A. Vitale, F. Taylor, M. Ross, and S. L. Moran, "Trapezium Prosthetic Arthroplasty (Silicone, Artelon, Metal, and Pyrocarbon)," *Hand Clin.*, vol. 29, no. 1, pp. 37–55, 2013.

[140] R. B. More and A. D. Haubold, "Surface chemistry and surface roughness of clinical pyrocarbons," *Cells Mater.*, vol. 6, no. 4, pp. 273–279, 1996.

[141] H. S. Shim and F. J. Schoen, "The wear resistance of pure and silicon-alloyed isotropic carbons.," *Biomater. Med. Devices. Artif. Organs*, vol. 2, no. 1, pp. 103–18, 1974.

[142] F. J. Schoen, J. L. Titus, and G. M. Lawrie, "Durability of pyrolytic carbon-containing heart valve prostheses," *J. Biomed. Mater. Res.*, vol. 16, no. 5, pp. 559–570, Sep. 1982.

[143] M. Hassler, R. Ranc, S. Carle, and F. Moutet, *Intéret d pyrocarbone dans la réalisation d'implants articulaires*. 1996.

[144] M. Sankar, J. Vishnu, M. Gupta, and G. Manivasagam, "Magnesium-based alloys and nanocomposites for biomedical application," in *Applications of Nanocomposite Materials in Orthopedics*, 2019.

[145] W. Daecke, K. Veyel, P. Wieloch, M. Jung, H. Lorenz, and A.-K. Martini, "Osseointegration and mechanical stability of pyrocarbon and titanium hand implants in a load-bearing in vivo model for small joint arthroplasty," *J. Hand Surg. Am.*, vol. 31, no. 1, pp. 90–97, 2006.

[146] R. D. Beckenbaugh, J. Klawitter, and S. Cook, "Osseointegration and Mechanical Stability of Pyrocarbon and Titanium Hand Implants in a Load-Bearing In Vivo Model for Small Joint Arthroplasty," *J. Hand Surg. Am.*, vol. 31, no. 7, pp. 1240–1241, 2006.

[147] B. Hohendorff, W. Zhang, K. J. Burkhart, L. P. Müller, and C. Ries, "Insertion of the Ascension PyroCarbon PIP total joint in 152 human cadaver fingers: analysis of implant positions and malpositions," *Arch. Orthop. Trauma Surg.*, vol. 135, no. 2, pp. 283–290, Feb. 2015.

[148] C. Ries, W. Zhang, K. J. Burkhart, W. F. Neiss, L. P. Muller, and B. Hohendorff, "Morphology of the proximal and middle phalanx of fingers with regard to the Ascension PyroCarbon PIP total joint," *J. Hand Surg. (European Vol.*, vol. 39, no. 6, pp. 596–603, 2014.

[149] J.-P. Pequignot, "APSI_Adaptative_proximal_scaphoid_implant_J_P_PEQUIGNOT_2004.pdf." 1994.

[150] D. J. Slutsky and J. F. Slade III, Eds., "35 Pyrocarbon Scaphoid Implant Allowing Adaptive Mobility in Proximal Scaphoid Pseudarthrosis," in *The Scaphoid*, Stuttgart: Georg Thieme Verlag, 2011.

[151] M. Driver, *Coatings for biomedical applications*. Woodhead Publishing, 2012.

[152] S. L. Salkeld, L. P. Patron, J. C. Lien, S. D. Cook, and D. G. Jones, "Biological and functional evaluation of a novel pyrolytic carbon implant for the treatment of focal osteochondral defects in the medial femoral condyle: assessment in a canine model," *J. Orthop. Surg. Res.*, vol. 11, no. 1, p. 155, 2016.

[153] M. Jung *et al.*, "Comparison of cobalt chromium, ceramic and pyrocarbon hemiprostheses in a rabbit model: Ceramic leads to more cartilage damage than cobalt chromium," *J. Biomed. Mater. Res. - Part B Appl. Biomater.*, vol. 85, no. 2, pp. 427–434, 2008.

[154] P. Strzepa and J. Klawitter, "ASCENSION PYROCARBON HEMISPHERE WEAR TESTING AGAINST BONE," *51st Annu. Meet. Orthop. Res. Soc. Poster No 0897*, vol. 71, no. 2, p. 1880, 2005.

[155] C. A. Pacione, S. Chubinskaya, and M. A. Wimmer, "Biological Response of Cartilage Articulating Against Pyrolytic Carbon in Comparison to Cobalt-Chromium Alloy," vol. 10, no. 0674, pp. 1–13, 2012.

[156] C. J. Lavernia, S. D. Cook, A. M. Weinstein, and J. J. Klawitter, "An analysis of stresses in a dental implant system," *J. Biomech.*, vol. 14, no. 8, pp. 555–560, 1981.

[157] J. N. Kent, S. D. Cook, A. M. Weinstein, and J. J. Klawitter, "A clinical comparison of LTI carbon, alumina, and carbon???coated alumina blade???type implants in baboons," *J. Biomed. Mater. Res.*, vol. 16, no. 6, pp. 887–899, 1982.

[158] R. E. Luedemann and S. D. Cook, "Radiographic and histologic evaluation of intramedullary implants intended for biological fixation.," *Biomater. Med. Devices. Artif. Organs*, vol. 11, no. 2–3, pp. 197–210, 1983.

[159] A. Hannoun *et al.*, "Pyrocarbon versus cobalt-chromium in the context of spherical interposition implants: an in vitro study on cultured chondrocytes," *Eur. Cells Mater.*, vol. 37, pp. 1–15, 2019.

[160] V. I. Sikavitsas, J. S. Temenoff, and A. G. Mikos, "Biomaterials and bone mechanotransduction," *Biomaterials*, vol. 22, no. 19, pp. 2581–2593, 2001.

[161] R. A. Gittens, R. Olivares-Navarrete, Z. Schwartz, and B. D. Boyan, "Implant osseointegration and the role of microroughness and nanostructures: Lessons for spine implants," *Acta Biomater.*, vol. 10, no. 8, pp. 3363–3371, 2014.

[162] D. L. Kerboull *et al.*, "Pyrocarbon interposition shoulder arthroplasty: preliminary results from a prospective multicenter study at 2 years of follow-up," *Biomaterials*, vol. 26, no. 1, pp. 1–9, 2012.

[163] G. Ouenzerfi *et al.*, "Characterization of cell cultures in contact with different orthopedic implants biomaterials," *IOP Conf. Ser. Mater. Sci. Eng.*, vol. 147, no. 1, p. 012015, Aug. 2016.

[164] R. Martins-Noguerol *et al.*, "Lipidomic Analysis of Plastidial Octanoyltransferase Mutants of Arabidopsis thaliana," *Metabolites*, vol. 9, no. 10, p. 209, Sep. 2019.

[165] M. Guichardant and M. Lagarde, "Phospholipid analysis and fatty acid content in platelets by the combination of high-performance liquid chromatography and glass capillary gas-liquid chromatography," *J. Chromatogr. B Biomed. Sci. Appl.*, 1983.

[166] M. Guichardant and M. Lagarde, "Studies on platelet lipoxygenase specificity towards icosapolyenoic and docosapolyenoic acids," *Biochim. Biophys. Acta (BBA)/Lipids Lipid Metab.*, 1985.

[167] B. A. Hills and B. D. Buttler, "Surfactants identified in synovial fluid and their ability to act as boundary lubricants," *Ann. Rheum. Dis.*, 1984.

[168] M.-C. Corneci, F. Dekkiche, A.-M. Trunfio-Sfarghiu, M.-H. Meurisse, Y. Berthier, and J.-P. Rieu, "Tribological properties of fluid phase phospholipid bilayers," *Tribol. Int.*, vol. 44, no. 12, pp. 1959–1968, Nov. 2011.

[169] A. M. Trunfio-Sfarghiu, Y. Berthier, M. H. Meurisse, and J. P. Rieu, "Role of nanomechanical properties in the tribological performance of phospholipid biomimetic surfaces," *Langmuir*, 2008.

Amira HANNOUN/ Thesis in Biomechanics 2020/ INSA Lyon

[170] E. Edston and L. Gröntoft, "Saffron—A Connective Tissue Counterstain in Routine Pathology," *J. Histotechnol.*, vol. 20, no. 2, pp. 123–125, Jun. 1997.

[171] C. S. Mears, T. D. Langston, C. M. Phippen, W. Z. Burkhead, and J. G. Skedros, "Humeral head circle-fit method greatly increases reliability and accuracy when measuring anterior–posterior radiographs of the proximal humerus," *J. Orthop. Res.*, 2017.

[172] G. Walch, R. Badet, A. Boulahia, and A. Khoury, "Morphologic study of the glenoid in primary glenohumeral osteoarthritis.," *J. Arthroplasty*, vol. 14, no. 6, pp. 756–60, Sep. 1999.

[173] K. V Vo, D. J. Hackett, A. O. Gee, and J. E. Hsu, "Classifications in Brief: Walch Classification of Primary Glenohumeral Osteoarthritis.," *Clin. Orthop. Relat. Res.*, vol. 475, no. 9, pp. 2335–2340, 2017.

[174] R. J. Hinton, Y. Jing, J. Jing, and J. Q. Feng, "Roles of Chondrocytes in Endochondral Bone Formation and Fracture Repair," *J. Dent. Res.*, vol. 96, no. 1, pp. 23–30, 2017.

[175] D. P. Hu *et al.*, "Cartilage to bone transformation during fracture healing is coordinated by the invading vasculature and induction of the core pluripotency genes," *Dev.*, vol. 144, no. 2, pp. 221–234, 2017.

[176] J. Filipowska, K. A. Tomaszewski, Ł. Niedźwiedzki, J. A. Walocha, and T. Niedźwiedzki, "The role of vasculature in bone development, regeneration and proper systemic functioning," *Angiogenesis*, vol. 20, no. 3, pp. 291–302, 2017.

[177] L. Szabova *et al.*, "MT1-MMP and type II collagen specify skeletal stem cells and their bone and cartilage progeny," *J. Bone Miner. Res.*, vol. 24, no. 11, pp. 1905–1916, 2009.

[178] L. M. Biga *et al.*, "Bone Structure – Anatomy and Physiology," *Creative Commons Attribution 4.0 International License*, 2018. [Online]. Available: http://library.open.oregonstate.edu/aandp/chapter/6-3-bone-structure/. [Accessed: 23-Jul-2019].

[179] V. I. Shubayev, R. Branemark, J. Steinauer, and R. R. Myers, "Titanium implants induce expression of matrix metalloproteinases in bone during osseointegration," *J. Rehabil. Res. Dev.*, vol. 41, no. 6, p. 757, 2004.

[180] H. A. Declercq, R. M. H. Verbeeck, L. I. F. J. M. De Ridder, E. H. Schacht, and M. J. Cornelissen, "Calcification as an indicator of osteoinductive capacity of biomaterials in osteoblastic cell cultures," *Biomaterials*, vol. 26, no. 24, pp. 4964–4974, 2005.

[181] T. Albrektsson and H. A. Hansson, "An ultrastructural characterization of the interface between bone and sputtered titanium or stainless steel surfaces," *Biomaterials*, vol. 7, no. 3, pp. 201–205, 1986.

[182] G. L. Jones, A. Motta, M. J. Marshall, A. J. El Haj, and S. H. Cartmell, "Osteoblast: Osteoclast co-cultures on silk fibroin, chitosan and PLLA films," *Biomaterials*, vol. 30, no. 29, pp. 5376–5384, 2009.

[183] K. Anselme, "Osteoblast adhesion on biomaterials," *Biomaterials*, vol. 21, no. 7, pp. 667–681, 2000.

[184] B. D. Boyan, T. W. Hummert, D. D. Dean, and Z. Schwartz, "Role of material surfaces in regulating bone and cartilage cell response," *Biomaterials*, vol. 17, no. 2, pp. 137–146, 1996.

[185] M. J. Nine, D. Choudhury, A. C. Hee, R. Mootanah, and N. A. A. Osman, "Wear Debris Characterization and Corresponding Biological Response: Artificial Hip and Knee Joints.," *Mater. (Basel, Switzerland)*, vol. 7, no. 2, pp. 980–1016, Feb. 2014.

[186] M. Gosset, F. Berenbaum, S. Thirion, and C. Jacques, "Primary culture and phenotyping of murine chondrocytes.," *Nat. Protoc.*, vol. 3, no. 8, pp. 1253–1260, 2008.

[187] T. Mosmann, "Rapid colorimetric assay for cellular growth and survival: Application to proliferation and cytotoxicity assays," *J. Immunol. Methods*, vol. 65, no. 1–2, pp. 55–63, 1983.

[188] C. M. Stanford, P. A. Jacobson, E. D. Eanes, L. A. Lembke, and R. J. Midura, "Rapidly forming apatitic mineral in an osteoblastic cell line (UMR 106-01 BSP).," *J. Biol. Chem.*, vol. 270, no. 16, pp. 9420–8, Apr. 1995.

[189] K. Lorentz, "Improved determination of serum calcium with 2-cresolphthalein complexone," *Clin. Chim. Acta*, vol. 126, no. 3, pp. 327–334, 1982.

[190] W. R. Moorehead and H. G. Biggs, "2-Amino-2-methyl-1-propanol as the Alkalizing Agent in an Improved Continuous-Flow Cresolphthalein Complexone Procedure for Calcium in Serum," *Clin. Chem.*, vol. 20, no. 11, 1974.

[191] G. W. Cyboron and R. E. Wuthier, "Purification and initial characterization of intrinsic membrane-bound alkaline phosphatase from chicken epiphyseal cartilage.," *J. Biol. Chem.*, vol. 256, no. 14, pp. 7262–7268, 1981.

[192] J. David S, "Dynamic mechanical analysis of polymeric systems of pharmaceutical and biomedical significance," *Int. J. Pharm.*, vol. 179, pp. 167–178, 1999.

[193] E. A. Lewallen *et al.*, "Biological strategies for improved osseointegration and osteoinduction of porous metal orthopedic implants," *Tissue Eng. Part B Rev.*, vol. 21, no. 2, pp. 218–230, 2014.

[194] J. G. Steele *et al.*, "Attachment of human bone cells to tissue culture polystyrene and to unmodified polystyrene: the effect of surface chemistry upon initial cell attachment," *J. Biomater. Sci. Polym. Ed.*, vol. 5, no. 3, pp. 245–257, 1994.

[195] R. C. Anderson, S. D. Cook, A. M. Weinstein, and R. A. Y. J. HADDAD JR, "An evaluation of skeletal attachment to LTI pyrolytic carbon, porous titanium, and carbon-coated porous titanium implants.," *Clin. Orthop. Relat. Res.*, vol. 182, pp. 242–257, 1984.

[196] M. Wimmer, C. Pacione, V. Shekhawat, P. B.-T. ORS, and U. 2008, "In vitro wear testing of living cartilage tissue," *ors.org*, 2008.

[197] B. M. Wroblewski, "Wear of high-density polyethylene on bone and cartilage.," *J. Bone Joint Surg. Br.*, vol. 61-B, no. 4, pp. 498–500, Nov. 1979.

[198] M. Wimmer, C. Pacione, T. Uth, and Y. Dwivedi, "Final Study Report In Vitro Wear Testing of Living Cartilage against Pyrolytic Carbon," 2010.

[199] V. Coulson-Thomas and T. Gesteira, "Dimethylmethylene Blue Assay (DMMB)," *BIO-PROTOCOL*, 2014.

[200] D. D. Cissell, J. M. Link, J. C. Hu, and K. A. Athanasiou, "A Modified Hydroxyproline Assay Based on Hydrochloric Acid in Ehrlich's Solution Accurately Measures Tissue Collagen Content," *Tissue Eng. - Part C Methods*, 2017.

[201] A. V. Sarma, G. L. Powell, and M. LaBerge, "Phospholipid composition of articular cartilage boundary lubricant," *J. Orthop. Res.*, 2001.

[202] B. A. Hills, "Surface-active phospholipid: A Pandora's box of clinical applications. Part II. Barrier and lubricating properties," *Internal Medicine Journal*. 2002.

[203] T. Veselack, G. Aldebert, A. M. Trunfio-Sfarghiu, T. M. Schmid, M. P. Laurent, and M. A.

Wimmer, "Phospholipid vesicles in media for tribological studies against live cartilage," *Lubricants*, vol. 6, no. 1, 2018.

[204] G. Aldebert, "Biomechanical and tribological testing on cartilage," no. September 2016, 2016.

[205] R. L. Trevino, J. Stoia, M. P. Laurent, C. A. Pacione, S. Chubinskaya, and M. A. Wimmer, "ESTABLISHING A LIVE CARTILAGE-ON-CARTILAGE INTERFACE FOR TRIBOLOGICAL TESTING.," *Biotribology (Oxford)*, vol. 9, pp. 1–11, Mar. 2017.

[206] M. A. Wimmer *et al.*, "Tribology Approach to the Engineering and Study of Articular Cartilage," *Tissue Eng.*, vol. 10, no. 9–10, pp. 1436–1445, 2004.

[207] J. Jagur-Grodzinski, "Polymers for tissue engineering, medical devices, and regenerative medicine. Concise general review of recent studies," *Polym. Adv. Technol.*, vol. 17, no. 6, pp. 395–418, Jun. 2006.

[208] D. Antoni *et al.*, "Three-Dimensional Cell Culture: A Breakthrough in Vivo," *Int. J. Mol. Sci.*, vol. 16, no. 12, pp. 5517–5527, Mar. 2015.

[209] J. C. Bernhard and G. Vunjak-Novakovic, "Should we use cells, biomaterials, or tissue engineering for cartilage regeneration?," *Stem Cell Res. Ther.*, vol. 7, no. 1, p. 56, Apr. 2016.

[210] A. R. Armiento, M. J. Stoddart, M. Alini, and D. Eglin, "Biomaterials for Articular Cartilage Tissue Engineering: Learning from Biology.," *Acta Biomater.*, 2017.

[211] E. M. Darling and K. A. Athanasiou, "Articular Cartilage Bioreactors and Bioprocesses," *Tissue Eng.*, vol. 9, no. 1, pp. 9–26, Feb. 2003.

[212] I. Martin, T. Smith, and D. Wendt, "Bioreactor-based roadmap for the translation of tissue engineering strategies into clinical products," *Trends Biotechnol.*, vol. 27, no. 9, pp. 495–502, 2009.

[213] M. Demoor *et al.*, "Cartilage tissue engineering: Molecular control of chondrocyte differentiation for proper cartilage matrix reconstruction," *Biochimica et Biophysica Acta - General Subjects*. 2014.

[214] R. L. Mauck *et al.*, "Functional Tissue Engineering of Articular Cartilage Through Dynamic Loading of Chondrocyte-Seeded Agarose Gels," *ASME*, vol. 122, 2000.

[215] J. D. Kisiday, M. Jin, M. A. DiMicco, B. Kurz, and A. J. Grodzinsky, "Effects of dynamic compressive loading on chondrocyte biosynthesis in self-assembling peptide scaffolds," *J. Biomech.*, vol. 37, no. 5, pp. 595–604, 2004.

[216] D. E. Anderson and B. Johnstone, "Dynamic Mechanical Compression of Chondrocytes for Tissue Engineering: A Critical Review," *Front. Bioeng. Biotechnol.*, vol. 5, 2017.

[217] E. H. Frank, M. Jin, A. M. Loening, M. E. Levenston, and A. J. Grodzinsky, "A versatile shear and compression apparatus for mechanical stimulation of tissue culture explants," *J. Biomech.*, vol. 33, no. 11, pp. 1523–1527, 2000.

[218] S. D. Waldman, C. G. Spiteri, M. D. Grynpas, R. M. Pilliar, and R. A. Kandel, "Long-term intermittent shear deformation improves the quality of cartilaginous tissue formed in vitro," *J. Orthop. Res.*, vol. 21, no. 4, pp. 590–596, 2003.

[219] S. D. Waldman, D. C. Couto, M. D. Grynpas, R. M. Pilliar, and R. A. Kandel, "Multi-axial mechanical stimulation of tissue engineered cartilage: Review," *Eur. Cells Mater.*, vol. 13, no. 613, pp. 66–73, 2007.

[220] J. Engmann, C. Servais, and A. S. Burbidge, "Squeeze flow theory and applications to

rheometry: A review," *J. Nonnewton. Fluid Mech.*, vol. 132, no. 1–3, pp. 1–27, Dec. 2005.

[221]   L. Bostan *et al.*, "Mechanical and tribological properties of poly(hydroxyethyl methacrylate) hydrogels as articular cartilage substitutes," *Tribol. Int.*, vol. 46, pp. 215–224, 2012.

[222]   C. Bougault, "Identification de nouveaux acteurs moléculaires impliqués dans la mécanotransduction des chondrocytes," *http://www.theses.fr*, Nov. 2009.

[223]   A. Hautier *et al.*, "Bone morphogenetic protein-2 stimulates chondrogenic expression in human nasal chondrocytes expanded *in vitro*," *Growth Factors*, vol. 26, no. 4, pp. 201–211, Jan. 2008.

[224]   F. Legendre *et al.*, "Enhanced Hyaline Cartilage Matrix Synthesis in Collagen Sponge Scaffolds by Using siRNA to Stabilize Chondrocytes Phenotype Cultured with Bone Morphogenetic Protein-2 Under Hypoxia," *Tissue Eng. Part C Methods*, vol. 19, no. 7, pp. 550–567, Jul. 2013.

[225]   S. Claus *et al.*, "Cartilage-Characteristic Matrix Reconstruction by Sequential Addition of Soluble Factors During Expansion of Human Articular Chondrocytes and Their Cultivation in Collagen Sponges," *Tissue Eng. Part C Methods*, vol. 18, no. 2, pp. 104–112, Feb. 2012.

[226]   C. Bougault *et al.*, "Alteration of cartilage mechanical properties in absence of β1 integrins revealed by rheometry and FRAP analyses," *J. Biomech.*, vol. 46, no. 10, pp. 1633–1640, Jun. 2013.

[227]   D. Axelrod, D. E. Koppel, J. Schlessinger, E. Elson, and W. W. Webb, "Mobility measurement by analysis of fluorescence photobleaching recovery kinetics.," *Biophys. J.*, vol. 16, no. 9, pp. 1055–69, Sep. 1976.

[228]   C. Bougault *et al.*, "Dynamic compression of chondrocyte-agarose constructs reveals new candidate mechanosensitive genes.," *PLoS One*, vol. 7, no. 5, p. e36964, 2012.

[229]   P. Apelgren *et al.*, "Chondrocytes and stem cells in 3D-bioprinted structures create human cartilage in vivo," *PLoS One*, 2017.

[230]   J. Luo *et al.*, "Printing Functional 3D Microdevices by Laser-Induced Forward Transfer," *Small*, vol. 13, no. 9, p. 1602553, Mar. 2017.

[231]   J. Zouaoui *et al.*, "Multi-scale mechanical characterization of prostate cancer cell lines: Relevant biological markers to evaluate the cell metastatic potential," *Biochim. Biophys. Acta - Gen. Subj.*, vol. 1861, no. 12, pp. 3109–3119, Dec. 2017.

[232]   M. Mumme *et al.*, "Nasal chondrocyte-based engineered autologous cartilage tissue for repair of articular cartilage defects: an observational first-in-human trial," *Lancet*, vol. 388, no. 10055, pp. 1985–1994, Oct. 2016.

[233]   P. Akbari *et al.*, "Generating Mechanically Stable, Pediatric, and Scaffold-Free Nasal Cartilage Constructs *In Vitro*," *Tissue Eng. Part C Methods*, vol. 22, no. 12, pp. 1077–1084, Dec. 2016.

[234]   A. Impergre *et al.*, "Tribocorrosion of Polyethylene/Cobalt Contact Combined with Real-Time Fluorescence Assays on Living Macrophages: Development of A Multidisciplinary Biotribocorrosion Device," *Biotribology*, vol. 18, p. 100091, Jun. 2019.

[235]   J. F. Gonzalez, G. B. Alami, F. Baque, G. Walch, and P. Boileau, "Complications of unconstrained shoulder prostheses," *Journal of Shoulder and Elbow Surgery*, vol. 20, no. 4. Mosby, pp. 666–682, 01-Jun-2011.

FOLIO ADMINISTRATIF

THESE DE L'UNIVERSITE DE LYON OPEREE AU SEIN DE L'INSA LYON

NOM : HANNOUN

DATE de SOUTENANCE : 07/04/2020

(avec précision du nom de jeune fille, le cas échéant)

Prénom : Amira

TITRE : TRIBOLOGICAL ROLE OF PYROCARBON IN ARTICULAR CARTILAGE REGENERATION. APPLICATION IN THE SHOULDER ARTHROPLASTY

NATURE : Doctorat

Numéro d'ordre : 2020LYSEI025

Ecole doctorale : MEGA

Spécialité : Mécanique

RESUME: Degenerative shoulder pathologies are currently treated by total arthroplasty or hemiarthroplasty. In these cases, the complication rate reaches 22 %. Therefore, a new spherical interposition implant has been developed. The implant is made with pyrocarbon (PyC). It is inserted between the glenoid cartilage and a surgically-created humeral bone cavity. Short-term clinical results showed minimal cartilage wear and good bone remodelling in contact with the implant. However, the origin of these results is not yet well understood.

In a previous study on human explants, it was showed that humerus bone remodelling involves the synthesis of a neocartilaginous tissue, which partly explains the favourable clinical results. Therefore, the effect of PyC on the remodelling of the surrounding tissues needs investigation. Thus, this thesis aims to understand the origin of tissue remodelling on the bone and cartilage side.

Our strategy is: first, to carry out three parallel studies to dissociate the role of the biology, the material, and the transmission of mechanical stresses; and second, to validate the results thus obtained by associating the different aspects in an in vitro tissue bioengineering model. Our methodology was based on 1) the expertise of retrieved explants; 2) the development of chondrocytes cultures in contact with the biomaterials; 3) the in vitro biotribological simulations; and 4) the design of a simulator allowing to combine the biological, physicochemical and tribological results obtained previously.

The final results showed better chondrogenic and osteogenic cell activity in the case of PyC compared to CoCr. This was correlated with the PyC affinity to the phospholipids and with an optimal transmission of the mechanical stress. The in vivo control of transmission of mechanical stresses is essential to guarantee good results in the long-term. This thesis opens up fresh perspectives on the control of this transmission through biomaterials to regenerate the cartilage

MOTS-CLÉS :Cartilage regeneration, Pyrocarbon, shoulder arthroplasty, chondrocytes culture, tribological simulations

Laboratoire (s) de recherche : Laboratoire de mécanique des contacts et des structures LaMCoS

Directeur de thèse: Yves Berthier

Président de jury :

Composition du jury :

Yves Berthier, DR-CNRS, Emérite - INSA Lyon
Ana-Maria Trunfio-Sfargiu, CR-CNRS, HDR - INSA Lyon
Markus Wimmer, PR - Rush university Medical center
Astrid Pinzano, CR-CNRS, HDR - IMOPA-Université de Lorraine
Frédéric Mallein-Gerin, DR-CNRS - IBCP
Cristophe Drouet, DR-CNRS – CIRMAT
Michel Hassler, Directeur – Wright Medical
Carole bougault, MdC - Université Lyon
Pascal Boileau, PR-Chirurgien - Hôpital Pasteur 2 Nice